UNIVERSIDAD DE CÓRDOBA

ESCUELA POLITÉCNICA SUPERIOR
DEPARTAMENTO DE INGENIERÍA RURAL
ÁREA DE PROYECTOS DE INGENIERÍA

TESIS DOCTORAL

BIOCOMBUSTIBLES Y RUIDO EN MOTORES DE TRACTORES

BIOFUELS AND NOISE IN TRACTOR ENGINES

María Dolores Redel Macías

TITULO: *Biocombustibles y ruido en motores de tractores. Biofuels and noise in tractor engines*

AUTOR: *MARIA DOLORES REDEL MACIAS*

© Edita: Servicio de Publicaciones de la Universidad de Córdoba.
Campus de Rabanales
Ctra. Nacional IV, Km. 396 A
14071 Córdoba

www.uco.es/publicaciones
publicaciones@uco.es

UNIVERSIDAD DE CÓRDOBA

ESCUELA POLITÉCNICA SUPERIOR
DEPARTAMENTO DE INGENIERÍA RURAL
ÁREA DE PROYECTOS DE INGENIERÍA

BIOCOMBUSTIBLES Y RUIDO EN MOTORES DE TRACTORES

BIOFUELS AND NOISE IN TRACTOR ENGINES

TESIS DOCTORAL

AUTORA:

MªDOLORES REDEL MACÍAS

DIRECTORES:

ANTONIO JOSÉ CUBERO ATIENZA

MARÍA DEL PILAR DORADO PÉREZ

PAUL SAS

Marzo, 2012

BIOCOMBUSTIBLES Y RUIDO EN MOTORES DE TRACTORES

BIOFUELS AND NOISE IN TRACTOR ENGINES

Los/a directores/a,

Fdo.: A.J. Cubero Atienza Fdo.: María del Pilar Dorado Pérez

Fdo.: Paul Sas

Trabajo presentado para optar al grado de Doctor en la Universidad de Córdoba

Fdo.: MªDolores Redel Macías
Ingeniero en Automática y Electrónica Industrial

Marzo, 2012

A.J. Cubero Atienza, **María del Pilar Dorado Pérez** y **Paul Sas**, en calidad de directores de la Tesis Doctoral presentada por la Ingeniera MªDolores Redel Macías, con el título "*Biocombustibles y ruido en motores de tractores*",

INFORMA:

Que la Tesis Doctoral se ha realizado en el Área de Proyectos de Ingeniería, Departamento de Ingeniería Rural bajo nuestra supervisión y que, a nuestro juicio, reúne los requisitos necesarios exigidos para optar al grado de Doctor.

Y para que conste y surta los efectos oportunos, firmo el presente documento en Córdoba, a 16 de marzo de 2012.

Fdo.: A.J. Cubero Atienza Fdo.: María del Pilar Dorado Pérez

Fdo.: Paul Sas

A mi amor, mi vida, mi marido David,

Te quiero

ACKNOWLEDGEMENTS/AGRADECIMIENTOS

Durante la realización de esta tesis doctoral han pasado cosas dolorosas en mi vida que he podido superar gracias al apoyo y cariño de muchas personas.

Me gustaría en primer lugar agradecerles a mis directores Antonio y María del Pilar la confianza depositada en mi, su apoyo, cariño y su infinita comprensión. Siempre me habéis hecho sentir que lo difícil era fácil, y así todo resulta mucho más sencillo, necesitaría muchas más hojas para poder agradeceros vuestro tiempo y dedicación conmigo, además de todos los buenos momentos que hemos pasado juntos y por ser mucho más que directores de tesis…grandes amigos.

I'm grateful to Prof. Sas to give me the opportunity to work in his research group in KULeuven, where I've spent an amazing time and to introduce me in noise knowledge.

Quiero agradecerle al Prof. César Hervás y a su grupo de investigación el apoyo y soporte prestado en la realización de esta tesis, así como por transmitirme su gran experiencia en investigación.

I would like to thank to Dries for his kindness, his friendship and infinite patience with me in his explanations about sound synthesis and the measurement set up¡¡¡.

A Sara porque es la pieza clave que hace que todo funcione y vaya bien, así como por hacerme ver las cosas desde un punto de vista positivo, preocuparse siempre de mí y sacarme una sonrisa, gracias *chiquilla*, te devuelvo algo…tú sí que eres preciosa por fuera y por dentro. Como no, a David, Isa, Marta Inés, Kika y Javi, por compartir conmigo mucho más que trabajo, unos buenísimos momentos de risas y diversión, espero que vengan muchos más, porque trabajar con personas como vosotros es un placer. También a Pepe, nuestro personal trainer, que me sube la autoestima con esas cosillas que me dice. A mis chicas de hidráulica, con un cariño especial a Elena y Cris, porque ese pasillo del 'da Vinci' no sería igual sin vosotras.

También a muchos de mis compañeros, Ramón, ánimo, pronto serás tú doctor también, y gracias por preocuparte tanto por mí y hacer siempre que me ría. A Aurora, Javi y David, que fueron alumnos y ahora me alegro de poder contar con ellos como amigos. Al Prof. Antonio Moreno-Muñoz, que me inició en el maravilloso mundo de la investigación, y siempre me ha mostrado su cariño. Al Prof. Juan Vicente Giraldez por enseñarme el placer de la lectura, sus infinitas muestras de cariño y ser tan entrañable conmigo. A 'Los Manolos', Vaquero y Caballano, ambos, dos buenos compañeros y

todo un ejemplo de buenas personas. A la Prof. Pilar Martínez que tanto cariño y ánimo me ha dado siempre, es muy bonito poder trabajar con una persona como tú, ya sabes cuánto te admiro¡. Al Prof. Ignacio Benavides, por todos los cafés agradables que hemos compartido. A Rafa Pérez, porque a pesar de todas nuestras 'peleillas y riñas' siempre prevalece el aprecio mutuo que nos tenemos. Se merecen un agradecimiento especial, todos mis compañeros del área de proyectos y de mi departamento que siempre me han animado, incluso a los ya jubilados. Por supuesto no me puedo olvidar de mis alumnos y alumnas, especialmente a los/as de proyectos fin de carrera y trabajos fin de máster que me han sufrido¡.

A mi amiga Paula que me ha demostrado que a pesar de no vernos con la frecuencia que nos gustaría, está siempre tanto en los buenos como en los malos momentos.

A una persona muy especial y a la que adoro por muchas cosas, *mi Tany*, con el permiso de Carlos, muchas gracias por estar siempre ahí, y ayudarme tanto cuando más lo he necesitado, *gracias cielete*, como tú me dices, aunque el *cielete eres tú*. Me encanta poder contar con una amiga como tú. Ya te lo he dicho muchas veces, verdad, la suerte ha sido mía (eres una estrella con luz propia).

A mis suegros cuyo apoyo ha sido fundamental siempre y a todos mis cuñados y cuñadas, especialmente a MªCarmen y Manolo, decirles que al final *siempre sale el sol*…

A mis padres que me lo han dado todo en esta vida. A mi padre que me gustaría estuviese conmigo para poder compartir éste y muchos momentos más, *no pasa ni un día que no me acuerde de ti papa*, y a mi madre, siempre dispuesta a apoyarme en todo, *para que no me falte nunca*, tienes que ser fuerte y luchar por tus hijas, nietas y nieto, que tanto te queremos. A mis hermanas, cuñados, sobrinas y mi sobrino, por todo el tiempo que no les he dedicado siempre inmersa en el trabajo, pero a pesar de todo comprenderme y quererme tanto. Especialmente a Irene, mi sobrina mayor, porque yo también la admiro a ella por ser tan buena chica.

Al mayor regalo que la vida me ha dado, mi marido David. Gracias por permanecer conmigo, regalarme amor y felicidad todos y cada uno de los días durante estos diecisiete años juntos. Sin duda, esta tesis no sería posible sin ti, todo el mérito es tuyo, mi amor, porque sin ti nunca lo hubiese conseguido. No imagino una vida que no sea a tu lado, y sabes que…*lo mejor está aún por venir*…***te quiero mi amor***. *"Look at the stars, look how they shine for you and everything you do,.....my love,....., you know I love you so……..……(Yellow, Chris Martin)"*.

Contents

List of Figures

List of Tables

Symbols, acronyms and abbreviations

AFT	Adiabatic flame temperature
APCI	Atmospheric pressure chemical ionization
ANN	Artificial Neural Network
BD	Biodiesel
ASQ	Airborne Source Quantification
BM, β	Isentropic bulk modulus
BSFC	Brake specific fuel consumption
BTE	Brake thermal efficiency
CME	Coconut methyl ester
CN	Cetane number
CO	Carbon monoxide, Coconut oil
CO_2	Carbon dioxide
dB	Decibel
EA	Evolutionary Algortihm
EGR	Exhaust gas recirculation
EP	Evolutionary Programming
EU	European Union
FAEE	Fatty acid ethyl esters
FAME	Fatty acid methyl esters
FAO	Food and agriculture organization of the United Nations
GCV	Generalized Cross Validation
HC	Hydrocarbon
HCV	High calorific value
HEP	Hybrid Evolutionary Programming

HEPC	Hybrid Evolutionary Programming with clustering
KOH	Potassium hidroxide
KOME	Karanja oil methyl ester
LC	Length of chain
LCV	Low calorific value
LEA	Low erucic acid
LME	Linseed oil methyl ester
LO	Linseed oil
MLP	MultiLayer Perceptron
MSE	Mean Square Error
NAH	Nearfield AcoAcoustic Holography
NO	Monoxide of nitrogen
NO_2	Dioxide of nitrogen
NOME	Nagchampa oil methyl ester
NO_x	Nitrogen oxides
NVH	Noise, Vibration and Hardness
O_2	Oxygen
OPME	Olive-pomace oil methyl ester
OPO	Olive pomace oil
OCV	Cross Validation principle
PM	Particulate matter
PME	Palm oil methyl ester
PO	Palm oil
PUNN	Product Unit Neural Network
r^2	Coefficient of determination
RBFNN	Radial Basis Function Neural Network
RI	Refractive index
RME	Rapeseed methyl ester
RSM	Response surface modeling

SEP	Standard Error of Prediction
SFME	Sunflower oil methyl ester
SFO	Sunflower oil
SI	Sound Intensity
SPL	Sound Pressure Level
SQ	Sound Quality
SVD	Singular Value Decomposition
TAG	Triacilglycerides
THC	Total hydrocarbons
TotalG	Total glycerol
TP(A)	Transfer Path (Analysis)
UD	Unsaturation degree
μ	Kinematic viscosity
ρ	Density

Abstract

Transport is included among the most important noise sources due to continuous increasing number of vehicles. In order to comply with the European regulations related to both the presence of renewable origin based-fuels and pollution (air and noise) reduction, biodiesel emerges as an excellent alternative. Provided that biodiesel properties are closely correlated with the chemical composition of the raw material used to produce it, this PhD thesis aims to study the effect of the chemical composition on air and noise emissions to find out the "ideal" raw material to produce biodiesel. Moreover, to study the effect of biodiesel on noise emission different models of sound prediction were developed. Finally, the influence of biodiesel chemical composition on sound quality has been assessed. The thesis comprises five chapters. First chapter presents an introduction to the PhD thesis, where the study purpose and objectives are stated and justified. Second chapter focuses on the effect of biodiesel chemical properties on combustion and air and noise emissions. In chapter 3, to predict noise emissions and their relation with the percentage of biodiesel blended with diesel fuel, two ANN-based models considering saturated and monounsaturated fatty acid methyl esters are presented. In addition, several response surface models have been developed to show the relationship between biodiesel chemical properties and noise emission by means of simple models, as well as the trend of the exhaust emissions and noise radiated for different engine operating conditions. Chapter 4 is composed of three evaluations of substitution monopole models for engine noise sound synthesis: the first work is based on Airborne Source Quantification (ASQ) technique, improved by means of regularization strategies. In the second evaluation, a novel model based on Product Unit Neural Networks (PUNN) is proposed and compared to ASQ technique. In the third evaluation, to improve the results achieved with the PUNN-based model, an ensemble of evolutionary Product Unit (PU) and Radial Basis Function (RBF) Neural Networks is suggested. In the fifth chapter, the effect of biodiesel properties on the tractor cabin mock up comfort from the driver's point of view has been studied. Moreover, several response surface models have been developed to correlate different sound quality metrics with biodiesel chemical properties. Finally, a conclusions section, the proposal of future research lines and the compendium of references used in this PhD thesis are provided.

Resumen

Una de las principales fuentes de ruido la proporciona el transporte, debido al constante crecimiento del número de vehículos. Para cumplir con los objetivos establecidos por la UE relativos tanto al incremento del uso de energías renovables como a la reducción de emisiones contaminantes (gaseosa y acústica), el biodiésel surge como una excelente alternativa. Puesto que las propiedades del biodiésel están correlacionadas con la composición química de los aceites vegetales empleados, en esta tesis doctoral se ha estudiado el efecto de aquélla sobre las emisiones, con el objeto de encontrar la composición ideal para producir biodiésel. Además, se han desarrollado distintos modelos de predicción de ruido para comprobar el efecto del incremento del porcentaje de biodiésel en mezclas con gasóleo sobre el ruido emitido. La influencia de la composición química sobre la calidad del sonido también se ha analizado. De este modo, la tesis se compone de cinco capítulos. El primer capítulo presenta una introducción de la tesis doctoral, donde se muestran, justificadamente, los objetivos a alcanzar. El segundo capítulo estudia el efecto de la composición química del biodiésel sobre las emisiones contaminantes y el ruido emitido. En el capítulo tres, se desarrollan dos modelos de predicción de ruido basados en redes neuronales considerando biodiésel o ésteres metílicos de ácidos grasos de dos tipos, con alto grado de saturación y monoinsaturados. Además, se proponen varios modelos de predicción de ruido basados en propiedades y emisiones contaminantes del biodiésel. El capítulo cuatro se compone de la evaluación de modelos de fuentes de ruido en vehículos mediante distintas técnicas: primero por el método de cuantificación de fuentes aéreas (*Airborne Source Quantification* (ASQ)) con estrategias de regularización. La segunda técnica propuesta se basa en el empleo de redes neuronales para altas frecuencias y ASQ para bajas y medias frecuencias, siguiendo el comportamiento del sistema. Finalmente, en la tercera evaluación, se propone una mejora del método previo mediante la fusión de dos métodos de redes neuronales artificiales basados en Unidades Producto Evolutivas y Funciones de Base Radial. En el capítulo cinco, se estudia el efecto de las propiedades del biodiésel en el confort de la cabina de un tractor, desde el punto de vista del conductor. Este estudio se acompaña del desarrollo de modelos de predicción de parámetros de calidad del sonido, sonoridad (*loudness*) y aspereza (*roughness*), basados en propiedades del biodiésel. Finalmente, se ha incluido una sección de conclusiones generales, futuras líneas de investigación y un compendio de las referencias empleadas en esta tesis doctoral.

Chapter 1

Introduction

1.1 Introduction

According to the European Energy Agency, transport related emissions were responsible for aprox. 24% of all EU greenhouse gas (GHG) emissions in 2009 [1]. Moreover, the annual energy consumption in this sector grows up continuously, being the most energy-consuming one. Another important factor is the fuel price, which experienced an increase of around 15% from 1980 to 2011. For these reasons, cleaner alternatives to fossil fuels are required. In this context, the EU Eureopean Directive 2009/28/EC adopted a Climate Change Package (CCP), which includes a 10% minimum target for renewable energy consumed in transport to be achieved. In this sense, biofuels constitute an excellent alternative, including the sustainability criteria.

Biodiesel consists in monoalkyl esters of long chain fatty acids derived from renewable feedstocks, such as vegetable oils, animal fats or microorganisms [2, 3]. It is commonly composed of fatty acid methyl esters (FAME) that can be prepared from triglycerides by transesterification with methanol. Less common alcohols are ethanol (which leads to FAEE), propanol (providing FAPE), etc. FAME is environmentally less contaminant, non-toxic and biodegradable compared to diesel fuel [4]. Biodiesel is quite similar to petroleum-derived diesel fuel in its main properties, *i.e.* cetane number, energy content, viscosity and phase changes

[5]. Biodiesel contains no petroleum products, but it is compatible with conventional diesel fuel and can be blended in any proportion with fossil-based diesel fuel to create a stable biodiesel blend. Therefore, biodiesel has become one of the most common biofuels in the world [6].

In addition, transport, and particularly road traffic, is responsible of the main environmental noise problems [7]. Although the economic crisis has led to a shortage in energy consumption and pollutant emissions from transport since 2009, almost 20% of the EU population is exposed to unacceptable noise levels (above 65 dB(A)). Moreover, it is estimated that about 30% European citizens are exposed to road traffic noise at levels exceeding 55 dB(A) during the night (Figure 1.1).

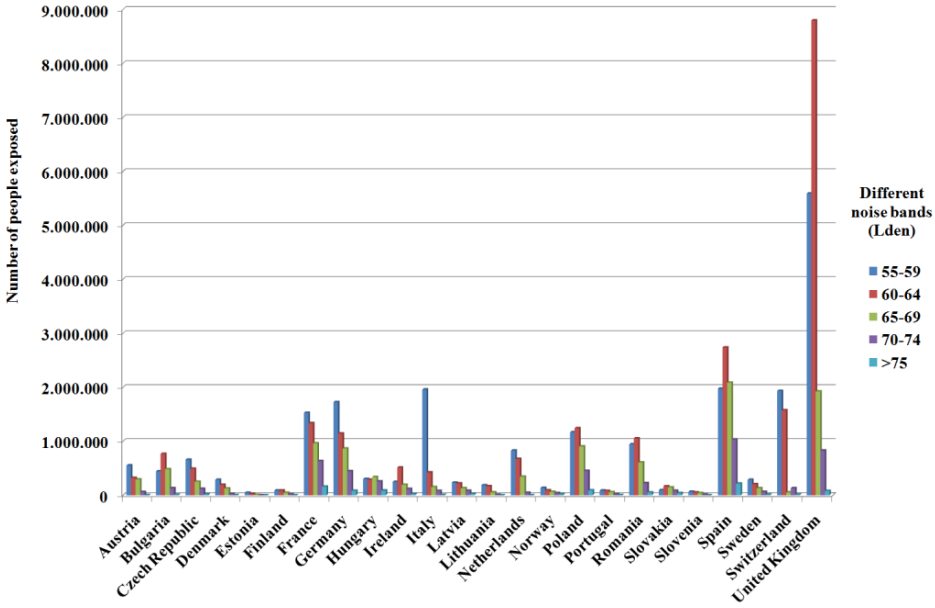

Figure 1.1. Agglomerations of people exposed to traffic road noise (L_{den}(dB(A)) (Source: The European Topic Centre on Spatial Information and Analysis, 2009)

Overnight noise levels over 55 dB(A) can produce sleep disturbance, annoyance, hearing impairment and cardiovascular disorders.

In addition, European Environmental Agency establishes that the impact of noise gets worse when it interacts with other environment stressors, such as air pollution. Therefore, new regulations on pollution emissions (including air and noise) are needed, to ensure that impacts will not increase dramatically in future strong economic growth periods. In this sense, the EU Directive 2002/49/EC that aimed to create a quieter and more pleasant environment for European citizens [8] is being discussed to focus on noise perception rather than on noise level. This represents an important challenge, which results in a need for new prediction models and noise abatement techniques. In this new context, different strategies may play an important role, *i.e.* auralization models or the use of alternative fuel, as discussed below [9].

1.2 The effect of biodiesel fatty acid composition on noise and exhaust emissions

The influence of the chemical structure of the raw material fatty acids on the quality of biodiesel has been proved in several studies [10-13], demonstrating the crucial importance of the raw materials used on biodiesel production [6]. Biodiesel properties are influenced by its fatty acids composition, which causes differences in the injection, combustion, performance and emissions of the engine. The knowledge of the fatty acid profile makes possible to study its influence on air and noise emissions.

According to several authors, biodiesel seems to provide a substantial reduction in unburned hydrocarbons (HC), carbon monoxide (CO) and smoke emissions, although it increases NO_x emissions compared to petroleum based-diesel fuel [14-18].

The origin of the diesel engine noise is the self-ignition of the air-fuel mixture, and both the level and sound quality depend on it. When combustion takes place, it produces an important sudden pressure increase giving rise to the well-known knock [19]. This abrupt pressure rise causes strong oscillations of the gas inside the combustion chamber, inducing the

vibration of the engine block. The combustion process is mainly responsible for block vibration through two excitation sources: the pressure and the mechanical forces (Figure 1.2). Pressure forces act directly on the combustion chamber walls as a result of the heat released during fuel combustion and in part, due to the piston motion. Mechanical forces due to the pressure forces on the mechanical systems in the cylinder are originated by piston slap, bearing clearances, element deformation, friction, etc. [20, 21]. Additionally, pressure forces are strongly dependent on the combustion process, which is mainly dominated by the fuel-burning rate.

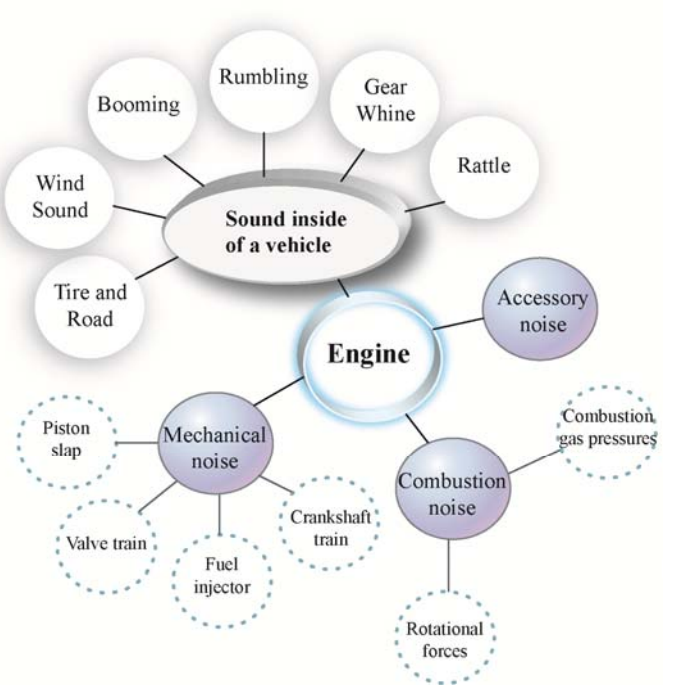

Figure 1.2. Components of a sound inside a vehicle

Switching to biodiesel, it may be interesting to find out whether the presence of biodiesel blended with diesel fuel (considering the new European regulations Directive 2009/28/EC [22]) may deteriorate the engine sound quality. This is of especial interest provided that, automotive customers demand sound quality. Therefore, it is important to increase the

knowledge on how biodiesel properties may influence radiated noise, sound quality and exhaust emissions. Eventually, this information will provide a guidance of the optimal biofuel composition to both improve the sound quality and reduce air emissions.

In section 1.2.2 a literature review of important chemical and physical properties of biodiesel is carried out. According to this review, the main fuel properties and their influence on engine performance and air and noise emissions are shown (Figure 1.3).

1.2.1 Chemical properties

One important chemical property is the oxygen content, which helps to achieve a more complete combustion and to prevent the formation of local rich zones in the combustion chamber and the formation of particle precursors. It is reported that oxygenated fuels are beneficial for lowering diesel engine emissions, especially particulate matter (PM) and in lowering the presence of CO, NO_x, total hydrocarbons (THC) and soot [23-25]. Moreover, it has been found that the peak of cylinder pressure increases in line with the increased proportion of oxygen in the fuel [26]. This indicates that the higher the content of oxygen in the fuel the higher the combustion noise due to the increase of the in-cylinder pressure peak.

By means of the adiabatic flame temperature (*AFT*) it is possible to know the maximum local temperature in the combustion chamber. Although there are some concerns about the accuracy of this theoretical parameter (as the combustion process is not strictly adiabatic), this property provides an interesting approach [23]. Adiabatic flame temperature increases slightly with the lengthening of the methyl ester chain and rises considerably when the number of double bonds is increased [6]. Lean premixed combustion decreases the adiabatic flame temperature and consequently reduces the production rate of NO_x emission which is highly temperature dependent. However the appearance of thermo-acoustic instabilities is becoming a key issue for diesel engines. Thermo-acoustic oscillations occur due to the coupling between the flame heat release behavior and oscillations that arise in the combustor flow field [27, 28]. In this condition the resulting coupled system dynamics emerges as high-amplitude oscillations of both neat

release and flow field variables. The result flow and structural vibrations have adverse effects on the performance [29].

In order to measure the fluid resistance to uniform compression, the bulk modulus property of the fuel is used. It is defined as the increase in pressure needed to cause a given relative decrease in volume. This is the inverse of compressibility. Diesel engines operate by compressing fuel using a high pressure and injecting it into the cylinder where the fuel spontaneously ignites. Injection begins when the pressure at the injector exceeds a critical pressure, known as the nozzle opening pressure [6]. The influence of a biodiesel with higher bulk modulus could increase the NO_x emissions mainly due to an advance of the start of injection time. This happens when biodiesel is injected, as the pressure rise produced by the pump is achieved quicker due to the lower compressibility (higher bulk modulus) and is also associated to higher speed of sound values, leading to a faster propagation of pressure waves from the pump to the injector needle, and thus resulting in an earlier needle lift [30-33]. All of these factors result in an increased injection line pressure and, therefore, NO_x and noise emissions. However, this assumption is not valid when referring to common-rail systems, because the opening and closing mechanisms are different [34-36].

The cetane number (*CN*) is an indicator of the combustion quality during ignition. It provides information about the ignition delay (*ID*) of a diesel fuel upon injection into the combustion chamber. Higher cetane numbers indicate less time between the initiation of fuel injection and ignition, which is a desirable property in a diesel fuel [37]. With regard to *CN* effect on exhaust and noise emissions, high *CN* reduces the maximum pressure rise as a consequence of a reduced ignition delay period. Thus, it leads to a reduction of NO_x, THC, CO and noise radiated, while PM increases [38].

Both gross calorific value (also known as higher heating value) and net calorific value (also known as lower heating value) indicate the suitability of fatty compounds as diesel fuel. Due to higher oxygen content, FAME exhibit lower heating values than fossil diesel fuel. Therefore, to achieve adequate engine torque and power, an increase of injection volumes is needed [39]. However, this leads to higher specific fuel consumption. Calorific value is not included in most fuel standards, but it is a limiting

parameter within the European standard for FAME used as heating fuel (EN 14213). Freedman and Bagby [40] developed a model to predict heating values from raw materials exhibiting different fatty acid composition [6]. Some authors have been found that the higher the injection pressure the lower the injection duration, causing more fuel to enter the cylinder in a shorter amount of time. This creates a greater rate of heat release, resulting in increased peak pressures and temperatures. Usually, it results in higher engine torque (lower *BSFC*), NO_x and noise emissions [41-43].

Fuel kinematic viscosity has an impact on both injection and combustion efficiency. High viscosity leads to poorer atomization of the fuel spray and less accurate operation of the fuel injectors [37], especially at low engine operating temperatures [6]. Moreover, higher viscosity reduces pump leakage resulting in increased injection line pressure, higher temperature peaks and greater rates of NO_x and noise radiated [35].

The second chapter of this thesis focuses on the effect of the chemical properties of biodiesel on combustion, air and noise emissions, in order to provide with recommendations about the ideal chemical structure of future biodiesel raw materials with the aim of reducing exhaust emissions and improving sound quality of biodiesel.

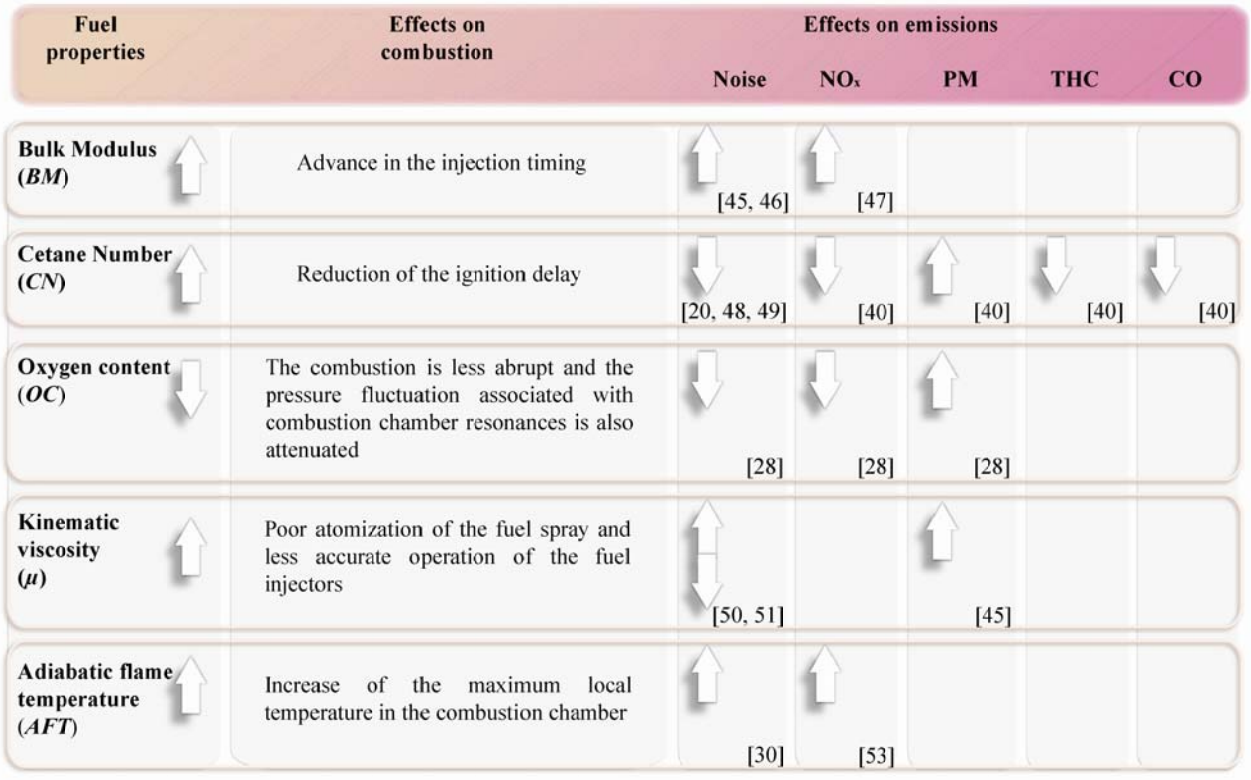

Figure 1.3. Chemical properties of biodiesel and their relationship with the exhaust and noise emissions

1.3 Models of noise prediction in biodiesel

Drastic upcoming limitations on exhaust emissions (the European EURO VI will come in force in 2014; EURO V in force since 2009) and sound quality are expected [44]. Besides, as mentioned above, alternative fuels will have to be introduced into the market to achieve the 10% minimum target for renewable energy consumption (Directive 2009/28EC [22]). In any case, engine manufacturers will have to optimize combustion parameters to comply with the regulations and for this purpose the development of prediction models in the design phase may help to face an unprecedented and challenging situation.

Traditionally, the effect of the in-cylinder pressure spectrum on combustion noise has been studied. Some authors proposed the 'attenuation curve' approach, from which a relationship between the in-cylinder sound pressure level and radiated noise level is established [45]. In this method, it is assumed that the engine block behaves as a linear system, and that it is the basis of several combustion noise meters frequently used by developing engineers to estimate radiated noise level from the in-cylinder pressure trace. Although, comparing different engines may be quantitatively useful, quantitative analysis is not recommended as a linear response of the block independently of the engine operating conditions is assumed.

Some works have shown that there are different patterns of acoustic energy propagation through the engine block, being highly nonlinear and time dependent [46-48]. Moreover, in-cylinder excitation propagates through multiple complex paths, either directly through the action of the forces exerted by the gases on the cylinder walls or though the mechanical elements of the engine. Mechanical forces applied to the moving parts in the cylinder depend on the engine operating conditions and also on the relative position of the piston inside the cylinder. Therefore, the deformation suffered by these elements (including the block) is load dependent and non-stationary.

Nivesrangsan *et al.* [49] suggested a method of mapping acoustic emission signals and wave propagation in engines and focused on source location techniques for complex structures typical of machinery applications. However, the used wave speed needed to be known for the particular source to allow accurate source location. They concluded that the accuracy of this technique depends on the accuracy of the determination of the attenuation coefficients.

Bao and He [50] studied the noise of rapeseed oil blends. They also proposed a nonlinear model, although they considered just two operating conditions and four working parameters, such as intake-valve-closing angle, exhaust-valve-opening angle, fuel delivery angle and injection pressure in a single cylinder diesel engine. This study provided useful reference material for the selection of the most preferable combination of working parameters.

Recently, Payri *et al.* [51] developed a new methodology for the analysis of in-cylinder pressure in direct injection diesel engines showing a fair qualitative correlation between in-cylinder pressure and combustion noise. It has been shown that the combustion signal is mostly controlled by speed, while the resonance signal is mostly controlled by load, because of its strong dependence on temperature. However, to confirm the tendencies found, it would be interesting to extend this analysis to other engine parameters such as injection strategy, bowl geometry, exhaust gas recirculation (EGR), coolant temperature, etc. Moreover, it has been shown that both vibration and angular speed signals contain information about the cylinder pressure but mainly in different frequency regions [52, 53]. Angular speed fluctuation comes from the low frequency content of cylinder pressure, as angular velocity is not as sensitive as structural

vibrations to instantaneous pressure changes. Engine structure vibration measurements, on the other hand, suffer from low signal-to-noise ratio at low frequencies, making the reconstruction of the compression/decompression phase of the combustion process uncertain. In both cases the relationship between cylinder pressure, vibration response and crankshaft speed is non-linear and changes with the running condition [52].

According to the last comments, the main problem of the mentioned classical methodologies is that they do not seem to be feasible in practice for the analysis of noise radiated by an engine. This situation induces to attempt the noise of an engine by means of other nonlinear techniques, such as Artificial Neural Networks (ANN) taking into account other kinds of parameters, like chemical properties of biodiesel, diesel fuel noise, speed and power, among others.

ANN are computer systems developed to have certain abilities such as generating and forming knowledge as well as learning and discovering new knowledge without any help, imitating the human brain. Furthermore, their advantages include their ability to model non-linear processes, adaptive learning, self organization, real-time operation and ease of insertion into existing technologies. This gives ANN a competitive edge over traditional experimental-based models [54].

According to literature, several studies have revealed the importance of the use of ANN in exhaust and noise emissions prediction as an alternative to regression techniques, due to their flexibility and high degree of accuracy to fit experimental data [55]. Sayin *et al*. [56] used ANN to predict spark ignition engine performance, exhaust emissions and temperatures. The study demonstrated accurate predictions with maximum root mean square error (RMSE) of 6.66%. Oguz *et al*. [57] successfully predicted engine performances with a reliability value of 99.94%. Kiani *et al*. [58] incorporate an ANN modeling of a spark ignition engine to predict brake power, output torque and exhaust emissions. Results showed high accuracies achieved with correlation factors in the range from 0.71 to 0.98. Kara Togun and Baysec [59] studied the use of ANN and successfully predicted the torque and specific fuel consumption of a spark ignition engine, with maximum RMSE of 2%. Yusaf *et al.* [60] conducted experiments in a diesel engine fueled with a combination of both

compressed natural gas and diesel fuel. ANN modeling was used to predict brake power, torque, brake specific fuel consumption and engine emissions. Good correlation values were achieved ranging between 0.92 and 0.99. Canakci *et al.* [61] used ANN for engine performance and emissions prediction of a diesel engine fueled with biodiesel produced from waste frying palm oil. They concluded that the use of ANN in engine predictive modeling achieved regression values closed to unity. Hashemi and Clark [62] applied ANN as emission predictive tools for heavy-duty diesel vehicles. The ANN were trained using driving cycle data, which provide a diverse data range, and varying the number of inputs to the model. Results showed accurate predictions. Arcaklioglu and Celikten [63] used ANN to predict emissions and engine performance of a diesel engine. The input parameters used for this study were injection pressure and engine speed at throttle position. RMSE achieved were below 10%. Yucesu *et al*. [64] used ANN to model the engine torque and specific fuel consumption based on the injection timing, air/fuel ratio, compression ration and fuel type. The correlation values achieved were all above 0.99 which demonstrated accurate predictability of ANN.

In summary, it can be seen that most of the studies conducted using ANN provided accurate predictions. Although, if ANN are compared to response surface models, the number of parameters needed for ANN could not be competitive due to the increase in the number of parameters in a non-linear system, when the number of conditions and/or the degree of the response surface model increases.

In chapter 3 of this PhD thesis, two models based on ANN considering saturated and monounsaturated fatty acid methyl esters to predict noise emission with the increase of the percentage of biodiesel in biodiesel/diesel fuel blends are proposed. Moreover, several response surface models have been developed to show the relationship between chemical properties, noise and exhaust emissions under several engine operating conditions.

1.4 Models of sound source prediction

Nowadays, the great majority of noise sources in vehicles have similar noise levels and thus, the so-called Noise, Vibration and Harshness (NVH) problems in a vehicle focus on improving acoustical comfort. On one hand, it involves a thorough understanding of the different noise and vibration sources and on the other hand, transfer paths of structural and acoustical energy. In order to reduce development time of the new vehicles, automotive engineering needs prediction models, which help to test different configurations earlier in the design phase. Therefore, human sound perception must be taken into account to improve the sound quality of the vehicles.

In this sense, it is possible to know the real listening experience by means of rendering audible the sound field of a physical sound source in a space. This process is known as auralization and emerges like an ever more important aspect of product development often being very useful in the treatment of NVH-related problem. Auralization has become a success allowing to vehicle manufactures to comply with all the obliged noise standards and sound quality, including changes in the ISO 362 procedure for vehicle pass-by noise testing.

The auralization process can be summarized in the modeling of the

physical sound source, the determination of transfer paths and the calculation of the sound spectrum at the receiver position. For sound synthesis purposes, there are different sound source reconstruction techniques that are composed of just a limited number of elementary substitute sources [65]. Cremer and Wang [66] proposed a new concept based on spherical wave field for calculating the sound radiated from a vibration body. Later, this idea was generalized by Heckl [67]. Koopmann *et al.* [68] established that the synthesized sound field obtained by superposition of substitute sources is equivalent to Helmholtz-Kirchhoff equation-based boundary element methods (BEM) [69]. The main advantages are the simplicity of generating the matrix elements used in the numerical formulation and the improved accuracy due to the avoidance of unique and singularity problems that are inherent in the BEM formulation. Ochmann [70] developed a method using multipole substitute sources and analyzed the ill-conditioning effects of the method to substitute sources in detail. Other authors have used the aforementioned ideas to develop a more refined method [71]. These last models are relatively simple and easy to handle, however the quantification of the substitute sources depends on the source and acoustic environment. In order to solve these problems, Bobrovnitskii and Pavic [65] suggest acoustic source models based on the blocked pressure and the internal source impedance although the measurements are complicated making it unfeasible for common use. All these methods are applicable in theory for the prediction of sound field radiated by a physical source. However, their practical application results are very complicated due to both the restrictions of the source geometry and the high computational effort. By means of acoustic equivalent source models, the physical sound source with only a limited amount of elementary source descriptors distributed on the surface of the physical source can also be represented [72]. The main drawback of this method is the ill-conditioning effect, which makes it necessary to use regularization techniques.

Chapter 4 of this PhD thesis is composed of three evaluations of substitution monopole models for engine noise sound synthesis: the first work is based on Airborne Source Quantification (ASQ) technique improved by means of regularization strategies. In the second evaluation, a novel model based on Product Unit Neural Networks (PUNN) is proposed and compared to ASQ technique. Finally, in the third evaluation, a hybrid

Artificial Neural Network model based on Product Unit (PU) and Radial Basis Function (RBF) Neural Networks is suggested.

1.5 Sound quality inside a tractor driver cabin based on biodiesel fatty acid composition

The trend in farm practices and machinery development suggest that noise is still an unfixed problem in agriculture, even though there has been a steady increase in the availability of equipments for noise control over recent year. Some examples of noise levels in agriculture given by the European agency for safety and health at work (EASHW) are shown in Table 1.1. Tractors are among the most used machineries in agriculture; their sales have increased in the last years as can be observed from Figure 1.4, showing this machine is the main source of noise present in the agricultural environment. In addition, studies carried out among 128 private farmers confirmed a considerable hearing impairment in this occupational group, which increased with age and duration of the period of employment [73, 74]. Results clearly show that the excessive noise produced by tractors and agricultural machinery used by farmers are the primary cause of development of such a significant hearing loss [75]. It is important to mention that workers without personal protective equipments may be exposed to up to 85 dB(A), while the maximum permitted value using

personal protective equipments is 87 dB(A), according to the European directive 96/58/EC.

Table 1.1. Noise sources in agricultural machinery (Source: European agency for safety and health at work, 2009)

Agricultural machinery	**Noise dB(A)**
Cascade grain drier	93.4
Cross flow grain drier	93.8
Green crop drier	89.8
Roller/crusher mill for feed preparation	92.3
Hop cleaner/picker	93.9
Vegetable preparation area/packing shed	91.6
Beet harvester	91.7
Tracklayer	97.5
Blower/duster (man carried)	89.4
Chain saw	103.9
Turkey plucker	99.8
Turkey house	94.4
Orchard sprayer	85-100
Use of Tractors	
Tractor with disc mower	91.1
Tractor with high density baler	96.8
Tractor with hedge cutter	89.6
Tractor with orchard sprayer	97.9
Tractor with straw chopper	90.4
Tractor with cab	73-90
Tractor without a cab	91-99
Tractor at full throttle	105
Tractor at full Load	120
All terrain vehicle	100

In Spain, the agricultural area is established in 27 900 000 ha, resulting around 27 ha per tractor in 2009. It places Spain as the most mechanized European country per area (FAOSTAT, 2011 [76]). Although tractor helps workers in agricultural and forestry tasks, it contributes to increase exhaust and noise emissions, besides fuel consumption.

One option to both pollution and fossil energy consumption reduction, besides increasing the sustainability, is provided by the use of biofuel based on raw materials cultivated by farmers. However; the production of biodiesel from edible oils is controversial, as some non-governmental organizations and social movements pinpoint the making of biofuels from edible raw materials as the main cause of increased global food market prices [6]. Despite this controversial topic related to the use of biodiesel from edible oils, it is environmentally less contaminant, non–toxic and biodegradable compared to diesel fuel [4].

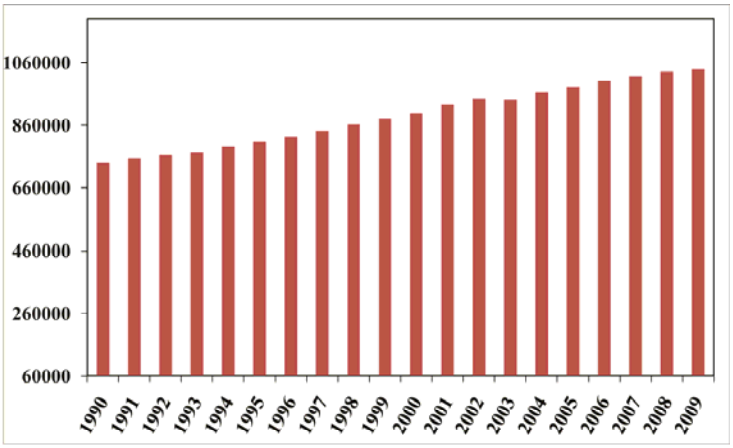

Figure 1.4. Evolution of tractor sales in Spain (Source: FAOSTAT, 2009)

In the fifth chapter the effect of biodiesel properties on the comfort of a tractor driver cabin mock up has been studied. Moreover, several response surface models have been developed to correlate different sound quality metrics with biodiesel chemical properties.

1.6 Objectives

The main purpose of this thesis is to characterize noise emissions of a combustion compression ignition engine fuelled with different biodiesel blends at several engine operating conditions. Moreover, their influence over sound quality considering a tractor cabin model will be studied. Inside the cabin, a noise prediction model will be developed. In addition, other secondary objectives are the following:

- Measurement and characterization of the emitted noise by the compression ignition engine fuelled with different biodiesel blends at several engine operating conditions:
  - ✓ Characterization of radiated noise.
  - ✓ Study of the sound quality for different biodiesel blends.
  - ✓ Establishment of a prediction model based on the psychochemical properties of the biodiesel blends.
- Study of the acoustic environment in the tractor cabin by modelling and simulating techniques:

- ✓ Design and construction of a scaled tractor cabin.
- ✓ Replay in the cabin the recorded files from the radiated engine noise fuelled with different biodiesel blends at several operating conditions and data analysis.
- ✓ Establishment of a noise prediction model inside the tractor cabin using the mock up.

- Establishment, design and evaluation of the different noise prediction models for these experiences. Comparative analysis:
  - ✓ Airbone Source Quantification (ASQ) prediction model.
  - ✓ Model based on Artificial Neural Networks (ANN).

1.7 References

[1] E.E. Agency, http://www.eea.europa.eu/themes/noise, in, 2012.

[2] L.C. Meher, D. Vidya Sagar, S.N. Naik, Technical aspects of biodiesel production by transesterification--a review, Renewable and Sustainable Energy Reviews, 10 (2006) 248-268.

[3] M. Dorado, Raw materials to produce low cost biodiesel. Chapter 4., in: A. Nag (Ed.) Biofuels refining and performance, McGraw Hill Professional, 2008, pp. 107-148.

[4] M. Azam, A. Waris, N.M. Nahar, Prospects and potential of fatty acid methyl esters of some non-traditional seed oils for use as biodiesel in India, Biomass and Bioenergy, 29 (2005) 293-302.

[5] L. Lin, Z. Cunshan, S. Vittayapadung, S. Xiangqian, D. Mingdong, Opportunities and challenges for biodiesel fuel, Applied Energy, 88 (2011) 1020-1031.

[6] S. Pinzi, Phd Thesis. Biocombustibles para motores diésel a partir de diversas grasas vegetales, in: Departamento de química fisica y termodinamica aplicada, Universidad de Córdoba, Córdoba, 2011, pp. 318.

[7] A.L. GMBH, Community noise research strategy plan (CALM), in: G4RT-CT-2001-05043 (Ed.) Fifth Framework Programme 2001.

[8] Official Journal of the European Communities, Directive 2002/49/EC of the European Parliament and the Council (June 2002).

[9] D. Berckmans, P. Kindt, P. Sas, W. Desmet, Evaluation of substitution monopole models for tire noise sound synthesis, Mechanical Systems and Signal Processing, 24 (2010) 240-255.

[10] G. Knothe, "Designer" Biodiesel: Optimizing Fatty Ester Composition to Improve Fuel Properties, Energy & Fuels, 22 (2008) 1358-1364.

[11] G. Knothe, Dependence of biodiesel fuel properties on the structure of fatty acid alkyl esters, Fuel Processing Technology, 86 (2005) 1059-1070.

[12] M. Canakci, Sanli, H., Biodiesel production from various feedstocks and their effects on the fuel properties, Journal of Industrial Microbiological and Biotechnology, 35 (2008) 431-441.

[13] K.J. Harrington, Chemical and physical properties of vegetable oil esters and their effect on diesel fuel performance, Biomass, 9 (1986) 1-17.

[14] M.J. Haas, K.M. Scott, T.L. Alleman, R.L. McCormick, Engine performance of biodiesel fuel prepared from soybean soapstock: A high quality renewable fuel produced from a waste feedstock, Energy and Fuels, 15 (2001) 1207-1212.

[15] C.A. Sharp, S. Howell, J. Jobe, The efect of biodiesel fuels on transient emissions from modern diesel engines-part I:regulated emissions and performance, SAE paper 2000-01-1967, (2000).

[16] A. Senatore, C. M., V. Rocco, M.V. Prati, A comparative analysis of combustion process in DI diesel engine fueled with biodiesel and diesel fuel, SAE paper 2000-01-0691, (2000).

[17] M.P. Dorado, E. Ballesteros, J.M. Arnal, J. Gomez, F.J.L. Gimenez, Testing waste olive oil methyl ester as a fuel in a diesel engine, Energy & Fuels, 17 (2003) 1560-1565.

[18] M.P. Dorado, E. Ballesteros, J.M. Arnal, J. Gomez, F.J. Lopez, Exhaust emissions from a Diesel engine fueled with transesterified waste olive oil, Fuel, 82 (2003) 1311-1315.

[19] R. Hickling, D.A. Feldmaier, S.H. Sung, Knock-induced cavity resonances in open chamber diesel engines, Journal of the Acoustical Society of America, 65 (1979) 1474-1479.

[20] D. Anderton, Relation between combustion system and noise, SAE paper 1979-790270, (1979).

[21] Y.M. Cho, Noise source and transmission path identification via state-space system identification, Control Engineering Practice, 5 (1997) 1243-1251.

[22] Directive 2009/28/EC of the European Parliament and of the Council of 23 April 2009 on the promotion of the use of energy from renewable sources and amending and subsequently repealing Directives 2001/77/EC and 2003/30/EC, in, 2009.

[23] J.M. Herreros Arellano, Framework to optimise the use of alternative fuels. Case study: emission benefits in compression ignition engines, in: School of Apoplied Sciences, Cranfield University, 2010.

[24] H. Chen, J. Wang, S. Shuai, W. Chen, Study of oxygenated biomass fuel blends on a diesel engine, Fuel, 87 (2008) 3462-3468.

[25] X. Wang, C.S. Cheung, Y. Di, Z. Huang, Diesel engine gaseous and particle emissions fueled with diesel-oxygenate blends, Fuel.

[26] P. Rounce, A. Tsolakis, P. Leung, A.P.E. York, A comparison of diesel and biodiesel emissions using dimethyl carbonate as an oxygenated additive, Energy and Fuels, 24 (2010) 4812-4819.

[27] A. Chaparro, E. Landry, B.M. Cetegen, Transfer function characteristics of bluff-body stabilized, conical V-shaped premixed turbulent propane-air flames, Combustion and Flame, 145 (2006) 290-299.

[28] R. Riazi, M. Farshchi, M. Shimura, M. Tanahashi, T. Miyauchi, An Experimental Study on Combustion Dynamics and NOx Emission of a Swirl Stabilized Combustor with Secondary Fuel Injection, Journal of Thermal Science and Technology, 5 (2010) 266-281.

[29] S. Ducruix, T. Schuller, D. Durox, S. Candel, Combustion Dynamics and Instabilities: Elementary Coupling and Driving Mechanisms, Journal of Propulsion and Power, 19 (2003) 722-734.

[30] F. Cruz-Peragon, F.J. Jimenez-Espadafor, A genetic algorithm for determining cylinder pressure in internal combustion engines, Energy & Fuels, 21 (2007) 2600-2607.

[31] F. Cruz-Peragon, F.J. Jimenez-Espadafor, Design and optimization of

neural networks to estimate the chamber pressure in internal combustion engines by an indirect method, Energy & Fuels, 21 (2007) 2627-2636.

[32] F. Cruz-Peragon, F.J. Jimenez-Espadafor, J.A. Palomar, M.P. Dorado, Influence of a Combustion Parametric Model on the Cyclic Angular Speed of Internal Combustion Engines. Part I: Setup for Sensitivity Analysis, Energy & Fuels, 23 (2009) 2921-2929.

[33] E. Torres-Jimenez, M.P. Dorado, B. Kegl, Experimental investigation on injection characteristics of bioethanol-diesel fuel and bioethanol-biodiesel blends, Fuel, 90 (2011) 1968-1979.

[34] F. Boudy, P. Seers, Impact of physical properties of biodiesel on the injection process in a common-rail direct injection system, Energy Conversion and Management, 50 (2009) 2905-2912.

[35] R. Payri, F.J. Salvador, J. Gimeno, G. Bracho, The effect of temperature and pressure on thermodynamic properties of diesel and biodiesel fuels, Fuel, 90 (2011) 1172-1180.

[36] M.E. Tat, J.H. Van Gerpen, S. Soylu, M. Canakci, A. Monyem, S. Wormley, Speed of sound and isentropic bulk modulus of biodiesel at 21 °C from atmospheric pressure to 35 MPa, JAOCS, Journal of the American Oil Chemists' Society, 77 (2000) 285-289.

[37] M.S. Graboski, R.L. McCormick, Combustion of fat and vegetable oil derived fuels in diesel engines, Progress in Energy and Combustion Science, 24 (1998) 125-164.

[38] N. Ladommatos, M. Parsi, A. Knowles, The effect of fuel cetane improver on diesel pollutant emissions, Fuel, 75 (1996) 8-14.

[39] M. Mittelbach, C. Remschmidt, Biodiesel: The Comprehensive Handbook, Martin Mittelbach, Graz, Austria, 2004.

[40] B. Freedman, M. Bagby, Heats of combustion of fatty esters and triglycerides, Journal of the American Oil Chemists Society, 66 (1989) 1601-1605.

[41] M. Bunce, D. Snyder, G. Adi, C. Hall, J. Koehler, B. Davila, S. Kumar, P. Garimella, D. Stanton, G. Shaver, Optimization of soy-biodiesel combustion in a modern diesel engine, Fuel, 90 (2011) 2560-2570.

[42] T. Yoshizaki, K. Nishida, H. Hiroyasu, Approach to low NO_x and

smoke emission engines by using phenomenological simulation, SAE paper 930612 1993, (1993).

[43] G.J. Hampson, M.A. Patterson, S.C. Kong, R.D. Reitz, Modeling the effects of fuel injection characteristics on diesel engine soot and NO_x emissions, SAE paper 940523 1994, (1994).

[44] L. Pruvost, Q. Leclere, E. Parizet, Diesel engine combustion and mechanical noise separation using an improved spectrofilter, Mechanical Systems and Signal Processing, 23 (2009) 2072-2087.

[45] A.E.W. Austen, T. Priede, Origins of diesel engine noise, SAE paper, 590127 (1959).

[46] L. Stanković, J.F. Böhme, Time-frequency analysis of multiple resonances in combustion engine signals, Signal Processing, 79 (1999) 15-28.

[47] J.M. Desantes, J. Benajes, S. Molina, C.A. González, The modification of the fuel injection rate in heavy-duty diesel engines. Part 1: Effects on engine performance and emissions, Applied Thermal Engineering, 24 (2004) 2701-2714.

[48] J.M. Desantes, J. Benajes, S. Molina, C.A. González, The modification of the fuel injection rate in heavy-duty diesel engines: Part 2: Effects on combustion, Applied Thermal Engineering, 24 (2004) 2715-2726.

[49] P. Nivesrangsan, J.A. Steel, R.L. Reuben, AE mapping of engines for spatially located time series, Mechanical Systems and Signal Processing, 19 (2005) 1034-1054.

[50] Y.D. Bao, Y. He, Study on noise of rapeseed oil blends in a single-cylinder diesel engine, Renewable Energy, 31 (2006) 1789-1798.

[51] F. Payri, A. Broatch, B. Tormos, V. Marant, New methodology for in-cylinder pressure analysis in direct injection diesel engines - application to combustion noise, Measurement Science & Technology, 16 (2005) 540-547.

[52] R. Johnsson, Cylinder pressure reconstruction based on complex radial basis function networks from vibration and speed signals, Mechanical Systems and Signal Processing, 20 (2006) 1923-1940.

[53] H. Du, L. Zhang, X. Shi, Reconstructing cylinder pressure from vibration signals based on radial basis function networks, Proceedings of the

Institution of Mechanical Engineers, Part D: Journal of Automobile Engineering, 215 (2001) 761-767.

[54] W.K. Yap, V. Karri, ANN virtual sensors for emissions prediction and control, Applied Energy, 88 (2011) 4505-4516.

[55] A.J. Yuste, M.P. Dorado, A neural network approach to simulate biodiesel production from waste olive oil, Energy & Fuels, 20 (2006) 399-402.

[56] C. Sayin, H.M. Ertunc, M. Hosoz, I. Kilicaslan, M. Canakci, Performance and exhaust emissions of a gasoline engine using artificial neural network, Applied Thermal Engineering, 27 (2007) 46-54.

[57] H. Oğuz, I. Saritas, H.E. Baydan, Prediction of diesel engine performance using biofuels with artificial neural network, Expert Systems with Applications, 37 (2010) 6579-6586.

[58] M.K. Deh Kiani, B. Ghobadian, T. Tavakoli, A.M. Nikbakht, G. Najafi, Application of artificial neural networks for the prediction of performance and exhaust emissions in SI engine using ethanol- gasoline blends, Energy, 35 (2009) 65-69.

[59] N. Kara Togun, S. Baysec, Prediction of torque and specific fuel consumption of a gasoline engine by using artificial neural networks, Applied Energy, 87 (2010) 349-355.

[60] T.F. Yusaf, D.R. Buttsworth, K.H. Saleh, B.F. Yousif, CNG-diesel engine performance and exhaust emission analysis with the aid of artificial neural network, Applied Energy, 87 (2010) 1661-1669.

[61] M. Canakci, A.N. Ozsezen, E. Arcaklioglu, A. Erdil, Prediction of performance and exhaust emissions of a diesel engine fueled with biodiesel produced from waste frying palm oil, Expert Systems with Applications, 36 (2009) 9268-9280.

[62] N. Hashemi, N.N. Clark, Artificial neural network as a predictive tool for emissions from heavy-duty diesel vehicles in Southern California, International Journal of Engine Research, 8 (2007) 321-336.

[63] E. Arcaklioğlu, I. Çelikten, A diesel engine's performance and exhaust emissions, Applied Energy, 80 (2005) 11-22.

[64] H.S. Yücesu, A. Sozen, T. Topgül, E. Arcaklioğlu, Comparative study

of mathematical and experimental analysis of spark ignition engine performance used ethanol-gasoline blend fuel, Applied Thermal Engineering, 27 (2007) 358-368.

[65] Y.I. Bobrovnitskii, G. Pavic, Modelling and characterization of airborne noise sources, Journal of Sound and Vibration, 261 (2003) 527-555.

[66] L. Cremer, M. Wang, Synthesis of Spherical Wave Fields to Generate the Sound Radiated from Bodies of Arbitrary Shape, its Realization by Calculation and Experiment, Die synthese eines von einem beliebigen koerper in luft erzeugten feldes aus kugelschallfeldern und deren realisierung in durchrechnung und experiment., 65 (1988) 53-74.

[67] M. Heckl, Remarks on the calculation of sound radiation using the method of spherical wave synthesis, Bemerkung zur Berechnung der Schallabstrahlung nach der Methode der Kugelfeldsynthese, 68 (1989) 251-257.

[68] G.H. Koopmann, L. Song, J.B. Fahnline, A method for computing acoustic fields based on the principle of wave superposition, Journal of the Acoustical Society of America, 86 (1989) 2433-2438.

[69] G.T. Kim, B.H. Lee, 3-D Sound source reconstruction and field reprediction using the Helmholtz integral-equation, Journal of Sound and Vibration, 136 (1990) 245-261.

[70] M. Ochmann, Source simulation technique for acoustic radiation problems, Acustica, 81 (1995) 512-527.

[71] J.M. Mason, F.J. Fahy, Development of a reciprocity technique for the prediction of propeller noise transmission through aircraft fuselages, Noise Control Engineering Journal, 34 (1990) 43-52.

[72] D. Berckmans, B. Pluymers, P. Sas, W. Desmet, Numerical case-study on the development of acoustic equivalent source models for use in sound synthesis methods, 2008.

[73] D. Pessina, M. Guerretti, Effectiveness of hearing protection devices in the hazard reduction of noise from used tractors, Journal of Agricultural Engineering Research, 75 (2000) 73-80.

[74] L. Solecki, Duration of exposure to noise among farmers as an important factor of occupational risk, Annals of Agricultural and Environmental Medicine, 7 (2000) 89-93.

[75] D. Monarca, M. Cecchini, M. Guerrieri, M. Santi, R. Bedini, A. Colantoni, Safety and health of workers: Exposure to dust, noise and vibrations, in, 2009, pp. 437-442.

[76] FAOSTAT., Food and agriculture organization of the united nations. (faostat.fao.org), 2012.

Chapter 2

The effect of biodiesel fatty acid composition on diesel noise and exhaust emissions

2.1 Air and noise pollution of a diesel engine fuelled with olive pomace oil methyl ester and petrodiesel blends

2.1.1 Abstract

Olive pomace oil derives from the oil left in the olive fruit pulp than remains after pressing extra virgin olive oil. To extract olive pomace oil, the pulp is treated with solvents. The resultant oil contains impurities and may undergo several heating and filtering processes to refine it to an acceptable standard. To make it satisfactory to consumers, it must be blended with virgin olive oil before use. Therefore, another uses for this oil could be soap production or its recycling to produce biodiesel. Exhaust emissions, noise and sound quality of a direct injection diesel engine fueled with olive pomace oil methyl ester (OPME) blends were studied at several steady-state engine operating conditions. Results showed that the higher the content of OPME in the blends, the lower the CO emissions, whereas NO_x increased, keeping fuel consumption constant. Moreover, it was found that cetane number exhibited a stronger effect over noise production than bulk modulus, whereas the reverse effect was found concerning NO_x emissions. Biodiesel blends reduced air and noise pollution, while improving sound quality. Therefore, the higher the percentage of biodiesel in blends, the

lower the CO and CO_2 pollution emitted by the engine.

2.1.2 Introduction

The Directive 2009/28/EC of the European Parliament and the Council sets out a package of measures to reduce greenhouse gas emissions, energy savings and increased energy efficiency, while complying with the Kyoto Protocol of the United Nations Framework Convention on Climate Change and with further Community and international greenhouse gas emissions reduction commitments beyond 2012. Moreover, it includes a mandatory 10% minimum target to be achieved by each Member State for the share of biofuels in transport by 2020. In this sense, biodiesel is a good alternative for diesel fuel since it can be used in diesel engines without major modifications. Biodiesel, commonly known as fatty acid methyl esters (FAME), is produced through the transesterification of vegetable oils or animal fats.

A highly valuable oil that is mainly produced in Mediterranean countries, i.e. Greece, Spain, Italy, Tunisia, Portugal, Syria and Lebanon is olive oil. Once virgin olive oil has been extracted by pressing, there is still some oil that remains in the olive fruit pulp. To extract the so-called olive pomace oil, the pulp is treated with solvents. Although, olive pomace oil may be used for consumption, it cannot be described as olive oil. In fact, it has a more neutral flavor than virgin olive oil, making it undesirable among experts; however, it has the same fatty acid composition as regular olive oil. Therefore, another uses such as raw material to produce soap or its recycling for biodiesel production must be taken into consideration.

In recent studies, the relationship between the fatty acid composition of biodiesel and its chemical and physical properties has been determined [1]. Several authors have suggested that biodiesel with a high level of methyl oleate (or monounsaturated fatty acid) may have excellent characteristics in regard to ignition quality, fuel stability, flow properties at low temperature and iodine number (according to the European biodiesel standard EN 14214) [1, 2]. For this reason, olive pomace oil (that contains more than 75% wt. of oleic acid) should be a suitable raw material for biodiesel production, especially in the South of Europe where it is obtained as a secondary product in the virgin olive oil industry.

Although biodiesel is an important option for alternative uses of olive pomace oil, it results imperative to study the pollution (air and noise emissions) produced from a diesel engine when it is fuelled with olive pomace oil biodiesel compared to conventional diesel fuel. In this sense, many researchers have addressed the suitability of the use of methyl esters of vegetable oils as fuel or additives to diesel fuel to reduce exhaust emissions, such as particulate matters (PM) [3, 4], carbon monoxide (CO) [5] or total hydrocarbons (THC) [6]. However, using biodiesel, an increase of NO_x emissions has been observed [2, 5, 7-9].

Since noise is one of the most important environmental factors, which affects comfort and human health, it seems logical to consider acoustic pollution in the same level of importance as air contamination. This is of special interest in protected landscapes, where flora and fauna need to be preserved from air and noise pollution that may imperil the ecosystem. Reduction of the ever-increasing noise levels in the environment may improve our quality of life. Vehicle noise, which constitutes about 40% of city environmental noise, has been considered in the past few decades, and vehicle noise control has accordingly become a very active research area. A large research effort related to sound quality (SQ) of vehicle has recently been conducted [10, 11]. It has been found that the characteristics of a sound as it is perceived are not exactly the same as those of the sound being emitted. Traditionally, acoustic engineers have employed measuring units such as A-weighted decibels (dBA), which, in spite of showing a correlation with human perception, they simply give weight to the effects of the different components, specially in low frequency noise, using a family of curves defined in the International standard IEC 61672. In this sense, it neglects an important mechanism within the ear transduction of pressure fluctuations into signals to the brain, namely frequency masking. Understanding the basic anatomy of human hearing is vital to facilitate the fundamental psychoacoustic findings relevant to the perception of the sound [12]. By means of a study of the sound and psychoacoustic quality, a more than mathematical interpretation is made of the pressure signals in order to correlate the acoustic stimulus with the hearing sensation [13].

It is also important to define the most appropriate set of metrics for each application. The International Standardization Organization (ISO) has generalized sound quality (SQ) methods into two classes. The first is the

octave-band analysis (OBA) for linear and/or weighted sound pressure levels (SPLs). The second refers to more appropriate values based on the human sensation of loudness. Typically, the standard ISO 532 and further updated versions BS 5727 and EN 61260, which provide a graphic method for loudness calculation by means of third-octave bands, have been proven very useful for SQ design in automotive engineering in the areas of engine noise [14-16]. The most important metrics in sound quality evaluation of vehicle related sounds are Zwicker loudness, sharpness, roughness and fluctuation strength. Some researchers recommend loudness and roughness as the most important sound quality metrics for the evaluation of engine noise [10]. However, other authors indicate that roughness and fluctuation strength seem to correlate well with engine related noise [17]. Also, loudness and sharpness have been proposed to evaluate the sound quality in vehicles [18]. According to these researches, it seems that an established criterion for determining the best parameters to assess the sound quality of an engine is missing. The so-called Just Noticiable Difference (JND) of amplitude and frequency, as well as duration changes of pure/complex tones or broad band noise, have been investigated for decades, but little is known regarding the JND of sound quality metrics in real noise [19, 20].

The aim of this work is to study the sound quality of a diesel engine fuelled with olive pomace oil methyl ester (OPME) considering loudness, sharpness and roughness psychoacoustic metrics to evaluate the noise emission in a receptor position as a human being could listen it. The study includes the influence of the use of OPME as a fuel for diesel engines in some of the main exhaust emissions. Finally, noise and air pollution of a diesel engine fuelled with OPME are assessed.

2.1.3 Materials and Methods

2.1.3.1 Fuel description

OPME was produced after basic-catalyzed transesterification of olive pomace oil (OPO) that was acquired from KOIPESOL (Sevilla, Spain). KOH and methanol were the catalyst and alcohol used during the transesterification to produce biodiesel, respectively. KOH pellets [85% p.a. CODEX (USP_NF)] and methanol ACS-ISO were acquired from PANREAC (Barcelona, Spain). Transesterification and purification

processes carried out to produce OPME have been previously described [21].

Fatty acids composition of OPME was analyzed following the EU standard EN14103, while glycerides content was determined following EN14105 standard. The most important chemical and physical properties of OPME and no. 2 diesel fuel were analyzed following the EU Standard EN 14214 and EN 590, respectively.

Pure diesel fuel and blends of 20% and 50% (v/v) of OPME and diesel fuel (OPME20 and OPME50, respectively) were tested in a direct injection diesel engine.

2.1.3.2 Description of the engine

Fuel tests were performed in a 2500 cm3, three cylinder, four-stroke, water-cooled, 18.5:1 compression ratio, direct injection diesel engine Perkins AD 3-152. The maximum torque was 162.8 Nm at 1300 rpm and the maximum engine power was 44 kW at 2132 rpm (DIN 6270-A). The engine was not new but reconditioned to original specifications. In order to measure the emissions and brake-specific fuel consumption (BSFC) during operation, the actual driving conditions on the road were simulated on a dynamometer bench. The dynamometer was an electric Froment testing device (model XT200), with maximum engine power of 136 kW and ±1.44 kW of accuracy at 100% of the engine speed (reported by the National Institute of Agricultural Engineering, UK), as described by Dorado *et al*. [5]. The fuel was metered by a positive displacement gear type sensor, using a Froment Electronic Fuel Flow Monitor (FM502), as described by Dorado *et al*. [5]. The engine speed was measured by the Froment testing device and monitored electronically to the nearest 5 rpm. Atmospheric condition data were collected to correct the engine power following the SAE standard J1349 (revised August 2004).

2.1.3.3 Emission tests

Emission tests were carried out with a portable Testo 350-S exhaust emissions monitor. The engine test cycle was tailored after the ‘8-mode cycle’ for engine dynamometer operation, according to ISO 8178-4.

Emission test plan adapted to diesel engine Perkins AD 3-152 is shown in Table 2.1. Each running step was held for 10 min until exhaust emissions were stabilized and maintained while each parameter was measured and recorded, during the last 3 min of each running step. The following principles of calculation were used:

$$NO_x = NO + (NO_{2add} NO) \quad (2.1)$$

where NO_x is the nitrogen oxide value (ppm), NO is the measured nitrogen monoxide value (ppm) and NO_{2add} is the nitrogen addition factor.

$$uCO=\lambda CO \quad (2.2)$$

where uCO is the carbon monoxide undiluted (ppm), CO is the measured carbon monoxide value (ppm) and λ is the calculated air ratio defined like the relationship between the fuel-specific carbon dioxide value, CO_{2max} (ppm), and calculated carbon dioxide value, CO_2 (ppm).

For the conversion from ppm to mg/m^3, the following expressions were used:

$$CO(mg/m^3) = 1.25 \frac{O_{2ref} - O_{2Bez}}{O_{2ref} - O_2} CO(ppm) \quad (2.3)$$

$$NO_X(mg/m^3) = 2.05 \frac{O_{2ref} - O_{2Bez}}{O_{2ref} - O_2} NO_X(ppm) \quad (2.4)$$

where O_2 is the measured oxygen content (%), O_{2ref} is the O_2 reference value (%) and O_{2Bez} is the fuel-specific oxygen reference number (%).

A first test was run with straight diesel fuel at the beginning, followed by the OPME blends test run, in order to compare exhaust emissions and *BSFC* with the fuels. Engine tests were run on the same engine and same day, in order to have almost the same conditions within the three repetitions of each test [22].

Table 2.1. Test plan for emission tests

Step number	Engine speed (equivalence in rpm)	Load (%) (equivalence in kW)
1	Rated (2132)	100 (44)
2	Rated (2304)	75 (33)
3	Rated (2348)	50 (22)
4	Rated (2392)	25 (11)
5	Medium (1376)	100 (28)
6	Medium (1448)	75 (21)
7	Medium (1500)	50 (14)
8	Low idle (1160)	-

2.1.3.4 Description of the noise meter

The set-up used for measuring noise consisted of one microphone placed at 1 m of the engine (Figure 2.1). A Soundbook instrumentation series, consisting of a portable and multi-channel meter and a GRAS prepolarized free-field half-inch microphone was utilized as the measuring device. Samurai v1.7 from SINUS Messtechnik GmbH (Germany) was the measurement software package used and the microphone was calibrated with a B&K calibrator. Recorded measurements were post processed using Matlab R2008a from MathWorks Inc (USA). All recordings were carried out following ISO 362-1:2007.

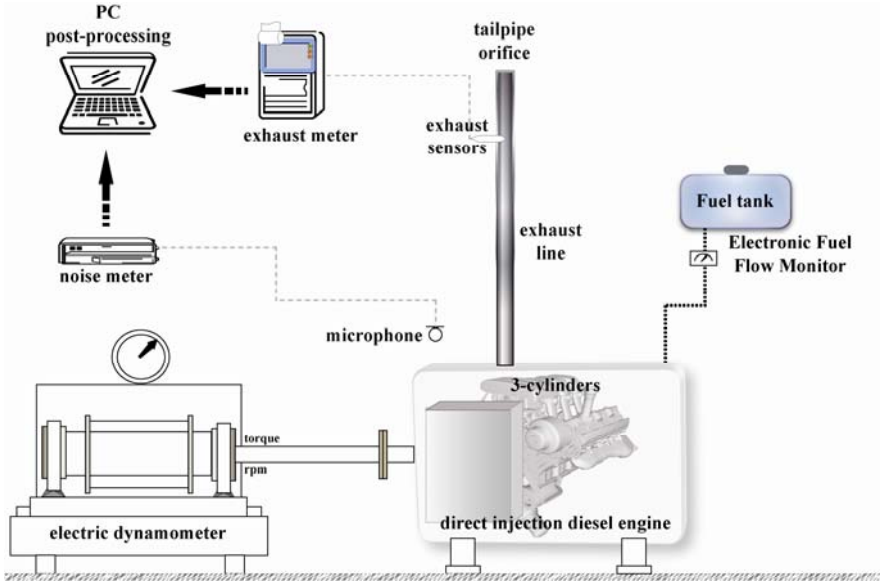

Figure 2.1. Set up of the experiment

2.1.3.5 Sound quality metrics

Although the term "sound quality" is widely used, its meaning often seems to appear diffuse. Sound quality is used to define the relationship between the physical quantities of sound and the subjective impression as heard by the human ear. A further difference may be explained by the evaluation of sound signals in the hearing. While evaluations by means of conventional acoustic measuring techniques are made with a simple A-weighting, human hearing involves more complicated level-dependent evaluation mechanisms. A sound impression is not only determined by the sound pressure level, but also by psychoacoustic properties such as loudness, sharpness and roughness. Besides, the reduction of sound pressure level often does not lead to subjectively perceived improvements [23].

Beyond the mathematical interpretation of pressure signals, SQ and psychoacoustics try to correlate acoustic stimuli with hearing sensation. For this purpose, a set of algorithms have been developed from the science of psychoacoustics which analyzes sound pressures level, frequency and

modulation depth to correlate them to human hearing perception [24]. In this research, the engine sound has been characterized only by means of loudness, sharpness and roughness.

Loudness. This parameter does not only depend on the sound pressure level, but also on the spectral composition of the sound. However, calculation of the loudness of more complex sounds requires the consideration of other aspects, i.e. the critical band-width. Critical band-width is a measure of the frequency resolution of the ear depending on the excitation level in the cochlea and surroundings, regarding a tonal (or narrow band) stimulus, measured in Barks. Considering the available techniques, only the method developed by Zwicker and Fastl [24] is valid to broadband excitation. Therefore, this procedure was considered in this research, as it is in compliance with ISO 532B, DIN 45631 and ISO/R 131.

Roughness. Roughness is another algorithm used to determine the subjective judgment of sound quality. Roughness correlates to how noticeable or annoying is heard a sound by the human ear. This is a complex effect, which quantifies the subjective perception of rapid amplitude modulation of a sound. The unit of measure is the Asper. However, the roughness metric has not yet been standardized and there are several methods of calculation. In this research, the procedure of calculation proposed by Aures [25] has been used.

Sharpness. Sharpness is a measure of the high frequency content of a sound relative to the overall level, its unit is the Acum. The high frequency content of a sound affects product quality, so sharpness can be a useful measure. The most important variables influencing sharpness are the spectral envelope of the sound and, for narrowband sounds, the center frequency. Despite, JND in sharpness does not vary much within the overall level. Therefore, it is still not very clear which sharpness changes can be perceived [24]. However, it has been found that sharpness shows a high correlation with perceived annoyance [26]. There are several methods to calculate SQ metrics, including Von Bismarck's method [26], Aures's method [25] and Zwicker and Fastl's method [24]. Since Zwicker and Fastl's method for calculating the sharpness is the most extended approach, it has been used along this research.

Just noticeable difference (JND). The concept of differential threshold or

just noticeable difference emerges from the need to verify the efficacy of some noise control solutions in improving operator comfort conditions in vehicles [24]. Since knowledge of the correlation between stimulus and sensation is not sufficient, it is therefore necessary to detect the step size of the stimulus that leads to a difference in the hearing sensation.

2.1.4 Results and discussion

2.1.4.1 Fuel properties and consumption

Fatty acid composition and the most important properties of the tested OPME blends, besides diesel fuel properties are shown in Table 2.2. As the fatty acid composition of olive pomace oil is that of olive oil a good engine performance is expected [5, 27].

Table 2.2. Fuels properties (OPME: olive pomace oil methyl ester)

Property	**OPME**	**No. 2 diesel fuel**
Kinematic viscosity (□) at 40ºC (mm^2/s)	5.2	2.47
High Calorific Value (*HCV*) (kJ/kg)	40220	42700
Cetane number (*CN*)	61.72	53.8
Fatty acid composition (%)		
Palmitic (C16:0)	11	
Palmitoleic (C16:1)	0.8	
Stearic (C18:0)	3	
Oleic (C18:1)	75.2	
Linoleic (C18:2)	9.5	
Linolenic (C18:3)	0.5	

No significant differences between *BSFC* of OPME20 and diesel fuel were observed and only a very slight increase on *BSFC* for OPME50 (lower than 6%) was recorded (Figure 2.2). Generally, biodiesel shows a

higher *BSFC* value than that of diesel fuel, mainly due to the lower calorific value of FAME with respect to diesel fuel [28]. Characterized by a high content of monounsaturated fatty acid methyl esters (Table 2.2), OPME depicts higher calorific value (*HCV*) than FAME produced from other raw materials, allowing values of *HCV* similar to diesel fuel, as shown in Table 2.2 [29]. For this reason, no significant differences on *BSFC* between the tested fuels were observed.

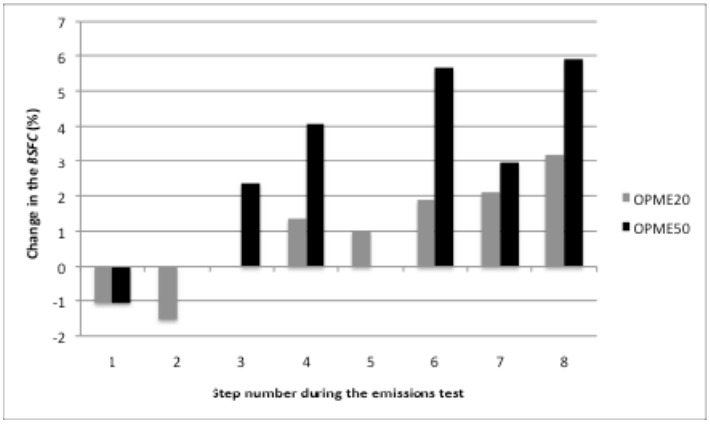

Figure 2.2. Percent changes in *BSFC* of a Perkins engine fuelled with different blends of OPME compared to 100% diesel fuel (OPME20: 20% OPME/80% diesel fuel; OPME50: 50% OPME/50% diesel fuel blends)

2.1.4.2 Exhaust emissions

Results including CO, NO and NO_x emissions are depicted in Figure 2.3. It is possible to appreciate that CO exhaust emissions clearly decrease with the content of OPME in diesel fuel (Figure 2.3). This trend can be explained by the oxygen content on biodiesel which leads to a more complete and cleaner combustion .[30, 31]. The main advantage is that CO_2 emissions, in case of biodiesel, can be regarded as carbon credit as it was produced by photosynthesis.

However, despite the higher value of *CN* of OPME (55.4 for OPME20 and 57.8 for OMPE50) compared to diesel fuel (53.9), the

emissions of NO and NO_x increased with the increment of the percentage of OPME in the blends, in general terms at higher torque values (Figure 2.3). Taking into account that the bulk modulus of the oleic acid methyl ester (the most important component of OPME) is 1538 MPa and the bulk modulus of diesel fuel is 1410 MPa [32], OPME20 and OPME50 blends depict higher bulk modulus than pure diesel fuel, and subsequently, using a mechanical injection system, an advance in the injection timing is expected [33].

This advance may cause higher NO_x formation. It may be inferred that the bulk modulus depicts a stronger effect over NO_x formation than *CN* influence.

Additionally, the oleic acid methyl ester (the most important component in OPME, according to Table 2.2) has higher adiabatic flame temperature (*AFT*) with respect to diesel fuel [34] and this difference may be responsible for an increase in thermally formed NO_x [35]. Moreover, OPME oxygen content may enhance NO formation reactions, increasing NO_x emissions [36]. For these reasons, the increase of NO emissions when OPME-based fuels are used is higher than the production of total NO_x exhaust emissions. Exhaust emissions results are in agreement with previous works related to the use of biodiesel from different origin in diesel engines [30].

2.1.4.3 Noise emissions

Figure 2.4 shows the frequency spectrograph on 1/3rd octave band number ascribing different colors at 1/3rd octave level (dB), considering tested fuels. Each row from 1 to 8 represents the sound considering the tested engine operating conditions (8-mode cycle), as described in Table 2.1. It may be noticed that the maximum noise level was achieved at rated engine speed. The maximum noise value was achieved by the use of diesel fuel (98 dB), providing a noise reduction of approximately 1-2 dB when both OPME20 (97 dB) and OPME50 (96 dB) were used. At medium rpm (mode 5) the most meaningful difference was a noise 4 dB higher for diesel fuel (78 dB) compared to the blends (74 dB for OPME20 and OPME50). At low rpm (mode 8), the fuels depicted similar behavior compared to medium rpm values. Only in the second $1/3^{rd}$ octave band, a difference of 3-4 dB between diesel fuel (89 dB), OPME20 (86 dB) and OPME50 (85 dB) was found.

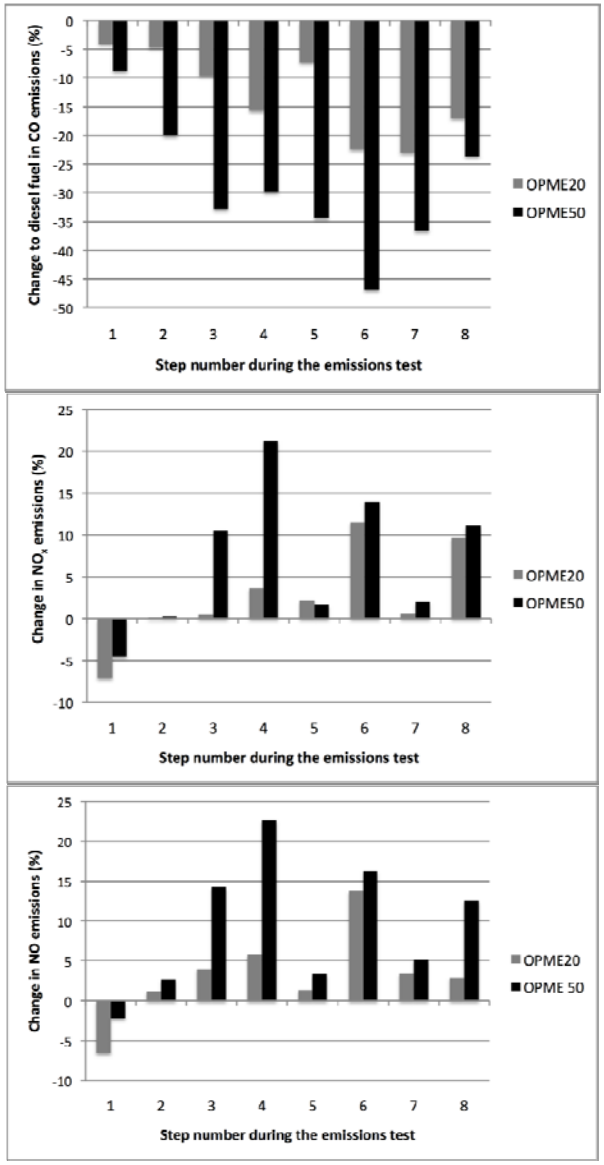

Figure 2.3. Percent changes in CO (a), NO (b) and NO_x (c) exhaust emissions of a Perkins engine fuelled with different blends of OPME compared to 100% diesel fuel (OPME20: 20% OPME/80% diesel fuel; OPME50: 50% OPME/50% diesel fuel blends)

Table 2.3 shows the relative change in SQ metrics (%), including sharpness, total loudness and total roughness. Total loudness and total roughness refer to the global parameters (total Zwicker loudness, sharpness and total roughness) regardless the frequency bands. The values of measured sharpness are low, thus indicating the high frequency provided by the engine sound is not meaningful. As shown in Figure 2.4, low values of noise (dB) are found between 25-30 1/3rd octave band numbers (related to 16-40 kHz frequency), which indicates a low sharpness value. Considering the blends, similar sharpness values are found. The most important difference between fuels (*circa* 5.33%, which is not too noteworthy) was provided by OPME50 compared to diesel fuel, when mode number 4 was tested. It has been found that JND in sharpness does not exhibit a relevant variation considering the overall level, although in general terms it is still unclear which changes in sharpness can be perceived [24, 25]. It is, however, clear that sharpness has a high correlation with perceived annoyance [26]. In general, it seems that OPME20 and OPME50 blends present a slightly lower attenuation of the sharpness level. The perception of sharpness corresponds to very high frequency spectral contents and the most predominant sound sources in an engine are found at low-medium frequencies. This result concerning sharpness attenuation is not correlated with the improvement of the engine sound quality and comfort. Changes in total loudness (%) for each blend compared to diesel fuel reveal no significant differences. However, a slight attenuation, around 3% of total Zwicker loudness for OPME20 and OPME50 compared to diesel fuel was noticed considering mode number no. 3 (Table 2.3). There was a little improvement when the blends were used compared to diesel fuel, although JND in amplitude (dB) were perceived in the loudness level. From the application of the Zwicker loudness method, it may be inferred that the use of the proposed biofuels decreases the loudness of the engine radiated noise, thus directly indicating the reduction of the noise perception. Also, from the spectrogram, it is evident that the noise improvement is achieved in the whole range frequency band, being more noticeable at low-medium frequencies (Figure 2.4).

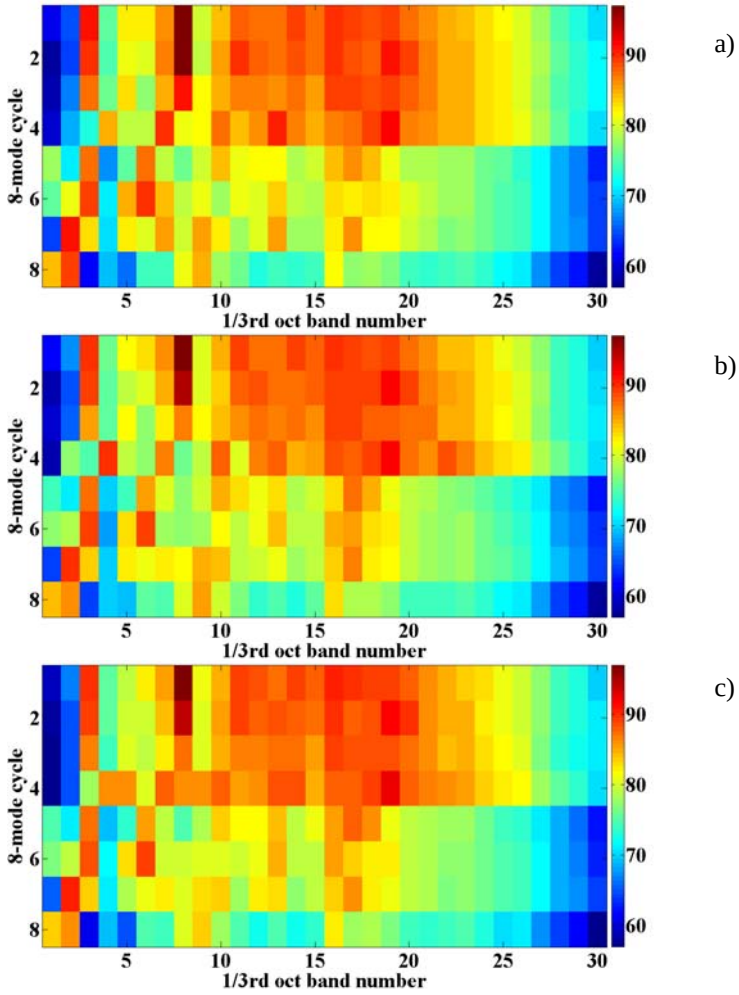

Figure 2.4. Spectrogram 1/3rd octave band level (dB) for all engine operating conditions: a) diesel fuel, b) OPME20 and c) OPME50

Similar conclusions may be withdrawn from the roughness parameters evaluation. OPME20 and OPME20 blends provide a decrease in roughness ca. 51.81% and 55.44%, compared to diesel fuel, respectively. As found by Coen *et al* [26], the minimum JND value to roughness detection

must be above 17%. Therefore, a good reduction of roughness was achieved with the use of the blends. Acoustic roughness is defined as medium frequency modulation of engine noise. The principal cause of roughness is medium frequency vibration of power train, which modulates radiated noise. Generally, medium frequency vibration is caused by dynamics of engine moving parts, e.g. crankshaft, camshafts, etc. Therefore, it seems that using OPME20 and OPME50 the roughness decreased, reducing also the low-medium frequency vibration in the engine. These vibrations are particularly penalizing for passenger vibration comfort and subsequently may be attenuated with the use of the proposed blends.

Table 2.3. Change in sharpness, total loudness and total roughness (%) for OPME20 and OPME50 for all engine conditions

Step number	**OPME20**	**OPME50**	**OPME20**	**OPME50**	**OPME20**	**OPME50**
	Sharpness		**Total Loudness**		**Total Roughness**	
1	0.74	0.74	0.66	1.18	19.50	19.50
2	0.00	0.72	1.43	2.17	13.49	14.29
3	0.69	1.38	2.88	2.91	12.73	16.36
4	0.67	5.33	0.07	0.50	20.83	35.42
5	2.21	2.94	0.41	1.56	51.81	55.44
6	0.74	0.74	0.64	1.12	18.18	36.36
7	0.00	0.00	1.35	1.81	4.65	3.49
8	2.16	2.88	0.40	0.54	21.21	26.26

Figure 2.5 provides a first overview of the absolute change in specific loudness values of the OPME20 and OPME50 blends compared to diesel fuel. As expected, the specific loudness values are slightly attenuated as happened to the total loudness. As shown in Figure 2.5 for for the majory of engine operating conditions, the attenuation of specific loudness at low frequencies is most important than at mid-high frequencies. Results for modes no. 4 and 6 provide the higher reduction of specific loudness (around 3 Bark) provided by the blends in comparison to diesel fuel. For the rest of the operating conditions or modes, no significant differences between the specific loudness values of the blends compared to diesel fuel were found.

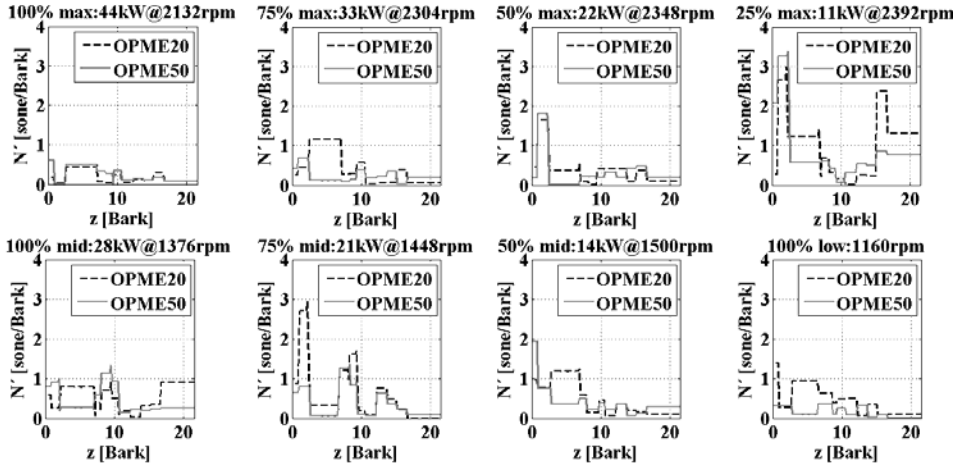

Figure 2.5. Absolute change in Zwicker Loudness for OPME20 and OPME50compared to diesel fuel at several engine operating conditions

Figure 2.6 shows the roughness for all engine conditions (8-mode cycle) regarding the frequency. Again, the reduction of the roughness level of the blends compared diesel fuel is highly noticeable. The gray scale is kept constant for the plots, to allow the visualization of the contrast between the different biofuels and diesel fuel. As depicted in Figure 2.6, the roughness level diminishes at low frequencies. In this range of frequencies and considering all engine operating conditions, the higher differences between the blends and diesel fuel were achieved. Concerning the influence of the blends, it is important to notice that the reduction in roughness (total and specific) is much more noticeable than the change of loudness (total and specific). However, besides being responsible of the feeling of power and sportiveness in an engine, roughness is usually associated with unpleasantness. In this way, blends with a higher content of OPME are expected to behave in a more pleasant way.

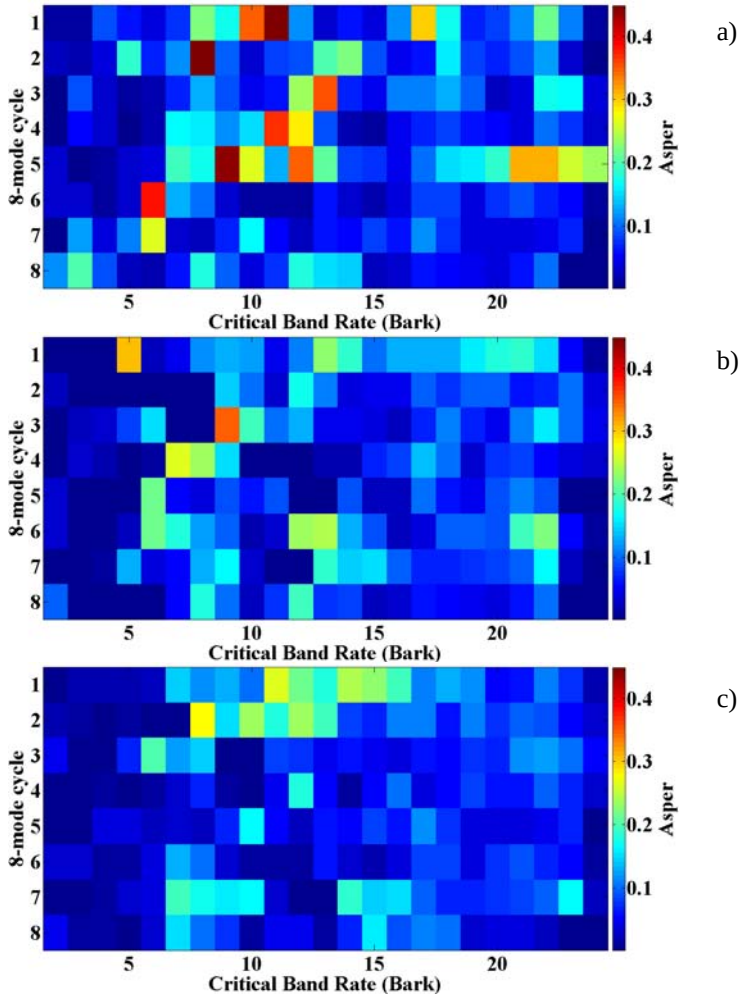

Figure 2.6. Roughness for all engine operating conditions: a) diesel fuel, b) OPME20 and c) OPME50

Moreover, it is known that the combustion noise in direct injection diesel engines originates from pressure and mechanical forces produced inside the cylinder [37]. Combustion noise is determined by cylinder pressure rise rate and is influenced by a variety of parameters, including injection timing and ignition delay. Moreover, the injection and the

combustion process vary between diesel fuel and the blends because of the difference of cetane number and bulk modulus (when a mechanical injection system is used). The higher the bulk modulus the longer the advance in the injection timing, thus increasing the noise radiation. On the other hand, as mentioned above, OMPE20 and OMPE50 have a higher cetane number compared to conventional diesel fuel. Then, a shorter ignition delay period is expected, hence steeper pressure gradients and so lower noise radiation [38, 39]. Taking into account the current results, it may be inferred that the use of biodiesel as partial diesel fuel substitute attenuate the emitted sound and improve the sound quality, too. In sum, it indicates that the effect of the ignition delay (*CN*) over combustion noise production is stronger than that of the injection timing (bulk modulus). This finding is partially in agreement with the results show by other researchers [26]. In addition, it is important to mention that the attenuation achieved for the blends in the range of low frequency is better than in mid and high frequencies, revealing a high agreement with previous results [40].

2.1.5 Conclusions

A diesel engine running on diesel fuel, straight and blended with olive pomace oil methyl ester, has been tested. This paper has shown that the tested blends are particularly attractive from an environmental perspective, because they attenuate both air and noise pollution without increasing *BSFC*. The use of biodiesel as partial diesel fuel substitute can also improve the engine sound quality, therefore making the engine sound more pleasant. Moreover, the effect of *CN* over noise production is stronger than that of bulk modulus; the reverse effect was found concerning NO_x emissions. It can be concluded that the higher the percentage of biodiesel in the blend, the lower the environmental pollution (air and noise) emitted by the engine, with the exception of NO_x emissions.

2.2 Biodiesel from saturated and monounsaturated fatty acid methyl esters and their influence over noise and air pollution

2.2.1 Abstract

A combined analysis of exhaust and noise emissions of an three-cylinder direct injection diesel engine running on palm oil methyl esters (PME) and olive pomace oil methyl esters (OPME), both blended with diesel fuel in different proportions, is proposed to evaluate their suitability as partial substitute to fossil fuels. Moreover, engine sound quality (derived from the use of these fuels) based on loudness and roughness metrics has been analyzed. A strong correlation between sound pressure maximum level and loudness was found. Although it was observed that both parameters improved with the use of both set of blends, PME blends depicted the best behavior. In terms of roughness, OPME blends achieved the maximum attenuation. In addition, roughness attenuation was found to be most meaningful than loudness when the blends were used. Considering the exhaust emissions tests, it was observed that the use of both sets of fatty acid methyl ester blends allows a significant reduction of CO emissions.

Moreover, lower NO exhaust emissions were produced when PME blends were used instead of OPME blends or diesel fuel. NO_x emissions were lower when PME blends were used instead of OPME blends, though diesel fuel depicts the lowest values. In general terms, it may be concluded that saturated fatty acid methyl esters produce biodiesel with a positive influence over air and noise emissions.

2.2.2 Introduction

Nowadays, the reduction of greenhouse gas (GHG) emissions is one of the most important targets for vehicle manufacturers. The "ecological conscience" of consumers, besides the fact that about one-third of the vehicles sold in Europe and United States are diesel-powered [41] are leading the scientific community to search for a new generation of fuels for diesel engines. To contribute to an effective reduction of GHG and to promote cleaner transport, the Directive 2009/28/EC establishes that the share of energy from renewable sources in the transport sector must amount to at least 10% of final energy consumption in the sector by 2020. In this context, biofuels need to meet certain criteria to be considered a cleaner option, including sustainability. In particular, biodiesel has received wide attention as a replacement for diesel fuel because it is biodegradable, nontoxic and environmentally less contaminant, being compatible with conventional diesel fuel. Also, it can be blended in any proportion with fossil-based diesel fuel to create a stable biodiesel blend [42]. Biodiesel is obtained from different vegetable oils or animal fats through their transesterification with an alcohol and a catalyst. The usual feedstocks for biodiesel production are rapeseed, soybean, palm, sunflower and other oleaginous plants. The use of palm oil biodiesel, also known as palm oil methyl ester (PME), is increasing due its low cost and productivity. Biodiesel from palm oil is characterized by a high level of saturated fatty acids and shows excellent combustion properties, such as cetane number and high calorific value, despite its poor cold properties or high kinematic viscosity. In recent studies [1, 21, 43] it has been observed that biodiesel from triglycerides with high concentration of monounsaturated fatty acids (such as rapeseed oil or olive pomace oil) may have optimal characteristics in regard to chemical and physical properties. Olive pomace oil is the residual oil that remains in the olive fruit pulp, once virgin olive oil has been extracted. It cannot be described as olive oil due to its poor

organoleptic properties, but it provides high-quality biodiesel [44].

On the other hand, the Directive 2002/49/EC aims to provide a common approach that intends to avoid, prevent or reduce on a prioritized basis, the harmful effects, including annoyance, due to exposure to environmental noise. Generally, the radiated noise from diesel engines can be broken down into mechanical noise and combustion noise, as shown in Figure 2.7. Combustion noise is separated into direct combustion noise (directly proportional to the combustion gas pressure) and indirect combustion noise (proportional to rotational forces as well as combustion-induced piston side forces) [45, 46].

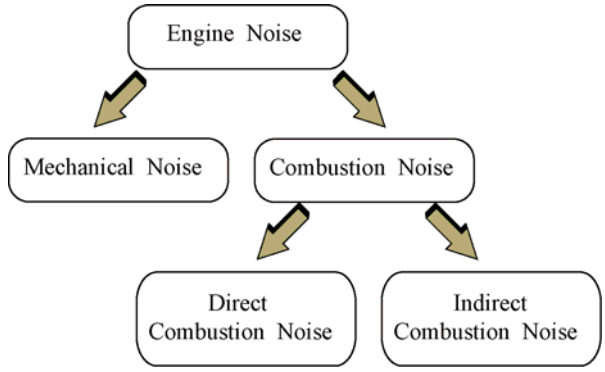

Figure 2.7. Engine noise contributions

When combustion takes place, a sudden pressure rise is produced causing the vibration of the engine block, which in turn radiates air-borne noise. The block vibration is caused by pressure forces exerted directly by the gas and the mechanical forces associated with piston slap, bearing clearances and friction. Pressure forces strongly depend on the combustion process, which is mainly dominated by the fuel-burning velocity. In addition, this velocity is controlled by the injection rate [47]. The excitation source, pressure and mechanical forces of combustion noise are characterized by in-cylinder pressure; the system response is associated with the vibration of the block wall and the radiated noise is the final effect of such vibration [48, 49]. As shown in Figure 2.8, combustion noise, which is audible in the vehicle, is associated with the vibration of the block wall,

while the radiated noise is the final effect of such vibration. It is transferred to the passenger as annoying noise in a frequency range between 800 Hz and 4000 Hz [50]. It is important to mention that engine performance, also related to combustion and hence to exhaust emissions, is a result of fuel properties, including molecular composition and structure, cetane number and viscosity [39, 51, 52]. Therefore, it is important to achieve the reduction both exhaust emissions and combustion noise when different fuels are used.

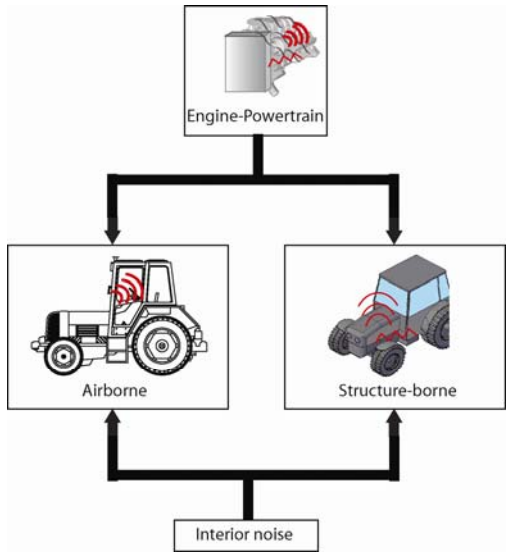

Figure 2.8. Transfer path of combustion noise in a vehicle

In this work, to evaluate the suitability of low and high saturation degree biodiesel blends as partial fossil fuel substitutes, a combined analysis of exhaust and noise emissions of a diesel engine fuelled with palm oil methyl ester and olive pomace oil methyl ester (OPME) is proposed. Moreover, sound quality based on loudness and roughness metrics has been considered, besides other important parameters.

2.2.3 Materials and Methods

2.2.3.1 Materials and experimental set-up

Both methyl esters of olive-pomace oil and palm oil were produced by alkaline transesterification and further purification processes as described by Pinzi *et al*.[21]. Olive pomace oil (OPO) was acquired from KOIPESOL (Sevilla, Spain) and palm oil (PO) that was purchased from Quimics Dalmau (Barcelona, Spain). KOH and methanol were the catalyst and alcohol used during the transesterification to produce biodiesel, respectively. KOH pellets [85% p.a. CODEX (USP_NF)] and methanol ACS-ISO were acquired from PANREAC (Barcelona, Spain). Fatty acid composition of OPME and PME were analyzed following the EU standard EN14103 and glycerides content was determined following EN14105 standard. The most important chemical and physical properties of OPME, PME and no. 2 diesel fuel were analyzed following the EU Standard EN14214 and EN 590, respectively.

Biodiesel blends of 20% and 50% (v/v) of OPME with diesel fuel (OPME20 and OPME50) and 20% and 50% (v/v) of PME with diesel fuel (PME20 and PME50) were tested in a diesel engine test bench.

Instruments, apparatus, software used, experimental set up and the emission test plan are depicted in depth in the section 2.1.3 of this chapter. Key properties of the biodiesel are shown in Table 2.4.

2.2.3.2 Noise characterization

By means of sound quality (SQ), sounds are not only considered pressure signals, because a correlation between acoustic stimuli and hearing sensation is established [53]. SQ is widely used in automotive engineering; in fact, manufactures have invested a lot of efforts and money to improve the sound of vehicles, e.g. the closing of a door lock, the feeling of sportiveness of a car engine during acceleration, etc.

Table 2.4. Main chemical and physical properties influencing combustion of biodiesel blends and diesel fuel

Fuel	Cetane number (*CN*)	Kinematic viscosity (μ) at 40 °C (mm^2/s)	*HCV* (kJ/kg)	C (%)	H (%)	O (%)
	[54]	EN ISO 3679	ASTM D 2382-88			
Diesel fuel	53.90	2.47	42700	86.5	13.5	0.0
OPME20	55.46	3.01	42203	84.5	13.2	2.2
OPME50	57.81	3.83	41459	81.7	12.8	5.4
PME20	57.54	3.10	42154	84.4	13.3	2.3
PME50	63.00	4.05	41333	81.4	12.9	5.6

The change of fuel in a vehicle could modify the original vibro-acoustic perception. For this reason, it is important to study the influence of the use of other fuels in both engine performance and SQ to take it into consideration in an early design stage.

As previously mentioned, the most important metrics in the sound quality evaluation of vehicle are loudness, sharpness, roughness and fluctuation strength [53]. There are many procedures to estimate SQ, due to the underlying psychoacoustic basis of this study. The choice of the most appropriate sound quality metrics depends on each individual application. Individual metrics do not give an indication of sound quality as a whole for many applications, so currently no metrics adequately quantify this subjective impression. Therefore, first of all it is important to decide which metric will be used since the use of wrong metrics can lead to misinterpretations. Loudness and roughness have been described in section 2.2.3.5 of this chapter.

2.2.4 Results and discussion

The absolute change of the sound pressure maximum level (SPL) for OPME and PME blends compared to diesel fuel, considering different engine operating conditions, is plotted in Figure 2.9. As may be seen, the sound pressure maximum level produced by PME50 is lower compared to that of the other blends and diesel fuel for all engine operating conditions,

excepting mode 3. The most important difference between the blends and diesel fuel is achieved in mode 7 (about 9 dB). It is a clear improvement provided by the blends: as noise behavior depicts a logarithmic trend, an attenuation of 3 dB means energy noise emissions are halved. Therefore, the maximum energy noise emitted by an engine may be attenuated up to almost 87.5% with the use of PME50 blend (corresponding to 9 dB).

Results concerning loudness are shown in Figure 2.10. It may be observed that sound pressure maximum level and loudness are highly correlated (Figure 2.9), PME50 showing the best behavior. The relative difference between diesel fuel and PME blends is slightly higher compared to the difference between OPME blends and diesel fuel. Provided that both sets of blends depict a similar trend, it may be inferred that the higher the percentage of biodiesel the lower the loudness of engine radiated noise, thus directly reducing the level of annoyance to the perceived engine noise.

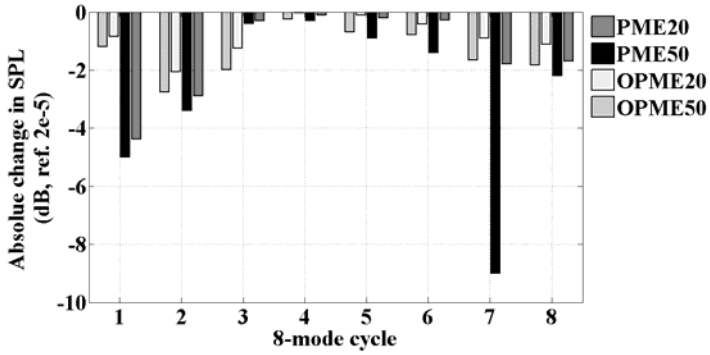

Figure 2.9. Absolute change in sound pressure maximum level (SPL) of a Perkins engine fuelled with different blends of OPME/diesel fuel and PME/diesel fuel compared to diesel fuel

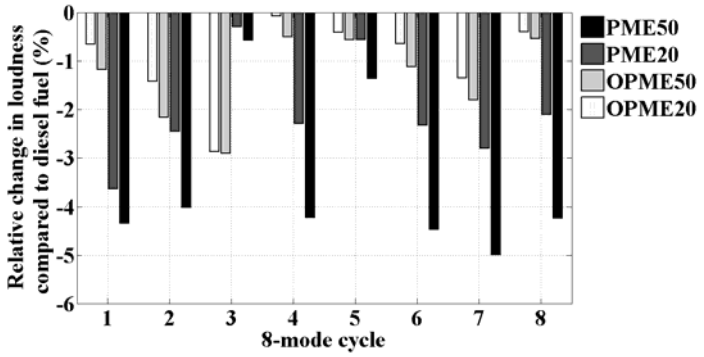

Figure 2.10. Relative change in total loudness level (%) of a Perkins engine fuelled with different blends of OPME/diesel fuel and PME/diesel fuel compared to diesel fuel

Roughness also improves considerably with the use of biodiesel blends, as depicted in Figure 2.11. The influence of OPME and PME blends on roughness is stronger compared to loudness. Roughness is attenuated around 40% for both sets of blends compared to that of diesel fuel, achieving a maximum reduction of almost 60% when both blends of OPME are used under mode 5.

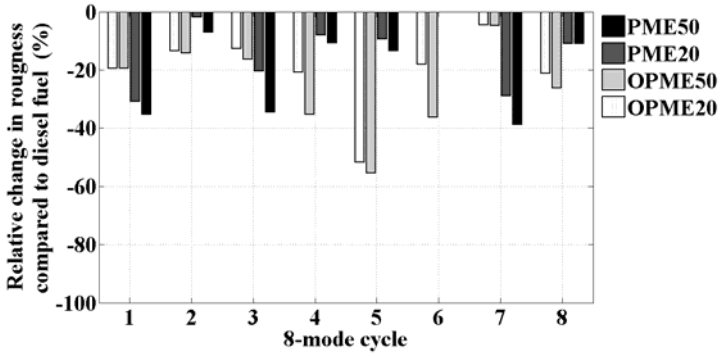

Figure 2.11. Relative change in total roughness level (%) of a Perkins engine fuelled with different blends of OPME/diesel fuel and PME/diesel fuel compared to diesel fuel

Results of loudness and roughness derived from the use of OPME and PME blends show an improvement of the engine sound quality at different operating conditions, compared to the use of diesel fuel. For both sets of blends, the higher the percentage of biodiesel the better the attenuation achieved. In general terms, results are better for PME blends than OPME blends.

Chemical and physical properties of biodiesel blends influence the previous results, provided that oxygen content, cetane number (*CN*) or kinematic viscosity (μ), among other properties, have an impact on combustion efficiency and therefore on combustion noise. Table 2.4 depicts some of the main properties of the tested fuels that influence their combustion behavior. As reported by Albarbar *et al*. [55] combustion noise is produced by the rapid rate of increase of cylinder pressure, which besides being a source of engine structural vibrations also excites resonances in the gas inside the combustion chamber cavity. The latter is also a source of vibration and air-borne acoustics. The excitation force, i.e. combustion pressure, first distorts the engine structure in an impulsive manner and then the engine structure begins to vibrate as damped free oscillations. Moreover, a rise in the cylinder pressure due to combustion cause an abrupt movement of piston which impacts with the cylinder walls, being another major source of engine noise. In this sense, a higher *CN* of fuel indicates less time between the beginning of fuel injection and further ignition in the cylinder, thus improving combustion. *CN* of OPME and PME blends is higher than that of diesel fuel (Table 2.4). The attenuation of the radiated noise may have resulted from the reduction of the maximum pressure rise rate due to the improved *CN* of biodiesel blends and therefore, the reduced ignition delay. The higher the ignition delay the higher the liquid fuel injected before it starts to ignite. This makes the combustion pressure rise rate higher, as a higher amount of mass is exploded, which cause noise increase [56]. As expected, sound pressure maximum level and sound quality have improved with the use of biodiesel blends, especially when PME is utilized. According to other researchers, apart from *CN*, other parameters such as the high viscosity of the blends (Table 2.4) may explain the effect on the attenuation of noise radiation as a result of the influence on the start of injection and injection pressure [51, 57]. In fact, spray properties may be altered due to differences in viscosity of the fuels. Affected spray properties may include droplet size, droplet momentum and hence degree of mixing

and penetration, evaporation rate and radiant heat transfer rate. A change in any of these properties might lead to different relative duration of the premixed versus diffusional burn regimes [3]. In this sense, high viscosity provides worse pulverization, leading to an increase in the fuel droplet size inside the combustion chamber and to a lower amount of fuel being burnt during the premixed regime, thus leading to a decrease of the maximum in-cylinder pressure.

According to previous results [44] and in agreement with Figure 2.12, a significant reduction of CO emissions was achieved when biodiesel blends were used. NO and NO_x emissions are generally lower when PME blends are used instead OPME blends (Figures 2.13 and 2.14). In accordance with other authors, this result confirms that the higher the number of double bounds in the chemical structure of biodiesel the higher the emission of NO_x (mainly consisting of NO_2 and NO) [30, 58]. In a recent work, it was found that the higher the unsaturation degree of methyl esters the higher the ignition delay (lower *CN*), the adiabatic flame temperature (AFT) and the advance of injection (higher bulk modulus), consequently increasing NO prompt of NO_x emissions [32]. This trend is depicted in Figure 2.13, where a reduction of NO emissions of PME blends with respect to diesel fuel is observed. In agreement with the previous statements, significant differences between NO_x emissions considering the different feedstocks used to produce biodiesel were reported (Figure 2.14).

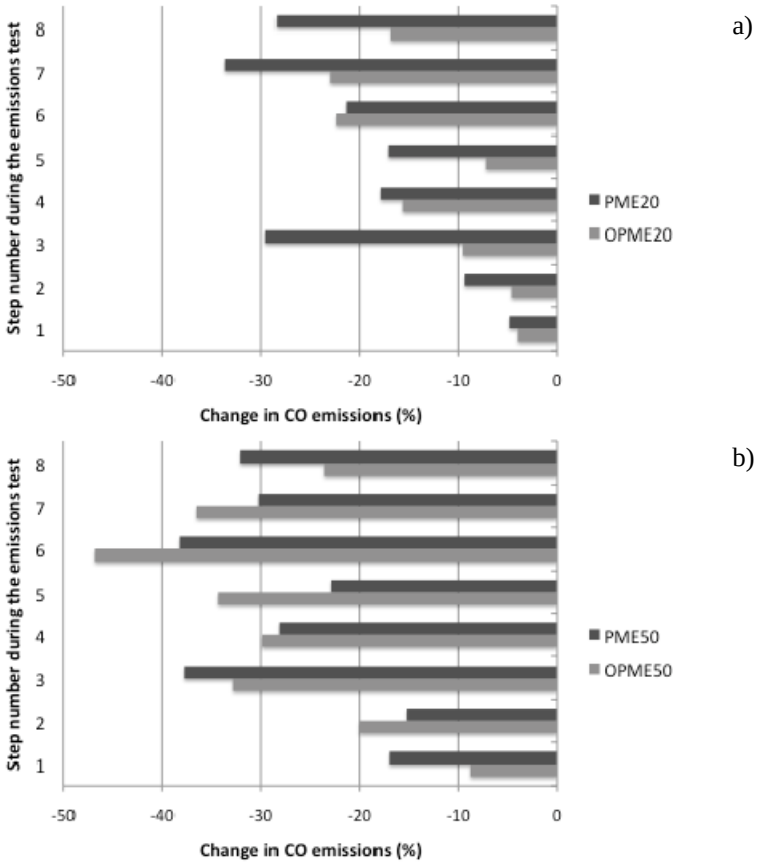

Figure 2.12. Percent changes in CO exhaust emissions of a Perkins engine fuelled with different blends of OPME and PME compared to diesel fuel (a) 20% biodiesel/80% diesel fuel; (b) 50% biodiesel/50% diesel fuel blends

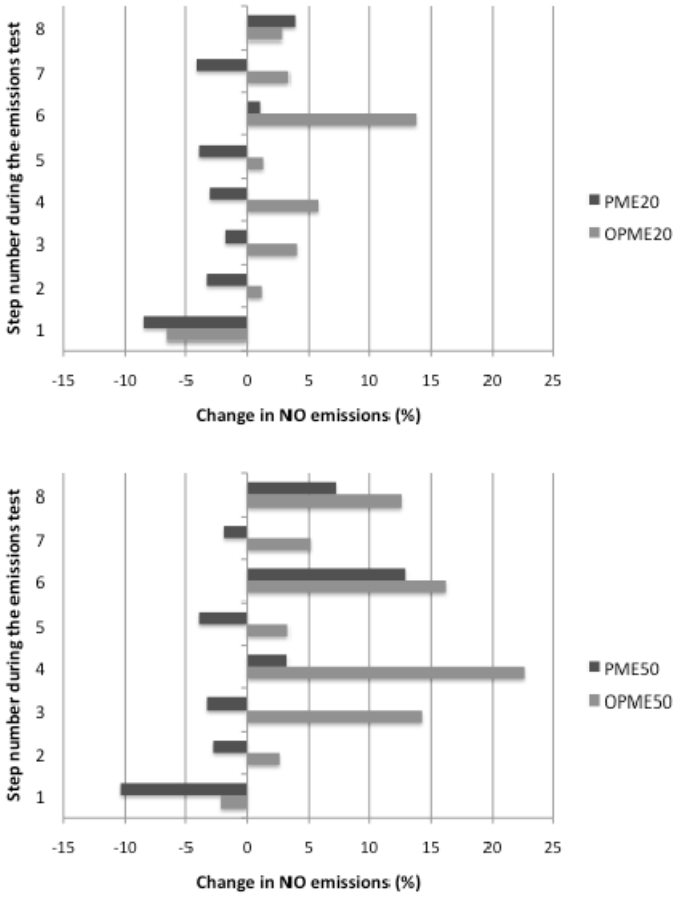

Figure 2.13. Percent changes in NO exhaust emissions of a Perkins engine fuelled with different blends of OPME and PME compared to diesel fuel (a) 20% biodiesel/80% diesel fuel; (b) 50% biodiesel/50% diesel fuel blends

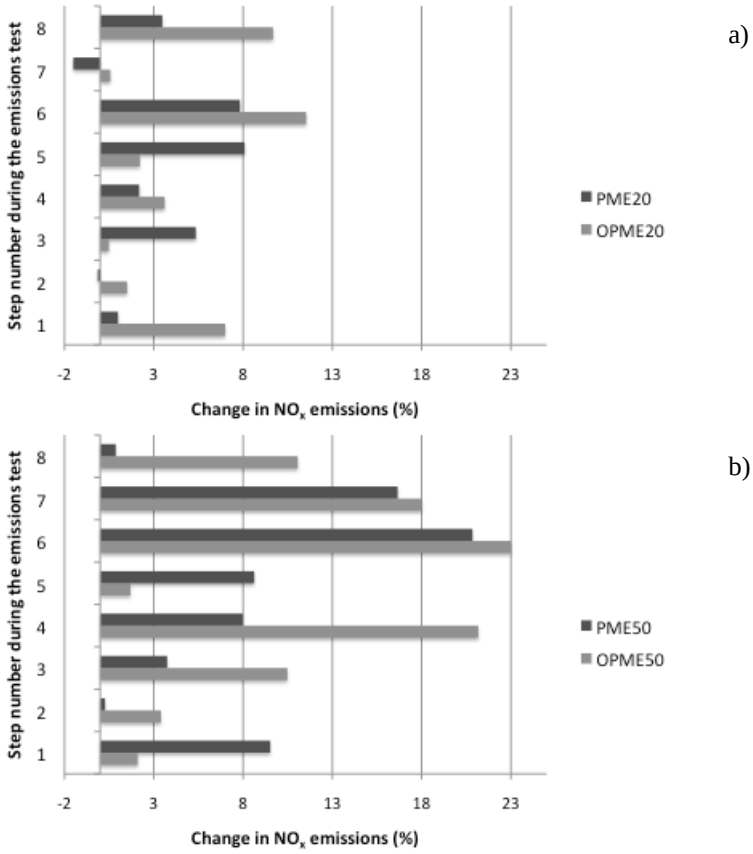

Figure 2.14. Percent changes in NO_x exhaust emissions of a Perkins engine fuelled with different blends of OPME and PME compared to diesel fuel (a) 20% biodiesel/80% diesel fuel; (b) 50% biodiesel/50% diesel fuel blends

2.2.5 Conclusions

A set of engine tests using OPME and PME blended with diesel fuel have proved that 20% and 50% (v/v) blends of biodiesel could be an attractive alternative to partially substitute fossil fuels and to reduce some exhaust and noise emissions. A strong correlation between maximum SPL and loudness was found. Moreover, it was observed that both sets of blends

improve the engine sound quality. During this field trial, high percentage of biodiesel from saturated fatty acid methyl esters (PME) in blends depicted the higher attenuation of the maximum engine noise in terms of loudness, while high percentage of biodiesel from monounsaturated fatty acid methyl esters (OPME) in blends achieved the maximum attenuation of roughness. In addition, roughness attenuation was found to be most meaningful than loudness when the blends were used. Generally, the use of both PME and OPME blends allows a significant reduction of CO emissions. In addition, lower NO exhaust emissions were observed when PME blends were used instead of OPME blends. In this way, although both sets of blends are expected to behave in a more pleasant way (especially when a higher content of OPME and PME is used in the blends), the saturation degree of the raw materials used to produce biodiesel seems to have a positive influence over air and noise emissions.

2.3 Influence of fatty acids saturation degree over exhaust and noise emissions through biodiesel combustion

2.3.1 Abstract

Environmental concerns are driving the scientific community to search for alternative fuels to substitute fossil-based ones. In this context, biodiesel is probably the most extended alternative to fuel diesel engines due to its renewable nature. In fact, the EU members aim at increasing the market share of biofuels within the coming years. However, the chemical composition of the raw materials used to produce biodiesel is variable, thus providing a wide range of types of biodiesel showing diverse affinity to diesel engines (cold weather behavior properties, etc.). Moreover, depending on the fuel properties, engine exhaust and noise emissions may be affected. For these reasons, it is important to increase the knowledge about the implications of biodiesel chemical composition and properties over engine exhaust and noise emissions. An experimental study with vegetable oils (covering a wide range of fatty acids) to produce biodiesel has been carried out. Selected raw materials included highly, medium and low saturated fatty acids, i.e. palm, sunflower, olive-pomace, coconut and linseed oil. Later, their methyl esters blended with diesel fuel were tested in

a direct injection diesel engine. Effects of chemical properties of biodiesel on exhaust and noise emissions have been studied at several engine operating conditions. In general terms, results showed results showed that the use of biodiesel/diesel fuel blends reduced the emissions of CO and noise, , thus improving the sound quality, although, NO_x increased. Particularly, it was found that the higher the unsaturation degree the higher the emission of NO_x and the higher the reduction of CO emissions. A linear correlation between fatty acids saturation level and sound pressure level was found at high power values. In sum, the use of unsaturated biodiesel as partial diesel fuel substitute is strongly recommended to improve CO and NO_x emissions, besides engine sound quality, therefore making the engine sound more pleasant.

2.3.2 Introduction

Due to the increasing interest in environmental problems and also motivated by the European legislation, the reduction of noise and pollutant emissions is one of the main targets for vehicle manufactures. Last years and mainly due to their lower fuel consumption, compression ignition engine cars, commonly known as diesel vehicles, have increased their share in the European passenger car market, in detriment of spark ignition engines-based cars. In fact, about one-third of the vehicles sold in the EU and the States are diesel powered [59]. Moreover, diesel engines are also used in industrial activities, power generators and construction. However, provided that engines are fuelled with fossil fuels, being highly responsible of the increase of hazardous pollutants to both humans and environment, alternatives to petroleum-based fuels are needed. Because it is produced from renewable sources and can be produced domestically, biodiesel has emerged as an alternative to petroleum diesel fuel [52].

Biodiesel consists in monoalkyl esters of long chain fatty acids derived from renewable feedstocks, such as vegetable oils, animal fats or microorganisms [60, 61]. It is commonly composed of fatty acid methyl esters (FAME) that can be prepared from triglycerides by transesterification with methanol. Biodiesel is an attractive alternative fuel for diesel engines because it can be used in its pure form or in any combination with diesel fuel to create a stable biodiesel blend.

When used in diesel engines, biodiesel usually exhibits combustion-related advantages, including reductions in carbon monoxide (CO), unburned hydrocarbon (UHC) and PM emissions [6]. The reduction of these emissions is mainly credited to the physicochemical properties of biodiesel, i.e. density, bulk modulus, cetane number and heat capacity, among many others.

However, there are also several combustion-related disadvantages, obviously due to biodiesel chemical composition. Owing higher oxygen content, FAME exhibits lower heating values than fossil diesel fuel. So, to achieve adequate engine power and power, an increasing of injection volumes is need [62]. This fact results in a larger biodiesel fuel requirement to achieve the same brake power level as diesel fuel, resulting in higher specific fuel consumptions. Moreover, many authors have found that for some operating conditions, biodiesel combustion emits more NO_x than conventional diesel fuel [63, 64]. The reduction of NO_x exhaust emissions is one of the most important technical challenges facing biodiesel development, especially in view of the increasingly stricter exhaust emission regulations affecting diesel engines.

There are several raw materials being exploited commercially to produce biodiesel, consisting of edible fatty oils derived from different oleaginous plants. Several studies have proved the influence of the chemical structure of the raw material on the physicochemical properties of biodiesel [1, 65, 66], demonstrating the crucial importance of the raw materials used on biodiesel production. It has been shown that the presence of saturated fatty acids in biodiesel improves combustion properties such as cetane number (*CN*) and calorific value, despite their poor cold-flow properties. Unsaturated, especially polyunsaturated fatty acid esters exhibit lower melting points (which are desirable for improved low-temperature properties) but also low cetane numbers and reduced oxidative stability, which are undesirable for a diesel fuel [1, 29].

Moreover, several studies have demonstrated that chemical and physical fuel properties influence the quality of engine combustion [28, 30, 67]. Besides, diesel engine combustion may be considered the most important source of noise in a vehicle. For these reasons, the study of the influence of the fuel chemical and physical properties over sound quality is needed [68]. Furthermore, the ultimate advances in combustion

technologies, conceived to further reduce NO_x or PM to comply with the European regulations without penalties, may affect this issue. The self-ignition of air-fuel mixture is the origin of the combustion noise, which produces an important sudden pressure increase giving rise to the well-known diesel knock [69]. Additionally, in-cylinder pressure forces are strongly dependent on the combustion process, which is mainly dominated by the fuel-burning rate. Moreover, for a given combustion system, the fuel burning velocity is controlled by the fuel injection rate. In this sense, biodiesel from different raw materials (showing different physicochemical properties) may influence the engine combustion process, i.e. ignition quality, fuel stability, flow properties at low temperature and iodine number (according to European fuel standard EN 14214) [54]. Although research has provided results about exhaust and noise emissions of a diesel engine fuelled with biofuels [39, 51, 52, 56, 70], the influence of biodiesel on engine sound quality remains unknown.

The aim of this work is to study the influence of the oleaginous raw materials fatty acid saturation degree used to produce biodiesel (in terms of physical and chemical properties of raw materials) on exhaust and combustion noise emissions. A preliminary exhaust emission test of a direct injection diesel engine fuelled with biodiesel produced from five different vegetable oils with fatty acids covering a wide range of saturation degree: sunflower oil (SO), olive pomace oil (OPO), palm oil (PO), coconut oil (CO) and linseed oil (LO) will be carried out. Finally, the influence of the saturation degree over biodiesel sound quality will be reported.

2.3.3 Materials and Methods

2.3.3.1 Fuels properties

Biodiesel samples were produced after basic-catalyzed transesterification of five different vegetable oils showing a wide range of fatty-acid composition [21, 71].Sunflower and olive pomace oils were acquired from KOIPESOL (Sevilla, Spain), linseed oil was purchased from Guinama (Valencia, Spain), while palm and coconut oils were acquired from Quimics Dalmau (Barcelona, Spain).

KOH and methanol were the catalyst and alcohol used to produce

biodiesel through transesterification, respectively. KOH pellets [85% p.a. CODEX (USP_NF)] and methanol ACS-ISO were acquired from PANREAC (Barcelona, Spain).

Yield on FAME (% wt.) and fatty acid composition of each fatty acid methyl ester sample were analyzed following the EU standard EN 14103. Coconut and palm oil methyl ester yields were analyzed using the modified EN 14103 (the initial oven temperature was raised from 150 ºC to 220 ºC at 5 ºC/min, with this last temperature being held for 15 min) and using as internal standard methyl tridecanoate (C13:0) to make possible the separation of short-chain fatty acid esters (C12–C14) in the chromatogram [72]. A Perkin Elmer (Waltham, Massachusetts, USA) Clarius 500 chromatograph (GC) equipped with a flame ionization detector (FID) was used for gas chromatographic determinations. A 30 m x 0.25 mm Elite 5-ms Perkin Elmer capillary column (film thickness of 0.25 µm) was selected.

Each biodiesel was blended with no. 2 diesel fuel (20% and 50% vol/vol biodiesel/diesel fuel). The most important fuel properties are depicted in Table 2.5.

Table 2.5. Chemical and physical properties of the tested fuels

Fuel	**HCV (J/g)**	**C (%)**	**H (%)**	**O (%)**	***CN***	**μ at 40 ºC (mm^2/s)**
No.2 diesel fuel	42700	86.50	13.50	0.00	53.9	2.467
OPME20	42204	84.59	13.23	2.18	55.5	3.014
OPME50	41460	81.72	12.83	5.45	57.8	3.834
SME20	42147	84.65	13.17	2.18	53.6	2.913
SME50	41317	81.87	12.67	5.45	53.2	3.582
LME20	42078	84.72	13.09	2.19	51.8	2.788
LME50	41144	82.05	12.47	5.48	48.8	3.270
CME20	41804	83.97	13.24	2.79	55.8	2.704
CME50	40459	80.18	12.85	6.97	58.6	3.059
PME20	42154	84.48	13.26	2.26	57.5	3.102
PME50	41336	81.45	12.90	5.64	63.0	4.054

Kinematic viscosity (μ) was measured with a Canon–Fenske capillary viscometer immersed in a constant temperature (40ºC) bath, following the European norm EN ISO 3104. High calorific value (*HCV*) analysis were carried out following the ASTM D240 standard, using an IKA (Staufen, Germany) Bomb Calorimeter, model C200.

Cetane number (*CN*) for biodiesel was calculated using the expression:

$$CN = \sum \mathrm{X_{ME}}\ (\mathrm{wt.\%})CN_{ME} \tag{2.5}$$

where X_{ME} is the weight of each methyl ester (%) and CN_{ME} is the cetane number of individual methyl esters [54]. Following the same expression, an estimation of *CN* of biodiesel/diesel fuel blends was calculated.

The methodology and apparatus used to perform each analysis has been explained more in depth in section 2.1.3 in this chapter.

A first test was run with straight diesel fuel at the beginning, followed by a test run with the blends at 20% and 50% of methyl esters of olive pomace oil (OPME), palm oil (PME), sunflower oil (SME), coconut oil (CME) and linseed oil (LME), in order to compare exhaust emissions and brake-specific fuel consumption (*BSFC*) with the fuels. Before every biofuel blend change, the engine fuel lines were cleaned and the engine was left to run a sufficient period of time to stabilize at its new condition. Engine tests were run on the same engine and same day, in order to have almost the same conditions within the three repetitions of each test [22].

2.3.3.2 Noise characterization

As mentioned before, radiated noise from diesel engines can be broken down into mechanical noise and combustion noise. At the start of combustion, an abrupt pressure rise that causes an important oscillation of the gas inside the combustion chamber is produced. Besides, it also excites resonances of the gas inside the combustion chamber cavity. The latter is also a source of vibration and air-borne acoustics. The excitation force, namely combustion pressure, first distorts the engine structure in an impulsive manner and then the engine structure begins to vibrate. During

this movement, the piston impacts with the cylinder walls; this phenomenon, known as piston slap, is another major source of engine noise. Rotating parts, such as the flywheel and front pulley, can excite noise with harmonic components. Mechanical noise consists mainly of piston slap impacts, timing gear rattle, bearing impacts, fuel injection system operations and valve impacts [55]. In the last years, researchers have found the solution to cancel or minimize the noise in a vehicle through active noise control [10, 73, 74]. However, controlling the fuel burning speed and hence the pressure gradient of the gas in the cylinder by means of the most appropriate fuel based on its properties may be an efficient procedure for combustion noise reduction. Figure 2.15 summarizes diesel air-borne acoustic signal excitation forces and generation mechanisms, besides fuel physical properties, which may influence them.

Traditionally, despite FFT analysis, A-weighted sound pressure and effective perceived noise level have been recommended as noise methods, they are no effective to assess the quality of perceived sound. Moreover, reducing the emitted noise may not ensure a good sound quality, provided that human perception is a very complex mechanism and many factors influence the sound quality evaluation process. Nowadays, automotive manufactures have invested a lot of effort and money to improve the sound of their vehicles, being the acoustic features a vehicle sound signature. In fact, while the control of the overall noise is imperative to fulfill the current legislation, sound quality and comfort also play an essential role in the customers purchasing decision. Even very quiet noises that are not associated with quality or do not meet personal expectations become noticeable and are potential cause for customer complaints. Besides, forthcoming legislation establishes an increase of the presence of biodiesel in fossil-based diesel fuel, which could modify the vibro-acoustic perception of the engine, initially conceived to run on straight diesel fuel. For these reasons, it is important to study the influence of the use of biodiesel, straight and blended with diesel fuel, in engine performance and emissions, to take them into consideration in the early design phase.

As previously mentioned, to establish relevant metrics to sound perception, different attempts have been undertaken. However, metrics unsuccessfully reflect the complete human sound quality perception. Despite this, they are very useful to determine specific parameters related to

sound quality, like loudness, tonality, sharpness and roughness. Besides, the overall sound quality study must include a jury test provided by a panel of listeners. However, this last option is more expensive and time consuming than metrics for evaluation purposes, so it is usually rejected. The correct choice of sound quality metrics depends on each individual application and is the most important issue to ensure a successful sound evaluation. Therefore, before the analysis starts, it is important to establish the appropriate metrics for engine noise, as using wrong metrics can lead to misinterpretations. Provided that loudness and roughness have been proposed as the most important indicators for engine noise, they have been utilized in this research [10, 75]. These sound quality metrics are detailed in depth in section 2.1.3.5 of this chapter.

2.3.4 Results and discussion

Results on NO_x and CO emissions are depicted in Figures 2.16 and 2.17, respectively. It is interesting to underline the trend on NO_x emissions observed for the blends (Figure 2.16). In agreement with other authors, increasing the number of double bounds of fatty acid methyl esters, as a general trend, an increase on NO_x emissions is observed [8, 21, 22]. The higher the unsaturation degree of methyl esters the higher the ignition delay (lower *CN*), the adiabatic flame temperature (AFT) and the advance of injection (higher bulk modulus), consequently increasing NO_x emissions.

A drastic reduction on CO exhaust emissions was observed when biodiesel blends were used instead of diesel fuel, especially with CME blends (Figure 2.18). In general terms, the higher the unsaturation degree the higher the reduction of CO emissions; CME being the exception. Moreover, observing Figure 2.18, it is possible to appreciate that the content of oxygen in the fuel depicts a linear dependence with CO emissions. This result agrees with previous finding provided by other authors [28].

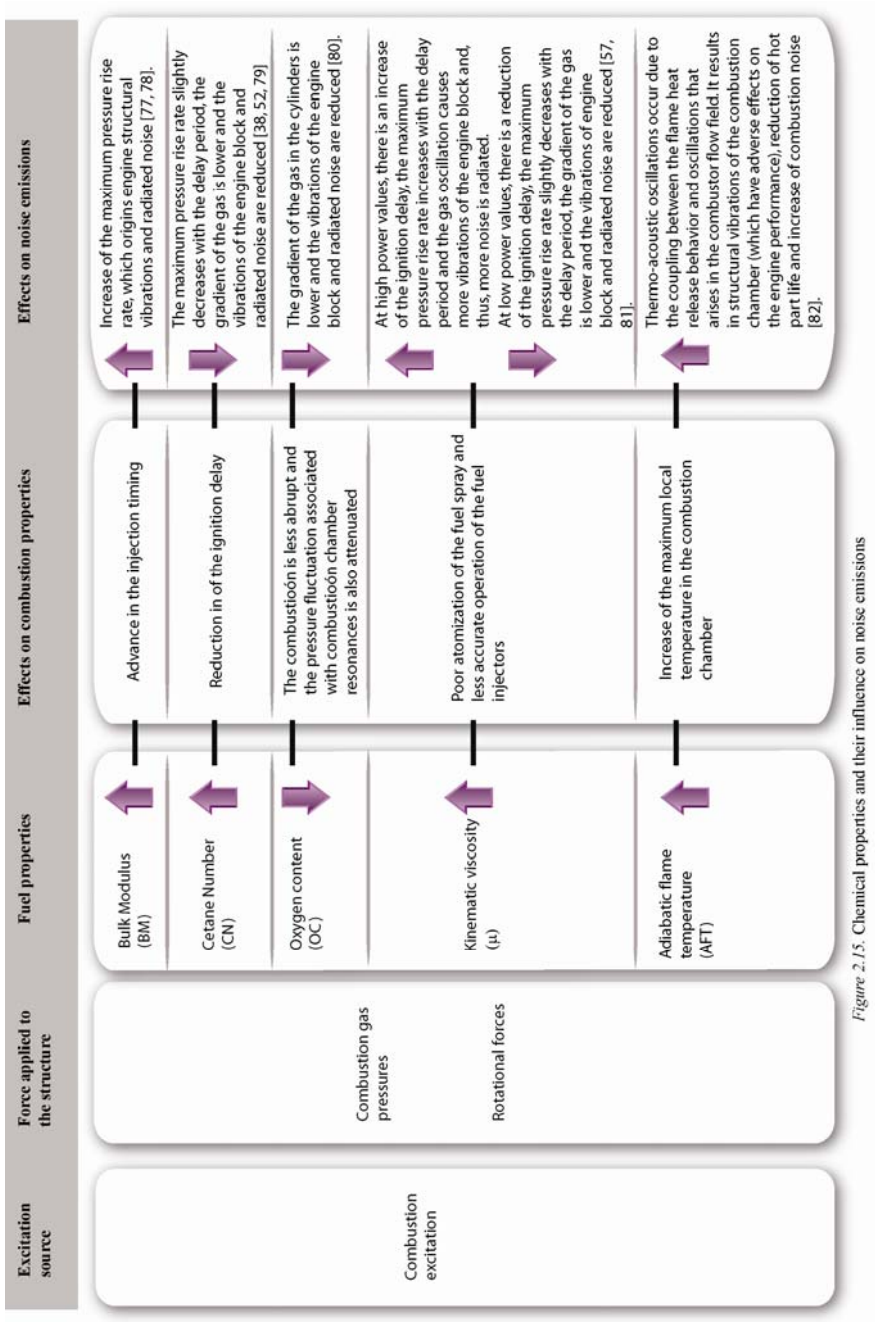

Figure 2.15. Chemical properties and their influence on noise emissions

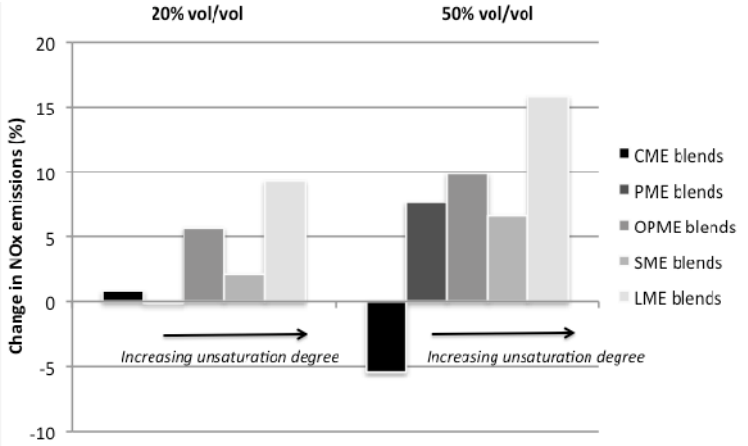

Figure 2.16. Percent changes in NO_x exhaust emissions of different blends of FAME compared to those of straight diesel fuel

In spite of the high number of publications concerning the analysis of the exhaust emissions derived from the use of biodiesel in diesel engines, there are only few works related to noise emission. Furthermore, to the best of our knowledge, there is no previous research describing listeners perception by means of sound quality metrics.

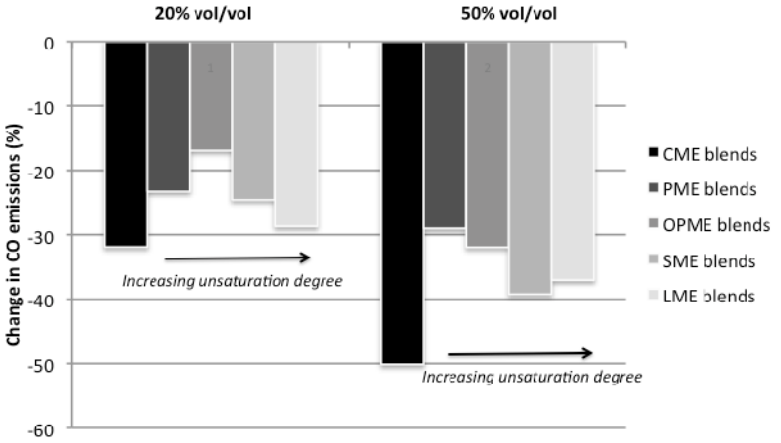

Figure 2.17. Percent changes in CO exhaust emissions of different blends of FAME compared to 100% diesel fuel

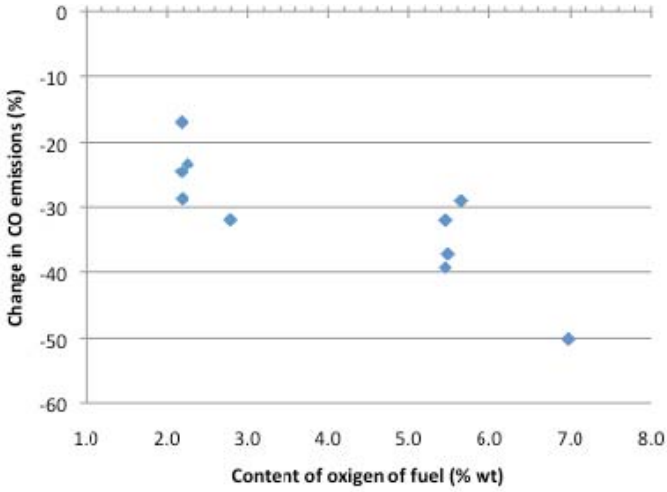

Figure 2.18. Percent changes in CO exhaust emissions of different blends of FAME compared to that of straight diesel fuel (% wt.)

Figure 2.19 shows the comparison of the mean sound pressure level for the biodiesel/diesel fuel blends sorted by their kinematic viscosity values (μ). The higher the value of μ (directly related to more saturated fatty acids) the higher the sound pressure level, especially under high power values and showing the reverse effect under very low power values. This influence of viscosity over noise emissions means that biodiesel blends with high μ cannot be recommended as a fuel substitute as they will provoke injection problems with impact on both injection and combustion efficiency [51]. In fact, high kinematic viscosity leads to poorer atomization of the fuel spray and less accurate operation of the fuel injectors, especially at low engine operating temperature [3]. Spray properties may be altered due to differences in the viscosity value of the fuels. Affected spray properties may include droplet size, droplet momentum and hence degree of mixing and penetration, evaporation rate and radiant heat transfer rate. A change in any of these properties might lead to different relative duration of the premixed *versus* diffusional burn regimes [3].

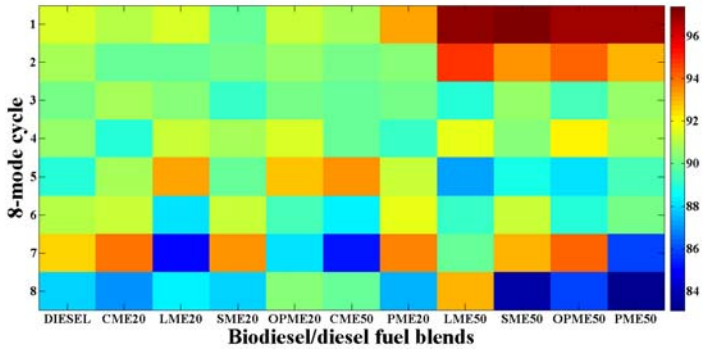

Figure 2.19. Spectrogram of sound level (dB) for biodiesel/diesel fuel blends and straight diesel fuel at several engine operating conditions

The effect of the increase of *CN* on total loudness at several engine operating conditions may be seen in Figure 2.20 (biodiesel blends being sorted by increasing *CN*). Concerning total loudness, the maximum values are achieved under high power conditions, thus suggesting *CN* provides the dominant effect. The higher the *CN* (directly correlated to the saturation degree) the higher the total loudness under high power values, while medium and low power values provide the opposite effect, total loudness decreasing when *CN* increases. In recent studies an increase of cylinder pressure and the rate of heat release in the premixed combustion phase increasing the number of double bounds of FAME was observed [34]. Provided that combustion noise originates from cylinder pressure, it may be inferred that combustion pressure rise rate exhibits slight decrease with engine speed due to the increased turbulence and improved mixing between air and fuel. This may be related to the increased cycle temperature when more fuel is injected, which can reduce both the ignition delay period and the pressure rise rate.

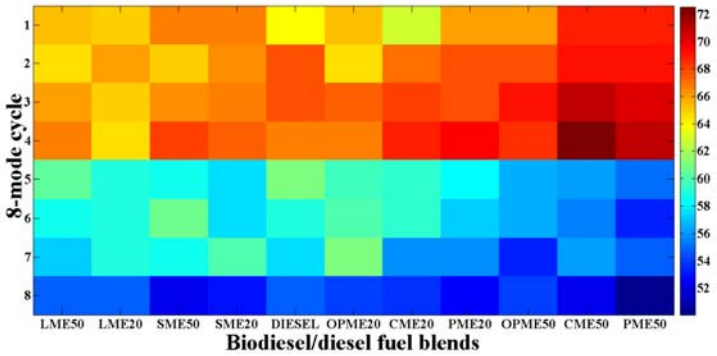

Figure 2.20. Spectrogram of total loudness level (Sone) for biodiesel/diesel fuel blends and straight diesel fuel at several engine operating conditions

Also, the reduction of the maximum pressure rise rate may have resulted from the improved *CN* and reduced ignition delay period provided by the biodiesel/diesel fuel blends. The higher the ignition delay period the higher the fuel injected before ignition starts [67]. Thus, the combustion pressure rise rate increases as more mass is exploded, which causes the noise to increase.

In Figure 2.21, the spectrogram of total roughness for biodiesel/diesel fuel blends at several operating conditions is presented. This plot shows that total roughness content decreases increasing unsaturation degree,, with the exception of CME blends. It is possible to observe that the total roughness follows the same trend that CO emissions. This can also be explained by the oxygen content having increased cylinder pressure with higher temperatures [28]. This increase of pressure may originate more forces in combustion chamber and therefore, more vibrations which can be transmitted through power train. Acoustic roughness is defined at medium frequency modulation of the engine noise. The main cause of roughness is a medium frequency vibration of the power train, which modules radiated noise. Generally, medium frequency vibration is caused by dynamics of engine moving parts, i.e. crankshaft, camshafts, etc. Moreover, insufficient power train rigidity may amplify vibration amplitudes. For a three-cylinder engine, it is especially important if the engine is not equipped with

balancing shaft, because vehicle structure modes can be excited causing more undesired low frequency vibration of passenger seat or drive wheel. Particularly, high load and low engine speed are penalising for passenger vibration comfort. From the results achieved with the blends it may be inferred that total roughness level is attenuated compared to the use of diesel fuel, thus reducing the vibrations of engine and power train. In this sense, taking into account the physical and chemical properties shown in Figure 2.15, the higher acoustic roughness values depicted by diesel fuel may be correlated with its low viscosity.

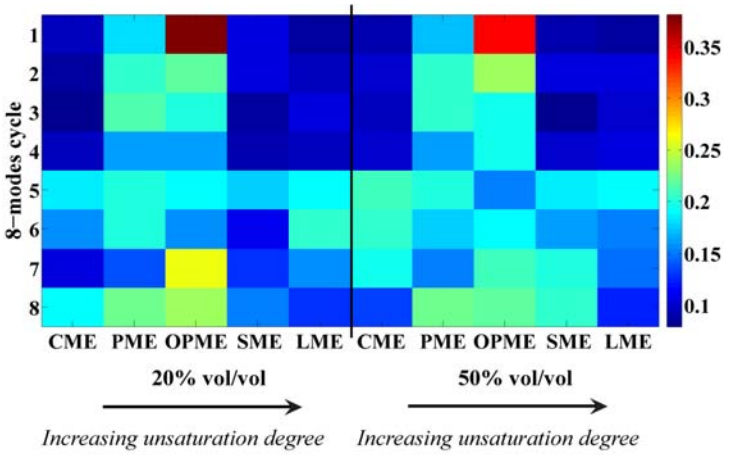

Figure 2.21. Total roughness level (Asper) for biodiesel/diesel fuel blends at several engine operating conditions

2.3.5 Conclusions

The influence of the saturation degree of fatty acid methyl esters (FAME) over noise and exhaust emissions has been studied. A series of engine tests performed under controlled road conditions with blends of biodiesel (covering a wide range of fatty acid composition) in diesel fuel showed the higher the number of double bonds (higher unsaturation degree) the higher the emission of NO_x and the higher the reduction of CO emissions. In general terms, NO_x emissions increased when biodiesel was used to substitute diesel fuel, however a reduction of CO and noise

emissions was achieved. In this sense, a linear correlation between kinematic viscosity (saturation level) and sound pressure level was found at high power values. In sum, the use of mono- and poly-unsaturated biodiesel as partial diesel fuel substitute is strongly recommended to improve CO and NO_x emissions, besides engine sound quality, therefore making the engine sound more pleasant.

2.4 References

[1] G. Knothe, "Designer" biodiesel: Optimizing fatty ester (composition to improve fuel properties, Energy & Fuels, 22 (2008) 1358-1364.

[2] M.J. Ramos, C.M. Fernandez, A. Casas, L. Rodriguez, A. Perez, Influence of fatty acid composition of raw materials on biodiesel properties, Bioresource Technology, 100 (2009) 261-268.

[3] M.S. Graboski, R.L. McCormick, Combustion of fat and vegetable oil derived fuels in diesel engines, Progress in Energy and Combustion Science, 24 (1998) 125-164.

[4] M. Lapuerta, O. Armas, R. Ballesteros, J. Fernandez, Diesel emissions from biofuels derived from Spanish potential vegetable oils, Fuel, 84 (2005) 773-780.

[5] M.P. Dorado, E. Ballesteros, J.M. Arnal, J. Gomez, F.J. Lopez, Exhaust emissions from a Diesel engine fueled with transesterified waste olive oil, Fuel, 82 (2003) 1311-1315.

[6] M. Lapuerta, J.M. Herreros, L.L. Lyons, R. Garcia-Contreras, Y. Briceno, Effect of the alcohol type used in the production of waste cooking oil biodiesel on diesel performance and emissions, Fuel, 87 (2008) 3161-3169.

[7] A. Tsolakis, A. Megaritis, M.L. Wyszynski, K. Theinnoi, Engine performance and emissions of a diesel engine operating on diesel-RME (rapeseed methyl ester) blends with EGR (exhaust gas recirculation), Energy, 32 (2007) 2072-2080.

[8] S.A. Basha, K.R. Gopal, S. Jebaraj, A review on biodiesel production, combustion, emissions and performance, Renewable and Sustainable Energy Reviews, 13 (2009) 1628-1634.

[9] R.L. McCormick, M.S. Graboski, T.L. Alleman, A.M. Herring, K.S. Tyson, Impact of biodiesel source material and chemical structure on emissions of criteria pollutants from a heavy-duty engine, Environ. Sci. Technol, 35 (2001) 1742–1747.

[10] L.P.R. de Oliveira, K. Janssens, P. Gajdatsy, H. Van der Auweraer, P.S. Varoto, P. Sas, W. Desmet, Active sound quality control of engine induced cavity noise, Mechanical Systems and Signal Processing, 23 (2009) 476-488.

[11] M.H. Fouladi, M.J.M. Nor, A.K. Ariffin, Spectral analysis methods for vehicle interior vibro-acoustics identification, Mechanical Systems and Signal Processing, 23 (2009) 489-500.

[12] M.J.M. Nor, M.H. Fouladi, H. Nahvi, A.K. Ariffin, Index for vehicle acoustical comfort inside a passenger car, Applied Acoustics, 69 (2008) 343-353.

[13] H. Fastl, The psychoacoustics of sound-quality evaluation, Acustica, 83 (1997) 754-764.

[14] A. Miskiewicz, Letowski, T., Psychoacoustic in the automotive industry, Acustica, 83 (1999) 5.

[15] E. Zwicker, H. Fastl, C. Dalmayr, BASIC-program for calculating the loudness of sounds from their 1/3-oct band spectra according to ISO 532B, Acustica, 55 (1984) 4.

[16] E. Zwicker, H. Fastl, U. Widmann, K. Kurakata, S. Kuwano, S. Namba, Program for calculating loudness according to DIN 45631 (ISO 532B), Journal of Acoustic Society of Japan, 12 (1991) 3.

[17] D. Berckmans, P. Kindt, P. Sas, W. Desmet, Evaluation of substitution monopole models for tire noise sound synthesis, Mechanical Systems and Signal Processing, 24 (2010) 240-255.

[18] S.G. Park, H.J. Sim, J.H. Yoon, J.E. Jeong, B.J. Choi, J.E. Oh, Analysis of the HVAC system's sound quality using the design of experiments, Journal of Mechanical Science and Technology, 23 (2009) 2801-2806.

[19] Y.-K. Oh, H.-J. Kim, S. Park, M.-S. Kim, D.D.Y. Ryu, Metabolic-flux analysis of hydrogen production pathway in Citrobacter amalonaticus Y19, International Journal of Hydrogen Energy, 33 (2008) 1471-1482.

[20] Y. You, Jeon, Y., Just noticeable differences of sound quality metrics of refrigerators noise, in: Proceedings of 19th ICA, Madrid, 2007.

[21] S. Pinzi, J.M. Mata-Granados, F.J. Lopez-Gimenez, M.D. Luque de Castro, M.P. Dorado, Influence of vegetable oils fatty-acid composition on biodiesel optimization, Bioresource Technology, 102 (2011) 1059-1065.

[22] M.P. Dorado, E. Ballesteros, J.M. Arnal, J. Gomez, F.J.L. Gimenez, Testing waste olive oil methyl ester as a fuel in a diesel engine, Energy & Fuels, 17 (2003) 1560-1565.

[23] K. Genuit, The sound quality of vehicle interior noise: a challenge for the NVH-engineers, International Journal Vehicle Noise and Vibration, 1 (2004) 11.

[24] H. Fastl, E. Zwicker, Psycho-Acoustics: Facts and Models, Springer, New York, 2007.

[25] W. Aures, A procedure for calculating auditory roughness, Acustica, 58 (1985) 268-281.

[26] T.J. Coen, N.; Van de Ponseele, P.; Goethals, I.; De Baerdemaeker, J.; De Moor, B., Engine sound comfortability: Relevant sound quality parameters and classification, in: Proceeding of IFAC 2005, Prague, Czech Republic, 2005, pp. 6.

[27] K.F. Hansen, M.G. Jensen, Chemical and biological characteristics of exhaust emissions from a diesel engine fuelled with rapeseed oil methyl ester (RME), SAE paper, 971689 (1997).

[28] P. Rounce, A. Tsolakis, P. Leung, A.P.E. York, A comparison of diesel and biodiesel emissions using dimethyl carbonate as an oxygenated additive, Energy and Fuels, 24 (2010) 4812-4819.

[29] S. Pinzi, D. Leiva, G. Arzamendi, L.M. Gandia, M.P. Dorado, Multiple response optimization of vegetable oils fatty acid composition to improve

biodiesel physical properties, Bioresource Technology, 102 (2011) 7280-7288.

[30] M. Lapuerta, O. Armas, J. Rodriguez-Fernandez, Effect of biodiesel fuels on diesel engine emissions, Progress in Energy and Combustion Science, 34 (2008) 198-223.

[31] C.D. Rakopoulos, D.T. Hountalas, T.C. Zannis, Y.A. Levendis, Operational and enviromental evaluation of diesel engines burning oxygen-enriched intake air or oxygen-enriched fuels: a review, SAE paper, 2004-01-2924 (2004).

[32] S. Pinzi, P. Rounce, J.M. Herreros, A. Tsolakis, M.P. Dorado, The effect of biodiesel fatty acid composition on combustion behavior and diesel engine exhaust emissions, Fuel, (In press).

[33] A.L. Boehman, D. Morris, J. Szybist, E. Esen, The Impact of the Bulk Modulus of Diesel Fuels on Fuel Injection Timing, Energy & Fuels, 18 (2004) 1877-1882.

[34] A. Schönborn, N. Ladommatos, J. Williams, R. Allan, J. Rogerson, The influence of molecular structure of fatty acid monoalkyl esters on diesel combustion, Combustion and Flame, 156 (2009) 1396-1412.

[35] G.A. Ban-Weiss, J.Y. Chen, B.A. Buchholz, R.W. Dibble, A numerical investigation into the anomalous slight NOx increase when burning biodiesel; A new (old) theory, Fuel Processing Technology, 88 (2007) 659-667.

[36] K. Schmidt, J. Van Gerpen, The Effect of Biodiesel Fuel Composition on Diesel Combustion and Emissions, SAE paper, 961086 (1996).

[37] F. Payri, A. Broatch, X. Margot, L. Monelletta, Sound quality assessment of Diesel combustion noise using in-cylinder pressure components, Measurement Science & Technology, 20 (2009).

[38] N. Bezaire, K. Wadumesthrige, K.Y.S. Ng, S.O. Salley, Limitations of the use of cetane index for alternative compression ignition engine fuels, Fuel, 89 (2010) 3807-3813.

[39] C.D. Rakopoulos, A.M. Dimaratos, E.G. Giakoumis, D.C. Rakopoulos, Study of turbocharged diesel engine operation, pollutant emissions and combustion noise radiation during starting with bio-diesel or n-butanol diesel fuel blends, Applied Energy, 88 (2011) 3905-3916.

[40] A.J. Torregrosa, A. Broatch, J. Martin, L. Monelletta, Combustion noise level assessment in direct injection Diesel engines by means of in-cylinder pressure components, Measurement Science & Technology, 18 (2007) 2131-2142.

[41] M.H. Jayed, H.H. Masjuki, M.A. Kalam, T.M.I. Mahlia, M. Husnawan, A.M. Liaquat, Prospects of dedicated biodiesel engine vehicles in Malaysia and Indonesia, Renewable & Sustainable Energy Reviews, 15 (2011) 220-235.

[42] S. Pinzi, I.L. Garcia, F.J. Lopez-Gimenez, M.D. Luque de Castro, G. Dorado, M.P. Dorado, The ideal vegetable oil-based biodiesel composition: a review of social, economical and technical implications, Energy & Fuels, 23 (2009) 2325–2341.

[43] S. Pinzi, F.P. Capote, J.R. Jimenez, M.P. Dorado, M.D.L. de Castro, Flow injection analysis-based methodology for automatic on-line monitoring and quality control for biodiesel production, Bioresource Technology, 100 (2009) 421-427.

[44] M.D. Redel-Macías, S. Pinzi, D. Leiva, A.J. Cubero-Atienza, M.P. Dorado, Air and noise pollution of a diesel engine fueled with olive pomace oil methyl ester and petrodiesel blends, Fuel, 95 (2012) 615-621.

[45] L. Pruvost, Q. Leclere, E. Parizet, Diesel engine combustion and mechanical noise separation using an improved spectrofilter, Mechanical Systems and Signal Processing, 23 (2009) 2072-2087.

[46] T. Tousignant, Wellmann, T., Govindswamy, K.,, Application of combustion sound level (CSL) analysis for powertrain NVH development and benchmarking, SAE paper 2009-01-2168, (2009).

[47] F. Payri, A.J. Torregrosa, A. Broatch, L. Monelletta, Assessment of diesel combustion noise overall level in transient operation, International Journal of Automotive Technology, 10 (2009) 761-769.

[48] D. Anderton, Relation between combustion system and noise, SAE paper 1979-790270, (1979).

[49] F. Payri, A. Broatch, B. Tormos, V. Marant, New methodology for in-cylinder pressure analysis in direct injection diesel engines - application to combustion noise, Measurement Science & Technology, 16 (2005) 540-547.

[50] N.W. Alt, J. Nehl, S. Heuer, M.W. Schlitzer, Prediction of combustion

process induced vehicles interior noise, SAE paper 2003-01-1435, (2003).

[51] Y. Bayhan, E. Kilic, S. Arin, Effect of Pure Biodiesel on Fuel Injection Systems and Noise Level in Agricultural Diesel Engines, Ama-Agricultural Mechanization in Asia Africa and Latin America, 41 (2010) 78-81.

[52] M. Bunce, D. Snyder, G. Adi, C. Hall, J. Koehler, B. Davila, S. Kumar, P. Garimella, D. Stanton, G. Shaver, Optimization of soy-biodiesel combustion in a modern diesel engine, Fuel, 90 (2011) 2560-2570.

[53] E. Zwicker, H. Fastl, Psychoacoustic: Facts and Models, second ed., Heidelberg, 1999.

[54] M.J. Ramos, C.M. Fernández, A. Casas, L. Rodríguez, Á. Pérez, Influence of fatty acid composition of raw materials on biodiesel properties, Bioresource Technology, 100 (2009) 261-268.

[55] A. Albarbar, F. Gu, A.D. Ball, Diesel engine fuel injection monitoring using acoustic measurements and independent component analysis, Measurement, 43 (2010) 1376-1386.

[56] Y.H.Y. Haik, M.Y.E. Selim, T. Abdulrehman, Combustion of algae oil methyl ester in an indirect injection diesel engine, Energy, 36 (2011) 1827-1835.

[57] A.J. Torregrosa, A. Broatch, R. Novella, L.F. Monico, Suitability analysis of advanced diesel combustion concepts for emissions and noise control, Energy, 36 (2011) 825-838.

[58] A. Schonborn, N. Ladommatos, J. Williams, R. Allan, J. Rogerson, The influence of molecular structure of fatty acid monoalkyl esters on diesel combustion, Combustion and Flame, 156 (2009) 1396-1412.

[59] M.A. Kalam, H.H. Masjuki, M.H. Jayed, A.M. Liaquat, Emission and performance characteristics of an indirect ignition diesel engine fuelled with waste cooking oil, Energy, 36 (2011) 397-402.

[60] P.S. Luque R, Campelo JM, Ruiz JJ, Lopez I, Luna D, Marinas JM, Romero AA, Dorado MP, Biofuels for Transport: Prospects and Challenges, in Emerging Enviromental Technologies, Springer:New York (USA), 2010.

[61] M. Dorado, Raw materials to produce low cost biodiesel, in: A. Nag (Ed.) Biofuels refining and performance, 2008, pp. 107-148.

[62] M. Mittelbach, Remschmidt, C.,, Biodiesel: The comprehensive

handbook, Graz, Austria:Martin Mittelbach, 2004.

[63] G. Knothe, C.A. Sharp, T.W. Ryan, Exhaust emissions of biodiesel, petrodiesel, neat methyl esters, and alkanes in a new technology engine, Energy & Fuels, 20 (2006) 403-408.

[64] J.P. Szybist, J.H. Song, M. Alam, A.L. Boehman, Biodiesel combustion, emissions and emission control, Fuel Processing Technology, 88 (2007) 679-691.

[65] M. Canakci, A.N. Ozsezen, E. Arcaklioglu, A. Erdil, Prediction of performance and exhaust emissions of a diesel engine fueled with biodiesel produced from waste frying palm oil, Expert Systems with Applications, 36 (2009) 9268-9280.

[66] G. Knothe, K.R. Steidley, Kinematic viscosity of biodiesel fuel components and related compounds. Influence of compound structure and comparison to petrodiesel fuel components, Fuel, 84 (2005) 1059-1065.

[67] N. Ladommatos, M. Parsi, A. Knowles, The effect of fuel cetane improver on diesel pollutant emissions, Fuel, 75 (1996) 8-14.

[68] K.K. InSoo J., New experimental approach for developing combustion noise of diesel engines, in: Aachen Acoustic Colloquium, Aachen, 2010, pp. 81-89.

[69] Y. Ren, R.B. Randall, B.E. Milton, Influence of the resonant frequency on the control of knock in diesel engines, Proceedings of the Institution of Mechanical Engineers Part D-Journal of Automobile Engineering, 213 (1999) 127-133.

[70] Y.D. Bao, Y. He, Study on noise of rapeseed oil blends in a single-cylinder diesel engine, Renewable Energy, 31 (2006) 1789-1798.

[71] S. Pinzi, L.M. Gandía, G. Arzamendi, J.J. Ruiz, M.P. Dorado, Influence of vegetable oils fatty acid composition on reaction temperature and glycerides conversion to biodiesel during transesterification, Bioresource Technology, 102 (2011) 1044-1050.

[72] S. Schober, I. Seidl, M. Mittelbach, Ester content evaluation in biodiesel from animal fats and lauric oils, European Journal of Lipid Science and Technology, 108 (2006) 309-314.

[73] C. Bohn, A. Cortabarria, V. Hartel, K. Kowalczyk, Active control of

engine-induced vibrations in automotive vehicles using disturbance observer gain scheduling, Control Engineering Practice, 12 (2004) 1029-1039.

[74] M.O. Tokhi, R. Wood, Active noise control using radial basis function networks, Control Engineering Practice, 5 (1997) 1311-1322.

[75] L.C. Meher, D.V. Sagar, S.N. Naik, Technical aspects of biodiesel production by transesterification - a review, Renewable & Sustainable Energy Reviews, 10 (2006) 248-268.

Chapter 3

Models of noise prediction in biodiesel

3.1 Multivariable models for noise prediction based on chemical composition of biodiesel blended with diesel fuel

3.1.1 Abstract

Biodiesel is considered a promising alternative to substitute petroleum-based diesel fuel. Cetane number, viscosity, oxygen content and higher heating value are among the most important fuel properties that affect engine noise emissions, provided that they are involved in combustion quality. In the present work, predictive noise emission models including previous properties as input data have been developed. To analyze the influence of the fuel chemical composition on engine noise emission, simple multivariable models have been proposed. In addition, the trend of the relationship between exhaust emissions, speed, power and noise emission has been studied. To carry out this work, the characterization of several biodiesel blends (20% and 50% in volume with diesel fuel) from five different vegetable oils, i.e. sunflower, olive pomace, linseed, palm and coconut oils has been included. It can be concluded that chemical properties, as viscosity, depict a strong influence on engine noise emission.

3.1.2 Introduction

In recent years, exhaust emissions released by vehicles are showing an increase together with the increase in the number of diesel cars [1]. Moreover, the close relationship between the number of vehicles and fuel consumption makes necessary to find out new fuels [2]. Biodiesel, commonly known as fatty acid methyl esters (FAME), is an alternative fuel with great developing potential due to its environmentally friendly nature, non-toxicity and biodegradability compared to diesel fuel [3]. Despite the fact that its main fuel properties, *i.e.* cetane number (*CN*), energy content, kinematic viscosity (μ) and phase changes [4] are similar to those of diesel fuel, there are differences in some physical and chemical properties that could affect the combustion process, injection mechanism, fuel spray behavior, and consequently, influence the emission of pollutants [5]. Also, the influence of biodiesel properties on combustion noise has been researched. Combustion noise is determined by the cylinder pressure rise rate, specifically its gradient with respect to crank angle, during the engine cycle [6]. This rate is influenced by a variety of parameters, such as injection timing and ignition delay, which also affect the speed of burning [7, 8].

CN is an important fuel property in relation to combustion noise [9, 10]. This parameter is an indicator of combustion quality and provides information about the ignition delay (*ID*) of a diesel fuel upon injection into the combustion chamber. Lower *CN* indicates longer ignition delay period, hence more pronounced pressure gradients and therefore higher noise radiation. Higher *CN* guarantees good cold start behavior and a smooth run of the engine [9].

Kinematic viscosity influences both injection and combustion efficiency [11-13]. Low viscosity leads to better fuel atomization, the breakup of the bulk liquid jets into small droplets by using an atomizer and mixes to form a fuel air mixture, burning rapidly resulting in a large percentage of fuel burned in the premixed burning phase and a greater release of heat [13]. Also, the use of fuel with high viscosity negatively affects the injection, atomization and mixing process of the fuel with air. With the reduction of the viscosity, the ignition delay period is reduced and the fuel mixes faster and better with hot air to achieve the self-ignition

temperature, thus it self-ignites faster. Decreasing the ignition delay period causes the combustion to start faster and smoother for a smaller amount of injected fuel, with less pressure rise rate and thus, less combustion noise [14].

The presence of oxygen in a fuel enhances the combustion in several ways, achieving a complete combustion, helping to prevent the formation of local rich zones in the combustion chamber and the formation of particle precursors. When there is not enough oxygen, less fuel burnt means less useful power, as well as emissions of unburned hydrocarbons (HC) and carbon monoxide (CO) [15, 16]. It has been found that the peak of cylinder pressure increases in line with the increased proportion of oxygen in fuel [17], leading to an increment of the combustion noise.

With reference to the effects of the physical properties of biodiesel on the injection advance, a higher bulk modulus of biodiesel is connected to an advance in the start of injection timing. When biodiesel is injected, the pressure rise produced by the pump is achieved faster, due to the lower compressibility, and it also propagates faster towards the injectors as a consequence of its higher sound velocity. As a result, there is an advance in the injection of fuel with higher pressure and rate, corresponding to an increase of combustion noise [14, 18].

Another important physical property of fuel is the adiabatic flame temperature, which is an indicator of the maximum local temperature in the combustion chamber. It has been considered that most combustion oscillations or combustion instabilities are caused by the feedback interaction between natural acoustic modes of a combustor and the oscillations release rate [19]. Some experimental studies were carried out to characterize sound radiation from turbulent flames [20, 21]. Moreover, a methodology to predict noise radiation levels and the frequency peak of the radiated noise spectrum in turbulent premixed flames has been proposed [22].

With regard to biodiesel emissions, one of the most troublesome pollutants from DI engines is oxides of nitrogen (NO_x) [23-25]. It has been shown that NO_x emissions follow the same trend as combustion noise [8]. It may be due to the fact that both parameters are influenced by the same physical properties, like *CN* and oxygen concentration.

For practical purposes, efforts have been made to find out a wide range of useful methods to estimate some of the most important biodiesel physical and chemical properties from parameters related to its chemical structure [26-29]. However, in just a few studies, a direct correlation between the chemical structure of fatty acids and exhaust emissions has been found [30-32]. To the best of our knowledge, studies concerning models about noise emissions based on biodiesel chemical and physical properties are inexistent, thus more research is needed.

This work was developed as an answer to the need for simple and reliable methods to estimate noise emission based on biodiesel properties, thus preventing experimental work, which is difficult, costly and time consuming. For this purpose, several regression models have been developed. To predict the noise emission, some properties, like *CN*, μ, oxygen content and higher calorific value (*HCV*), were used. Moreover, the relationship between NO_x and noise emission has been stated by means of response surface models.

3.1.3 Materials and Methods

3.1.3.1 Fuel description and experimental set up

Fuel description and experimental set up have been depicted in section 2.3.3, chapter 2.

3.1.3.2 Modeling techniques

Combustion noise originates from the self-ignition of the air-fuel mixture, which produces an important sudden pressure increase giving rise to the well-known diesel knock [33]. It causes strong oscillations of the gas inside the combustion chamber inducing vibrations to the engine block. These block vibrations are caused by two excitation sources: the pressure forces, acting directly on the combustion chamber (piston motion) and mechanical forces, due to the pressure forces on the mechanical systems in the cylinder (piston slap, bearing clearances, etc) [34]. These pressure forces are strongly dependent on the combustion process and thus, on the fuel-burning rate. In a previous study, differences in radiated combustion noise

between olive-pomace oil methyl esters and diesel fuel were found [35]. These differences were mainly due to their different properties, such as *CN*, bulk modulus or μ. In accordance with the comments described above, several multiple surface response models have been developed in order to describe the relationship between noise and exhaust emissions and the properties of different biodiesel blends.

Multivariable regression models. The response surface model gives the relationships between several explanatory and one or more response variables. The case of one explanatory variable is called simple regression; more than one explanatory variable constitutes multiple regression. By means of a response surface model, the relationship between the independent and dependent variables have been described. In this case, the target variable is expressed as a combination of the attributes with predetermined weights, $y = \beta_0 + \beta_1 x + \beta_2 x^2 + \beta_3 x^3 + \cdots + \beta_j x^j + \varepsilon$ where $\beta_0, \rightleftharpoons, \beta_j$ are the weights to be estimated, *K* is the number of inputs and x_i is the *i*-th input variable. In this research, to predict the noise emission from a direct injection diesel engine Perkins AD-3-152 under the 8-mode cycle, different response surface models have been proposed. The target is to develop different models as simple as possible to show the influence of biodiesel properties and exhaust emissions (correlated with biodiesel combustion) on radiated noise. In this way, simple linear models such as $y = \beta_0 + \sum_{i=1}^{j} \beta_i x_i \varepsilon$, where *y* is the noise radiated and $x = (x, x^2, x^3, \ldots, x^k)$ is the vector of input variables that will later be specified for each model have been proposed. All models have been implemented using regression functions available in Matlab R2008a from MathWorks Inc (USA).

3.1.4 Results and discussion

Experimental data were collected while running the direct injection diesel engine Perkins AD 3-152 on sunflower oil methyl ester (SME), olive pomace oil methyl ester (OPME), palm oil methyl ester (PME), coconut oil methyl ester (CME) and linseed oil methyl ester (LME), all of them blended with diesel fuel (20% and 50% in volume) under the 8-mode cycle. For each model, *CN*, μ, oxygen content, higher calorific value (*HCV*), engine speed and power were considered independent variables. Moreover, the trend

between the most significant exhaust emissions, such as NO_x, CO, NO, and noise radiated was studied by means of response surface models, exhaust emissions being considered the independent variable. Results from the different models were evaluated based on the mean square error (MSE). Results show that the P-value for all proposed models is lower than 0.0001 (Table 3.1). Thus, there are statistically significant relationships between the variables, with more than 99.9% confidence level.

In addition, a holdout crossvalidation procedure was carried out in the experimental design using different functions from Matlab R2008a. The whole dataset *n* was divided into 3*n*/4 for training and *n*/4 for generalization proposes. Each model was performed using 88 points measured under the engine 8-modes cycle for 10 biodiesel blends and diesel fuel. Moreover, 30 holdout processes with different random splits of the data (by means of iterative loop) achieving 30 models were performed. For each model, the MSE and the standard deviation (SD) were recorded. The best model was selected based on the value of these parameters in the generalization set. Training results have not been considered since they are upward-biased.

Table 3.1. Multiple regression models for prediction of noise emissions based on biodiesel properties and diesel engine exhaust emissions

MSE (%)	**R^2**	**Model**	**Variables**			
			X_1	X_2	X_3	X_4
3.68	94.10	$y = 83.4628 - 0.0448665\,x_1 + 0.218615\,x_2 + 0.0799602\,x_3 + 0.00228615\,x_4$	*CN*	μ at 40 ºC (mm^2s^{-1})	Oxygen content (% wt.)	*n* (rpm)
5.30	90.51	$y = 13.2401 + 0.0089\,x_1 - 0.0356\,x_2 - 29.532\,x_3 - 2.1899\,x_3^2$	CO (ppm)	NO_x (ppm)	CO_2 (ppm)	---
3.76	98.45	$y = 80.2151 + 0.000147\,x_1 + 0.002468\,x_2 - 0.015888\,x_3$	*HCV (J/g)*	*n* (rpm)	*N (kW)*	---

3.1.4.1 Prediction of noise emission based on CN, μ, oxygen content and engine speed

In order to predict noise emission from biodiesel properties consideringengine speed (*n*), the following expression has been proposed:

Noise (dB) = 83.4628 – 0.0448665 CN + 0.218615 μ (40 ºC)(mm^2s^{-1}) *+0.0799602 O* (% wt) + *0.00228615 n* (rpm)

The model shows a coefficient of determination (R^2) of 94.10%. MSE depicts a low value (3.68), indicating prediction values are close to the experimental ones.

The coefficients of the model confirm the trends described by previous researches [35]. It can be observed that the higher the *μ* and the oxygen content the higher the noise emission. Moreover, the higher the *CN* the smaller the noise emission at a given speed. It is interesting to mention that the influence of *μ* on noise emission is stronger than that of *CN* and oxygen content as may be inferred from the higher value of its coefficient in the model. Viscosity affects the atomization quality, size of drop and penetration of fuel. Higher viscosity tends to form larger droplets on injection, which can cause poor fuel atomatization during the spray, increasing the engine deposits, the wear of both fuel pump elements and injectors, exhaust smoke and noise emissions. Besides, more energy to pump the fuel is needed [11, 12]. The effect of *CN*, *μ* and oxygen content at 2392 rpm of engine speed is shown in Figure 3.1 In this Figure, the modeled noise emission was evaluated by means of three-dimensional spectrograms, where red color indicates high noise and blue is used to show low noise. For the maximum value of oxygen content and *μ*, and lower *CN*, the noise emission increases (red color), achieving the lowest noise emission when *CN* and oxygen content decrease (blue color).

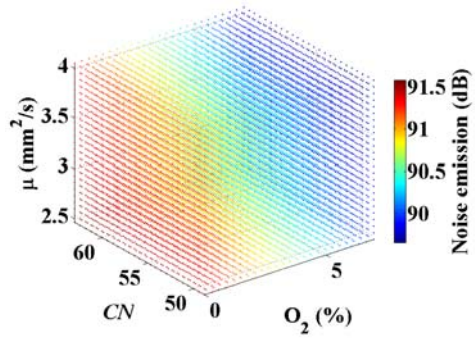

Figure 3.1. Response surface model considering *CN*, *μ at 40 ºC (mm²/s)*, oxygen content (%) and engine speed (2392 rpm)

3.1.4.2 Prediction of noise emission based on CO, NO_x and CO_2 emissions

The response surface model to predict noise emission based on CO, NO_x and CO_2 emissions, engine speed and power is given by the following expression:

$$Noise\ (dB) = 13.2401 + 0.0081\ CO\ (ppm) - 0.0356\ NO_x\ (ppm) - 29.532\ CO_2\ (ppm) - 2.1899\ (CO_2)^2$$

The model shows an R^2 of 90.51% and both MSE depicting a low values (5.30). CO is an intermediate combustion product that is formed in the absence of complete fuel oxidation and it has adverse effect on human health due to its toxicity [36, 37]. As can be observed from the model, lower NO_x reduce noise emissions. This result is consistent with the above explanation: timing advancement generally results in a more vigorous combustion process with higher temperatures in a smaller in-cylinder volume, leading an increase in NO_x emission and a decrease in noise radiated [38]. Moreover, modeled noise emissions increase drastically at high CO emissions, thus indicating the increase of the in-cylinder pressure. The same trend is showed by CO_2 emissions. The perfect combustion of a hydrocarbon should only produce CO_2 and H_2O. The higher the speed and CO_2 emissions the higher the noise emission, this may be attributed to an increased frequency of the combustion cycle [37]. Figure 3.2 plots the trend

of noise emission prediction based on CO, NO_x and CO_2 emissions. Again, it can be observed that NO_x emissions depict the opposite trend as noise emissions, increasing when the NO_x emission decreases.

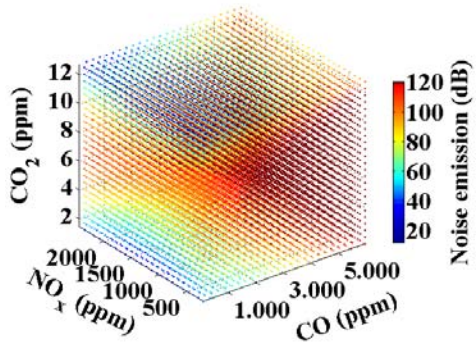

Figure 3.2. Response surface model considering CO (ppm), NO_x (ppm) and CO_2 (ppm)

3.1.4.3 Prediction of noise emission based on higher calorific value, speed and power

The term higher calorific value (*HCV*) is related to the brake specific fuel consumption and indicates the energy released when a fuel undergoes complete combustion [39, 40]. To achieve the same power of diesel fuel using fuels with higher *HCV*, a decrease of injection volumes is need, which leads to lower specific fuel consumption and noise emission [41, 42]. To predict noise emission, the model that best fits experimental results is a first-order equation with a R-square of 98.45%. The prediction from the proposed linear model was compared with experimental results and achieved a MSE of 3.76. It has been found that the estimation of the radiated noise level is correlated with the higher calorific value, the speed and power by means of the following response surface model:

Noise (dB) = 80.2151 + 0.000147 HCV (J/g) + 0.002468 n (rpm) – 0.015888 N (kW)

Therefore, it may be inferred from the proposed model that high

HCV increases noise emission and specific fuel consumption. This means an increased consumption of fuel mass, and thus, more noise is produced. In addition, both lower *CN* of the fuel and higher latent heat of vaporation may increase the ignition delay at low power and therefore, the noise radiated increases [43]. This trend can also be appreciated in Figure 3.3, which illustrates the effect of higher calorific value on modeled noise emission.

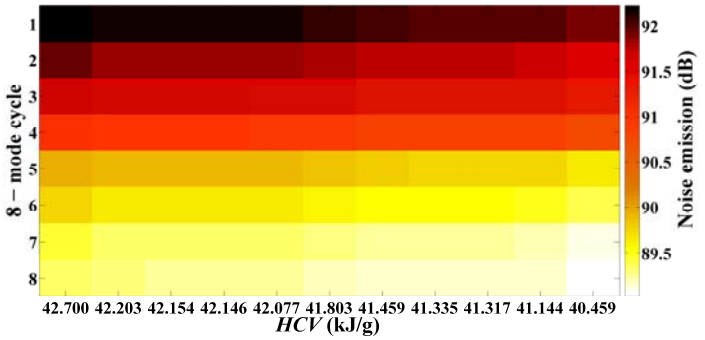

Figure 3.3. Spectrogram (in dB) of modeled noise emission based on *HCV* (kJ/g) at 8-mode cycle

3.1.5 Conclusions

Several response surface models have been developed to show the effect of chemical properties and exhaust emissions on noise radiated by a diesel engine when it is fuelled with different biodiesel blends.

The influence of viscosity is higher than that of oxygen or *CN* on noise emissions. Moreover, the trend of NO_x emissions is opposite to that of noise emissions. It can be concluded that there is a good agreement between experimental and modeled noise emissions.

3.2 Noise prediction of a diesel engine fuelled with olive pomace oil methyl ester blended with diesel fuel

3.2.1 Abstract

Two of the major challenges of the European Union policy are to reduce both greenhouse gas (GHG) emissions and the dependence on fossil-based fuels. Biodiesel, produced through the transesterification of vegetable oils or animal fats, seems to be an excellent support. Nowadays, new raw materials to produce biodiesel are under study, provided that the production of biodiesel from edible oils is controversial for some social organizations. Olive pomace oil derives from the oil left in the olive fruit pulp (once olive oil has been extracted) and may be an option to considerer since it exhibits high neutral flavor that makes it undesirable for consumption, unless it is treated and further blended with virgin olive oil. Therefore, other uses for this oil could be soap production or its recycling to produce biodiesel. In this paper, noise emissions of a direct injection diesel engine Perkins fueled with olive pomace oil methyl ester (OPME) at several steady-state engine operating conditions were studied. This study proposes the use of different approaches for sound prediction of a diesel engine, based on Artificial Neural Network (such as Evolutionary Product Unit Neural Networks,

PUNN and Radial Basic Function Neural Networks, RBFNN) and response surface models. Their accuracies are compared in terms of Mean Square Error (MSE) and Standard Error of Prediction (SEP). It can be concluded that the use of PUNN improves the accuracy achieving acceptable values for both MSE and SEP by means of a simpler model than the combined PU and RBF NN proposed model. Moreover, it was found that the variable power does not explain the noise value prediction, the noise emitted by the engine is inversely related to the 1/3rd octave band of the frequency value and diesel fuel noise plays the most important role and influence in the PUNN model. Response surface models are rejected, due to their unacceptable accuracy in terms of noise prediction.

3.2.2 Introduction

To meet the regulations of both permissible emission level and customer requirements, reduction and improvement of noise emissions are considered major factors in the design of modern engines [44]. In recent years, in the EU, the demand of compression ignition engine-based cars, commonly known as diesel vehicles, has increased with the development of technology. In turn, the increase of the number of vehicles involves a greater consumption of petroleum-based fuels and, therefore, the new European regulations force to meet this energy demand including environmental rules. In this context, biodiesel has the opportunity to contribute to the gradual substitution of fossil fuels, not only in the automotive sector but in industrial applications. Biodiesel, commonly known as fatty acid methyl esters (FAME), consists of monoalkyl esters of long chain acids derived from renewable feedstocks, such as vegetable oils, animal fats or microorganisms [45, 46]. The usual raw materials being commercially exploited to produce biodiesel consist of edible oils derived from rapessed, soybean, palm, sunflower and other oleaginous plants/trees such as olive oil.

Olive oil is produced in the South of Spain as well as in other Mediterranean countries, i.e. Greece, Italy, Tunisia, Portugal, Syria and Lebanon. Olive pomace oil (OPO) derives from the remaining pulp, once virgin olive oil has been extracted. The resultant oil contains many impurities and may undergo several heating and filtering processes to refine it to an acceptable standard. Although it may be used for consumption, it

must be blended with virgin olive oil before its use, due to its high neutral flavor, which makes it undesirable among experts. For this reason, its alternative use for biodiesel production must be taken into consideration [10].

As many studies have revealed [47-50], chemical and physical fuel properties are closely related to combustion parameters, such as ignition quality, fuel stability and flow properties at low temperature, among others. Since these parameters have important effects on the combustion quality, they could also modify the radiated combustion noise of the engine [6, 35, 51]. On the other hand, combustion noise in diesel engines is produced by pressure and mechanical forces, i.e. piston slap and connection mechanisms, inside the cylinder. Moreover, pressure forces mainly depend on the injection strategy, which is influenced by fuel chemical and physical properties, like cetane number (*CN*), bulk modulus and viscosity (μ) and, together with other design parameters, i.e. the combustion chamber geometry, they affect the combustion noise source. These forces cause the engine block to vibrate and thus noise is radiated [52].

The characterization of the radiated noise provided by diesel engines fueled with fossil fuel is well known [53, 54]. However, despite the great number of works related to exhaust emissions produced by different biofuels and their blends, studies about biodiesel noise emissions, and in particular about olive pomace oil biodiesel, are insufficient, thus more research is needed. In this sense, the mandatory 10% minimum target to be achieved by each Member State for the share of biofuels in transport by 2020 urges to increase the knowledge about exhaust and noise emissions provided by biodiesel, straight and blended with diesel fuel. Also, it could be interesting to provide automotive manufactures with prediction models that allow, in the early stages of a car design, to know the influence of alternative fuels on the vibro-acoustic behavior of the engine.

Nowadays, different models are used for regression purposes, including linear or response surface models. However, the great majority of the real-world problems are not linear and therefore, other modeling techniques are more and more used [55]. In this context, some works have shown that there are many patterns of sound energy propagation through the engine, whose response is a time-variant and nonlinear phenomenon [56,

57]. Furthermore, despite the fact that noise emission due to block vibration is mostly a linear phenomenon, nonlinearities become relevant again when the sound quality of noise is assessed [58].

According to the comments exposed above, combustion noise analysis of diesel engines seems to be unapproachable by means of the traditional linear regression models. In the last years, Artificial Neural Network (ANN), one of the most efficient computational methods broadly inspired by the organization of the human brain, has emerged as a powerful alternative to solve nonlinear problems. The main feature of ANN is the ability to learn based on optimization of nonlinear functions.

In this work, to model the combustion noise of a diesel engine fuelled with different olive pomace oil methyl ester (OPME)/diesel fuel blends at several engine operating conditions, a recent type of models based on hybrid artificial neural networks is proposed. In addition, results are compared to those provided by other artificial neural networks and response surface models, based on mean square error criterion, in order to check the accuracy of the best model.

3.2.3 Material and Methods

3.2.3.1 Fuel description and experimental set up

Biodiesel samples were produced after basic-catalyzed transterification of olive pomace oil (OPO) which was acquired from KOIPESOL (Sevilla, Spain). Reagents, instruments, apparatus, software used and experimental set up are depicted in depth in the section 2.1.3 of the chapter 2. Key properties of the biodiesel are shown in Table 2.2 in section 2.1.4.1.

Fatty acid composition of OPME was analyzed following the EU standard EN14103 and the glycerides content was determined following the EN14105 standard. The most important chemical and physical properties of OPME and no. 2 diesel fuel were analyzed following the EU Standard EN 14214 and EN 590, respectively.

Pure diesel fuel and blends of 20% and 50% (v/v) of OPME and

diesel fuel (OPME20 and OPME50, respectively) were tested in a direct injection diesel engine.

3.2.3.2 Modeling techniques

Diesel engines generate a complex noise, which is the result of different sources, although, specifically, both its level and sound quality strongly depend on a particular source, that is the burning of the fuel, producing the so-called combustion noise [59, 60]. Combustion noise is characterized by the rapid increasing rate of in-cylinder pressure, besides engine structural vibrations. This is because it excites resonances in the gas inside the combustion chamber cavity [52]. Both combustion noise and in-cylinder pressure-related differences between biodiesel and diesel fuel occur as a result of fuel property differences, including *CN*, μ or bulk modulus, among others [10, 35]. Furthermore, in terms of energy content derived from the boost pressure, both speed and load are also very important. It can be observed, from Figure 3.4, that combustion noise from different OPME blends decrease compared to that of diesel fuel at several engine speed and load conditions.

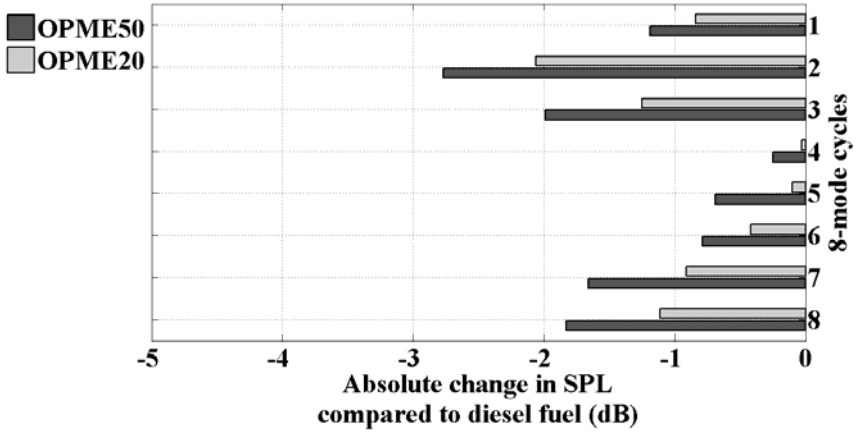

Figure 3.4. Absolute change in sound pressure level (SPL) between diesel fuel and OPME blends

Therefore, there is no doubt that noise radiation is mainly due to

combustion noise produced by the selection of the fuel. In agreement with these statements, it seems that the percentage of biodiesel in the blend, the engine speed and load and the diesel fuel noise for each frequency are the most important parameters to be taken into consideration as input variables in a prediction model; OPME noise for each frequency being considered the output. Based on the relationship between input and output variables, two response surface models (with and without interaction terms) and several ANN models have been compared.

Response surface models. By means of the response surface methodology, the relationship between several explanatory and one or more response variables can be explained. A polynomial model may be sufficient to determine which explanatory variables have an impact on the combination of the attributes with predetermined weights. In this work, two response surface models have been proposed, one with interaction terms:

$$y = \beta_0 + \sum_{i=1}^{k} \beta_i x_i + \sum_{i=1}^{k} \sum_{j<i}^{k} \beta_{ij}^{'} (x_i x_j) + \sum_{i=1}^{k} \beta_i^{''} x_i^2 + \varepsilon \tag{3.1}$$

and one without interactions terms:

$$y = \beta_0 + \sum_{i=1}^{K} \beta_i x_i + \sum_{i=1}^{K} \beta_i^{'} x_i^2 + \varepsilon \tag{3.2}$$

where y is OPME noise for each frequency, x_i is the i-th input variable, k is the number of inputs and ε is the error of the model. The vector of input variables $x = (x, x^2, x^3 \ldots x^K)$ will be later specified in the paper. Both models have been implemented using the regression functions available in Matlab R2008a from MathWorks Inc (USA).

Neural network structure and function form. In the area of neural network applications, some of the most interesting fields are classification and function regression. Its functional form, and specifically the nonlinear function (activation and transfer functions) used in the hidden layer, helps to define ANN taxonomy. In this sense, different types of ANN are being used for regression purposes, including, among others, MultiLayer Perceptron (MLP) neural networks [61] (with standard sigmoid functions applied to the

weighted sum of the inputs), Radial Basis Functions (RBF) neural network [62] (with kernel functions for the hidden layer, usually Gaussian kernels), General Regression Neural Networks [63] (where eacj hidden unit represents a pattern and an additional layer performs a summation of the activated units), Product Unit Neural Networks (PUNN) [64] (where the hidden units are weighted products of the inputs), etc.

In this work, a feed-forward ANN consisting of an input layer (where the scaled inputs are introduced), one hidden layer (where nonlinear transformations of the inputs are obtained) and one output layer (where the estimated outputs are read) has been considered. Although more hidden layers could be considered, there is no evidence that the additional complexity results in enhanced generalization performance. This hidden layer neural network can be considered as a generalized linear regression model, i.e. a linear combination of non-linear projections of the input variables (also known as basic functions or hidden neurons in the ANN terminology). Let $B_j(\mathbf{x},\mathbf{w}_j)$ be the output of the *j*-th hidden neuron for pattern $\mathbf{x}$, $\mathbf{w}_j$ being a vector that includes all the weights of the hidden neuron. Then, the output estimated by the model is provided by the following expression:

$$f(\mathbf{x},\theta) = \beta_0 + \sum_{j=1}^{m} \beta_j B_j(\mathbf{x},\mathbf{w}_j) \tag{3.3}$$

where β_j is the weight of the connection between the hidden node j and the output neuron and $\mathbf{w}_j$ is the vector of weights of the hidden neuron *j*, one for each input variable. For this model, the transfer function of all hidden and output neurons is the identity function. This part of the model is the same for Product Unit Neural Networks (PUNN) and Radial Basis Function Neural Networks (RBFNN). The difference between PUNN and RBFNN is related to the activation function considered in the hidden layer. Figure 3.5 includes the structure of neural networks and the functional equivalence, where the hidden neurons are differently defined for RBFNN and PUNN. RBF are functions built by a distance criterion with respect to a center, using hyper-ellipsoids to split the pattern space in the following way:

$$B_j(\mathbf{x},\mathbf{w}_j) = \exp\left(-\frac{\left\|\mathbf{x}-\mathbf{c}_j\right\|^2}{r_j^2}\right) \tag{3.4}$$

where $\mathbf{w}_j=(\mathbf{c}_j,r_j)$, $\mathbf{c}_j=(c_{j1}, c_{j2},\ldots, c_{jK})$ is the center or average of the j-th Gaussian RBF transformation, r_j is the corresponding radius or standard deviation and $\boldsymbol{c}_{ji},\boldsymbol{r}_j \in \mathbb{R}$. These are different from PUNN, which build their classifications on pseudo hyper-planes, defined by weighted product:

$$B_j(\mathbf{x},\mathbf{w}_j) = \prod_{i=1}^{k} x_i^{w_{ji}} \tag{3.5}$$

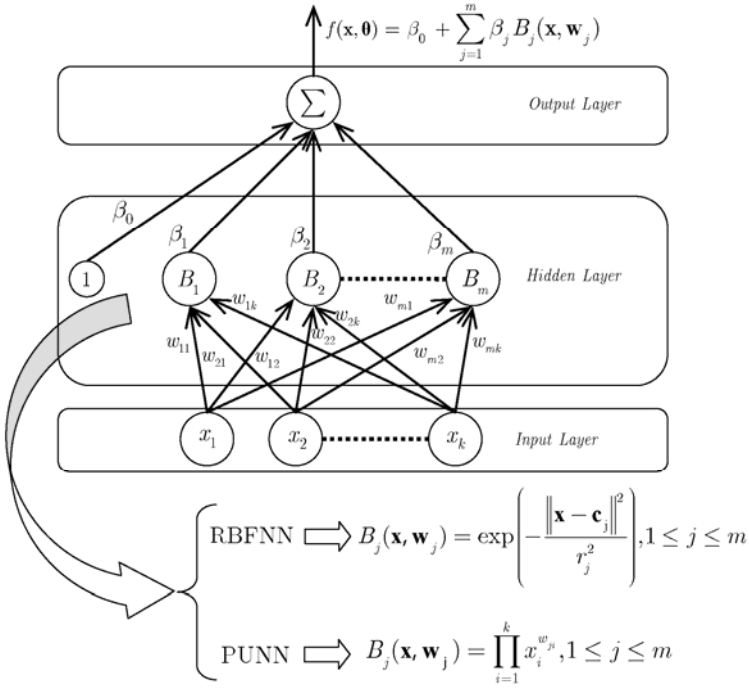

Figure 3.5. Structure of different basis function formulation for RBFNN and PUNN

PUNN have the capacity of reflecting the high order relationships between the inputs and the output, although their training is more difficult than the training of RBFNN. The main reason for this difficulty is that small changes in the exponents can cause large changes in the total error surface. RBFNN require less computation time for learning and they have also a more compact topology [65]. However, it is very difficult to determine the number of hidden centers and their locations.

On the other hand, the main problem involved in the application of ANN models is the selection of the most appropriate net architecture to be used. By means of Evolutionary Algorithms (EA), which are stochastic search algorithms that execute a global search in the input space preventing the fall to local optimum, it is possible to design a near optimal architecture with a great accuracy [66]. This fact and the complexity of the error surface associated with PUNN or RBFNN justify the use of EA to design the structure and adjust the weights of these models.

An alternative to both models has been proposed by means of the hybridization of different basis functions by using either one single hybrid hidden layer, or several connected pure layers. In this context, an Evolutionary Algorithm evolving one hidden layer model with kernel (RBF) functions and projection ones (PU) has been proposed [67]. This hybrid structure has emerged as an excellent alternative, concluding that the combination of RBF and PU offers a very competitive performance. As later discussed, both hybrid RBF and PU neural network and pure PUNN will be considered in this work.

Evolutionary Algorithm (EA). One of the main problems involved in the application of ANN models is the selection of the most appropriate net architecture (i.e., number of hidden nodes and number of connections). By means of Evolutionay Algorithms (EA), which are stochastic search algorithms that execute a global search in the input space preventing the fall to local optimum, it is possible to design a near optimal architecture with a great accuracy [66]. This fact and the complexity of the error surface associated with PUNN or RBFNN justify the use of EA to design the structure and adjust the weights of these models. As mentioned above, all the parameters and the structure of the models based on ANN are estimated by means of an EA. First, the random generation of N_p individuals is performed and then, the evolution process starts updating the population by

means of an algorithm. The population is subjected to replication and mutation operations due to the fact that the algorithm falls into the class of Evolutionary Programming (EP) paradigm [68], crossover not being considered.

Fitness of a neural network of the population that implements a function $f(x,\boldsymbol{\theta})$ is calculated using a training dataset, D={(x_l, y_l): l=1,2,…,n_T}, where the number of samples is n_T. To evaluate the error in the prediction, the Mean Squared Error (MSE) of *f(x)* will be considered,

$$MSE(f) = \frac{1}{n_T}\sum_{l=1}^{n_T}(y_l - f(x_l))^2 \tag{3.6}$$

where y_l are the observed values, and $f(x,\boldsymbol{\theta})$ are the predicted ones. The fitness function $A(f)$ is defined by means of a strictly decreasing transformation of the MSE:

$$A(f) = \frac{1}{1+MSE(f)}, \quad 0 < A(f) \leq 1 \tag{3.7}.$$

The adjustment of both weights and structure of the neural networks is performed by the complementary action of two mutation operators: parametric and structural mutation. The general structure of the algorithm is shown in Figure 3.6 and more details about the EP operators can be found in Hervás-Martinez et al. [69].

In this research, different models of ANN are considered with the following basic functions: RBF pure layer, PU pure layer and hybrid RBF and PU hybrid layer, all of them optimized by using EA for the calculation of the net parameters. It can be anticipated that the accuracy of the hybrid RBF and PU model is better than that of pure models, as previous works have found [67]. Although a model based on a pure RBF layer has been implemented, results are not included in this paper because they are worse than the use of a response surface model.

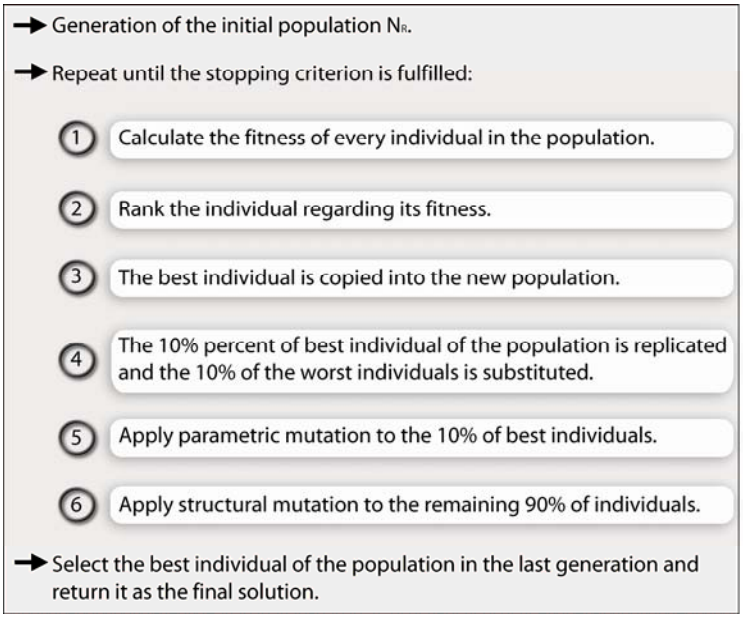

Figure 3.6. Evolutionary Algorithm framework

3.2.3.3 Description of the data set

Data were collected from the 8-mode cycle in the direct injection diesel engine Perkins AD 3-152 when it was fuelled with OPME20 and OPME50 at 26 1/3rd octave band of frequency. First, the input variables were scaled in the interval [0.1, 0.9] in the PUNN model and in the interval [1, 2] in the RBFNN model. For the surface response models, the input variables were also scaled in the interval [1, 2]. All the parameters used in the evolutionary algorithm have the same values in all methodologies. The vector elements $\mathbf{w}_j$ were initialized in the [–5, 5] interval for the PU nodes and in the [-2, 2] for the RBF ones; the coefficients β_j were given a random value in the [-5, 5] interval; the maximum number of hidden nodes are m=4 for PUNN model and m=7 for combined PU and RBFNN model, the size of the population being $N_P = 1,000$ and the number of generations 150. The number of nodes that can be added or removed in a structural mutation is within the [1, 2] interval, whereas the number of connections that can be

added or removed in a structural mutation is within the [1, 6] interval.

A holdout crossvalidation procedure was used in the experimental design, being the size of training set 3*n*/4, and *n*/4 for generalization set, where *n* is the size of the whole dataset. 480 data were collected and were randomly split in two dataset, a 360 instances dataset was used for training, while the remaining 120 instances provided the generalization one (used for assessing the performance of the models). Since the EP algorithm is a stochastic method, the algorithm was repeated 3 times, each one with a different random seed. Additionally, a total of 10 holdout validations were performed (with different random splits of the data), which resulted into 30 models. In the case of the response surface models (a deterministic method), one run was performed for each holdout, this time considering 30 holdout processes, with different random splits. In this way, the number of models was also 30. Then, the mean and the standard deviation of the error corresponding to the 30 models achieved were recorded. The evaluation of the models was based on the MSE and the Standard Error of Prediction (SEP) in the generalization set. SEP is defined as:

$$SEP = \frac{100}{|\bar{y}|}\sqrt{MSE} \tag{3.8}$$

where $\bar{y}$ is the average output of all patterns in the dataset.

3.2.4 Results and discussion

Results achieved with the different modeling approaches based on ANN were evaluated using both MSE and SEP, and the response surface regression models were also trained to verify that the compared models achieved an acceptable performance. Table 3.2 shows the comparison of the proposed techniques (PUNN and combined PU and RBF NN) and the response surface models (quadratic regression and pure quadratic regression), measured by using the mean MSE value and SEP in the generalization and training datasets. Although the training results have been included, they should not been considered because it is well-known that the results in the training sample are upward-biased. Based on the generalization results, it can be concluded that the combined model

considering PU and RBF clearly outperforms the remainder methodologies, since it is the most accurate in terms of MSE. Moreover, it also results in almost the lowest standard deviation, which means higher stability.

Taking into account that MSE values depend on the magnitude of the data, other kind of indicators should be used for the comparison between the different models, for instance, SEP values. The lowest value for SEP is achieved by the hybrid PU and RBF NN model. Thus, it should be adopted for predicting combustion noise radiated when the engine is fuelled with OPME. The Pearson's linear correlation coefficient was computed for all the models providing R^2=97.80% for the PUNN model, R^2= 97.67% for the combined PU and RBF NN model, and R^2=79.48% and 71.37% for the quadratic and pure quadratic response surface models, respectively. According to these results, it is possible to observe that the best correlation was achieved for the PUNN model.

Figure 3.7 shows the box plot obtained with the results of the different algorithms in MSE. Box plots depict algorithm results according to the smallest observation, lower quartile, median, upper quartile and largest observation. Both Table 3.2 and Figure 3.7 show that the proposed approaches based on ANN are robust enough to predict the radiated sound by engine when it is fuelled with OPME at different engine conditions. However, although the best model based on MSE and SEP seems to be the combined PU and RBF NN model, other considerations should be taken into account as the number of independent variables, or the simplicity of the model (number of links or number of hidden neurons). The structure of the interconnected neurons depends on the complexity of the given problem and the number of neurons in the hidden layer is related to the performance of a neural network. Too few hidden neurons limit the ability of the network to model the problem, and too many result in over-fitting input/output pair patterns presented in the training process. In this case, PUNN proposed models are not particularly complex, since they have neither a high number of neurons nor too many variables associated with each neuron.

Table 3.2. Comparative performance of the models based on MSE and SEP

	MSE (Mean±SD)		SEP (%)	
Method	**Training**	**Generalization**	**Training**	**Generalization**
PUNN	2.854±0.634	2.606±0.973	2.109±0.212	1.997±0.346
combined PU and RBF NN model	2.190±0.134	2.294±0.494	1.856±0.057	1.885±0.214
RS with interaction terms	0.046±0.109	2.570±2.579	0.269±0.536	2.011±0.422
RS without interaction terms	0.066±0.148	2.809±4.085	0.322±0.434	2.102±0.461

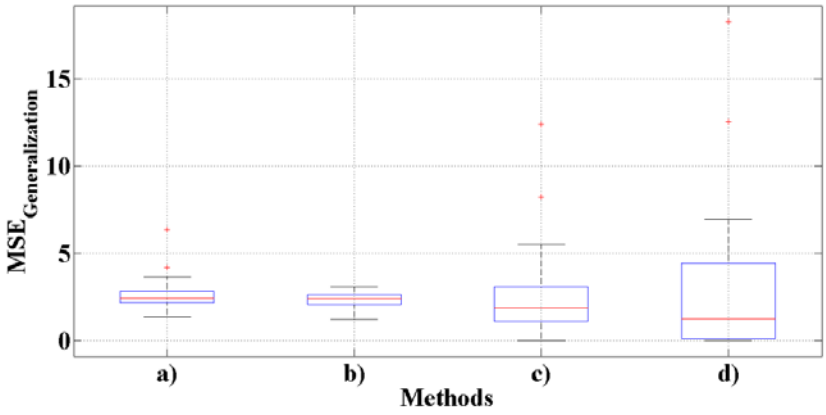

Figure 3.7. Box plots results of: a) PUNN model, b) combined PU and RBF NN model, c) response surface model with interaction terms, d) response surface model without interaction terms

As can be observed in Table 3.3 the PUNN model shows the simplest formula. In this model, x_1 represents the power, x_2 is the speed, x_3 is the percentage of OPME, x_4 is the noise emitted when the engine was fuelled with diesel fuel and x_5 is the 1/3rd octave band of the frequency. The influence of the input variables on the output depends not only on the value of their exponents but also on the coefficients corresponding to the hidden neurons in which they are included. Focusing on the PUNN model, the

variable power (x_1) does not appear in the equation of the model, which means that power was not able to explain the variability of noise emission with a significant confidence level. Moreover, from the equation shown in Table 3.3, the 1/3rd octave band of the frequency variable (x_5) only appears in the hidden neurons with negative coefficient, and its exponent is greater than 0. Therefore, the combustion noise emitted by the engine is inversely related to 1/3rd octave band of the frequency value. This finding agrees with previous studies on combustion noise, where it has been shown that the most meaningful contribution is achieved at low frequencies [35]. Moreover, observing the coefficients of diesel noise (x_4) in the model, it can be observed that it is the most important variable. When the diesel noise increased also does the OPME noise, although it never exceeds the diesel noise. In summary, although the combined PU and RBF NN model has shown a slightly better performance in both MSE and SEP, the best model based on its simplicity and R^2 is the PUNN model.

From the PUNN equation shown in Table 3.3, it can be interesting to fix some input variables such as the frequency at 1000 Hz, the engine speed and power for different conditions and the maximum level of diesel noise (99.94 dB), and to study the influence of the percentage of OPME blended with diesel fuel on the radiated noise. This is shown in Figure 3.8. At high speed (2132 rpm), the effect of the increase in the percentage of OPME is more noticeable, achieving a reduction of noise around 2 dB compared to diesel noise. However, at low speed (1160 rpm) the noise radiated is more or less constant despite the increase in the percentage of OPME in the blend. Concerning the effect of the increase of OPME percentage with respect to frequency, it seems that when the content of OPME increases the noise radiated decreases, being this attenuation more important at low frequencies, see Figure 3.9. Both trends agree to previous results found by authors [10], where the maximum attenuation is achieved by the highest percentage of OPME studied (50%) at low frequencies.

Table 3.3. Functions of the all the models compared

Models	
$\mathbf{f}_{\mathbf{PUNN}}$	$y = 0.363x_4^{1.737} - 0.235x_4^{-4.625} + 0.016\left(x_2^{-3.188}x_3^{-4.690}x_5^{-2.037}\right) + 0.023\left(x_2^{1.317}x_4^{-4.977}x_5^{-3.406}\right) - 0.184$
$\mathbf{f}_{\mathbf{combined\ PU\ and\ RBF\ NN}}$	$y = 0.632\left(x_4^{0.719}\right) + 0.632\left(x_4^{1.542}\right) +$ $0.038\left(exp\left(-0.5\left(+\frac{\left(\left(x_1^{-0.181}\right)^2+\left(x_2^{-0.181}\right)^2+\left(x_3^{-0.181}\right)^2+\left(x_4^{-0.181}\right)^2+\left(x_5^{-0.181}\right)^2\right)^{0.5}}{1.181}\right)^2\right)\right) +$ $0.032\left(exp\left(-0.5\left(+\frac{\left(\left(x_1^{-0.217}\right)^2+\left(x_2^{-0.842}\right)^2+\left(x_3^{-0.873}\right)^2+\left(x_4^{-0.500}\right)^2+\left(x_5^{-0.173}\right)^2\right)^{0.5}}{0.090}\right)^2\right)\right) -$ $0.155\left(exp\left(-0.5\left(+\frac{\left(\left(x_1^{-0.490}\right)^2+\left(x_2^{-0.512}\right)^2+\left(x_3^{-0.440}\right)^2+\left(x_4^{0.439}\right)^2+\left(x_5^{-0.531}\right)^2\right)^{0.5}}{0.448}\right)^2\right)\right) +$ $0.325\left(exp\left(-0.5\left(+\frac{\left(\left(x_1^{0.525}\right)^2+\left(x_2^{-0.253}\right)^2+\left(x_3^{0.379}\right)^2+\left(x_4^{-0.499}\right)^2+\left(x_5^{0.536}\right)^2\right)^{0.5}}{0.402}\right)^2\right)\right) +$ $0.501\left(exp\left(-0.5\left(+\frac{\left(\left(x_1^{0.243}\right)^2+\left(x_2^{-0.771}\right)^2+\left(x_3^{-0.333}\right)^2+\left(x_4^{-0.263}\right)^2+\left(x_5^{-0.608}\right)^2\right)^{0.5}}{0.229}\right)^2\right)\right) - 0.030$
$\mathbf{f}_{\mathbf{rs\ with\ interaction\ terms}}$	$y = 0.039x_2 - 0.014x_5 + 0.001x_1x_2 - 0.009x_1x_4 + 3.427e^{-0.5}x_1x_5 + 0.004x_2x_3 + 0.002x_2x_4$ $+4.987e^{-0.6}x_2x_5 + 0.072x_3x_4 + 4.225e^{-0.5}x_3x_5 + 2.227e^{-0.5}x_4x_5 - 0.0001x_2^2 + 0.008x_4^2 + 5.617e^{-0.8}x_5^2$
$\mathbf{f}_{\mathbf{rs\ without\ interaction\ terms}}$	$y = -0.028x_2 + 1.548x_4 + 0.0002x_5 + 0.0006x_1^2 + 7.91e^{-0.6}x_2^2$ $-0.0003x_3^2 - 0.003x_4^2 - 2.92e^{-0.8}x_5^2$

1 where x_1 is power; x_2 is speed; x_3 is the percentage of OPME; x_4 is the noise emitted when the engine was fuelled with diesel fuel and x_5 is the 1/3rd octave band of the frequency.

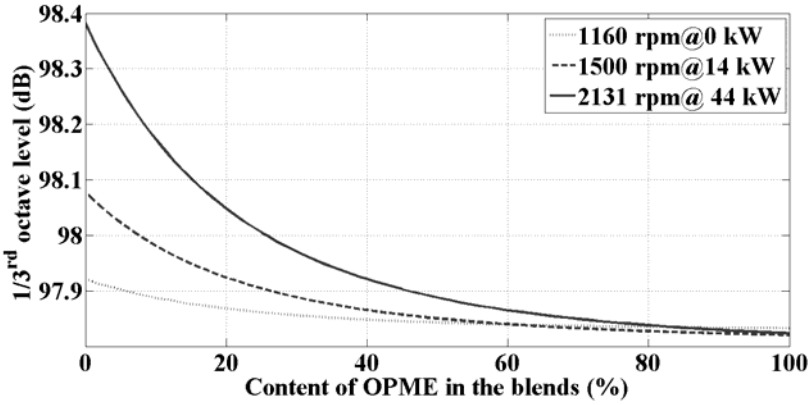

Figure 3.8. Noise radiated versus percentage of OPME blended with diesel fuel, considering 99.94 dB of maximum diesel engine noise, 1000 Hz of frequency and 1160, 1550 and 2131 rpm of engine speed

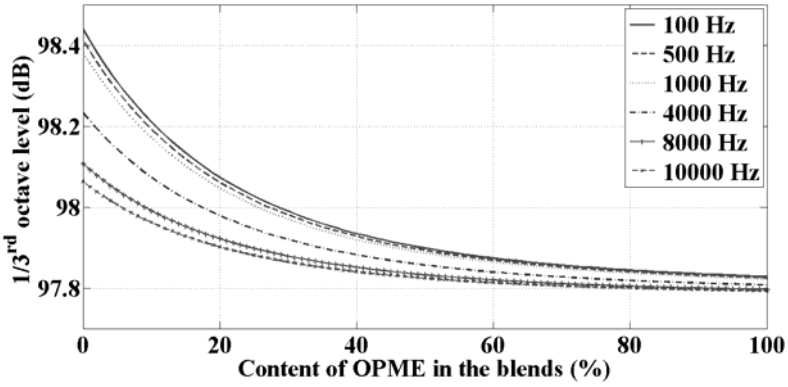

Figure 3.9. Noise radiated versus percentage of OPME blended with diesel fuel, considering 99.94 dB of maximum diesel engine noise, 2131 rpm of engine speed and 100, 500, 1000, 4000, 8000, 10000 Hz of frequency

Figures 3.10 (a-d) and 3.11 (a-d) show the frequency spectrographs of absolute error between observed and predicted noise by the model proposed at several engine operating conditions, both for OPME 20% and OPME 50%. Each row from 1 to 8 represents the sound considering the tested engine operating conditions (8-mode cycle), as described in Table 3.2. The gray scale allows the visualization of the contrast of the absolute error in terms of 1/3rd octave band level (dB). A good prediction is visible in both set of figures for the models based on ANN, in contrast to the response surface regression models. From the analysis of these results, in general terms, the models based on ANN are the most competitive ones, while the response surface models exhibit an unacceptable difference between observed and predicted noise (more than 5 dB). This difference is very important in terms of noise prediction, since 3 dB may means whether the noise has doubled or halved. For these reasons, the accuracy of the model is a critical factor for predicting the combustion noise radiated by an engine; thus, ANN is recommended for all cases in this study.

3.2.5 Conclusions

This study demonstrates the capability of ANN to identify the noise emitted by an engine when it is fuelled with OPME at several steady-state engine operating conditions. Moreover, two response surface regression models were evaluated to compare the accuracy with respect to the proposed ANN models. Results for both MSE and SEP show that combined PU and RBF NN model is the one that better simulate noise emissions. However, the best solution considering both the simplicity of the model and the R^2 is provided by the PUNN model. The simplicity of the PUNN model allows extracting interesting conclusions: the variable power does not explain the noise value prediction; the noise emitted of the engine is inversely related to the 1/3rd octave band of the frequency value; and the diesel noise has the most important role and influence in the model. Although results achieved for the response surface models may be acceptable in other context, from the noise prediction point of view, the accuracy of the model is a critical factor in this kind of prediction models, so they must be rejected.

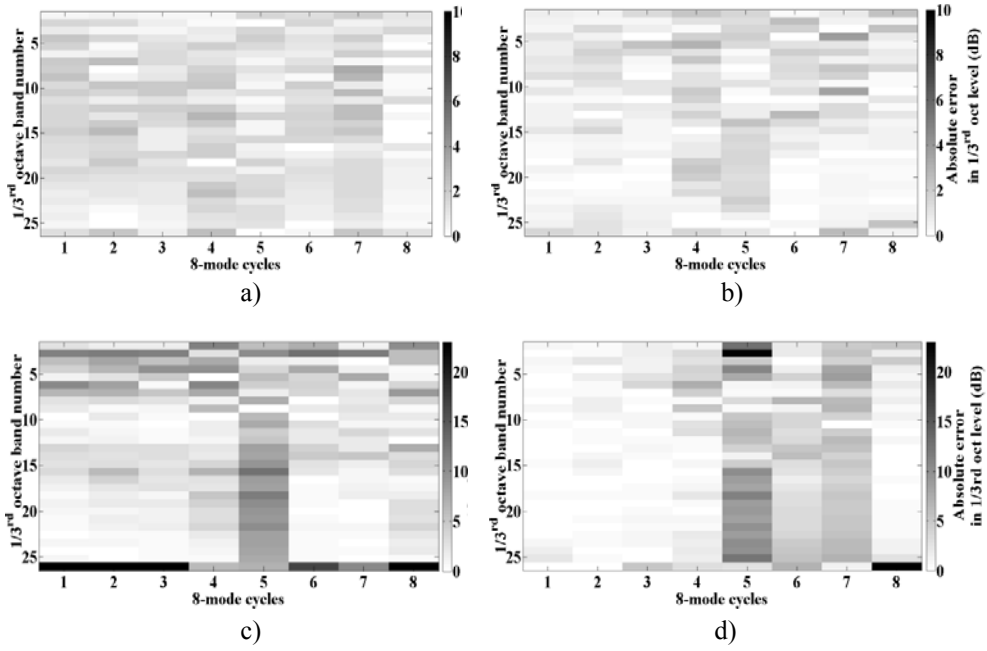

Figure 3.10. Absolute change in 1/3rd octave band level noise (dB) for OPME20 at 8-mode cycles: a) PUNN model, b) combined PU and RBF NN model, c) response surface model with interaction terms, d) response surface model without interaction terms

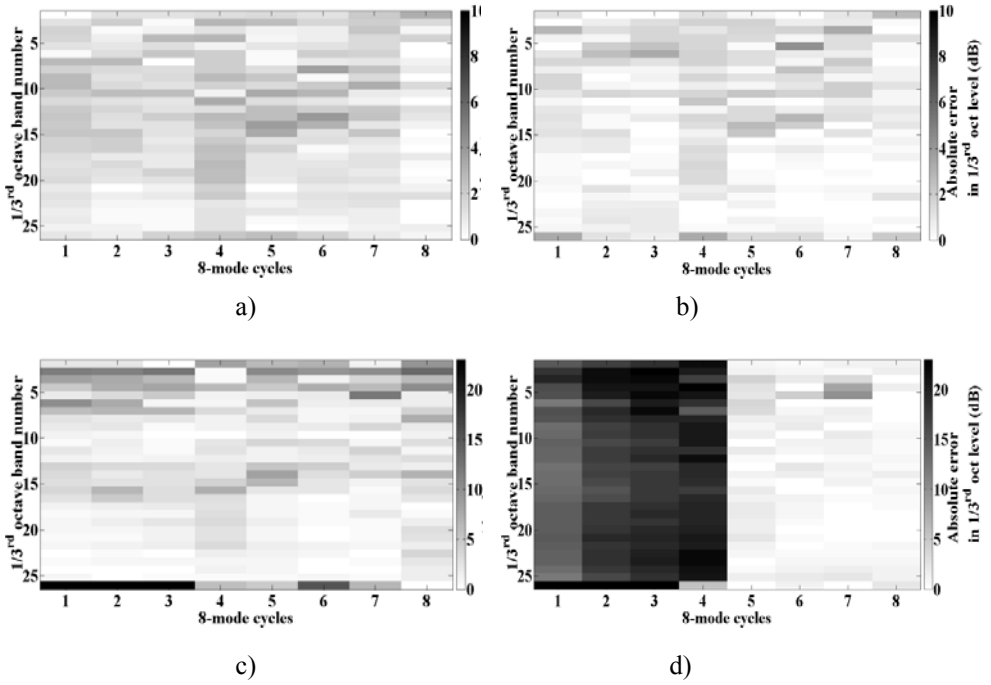

Figure 3.11. Absolute error of 1/3rd octave band level noise (dB) for OPME50 at 8-mode cycles: a) PUNN model, b) combined PU and RBF NN model, c) response surface model with interaction terms, d) response surface model without interaction terms

3.3 Prediction models of the noise emissions produced by a diesel engine fuelled with saturated and monounsaturated fatty acid methyl esters

3.3.1 Abstract

The low particular matter (PM), carbon monoxide (CO) and unburned hydrocarbon (UHC) emission achievable with biodiesel allowing to obey the new regularizations for pollution emission reduction make it an excellent alternative to derivate petroleum fuel.

The properties of biodiesel are different depending on their fatty acids content, in which the feedstocks used have influence. Moreover, it is well-known that combustion process changes with the use of different fuels. The noise emissions of a diesel direct injection Perkins engine fueled with olive pomace oil methyl ester (OPME) and palm oil methyl ester (PME) were studied at several steady-state engine operating conditions. Different approaches for sound prediction of engine have been proposed in this work based on Artificial Neural Networks (ANN), such as Evolutionary Product Unit Neural Networks (EPUNN), Radial Basic Function Neural Networks

(RBFNN), and polynomial regression to compare the accuracy in terms of Mean Square Error (MSE) and Standard Error of Prediction (SEP). It can be concluded that the use of EPUNN improves the accuracy achieving an acceptable values of both MSE and SEP by means of a model simpler than the combined EPUNN and RBFNN model proposed.

3.3.2 Introduction

Biodiesel are mono-alkyl esters produced from renewable sources and can be produced domestically. It has emerged as an attractive alternative to diesel fuel in order to help curb demand for petroleum due to the unceasing growing in the sales of passenger cars equipped with diesel engine [60]. When biodiesel is used as substitute fuel in diesel engines, it usually exhibits several emissions-related advantages as higher potential for particular matter (PM), carbon monoxide (CO) and unburned hydrocarbon (UHC) reductions [38]. However, the use of biodiesel, has also some disadvantages: lower energy density, due to the fact that its calorific value is 12% lower than diesel, and more emissions of nitrogen oxides (NO_x) than conventional diesel [70]. Despite these difficulties, the use of blends [71, 72], additives [17] or indeed modifying the fatty ester composition of biodiesel [27] has recovered its potential as a promising fuel for automotive diesel engine [73-75].

There are many potential feedstocks for biodiesels, including; rapeseed, soybean, sunflower, palm, peanut oils and olive oil, etc, showing some variations in the fuel properties of biodiesel given that its fatty acids content is different. These differences affect the injection, combustion, performance and emissions characteristics of the engine. Indeed, both air and noise emissions are strongly dependent on the operating setting of the fuel injection system (injection pressure, start of the injection and injection pattern), which depend on the chemical properties of biofuel [41, 50, 76]. Specifically, the fuel combustion produces the so-called combustion noise, which may be considered as the most important source of noise in an engine. For diesel engines, it is an unpleasant sound signature due to the harsh and irregular self-ignition of the fuel. Therefore, being able to control fuel combustion process by means of significant parameters of combustion such as injection timing and pressure, would be of prime interest for reducing noise emissions.

Most of the work in the literature on engine noise has been devoted to describing the effect of in-cylinder pressure spectrum. This effect has been established by Austen and Priede [77], who proposed the attenuation curve approach in which a relationship between the in-cylinder sound pressure level and radiated noise level is given. However, this method assumes that the noise of the engine block is linearly independent with respect to the engine operating conditions which make it unfeasible for quantitative analysis. Other classical approaches for acoustic energy propagation through the engine block [54, 78] are too complex in practice for the analysis of combustion noise due to the fact that in-cylinder excitation is propagated through multiple and extremely complex path. Recently, some authors [56, 59] have developed a procedure in order to assess the radiated engine noise level based on the in-cylinder pressure components during engine operating although the effect of diesel fuel has been only considered. In other research [51], the influence of four parameters, i.e. intake-valve-closing angle, exhaust-valve opening angle, fuel delivery angle and injection pressure, have also been also studied for rapeseed oil blends to design a regressive orthogonal method for predicting noise level in an engine. The weakness of this approach is that it is only validated for two operating engine conditions, 0 kW/2000 rpm and 8.82 kW/2000 rpm.

This situation induces working with other techniques more suitable for combustion noise, which is a time-variant and nonlinear phenomenon. In the last decades, Artificial Neural Networks (ANN) have emerged as a powerful alternative to solve nonlinear problems, one of their main advantages being their ability to learn based on the optimization of nonlinear functions. Different types of ANN are being used for regression purpose, including among others: MultiLayer Perceptron (MLP) neural networks [61], Radial Basis Functions (RBF) [62], General Regression Neural Networks [63] and Product Unit Neural Networks (PUNN) [64], etc.

The aim of this work is to predict combustion noise in an engine when it is fuelled with biofuel blends of OPME and PME at several engine operating conditions based on diesel fuel noise radiated by the same engine. In order to achieve this objective, several models based on ANN have been developed. These ANN are trained by means of evolutionary algorithms which define both the structure (number of nodes) and coefficients of the

models. In addition, the results are compared with surface response models based on the mean square error criterion in order to check the accuracy of the best model.

3.3.3 Materials and Methods

3.3.3.1 Fuel description and experimental set up

Both methyl esters of olive-pomace and palm oil were produced by alkaline transesterification and purification processes as is described in [76]. OPME and PME were produced after basic-catalyzed transesterification of olive pomace oil (OPO) that was acquired from KOIPESOL (Sevilla, Spain) and palm oil (PO) that was purchased from Quimics Dalmau (Barcelona, Spain). Key properties of the biodiesel are shown in Table 2.4 in section 2.2.3.2.

Fatty acid composition of OPME and PME were analyzed following the EU standard EN14103 and their glycerides content was determined following the EN14105 standard. The most important chemical and physical properties of OPME, PME and no. 2 diesel fuel were analyzed following the EU Standard EN 14214 and EN 590, respectively.

Pure ultra low sulfur diesel fuel (ULSD) and blends of 20% and 50% (v/v) of OPME (OPME20 and OPME50), blends of 20% and 50% (v/v) of PME (PME20 and PME50) and ULSD were tested in a direct injection diesel engine.

3.3.3.2 Modeling techniques

Combustion-induced noise and mechanical-induced noise are two major exciting forces-induced noise in an engine, which in certain conditions may be coupled [59]. When combustion take place, a sudden pressure rise is produced in the cylinder causing the vibration of the engine block and it turns in radiates air-borne noise. Both pressure forces and the mechanical forces associated with piston slap are the origin of this block vibration. Specifically, combustion noise is characterized by cylinder pressure whose evolution depends on the fuel burning, being different for

each particular fuel, and injection strategy among others. In this sense, as can be observed from Figures 3.12 (a-h), there are noticeable differences between the noise produced by engine when it is fuelled with a higher saturated fatty acids (PME) and when it is fuelled with a monosaturated fatty acids (OPME). Moreover, the energy content derived of the boost pressure is determined by engine speed and load. This situation induces considering these variables (percentage of biodiesel fuel, engine speed and power), diesel fuel noise for each frequency like input at our prediction models, being OPME and PME fuel noise for each frequency the output considered in each model.

Several non-linear models based on ANN and additionally, two polynomial regression models, have been developed in order to describe the relationship between the noise of diesel fuel and biofuel blends at different engine operating conditions for each 1/3rd octave band frequency. These modeling techniques have been detailed depth in section 3.2.3.2 of this chapter.

3.3.3.3 Description of the data set

Although, a model based on RBF has been implemented, the results are not included in this work because they were worse than those of the polynomial models. The dataset was randomly split in two dataset approximately 3*n*/4 (360 instances dataset) for training and *n*/4 (120 instances dataset) for the generalization set by means of a holdout crossvalidation. This procedure was repeated 10 times, so 10 random splits were used. To start processing the data each of the input variables was scaled in the rank [0.1, 0.9]. This was not necessary in the polynomial models. The parameters used in the evolutionary algorithm for learning the ANN models are common to all methodologies: the exponents w_j are initialized in the interval [-5, 5] for the PU nodes, this range is [0.1, 0.9] for the RBF nodes, and the coefficients β_j are initialized in the [–5, 5] range. The maximum number of hidden nodes is m=2 for EPUNN model and m=5 for combined EPUNN and RBFNN model; the size of the population is N_p=1,000 and the number of generation is 150. The number of nodes that can be added or removed in a structural mutation is within the [1, 2] interval. The number of connections that can be added or removed in a

structural mutation is within the interval [1, 6].

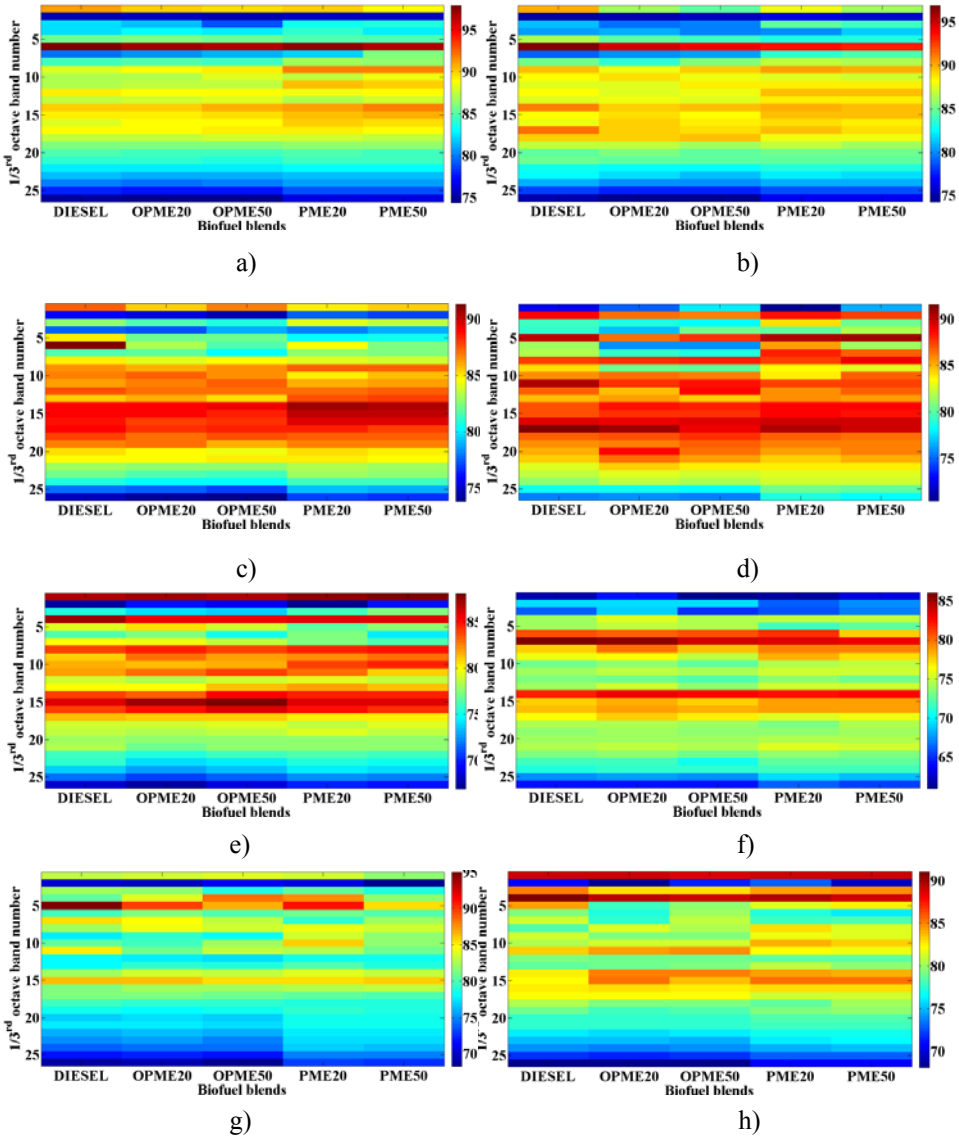

Figure 3.12. Spectrogram on 1/3rd octave band of frequency for all biofuel blends and diesel fuel at 8-modes cycle, a)-h)

For each ANN model, 3 repetitions of the EA were performed for each of the 10 holdouts due to the fact that these are stochastic methods and resulting into 30 results. The mean and the standard deviation of the error of these 30 results were recorded. For the response surface models (which are deterministic models), 30 splits were considered to obtain the same number of results.

The evaluation of the models was based on the MSE and the Standard Error of Prediction (SEP).

3.3.4 Results and discussion

With the aim of showing the interest of the methodology proposed in this work, combustion noise issues in a diesel engine fuelled with two different biofuel blends at several operating conditions will be analyzed in this section. For this application, the variables taken into account are the engine speed, the power, noise using diesel fuel, the frequency and the percentage of mixture.

The spectrogram on the 1/3rd octave band for all biofuel blends and the diesel fuel at several engine operating conditions are shown in Figure 3.12 (a-h). As can be appreciated, the effect of biofuel blends on engine noise is more noticeable at low-medium frequencies. For all the engine operating modes the maximum noise level is reached by the diesel fuel. As it is illustrated in Figure 3.12 (a-h), the engine noise rise when increasing the engine speed. Moreover, there are meaningful differences between the engine noise produced by the biofuel blends compared with the diesel fuel. Thus, it may be inferred that the origin of engine noise is mainly due to the combustion noise and not to the mechanical forces [79].

Table 3.4 shows a comparison of the generalization results of the different proposed algorithms based on the MSE and SEP values. The SEP values are only referred to the best model obtained over the 30 executions of all the algorithms. The training results have not been considered, since it is well-known that the results in the training sample are upward-biased. As mentioned above, the mean and standard deviation values of these MSE were calculated for the best models obtained in the 30 executions of the different algorithms and included in the table. From a quantitative point of

view, the best mean results in MSEG are achieved by the combined PU and RBF NN model for OPME biofuel blends and by the PUNN model for PME biofuel blends. Another aspect that is important to point out is that these methods are far more robust than the rest of the methods, which can be observed on analyzing the values of standard deviation generated. On the other hand, since MSE values depend on the magnitude of the data, SEP values provided better comparisons between the different models, the combined PU and RBF NN model achieving the lowest value for SEP OPME biofuel blend and the PUNN model for PME biofuel blends. Moreover, the Pearson's linear correlation coefficient (R^2) was computed in order to check if the methodology applied significantly affects the results obtained. The prediction models show a coefficient of determination (R^2) of 97.80% for the EPUNN model, R^2 of 97.67% for the combined PU and RBF NN model, being much higher than the 80% obtained for the polynomial models (79.48% and 71.37%) for OPME biofuel blends. In the case of PME, the result of the coefficients of correlation of the models based on ANN is worse than the results for OPME, 90.89% and 90.07% for EPUNN model and combined PU and RBF NN. However, for polynomial models of PME, this coefficient has improved reaching values of 86.57% for the quadratic one (with interaction terms) and of 88.02% for the pure quadratic models. Moreover, the p-values (probability of obtaining a test statistic) of all models were lower than 0.00001, meaning that there are statistically significant relationships between the variables with more than a 99.9% confidence level. From the analysis of these results, it is possible to observe that the best correlations were achieved for the ANN models, EPUNN model in the case of PME, and the combined EPUNN and RBFNN model for OPME.

Table 3.4. Comparative performance of the models based on MSE for OMPE and PME blends models in generalization test

	MSE_G (Mean±SD)		**SEP (%)**	
Method	**OMPE**	**PME**	**OMPE**	**PME**
PUNN	2.606±0.973	14.26±3.60	1.997±0.346	4.68±0.569
Combined PU and RBF NN model	2.294±0.494	14.46±3.58	1.885±0.214	4.72±0.567
Quadratic	2.570±2.579	15.78±4,12	2.011±0.422	4.95±0.671
Pure quadratic	2.809±4.085	16.19±4.61	2.102±0.461	5.01±0.683

This can also be seen in Figure 3.13, which shows the results of the different algorithms in terms of MSEG. Boxplots depict algorithm results according to the smallest observation, lower quartile, median, upper quartile and largest observation. The difference in MSEG for OPME and PME are really important. The reason for this is that the diesel fuel noise is included in the model as input variable presenting high deviations between diesel fuel noise and biofuels, and these differences being more noticeable for PME fuel noise, as depicted in Figure 3.12 (a-h). Therefore, the results in terms of MSE_G for PME fuel noise will be always worse than those of the OPME fuel noise. This difference in the trend of the noise radiated between OPME and PME may be explained by the higher the unsaturation level of methyl esters, the higher the ignition delay (*CN* for OPME fuel lower than *CN* for PME fuel), consequently increasing the pressure in the cylinder and thus, the noise radiated [41].

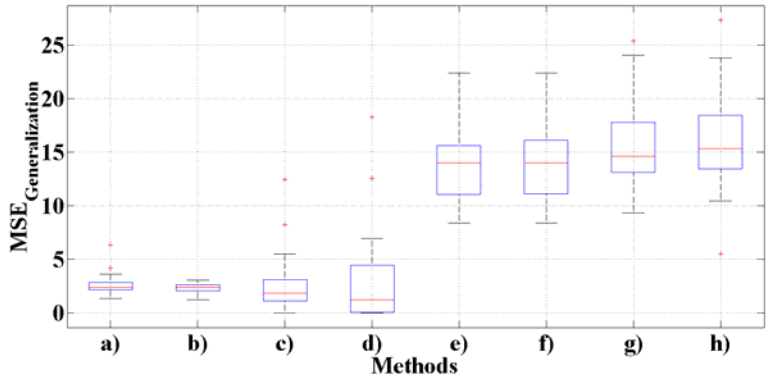

Figure 3.13. Box plots: results of the models: a) EPUNN for OPME, b) combined PU and RBF NN model for OPME, c) response surface model with interaction terms for OPME, d) response surface model without interaction terms for OPME, e) EPUNN for PME, f) combined PU and RBF NN model for PME, g) response surface model with interaction terms for PME and h) response surface model without interaction terms for PME

Regression equations of whole models are given in Tables 3.3 and

3.4. The number of effective links is 7 for EPUNN model and 22 for combined EPUNN and RBFNN model. Although the combined EPUNN and RBFNN model shows the best performance based on the MSE_G and SEP for OPME fuel, other considerations should be taken into account such as the simplicity of the model (number of links or number of hidden neurons, connections or variables, and number of hidden neurons). The structure of the interconnected neurons depends on the complexity of the given problem and the number of neurons in the hidden layers is related to the performance of a neural network.

Table 3.5. Functions of the proposed models for PME

Models	
$\mathbf{f_{PUNN}}$	$y = -2.077\left(x_2^{-0.148}\right) + 0.937\left(x_1^{0.132}x_4^{0.165}x_5^{-0.676}\right) + 2.553$
$\mathbf{f_{combined\ PU\ and\ RBF\ NN}}$	$y = 0.382\left(x_2^{0.619}x_4^{1.198}\right) - 0.421\left(x_5^{1.111}\right) - 3.299\left(exp\left(-0.5\left(+\frac{\left(\left(x_1^{0.569}\right)^2+\left(x_2^{-0.342}\right)^2+\left(x_3^{-0.515}\right)^2+\left(x_4^{-0.686}\right)^2+\left(x_5^{0.258}\right)^2\right)^{0.5}}{0.307}\right)^2\right)\right)\left(x_1^{1.026}x_2^{5.951}x_5^{5}\right) + 5.191\left(exp\left(-0.5\left(+\frac{\left(\left(x_1^{0.614}\right)^2+\left(x_2^{-0.477}\right)^2+\left(x_3^{-0.492}\right)^2+\left(x_4^{0.387}\right)^2+\left(x_5^{0.587}\right)^2\right)^{0.5}}{0.386}\right)^2\right)\right) + 0.507$
$\mathbf{f_{rs\ with\ interaction\ terms}}$	$y = 0.039x_2 - 0.014x_5 + 0.001x_1x_2 - 0.009x_1x_4 + 3.427e^{-0.5}x_1x_5 + 0.004x_2x_3 + 0.002x_2x_4 + 4.987e^{-0.6}x_2x_5 + 0.072x_3x_4 + 4.225e^{-0.5}x_3x_5 + 2.227e^{-0.5}x_4x_5 - 0.0001x_2^2 + 0.008x_4^2 + 5.617e^{-0.8}x_5^2$
$\mathbf{f_{rs\ without\ interaction\ terms}}$	$y = 0.063x_1 + 0.031x_2 + 0.361x_3 + 1.063x_4 - 0.001x_5 - 0.0004x_1^2 - 0.005x_3^2 - 0.006x_4^2$

[1] where x_1 is power; x_2 is speed; x_3 is the percentage of OPME; x_4 is the noise emitted when the engine was fuelled with diesel fuel and x_5 is the 1/3rd octave band of the frequency.

In this sense, despite the combined EPUNN and RBFNN model for OPME has shown a better performance both in MSE_G and SEP, the best model based on its simplicity and its accuracy, slightly different to the combined model and with a better R^2, is the EPUNN model. For PME fuel, the best model is also the EPUNN model.

Moreover, the influence of the input parameters on the output should be taken into account, not only for by analyzing the value of the exponents but also by analyzing the coefficient corresponding to the hidden neurons in which they are represented. Focusing on the EPUNN model for OPME fuel, the variable power (x_1) does not appear in the equation of the model, this means that power was not able to explain the variability of noise emission with a significant confidence level. In the case of PME fuel, the EPUNN model does not consider the variable percentage of biofuel blend (x_3), thus it may be inferred that the percentage of PME blend has not influenced on the noise radiated by engine. Moreover, from both equations of EPUNN models for OPME and PME fuel, shown in Tables 3.3 and 3.5, it follows that the 1/3rd octave band of the frequency variable (x_5) only appears in the hidden neurons with negative coefficient, and its exponent is greater than 0. Therefore, the combustion noise emitted by engine is inversely related to the 1/3rd octave band of the frequency value. This agrees with previous studies on combustion noise where it was shown that the most meaningful contribution is at low frequencies. Other important independent variable in the models is the diesel noise radiated (x_4). When diesel noise increases, an increase of the biodiesel blends noise takes place although it never reaches the value of the diesel noise.

As seen in the Figure 3.14, (where the noise value predicted by the EPUNN model is represented in relation to the frequency and the percentage of OPME in the blend variables), the noise radiated by the engine when it is fuelled with OPME decreases as the contents of OPME in the blend rises. Moreover, the figure reveals the inverse relationship with the frequency already mentioned. At low frequencies the noise radiated is higher than at high frequencies and the effect of increasing the biodiesel content is more noticeable at these frequencies. However, if the engine is fuelled with PME, taking into account the EPUNN model, the content of PME in the blend has no influence due to the fact that, as mentioned above, it does not appear in the equation of the model. Other significant variables

for PME in the model are the frequency and the power as can be observed in the Figure 3.15. The frequency has the same trend that in the case of OPME model, by increasing the frequencies, the noise radiated decreases. However, the power has a reverse effect compared to the frequency, at higher power conditions; an increase of the noise radiated can be observed.

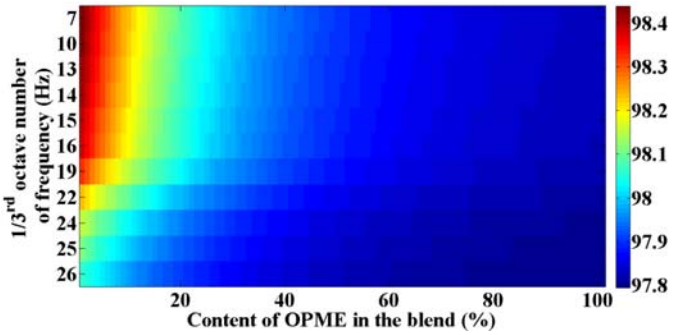

Figure 3.14. Spectrogram on 1/3rd octave band of frequency (dB) for EPUNN model of OPME

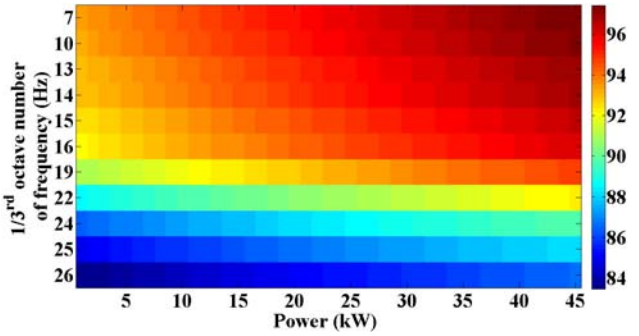

Figure 3.15. Spectrogram on 1/3rd octave band of frequency (dB) for EPUNN model of PME

Figures 3.16 (a-d) and 3.17 (a-d) show the observed and predicted noise by means of the EPUNN proposed models at different engine operating conditions both OPME and PME biofuel blends. A good accuracy of the models is essential for successful implementation of prediction noise due to in terms of noise prediction 3 dB more or less may means to double

or to be halved the noise. Taking into account the results of the observed and predicted noise by EPUNN models, a clear difference between the accuracy achieved for OPME compared with PME have been found.

The perception of sound by a human being is more than the pressure signal and thus, other kinds of metrics different from decibels (dB) are needed for relating acoustic stimuli with hearing sensation [80]. The metric selected for this propose is the Zwicker loudness, because it is related to the strength of the engine sound, this being very important for the overall noise and the main engine orders, especially at idle and during acceleration. Figures 3.18 (a-b) and 3.19 (a-b) show the relative error in Zwicker loudness by means of the EPUNN proposed models at different engine operating conditions, both for OPME and PME biofuel blends. In general, the results achieved for the EPUNN model of OPME blends based on the relative error in loudness are lower compared to the EPUNN model of PME blends. For PME, the error is even larger than 140% although, this happens only at low power. Based on these results, the proposed model for PME may be only valid at high and medium power due to the relative error on Zwicker loudness drops severely below 20% achieving a good accuracy. As expected, the model for OPME is the most competitive due to the fact that it shows the best MSE_G and R^2 and therefore, its accuracy is also the best one compared to the model for PME.

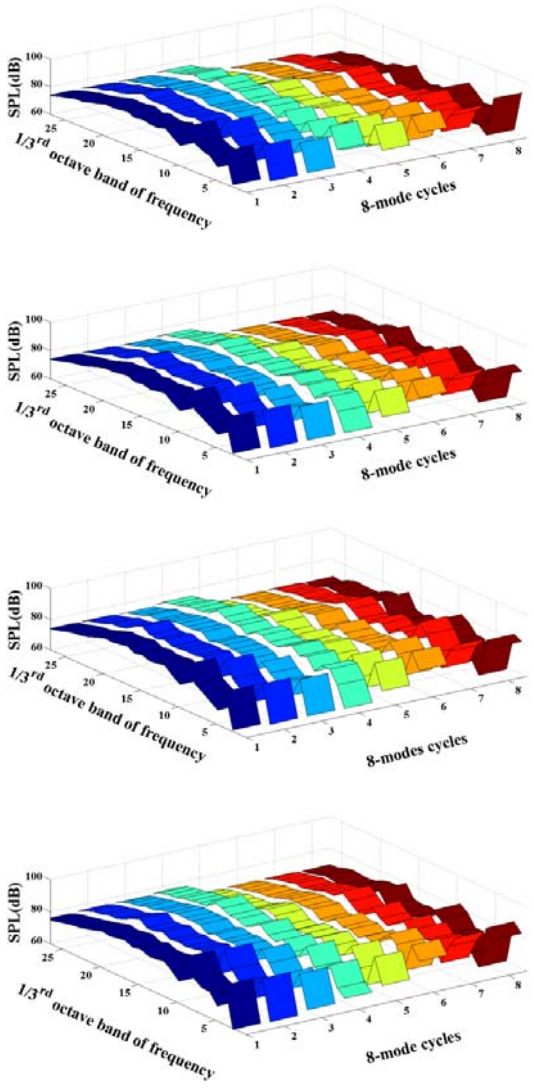

Figure 3.16. Observed and predicted noise by EPUNN model for OPME20 and OPME50 fuel blends at several engine operating conditions: a) observed OPME20 1, b) observed OPME50, c) predicted OPME20, d) predicted OPME50

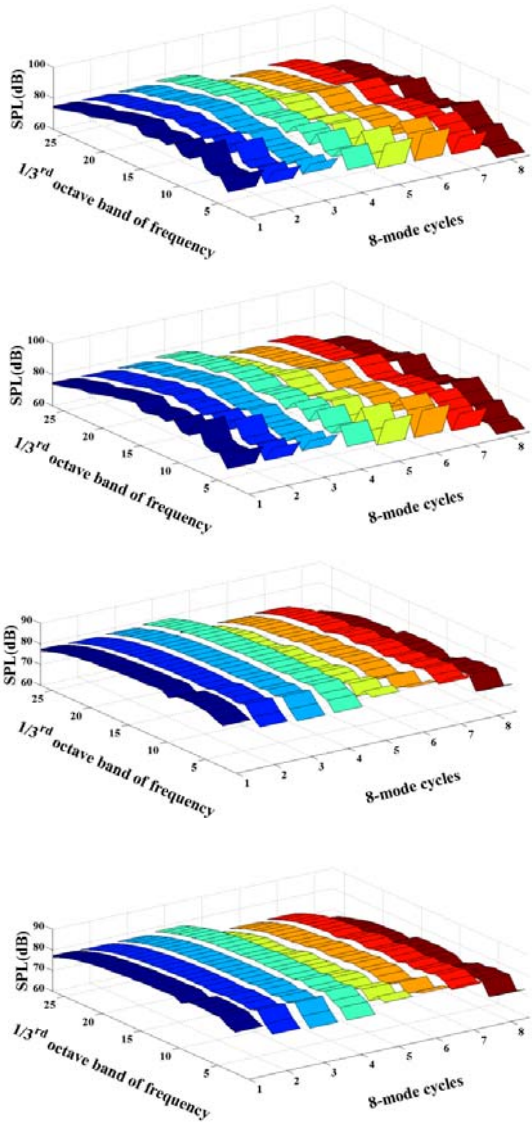

Figure 3.17. Observed and predicted noise by EPUNN model for PME20 and PME50 fuel blends at several engine operating conditions: a) observed PME20 1, b) observed PME50, c) predicted PME20, d) predicted PME50

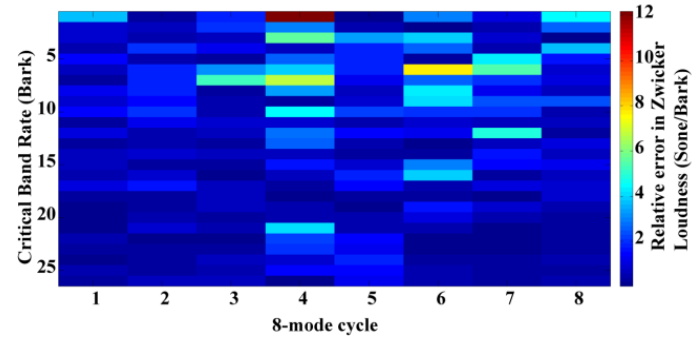

a)

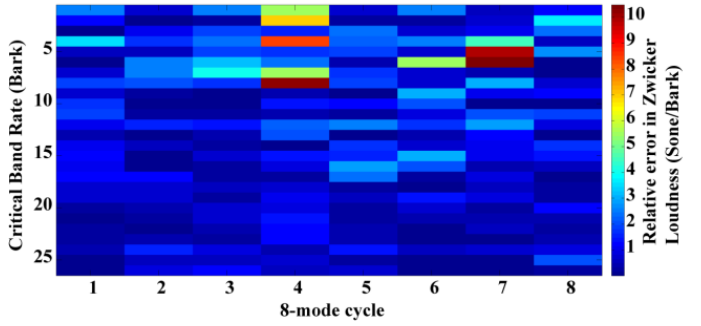

b)

Figure 3.18. Relative error in Zwicker loudness by: a) EPUNN model for OPME20 and b) EPUNN model for OPME50

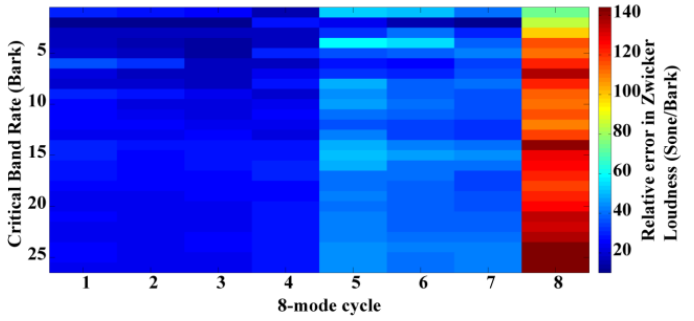

a)

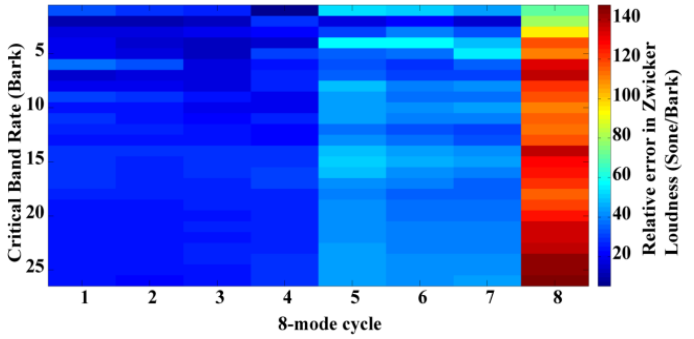

b)

Figure 3.19. Relative error in Zwicker loudness by: a) EPUNN model for PME20 and b) EPUNN model for PME50

3.3.5 Conclusions

A series of engines test performed under controlled engine operating conditions with a biofuel blends may cause slight improvements in combustion noise compared to straight diesel fuel. Moreover, this study demonstrated the capability of ANN to identify noise emitted by an engine when it is fuelled with OPME and PME fuel at several steady-state engine operating conditions. In order to evaluate the accuracy with respect to proposed ANN model, two polynomial regression models have been developed. The results for both MSE and SEP show that combined EPUNN and RBFNN model is the best one, taking into account also the simplicity of

the model, the best solution is EPUNN model.

Although the results achieve for the polynomial models may be acceptable in other context, from noise prediction point of view, an error superior to 3 dB means to double or to be halved the noise, being the accuracy of the model thus a critical factor in this kind of prediction models.

3.4 References

[1] D. Agarwal, L. Kumar, A.K. Agarwal, Performance evaluation of a vegetable oil fuelled compression ignition engine, Renewable Energy, 33 (2008) 1147-1156.

[2] A.K. Agarwal, K. Rajamanoharan, Experimental investigations of performance and emissions of Karanja oil and its blends in a single cylinder agricultural diesel engine, Applied Energy, 86 (2009) 106-112.

[3] M. Azam, A. Waris, N.M. Nahar, Prospects and potential of fatty acid methyl esters of some non-traditional seed oils for use as biodiesel in India, Biomass and Bioenergy, 29 (2005) 293-302.

[4] L. Lin, Z. Cunshan, S. Vittayapadung, S. Xiangqian, D. Mingdong, Opportunities and challenges for biodiesel fuel, Applied Energy, 88 (2011) 1020-1031.

[5] S.H. Park, H.J. Kim, H.K. Suh, C.S. Lee, Experimental and numerical analysis of spray-atomization characteristics of biodiesel fuel in various fuel and ambient temperatures conditions, International Journal of Heat and Fluid Flow, 30 (2009) 960-970.

[6] C.D. Rakopoulos, A.M. Dimaratos, E.G. Giakoumis, D.C. Rakopoulos, Study of turbocharged diesel engine operation, pollutant emissions and

combustion noise radiation during starting with bio-diesel or n-butanol diesel fuel blends, Applied Energy, 88 (2011) 3905-3916.

[7] Y.H.Y. Haik, M.Y.E. Selim, T. Abdulrehman, Combustion of algae oil methyl ester in an indirect injection diesel engine, Energy, 36 (2011) 1827-1835.

[8] A.J. Torregrosa, A. Broatch, R. Novella, L.F. Monico, Suitability analysis of advanced diesel combustion concepts for emissions and noise control, Energy, 36 (2011) 825-838.

[9] D.C. Rakopoulos, C.D. Rakopoulos, E.G. Giakoumis, A.M. Dimaratos, D.C. Kyritsis, Effects of butanol-diesel fuel blends on the performance and emissions of a high-speed DI diesel engine, Energy Conversion and Management, 51 (2010) 1989-1997.

[10] M.D. Redel-Macías, S. Pinzi, D. Leiva, A.J. Cubero-Atienza, M.P. Dorado, Air and noise pollution of a diesel engine fueled with olive pomace oil methyl ester and petrodiesel blends, Fuel, 95 (2012) 615-621.

[11] L.F. Ramírez-Verduzco, B.E. García-Flores, J.E. Rodríguez-Rodríguez, A. Del Rayo Jaramillo-Jacob, Prediction of the density and viscosity in biodiesel blends at various temperatures, Fuel, 90 (2011) 1751-1761.

[12] L.F. Ramírez-Verduzco, J.E. Rodríguez-Rodríguez, A.D.R. Jaramillo-Jacob, Predicting cetane number, kinematic viscosity, density and higher heating value of biodiesel from its fatty acid methyl ester composition, Fuel, 91 (2012) 102-111.

[13] M.Y.E. Selim, Reducing the viscosity of Jojoba Methyl Ester diesel fuel and effects on diesel engine performance and roughness, Energy Conversion and Management, 50 (2009) 1781-1788.

[14] F. Caresana, Impact of biodiesel bulk modulus on injection pressure and injection timing. the effect of residual pressure, Fuel, 90 (2011) 477-485.

[15] Y. Ren, Z. Huang, H. Miao, Y. Di, D. Jiang, K. Zeng, B. Liu, X. Wang, Combustion and emissions of a DI diesel engine fuelled with diesel-oxygenate blends, Fuel, 87 (2008) 2691-2697.

[16] X.C. Lü, J.G. Yang, W.G. Zhang, Z. Huang, Improving the combustion and emissions of direct injection compression ignition engines using oxygenated fuel additives combined with a cetane number improver, Energy

and Fuels, 19 (2005) 1879-1888.

[17] P. Rounce, A. Tsolakis, P. Leung, A.P.E. York, A comparison of diesel and biodiesel emissions using dimethyl carbonate as an oxygenated additive, Energy and Fuels, 24 (2010) 4812-4819.

[18] A. Abu-Jrai, J.A. Yamin, A.H. Al-Muhtaseb, M.A. Hararah, Combustion characteristics and engine emissions of a diesel engine fueled with diesel and treated waste cooking oil blends, Chemical Engineering Journal, 172 (2011) 129-136.

[19] G.M. Choi, M. Tanahashi, T. Miyauchi, Control of oscillating combustion and noise based on local flame structure, in: 30th International symposium on combustion, Combust Inst, Univ. Illinois Chicago, 2005, pp. 1807-1814.

[20] S. Kotake, K. Takamoto, Combustion noise: Effects of the velocity turbulence of unburned mixture, Journal of Sound and Vibration, 139 (1990) 9-20.

[21] K.K. Singh, S.H. Frankel, J.P. Gore, Study of spectral noise emissions from standard turbulent nonpremixed flames, Aiaa Journal, 42 (2004) 931-936.

[22] P. Duchaine, L. Zimmer, T. Schuller, Experimental investigation of mechanisms of sound production by partially premixed flames, in: Proceedings of the combustion institute, 2009, pp. 1027-1034.

[23] D.N. Mallikappa, R.P. Reddy, C. Murthy, Performance and emission characteristics of double cylinder CI engine operated with cardanol bio fuel blends, Renewable Energy, 38 (2012) 150-154.

[24] S. Mirheidari, M. Franchek, K. Grigoriadis, J. Mohammadpour, Y.Y. Wang, I. Haskara, Real-time and robust estimation of biodiesel blends, Fuel, 92 (2012) 37-48.

[25] S.L. Lin, W.J. Lee, C.f.F. Lee, Y.p. Wu, Reduction in emissions of nitrogen oxides, particulate matter, and polycyclic aromatic hydrocarbon by adding water-containing butanol into a diesel-fueled engine generator, Fuel, (2011).

[26] G. Knothe, "Designer" Biodiesel: Optimizing Fatty Ester Composition to Improve Fuel Properties, Energy & Fuels, 22 (2008) 1358-1364.

[27] G. Knothe, Dependence of biodiesel fuel properties on the structure of fatty acid alkyl esters, Fuel Processing Technology, 86 (2005) 1059-1070.

[28] M. Canakci, Sanli, H., Biodiesel production from various feedstocks and their effects on the fuel properties, Journal of Industrial Microbiological and Biotechnology, 35 (2008) 431-441.

[29] M.J. Ramos, C.M. Fernández, A. Casas, L. Rodríguez, Á. Pérez, Influence of fatty acid composition of raw materials on biodiesel properties, Bioresource Technology, 100 (2009) 261-268.

[30] G. Knothe, C.A. Sharp, T.W. Ryan, Exhaust emissions of biodiesel, petrodiesel, neat methyl esters, and alkanes in a new technology engine Energy & Fuels, 20 (2006) 403–408.

[31] M.S. Graboski, R.L. McCormick, T.L. Alleman, A.M. Herring, The Effect of Biodiesel Composition on Engine Emissions from a DDC Series60 Diesel Engine, in, National Renewable Energy Laboratory, Golden, Colorado, 2003.

[32] A. Schönborn, N. Ladommatos, J. Williams, R. Allan, J. Rogerson, The influence of molecular structure of fatty acid monoalkyl esters on diesel combustion, Combustion and Flame, 156 (2009) 1396-1412.

[33] R. Hickling, D.A. Feldmaier, S.H. Sung, Knock-induced cavity resonances in open chamber diesel engines, Journal of the Acoustical Society of America, 65 (1979) 1474-1479.

[34] F. Payri, A. Broatch, X. Margot, L. Monelletta, Sound quality assessment of Diesel combustion noise using in-cylinder pressure components, Measurement Science & Technology, 20 (2009).

[35] M.D. Redel-Macías, S. Pinzi, M.F. Ruz, A.J. Cubero-Atienza, M.P. Dorado, Biodiesel from saturated and monounsaturated fatty acid methyl esters and their influence over noise and air pollution, Fuel.D.O.I.: 10.1016/j.fuel.2012.01.070

[36] M.P. Dorado, E. Ballesteros, J.M. Arnal, J. Gomez, F.J. Lopez, Exhaust emissions from a Diesel engine fueled with transesterified waste olive oil, Fuel, 82 (2003) 1311-1315.

[37] J.H. Ng, H.K. Ng, S. Gan, Characterisation of engine-out responses from a light-duty diesel engine fuelled with palm methyl ester (PME), Applied Energy, 90 (2012) 58-67.

[38] M. Bunce, D. Snyder, G. Adi, C. Hall, J. Koehler, B. Davila, S. Kumar, P. Garimella, D. Stanton, G. Shaver, Optimization of soy-biodiesel combustion in a modern diesel engine, Fuel, 90 (2011) 2560-2570.

[39] A. Demirbaş, Direct route to the calculation of heating values of liquid fuels by using their density and viscosity measurements, Energy Conversion and Management, 41 (2000) 1609-1614.

[40] B. Freedman, M.O. Bagby, Heats of combustion of fatty esters and triglycerides, Journal of the American Oil Chemists' Society, 66 (1989) 1601-1605.

[41] S. Pinzi, D. Leiva, G. Arzamendi, L.M. Gandia, M.P. Dorado, Multiple response optimization of vegetable oils fatty acid composition to improve biodiesel physical properties, Bioresource Technology, 102 (2011) 7280-7288.

[42] S. Pinzi, F.J. Lopez-Gimenez, J.J. Ruiz, M.P. Dorado, Response surface modeling to predict biodiesel yield in a multi-feedstock biodiesel production plant, Bioresource Technology, 101 (2010) 9587-9593.

[43] D.B. Hulwan, S.V. Joshi, Performance, emission and combustion characteristic of a multicylinder DI diesel engine running on diesel-ethanol-biodiesel blends of high ethanol content, Applied Energy, 88 (2011) 5042-5055.

[44] Official Journal of the European Communities, Directive 2002/49/EC of the European Parliament and the Council (June 2002).

[45] M. Dorado, Raw materials to produce low cost biodiesel, in: A. Nag (Ed.) Biofuels refining and performance, 2008, pp. 107-148.

[46] A.P. Vyas, J.L. Verma, N. Subrahmanyam, A review on FAME production processes, Fuel, 89 (2010) 1-9.

[47] G. Knothe, "Designer" biodiesel: Optimizing fatty ester (composition to improve fuel properties, Energy & Fuels, 22 (2008) 1358-1364.

[48] G. Knothe, C.A. Sharp, T.W. Ryan, Effect of biodiesel composition on the formation of particulate matter exhaust emissions and comparison to petrodiesel components, in: Abstract of papers of the american chemical society, 2007, pp. 77-Fuel.

[49] M. Lapuerta, O. Armas, J. Rodriguez-Fernandez, Effect of biodiesel

fuels on diesel engine emissions, Progress in Energy and Combustion Science, 34 (2008) 198-223.

[50] S. Pinzi, I.L. Garcia, F.J. Lopez-Gimenez, M.D.L. de Castro, G. Dorado, M.P. Dorado, The Ideal Vegetable Oil-based Biodiesel Composition: A Review of Social, Economical and Technical Implications, Energy & Fuels, 23 (2009) 2325-2341.

[51] Y.D. Bao, Y. He, Study on noise of rapeseed oil blends in a single-cylinder diesel engine, Renewable Energy, 31 (2006) 1789-1798.

[52] A. Albarbar, F. Gu, A.D. Ball, Diesel engine fuel injection monitoring using acoustic measurements and independent component analysis, Measurement, 43 (2010) 1376-1386.

[53] A.E.W. Austen, T. Priede, Origins of diesel engine noise, SAE paper, 590127 (1959).

[54] M.F. Russell, R. Haworth, Combustion noise from high speed direct injection Diesel engines, SAE paper 850973, (1985).

[55] C.C. Sanchez, M.F. Pantoja, R.G. Martin, Design of Gradient Coil for Magnetic Resonance Imaging Applying Particle-Swarm Optimization, Magnetics, IEEE Transactions on, 47 (2011) 4761-4768.

[56] F. Payri, A. Broatch, B. Tormos, V. Marant, New methodology for in-cylinder pressure analysis in direct injection diesel engines - application to combustion noise, Measurement Science & Technology, 16 (2005) 540-547.

[57] K. Schmidt, J.H. Van Gerpen, The effect of biodiesel fuel composition on diesel combustion and emissions, SAE paper, 961086 (1996).

[58] F. Payri, A.J. Torregrosa, A. Broatch, L. Monelletta, Assessment of diesel combustion noise overall level in transient operation, International Journal of Automotive Technology, 10 (2009) 761-769.

[59] A.J. Torregrosa, A. Broatch, J. Martin, L. Monelletta, Combustion noise level assessment in direct injection Diesel engines by means of in-cylinder pressure components, Measurement Science & Technology, 18 (2007) 2131-2142.

[60] L. Pruvost, Q. Leclere, E. Parizet, Diesel engine combustion and mechanical noise separation using an improved spectrofilter, Mechanical Systems and Signal Processing, 23 (2009) 2072-2087.

[61] A.J. Yuste, M.P. Dorado, A neural network approach to simulate biodiesel production from waste olive oil, Energy & Fuels, 20 (2006) 399-402.

[62] M.C. Bishop, Pattern Recognition and Machine Learning, 1st ed., Hardcover, 2006.

[63] D.F. Specht, A general regression neural network, IEEE Transactions on Neural Networks, 2 (1991) 568-576.

[64] F.J. Martinez-Estudillo, C. Hervas-Martinez, P.A. Gutierrez, A.C. Martinez-Estudillo, Evolutionary product-unit neural networks classifiers, Neurocomputing, 72 (2008) 548-561.

[65] M.C. Bishop, Improving the generalization properties of radial basis function neural networks, Neural Computation, 4 (1991) 579-581.

[66] A.C. Martinez-Estudillo, C. Hervás-Martínez, F.J. Martinez-Estudillo, N. García-Pedrajas, Hybridization of evolutionary algorithms and local search by means of a clustering method, IEEE Transactions on Systems, Man, and Cybernetics, Part B: Cybernetics, 36 (2005) 534-545.

[67] P.A. Gutierrez, C. Hervas, M. Carbonero, J.C. Fernandez, Combined projection and kernel basis functions for classification in evolutionary neural networks, Neurocomputing, 72 (2009) 2731-2742.

[68] D.B. Fogel, Evolutionary Computation: A New Transactions, IEEE Transactions on Evolutionary Computation, 1 (1997) 1-2.

[69] C. Hervas-Martinez, F.J. Martinez-Estudillo, M. Carbonero-Ruz, Multilogistic regression by means of evolutionary product-unit neural networks, Neural Networks, 21 (2008) 951-961.

[70] M. Bunce, D. Snyder, G. Adi, C. Hall, J. Koehler, B. Davila, S. Kumar, P. Garimella, D. Stanton, G. Shaver, Stock and Optimized Performance and Emissions with 5 and 20% Soy Biodiesel Blends in a Modern Common Rail Turbo-Diesel Engine, Energy & Fuels, 24 (2010) 928-939.

[71] S. Godiganur, C.H. Suryanarayana Murthy, R.P. Reddy, 6BTA 5.9 G2-1 Cummins engine performance and emission tests using methyl ester mahua (Madhuca indica) oil/diesel blends, Renewable Energy, 34 (2009) 2172-2177.

[72] P. Rounce, A. Tsolakis, J. Rodriguez-Fernandez, R.F. Cracknell, R.

Clark, A. York, Diesel Engine Performance and Emissions when First Generation Meets Next Generation Biodiesel, SAE paper, 2009-01-1935 (2009).

[73] M. Lapuerta, O. Armas, R. Ballesteros, J. Fernandez, Diesel emissions from biofuels derived from Spanish potential vegetable oils, Fuel, 84 (2005) 773-780.

[74] M. Lapuerta, O. Armas, J.M. Herreros, Emissions from a diesel-bioethanol blend in an automotive diesel engine, Fuel, 87 (2008) 25-31.

[75] X.C. Lu, J.G. Yang, W.G. Zhang, Z. Huang, Effect of cetane number improver on heat release rate and emissions of high speed diesel engine fueled with ethanol-diesel blend fuel, Fuel, 83 (2004) 2013-2020.

[76] S. Pinzi, J.M. Mata-Granados, F.J. Lopez-Gimenez, M.D. Luque de Castro, M.P. Dorado, Influence of vegetable oils fatty-acid composition on biodiesel optimization, Bioresource Technology, 102 (2011) 1059-1065.

[77] A.E.W. Austen, Priede, T., Origins of Diesel engine noise, in: Proceedings IMechE Symp. on Engine Noise and Noise Supression, London, 1958, pp. 19-32.

[78] N. Lalor, M. Petit, Modes of engine structure vibration as a source of noise, SAE paper 750833, (1975).

[79] Z.C. Yuan, H. Fang, F.Q. Zhao, The Experiment Research on Related Factors of Influencing Combustion Noise of Diesel Engine, in: J.M. Zeng, Z.Y. Jiang, T. Li, D.G. Yang, Y.H. Kim (Eds.) Advances in Mechanical Design, Pts 1 and 2, 2011, pp. 1005-1009.

[80] L.P.R. de Oliveira, K. Janssens, P. Gajdatsy, H. Van der Auweraer, P.S. Varoto, P. Sas, W. Desmet, Active sound quality control of engine induced cavity noise, Mechanical Systems and Signal Processing, 23 (2009) 476-488.

Chapter 4

Models of sound source prediction

4.1 Evaluation of accuracy in an engine sound synthesis model for identifying sound sources in vehicles

4.1.1 Abstract

Sound quality is one of the principal factors intervening in customers' preferences when selecting a motor vehicle. For that reason, increasingly more precision in the models is demanded in the prediction of noise, as alternative to the traditional jury tests. Using the Sound Synthesis methods it is possible to obtain the auralization of the sound produced by a physical sound source as it would be heard in an arbitrary receptor position. The physical source is represented by an acoustic equivalent source model and the engine noise is experimentally characterized by means of the substitution monopole technique. However, some factors have an influence on the accuracy of the model obtained such as the number of descriptors of the source necessary for achieving the precision desired, the type of sound, the receptor position or the influence of the phase of the sound emitted, among others. In this study the influence of these factors in the precision of equivalent source models has been discussed. It was found that the configuration of the phase and the monopole exhibited a stronger effect over the precision of the model. Moreover, it was observed that the increasing of

the monopole number improves the error on loudness and sharpness and the number of iterations necessary in the regularization strategy to achieve a good accuracy is less.

4.1.2 Introduction

By means of auralization, the sound produced is rendered by a physical sound source in space, simulating the listening experience in a position given by the space model [1, 2]. A typical application is the measurement of acoustic transfer paths of sound radiated from a vehicle, see Figure 4.1. It is well known that there are different kinds of sound source in a vehicle which may be interesting to identify [3, 4]. In this sense, the auralization process begins with a source-transmission path-receiver model to predict the time-frequency spectrum of the sound field produced by an active source at the receiver position. The following step is to determine the transfer paths between the source and the receiver experimentally or numerically [5]. Combining the two previous steps we can calculate the time-frequency spectrum in the receptor position. For non stationary sources a discretization in the time should be made, although this can only be carried out by repeating the method of prediction of a simple spectrum in the time. If the receptor or the source is in movement it is also necessary to consider a discretization in the space and to determine the diverse transfer paths intervening in the process [6]. Once the monoaural or binaural time-frequency spectrum has been determined in a certain position, the temporal signal of the sound is synthesized based on the characteristics of the sound, like the different orders in an engine spectrum [7]. The result of this process is finding out the real experience of an observer in a specific position obtaining the possibility of assessing the sound quality perceived quickly and economically. Furthermore, sound quality is of great importance in achieving sound which is agreeable to the human ear, in fact noise annoyance not only depends on sound exposure levels [8].

Auralization models allow the definition of noise standards, thus more realistic and effective legislation can be developed. Moreover, the currently applied test procedures, such as the recent change in the ISO 362 procedure for vehicle pass-by noise testing can be referred. The new version of this standard, a new procedure has been proposed based on a series of experiments; with the aid of accurate auralization models. This work's

contribution is aimed at the assessment of accuracy on source models which are used in the first step of a vehicle pass-by sound synthesis. Within this study, the factors influencing the accuracy of the model and the number of descriptors necessary for obtaining the required precision in it have been considered, in order to simplify the models as much as possible. The influence of the receptor position, the order engine or the regularization strategies has been evaluated to establish the optimal configuration in each case. The accuracy of the models is evaluated using sound quality metrics for knowing the real listening experience.

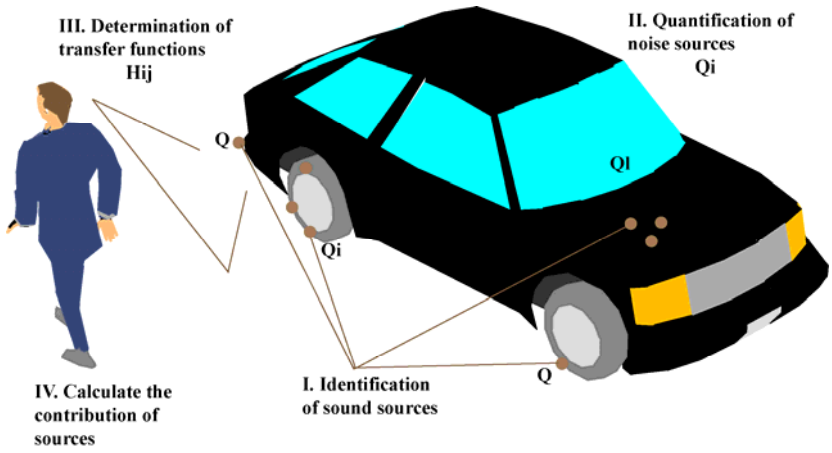

Figure 4.1. First steps in sound synthesis where Q_i are the noise sources and H_{ij} are the transfer functions between noise source and receptor position

4.1.3 Substitute source methods

First, the source model needs to be determined. Next, the type of descriptor and the method of quantification of these descriptors have to be selected. With regard to the source model, there are different alternatives developed in the literature [9], which can be classified as a function of frequency, understanding the latter to be the relation between the acoustic wavelength λ and the source dimension L. At low frequencies ($\lambda \gg L$), the simplest mathematical model of a sound source describing its behaviour is a pulsating sphere with a radius *a*, which expands and contracts harmoniously

with a perfect symmetry. If the sphere radius is much smaller than the wavelength ($ka \ll 1$), $k=\omega/c$, being the acoustic wavenumber, ω (rad·s-1) the angular frequency and c (m·s-1) the velocity of the sound, the source turns into a monopole, or, in other words, a point source. The point sources are also known as an omni directional sound source of a constant volume velocity, if two out of phase monopoles are combined to a distance d separated, are combined with ($kd \ll 1$), they would form a dipole and when two oppositive phase dipoles are combined they form a quadrupole. Monopole sound source are required for reciprocal measurements such as Noise Vibration and Harshness (NVH) applications [10]. It is due to very different space requirements of sound sources and sensors; measurements of acoustic transfer functions are often much easier done reciprocally, i.e. when source and sensor are interchanged. Once the model to be followed for the source is established, the type of descriptor to be used has to be fixed. In this sense, of the three descriptor types found: velocity patterns [5], pressure measurements at indicator positions [9], and acoustic particle velocity measurements at indicator positions [7], the one most widely used is that based on sound pressure levels at a specific distance from the sound source. In the source models applied here, the substitute sound sources are quantified by their volume velocities. Effectively, a monopole sound source has a volume velocity output in cubic meters per second and an omni directional directivity. Volume velocity is thus equal to the particle velocity (in meters per second) times the surface of the sound source. These are obtained from pressure measurements of microphones at indicator positions, since the employment of any other type of descriptor for engine sound is difficult to measure and costly.

For the quantification of these descriptors there are three techniques, mainly: 'Sound Intensity' [11], 'Acoustic Holography (NAH)' [12] and 'Airborne Source Quantification (ASQ)' [13].

The basic principle of the 'Sound Intensity' technique is the measurement of the acoustic energy which passes through the area unit. By means of the integration of the surface close to the study object, the power of the sound is calculated. The main advantage is that this permits the determination of the directionality of the sound, but its drawback is its high sensitivity to wind effects, which restricts the distance from the receptor, since the measurements have to be made very close to the surface of the

noise source. The NAH or AH techniques are based on the use of the fast Fourier transform, resulting in a low computational cost, this being its main advantage. However, its application is very limited by source geometry [14] and intrinsic errors due to sampling and finite measurement apertures. Compared with other acoustic array techniques, NAH or AH require a larger number of indicator microphones for a high resolution.

The Transfer Path Analysis (TPA) is a procedure by which it is possible to determine the flow of vibro-acoustic energy from the source, by means of solid structures and air, up to a specific receptor position. When it only intervenes as a means of air transmission the TPA is denominated ASQ. Although in some cases the post-processing time can be important, the inverse ASQ method is, in general, suitable for a sound synthesis approach, as will be described later on.

4.1.1.1 Acoustic source quantification

A real source model is obtained by a substitution source model, in which *M* monopoles are distributed over the radiating surface of the source with acoustic quantities in *N* field points or indicator points. The relation between the complex volume velocities *q* of the *M* monopoles and the pressures *p* in *N* field points is given by the ASQ method by (4.1), in which *H* is a frequency response matrix

$$\mathrm{P}_{(\mathrm{Nx1})} = \mathrm{H}_{(\mathrm{NxM})}\mathrm{q}_{(\mathrm{Mx1})} \tag{4.1}$$

each element of the transfer function matrix *H*, (4.1) is calculated using the monopole radiation formulation

$$\mathrm{H} = \mathrm{j}\rho\omega\frac{\mathrm{e}^{-\mathrm{jkr}}}{2\pi\mathrm{r}} \tag{4.2}$$

where *r* is the distance between the considered source-received couple (m), *k* the acoustic wavenumber (rad·m-1), ω the pulsation (rad·s-1), and ρ the density of the fluid (kg·m-3).

The calculation of *q* starting from *p* and *H* requires the inversion of a matrix. When the number *N* of indicator points is different from the number of monopoles, the inverse matrix H^{-1} has to be redefined as a least

square pseudo-inverse H^+. The method used the most to obtain the pseudo-inverse is the singular value decomposition (SVD), in which the matrix H is factorized, as indicated in (4.3)

$$\mathrm{H} = \mathrm{U}\sum \mathrm{V}^{\mathrm{H}} = \sum_{\mathrm{i}=1}^{\mathrm{M}} \mathrm{u}_{\mathrm{i}}\sigma_{\mathrm{i}}\mathrm{v}_{\mathrm{i}}^{\mathrm{H}} \tag{4.3}$$

in which U is an N-by-N unitary matrix; V is another M-by-M unitary matrix, the superscript H indicating the Hermitian transpose and σ a diagonal matrix with nonnegative real numbers on the diagonal ($\sigma_i \geq 0$) known as singular values of H matrix. A common convention is to order the diagonal entries σ in a descending order

$$\mathrm{H}^{+} = \mathrm{V}\sum{}^{+}\mathrm{U}^{\mathrm{H}} \tag{4.4}$$

$$\mathrm{q} = \mathrm{H}^{+}\tilde{\mathrm{p}} = \mathrm{V}\sum{}^{+}\mathrm{U}^{\mathrm{H}}\tilde{\mathrm{p}} = \sum_{\mathrm{i}=1}^{\mathrm{M}} \frac{\mathrm{u}_{\mathrm{i}}^{\mathrm{H}}\tilde{\mathrm{p}}}{\sigma_{\mathrm{i}}}\mathrm{v}_{\mathrm{i}} \tag{4.5}$$

being $\sum{}^{+} = \mathrm{diag}(\sigma_1^{-1},\sigma_2^{-1},...,\sigma_R^{-1},0,...,0)$.

The inversion of the matrix H taking (4.4) can be easily calculated due to the decomposition properties of the matrices. The difficulty lies in the fact that, often, this inversion poses the problem of being ill-conditioned, since most of the systems are overdetermined (i.e. with $N \geq M$), as stated in [15]. In this case, the application of pseudo-inverse does not ensure the obtaining of satisfactory results, so that the application of regularization methods is resorted to.

4.1.1.2 Regularization techniques

One of the most and well established regularization methods is the Tikhonov-Phillips one which finds the solution $\mathrm{x}_{\lambda}^{\delta}$ to the following minimization problem:

$$\min_{\mathrm{x}} \left\|\mathrm{Hx} - \mathrm{y}^{\delta}\right\|^2 + \lambda\left\|\mathrm{Lx}\right\|^2 \tag{4.6}$$

where λ is known as the regularization parameter whose value must be

determined. The operator L is used to impose some constraints about the smoothness of the solution.

The selection of regularization parameters is highly complex and, in this respect, a large amount of research works have been done to develop a suitable strategy for that selection [16]. Among these techniques are the *L-curve* criterion and the *generalized cross validation* (GCV) method. These techniques need to test a large number of regularization parameters in order to find reasonably good values and this can be very time-consuming although it has the advantage of not requiring any prior knowledge of the error level in p observations. However, other techniques require additional information on the noise present in the data, or on the amount of regularization prescribed by the optimal solution. In this work, the value of the ratio between the regularization part $\|\mathrm{Lx}\|^2$ and the value of the Tikhonov functional $\|\mathrm{Hx}-\mathrm{y}^{\delta}\|^2+\lambda\|\mathrm{Lx}\|^2$ were assigned, in the hypothesis that the regularization part would somehow preserve the fidelity to the data represented by the residual norm $\|\mathrm{Hx}-\mathrm{y}^{\delta}\|^2$. A method is proposed for the updating of regularization parameters, which decreases the Tikhonov functional if the regularization part is too large and increases it otherwise.

With the iterative algorithm, it was aimed to obtain a good solution to the problem posed for an acceptable number of iterations and without it being necessary to know or estimate $\|\mathrm{e}\|$. The results obtained were compared with a different number of iterations and with other traditional methods for the selection of regularization parameters, such as the *L-curve* criterion and the *generalized cross validation* (GCV) method.

The L-curve validation. The name *L-curve* comes from the curve representing the logarithm of the norm of the solution $\|\mathrm{x}\|$ as a function of the logarithm of the residue r, for different values of the regularization parameters β. With a small regularization, the norm of the regularized solution drops abruptly with β for a small variation in the residual norm, this being the 'vertical' part of the *L-curve*. With too much regularization, the residual norm significantly increases with β, whereas the norm of the regularization solution slightly decreases; this is the 'horizontal' part of the

L-curve. The best value for β is obtained in the vertex of the *L-curve*; this is the best compromise between the minimum of $\|x\|$ and *r*. The curve is represented on a log-log scale since both magnitudes are not comparable and a relative scale cannot therefore be employed. The curvature function is given by the following expression

$$J_{LCV}(\beta) = \frac{\rho'_\beta \eta''_\beta - \rho''_\beta \eta'_\beta}{\left(\rho'^2_\beta + \eta'^2_\beta\right)^{2/3}} \quad \text{with } \rho_\beta = \log(r_\beta); \eta_\beta = \log(\|x_\beta\|) \qquad (4.7)$$

$'$ and $''$, being, respectively, the first and second derivative with respect to β. The optimal value β_{LCV} corresponds to the curve's corner maximizing function $J_{LCV}(\beta)$.

Generalized cross validation. GCV is the first method for the fit of β. This method is an extension of the *Ordinary Cross Validation principle* (OCV), a method based on the capacity to obtain a solution with (*m-l*) observations to predict the *m-th* observation. The GCV function to be minimized is given by

$$J_{GCV}(\beta) = \frac{r_\beta^2}{\mathrm{Tr}\left(I_{(mxm)} - hh_\beta^{-1}\right)^2} \qquad (4.8)$$

Tr(x) being for the trace of matrix *x*. The denominator of the GCV function is an estimation of the trend induced by β. Without any regularization (β=0) since hh_β^{-1} is equal to I_{mxm}. When the amount of regularization increases, the matrix hh_β^{-1} moves away from the identity matrix, with the value of the denominator J_{GCV} being increased.

Iterative Tikhonov algorithm. The Tikhonov method establishes that the function (4.10) has a single minimum for any value λ>0, the same as $\theta(x,\lambda) = \|Hx - y^\delta\|^2 + \lambda\|Lx\|^2$ $N(H) \cap N(L) = \{0\}$ in which $N(\cdot)$ is a null space of the matrix.

$$\theta(x,\lambda) = \left\| Hx - y^{\delta} \right\|^2 + \lambda \left\| Lx \right\|^2 \tag{4.9}$$

Considering that x_λ is the minimum of the function, this can be characterized as the solution of the system:

$$(H^{*}H + \lambda L^{*}L)x_{\lambda} = H^{*}y^{\delta} \tag{4.10}$$

An iterative algorithm is used in this work to computerize the values (x_k,λ_k), where λ_k is updated in each iteration and x_k is obtained by applying the CG iterations to (4.10) with $\lambda=\lambda_k$.

The problem in the regularization techniques is how to determine the regularization parameters. This is because when the parameters are too large the solution will significantly deviate from the correct solution, and when they are too small, they complicate the problem too much. γ being the prescribed weight of regularization part $\hat{\gamma} = 1e^{-1} \left\| Lx \right\|^2$ with respect to the Tikhonov functional, for each given value of λ_k, x_k is computed resolving (4.7) and γ_k as:

$$\gamma_k = \frac{\left\| Lx_k \right\|^2}{\theta(x_k, \lambda_k)} \tag{4.11}$$

Employing the following rule for the updating of regularization parameters:

$$\lambda_{k+1} = \lambda_k + sign(\hat{\gamma} - \gamma_k)\mu \tag{4.12}$$

$$sign(\hat{\gamma} - \gamma_k) = \begin{cases} 1 & \text{if } (\hat{\gamma} - \gamma_k) > 0 \\ -1 & \text{if } (\hat{\gamma} - \gamma_k) < 0 \\ 0 & \text{if } (\hat{\gamma} - \gamma_k) = 0 \end{cases}$$

The precision of the solution obtained for a value of de $\hat{\gamma} = 1e^{-3}$ was verified.

4.1.1.3 Problem description

In previous sections have been shown, highly detailed, the reasons for the selection of the source model, the type of descriptors and the method for the quantification of monopoles. By means of the experiments carried out in this research, it was aimed to measure the influence of certain key factors which affect the precision of these types of models, evaluated in terms of sound quality, in response to some questions like: the number of monopoles necessary for obtaining a sufficient accuracy, the influence of the receptor position, the type of noise or the influence of the regularization strategies (regularization strategy used, selection of parameters or number of iterations). Some authors have evaluated tire sound source in vehicle based on the number of monopoles required and non iterative Tikhonov regularization [17]. However, for engine noise source, it is primordial to considerer several relationship of phase, to simulate the engine modes, and target positions, in order to achieve more realistic models based on the procedure established by the standard.

It can be anticipated that the accuracy of the model improved when the number of monopoles increased, if the number of significant singular values was less than the number of microphones. The superiority of other methods such as NAH or AH in the establishment of source strengths is known, although this was not the objective of this investigation, since what was aimed was not the reconstruction of the velocity pattern on the boundary of the source, but the prediction of the resulting spectrum at different receptor positions. With regard to frequency limits, their behaviour was similar to that of NAH or AH. At low frequencies, only some monopoles are necessary to reconstruct the radiation pattern of the source. However, at high frequencies the number of monopoles required is larger, although this depends on a compromise with the condition number as will be explained in the following sections.

4.1.1.4 Overview of different models

Figures 4.2 shows the 9 models with monopoles taken into account in this paper, classified in ascending order as a function of the number of monopoles studied. In all the models, the radiating engine is modelled as a limited set of radiating sub-sources. The radiation of these sub-sources can

be approximated to the radiation of a simple monopole by finding the mean of the transfer functions, although this does not modify the number of unknown source strengths q. The amount of points used in the mean of each FRF is determined considering the number of loudspeakers involved.

In addition, the phase of the loudspeakers in the set-up is modified individually and the signal transmitted via an amplifier to the loudspeakers. In this way, we represent phase changes of between 0º and 180º, and we can also activate and disactivate certain loudspeakers. Figure 4.3 represents all the phase configurations studied v1, v2, v3, v4, v5 and v6, respectively.

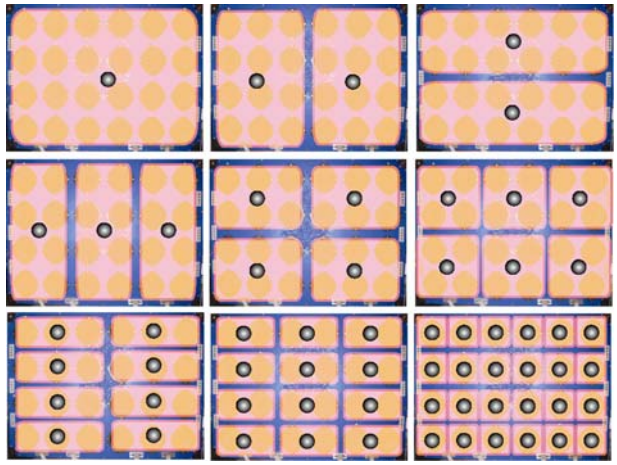

Figure 4.2. Overview of models studied

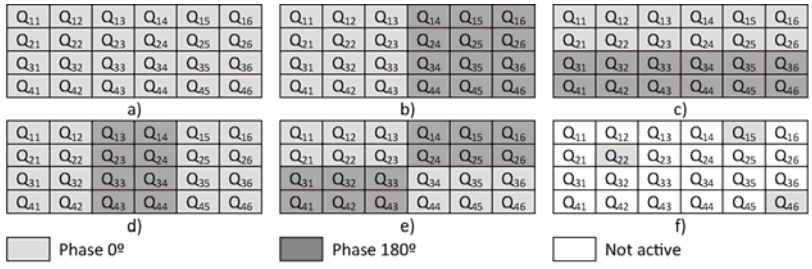

Figure 4.3. Phase configurations of the loudspeakers

Additionally, the sound emitted by the source was modified, making a study with a repetitive sound, blockwave at 400 Hz, and with a random burst noise of between 100-10000 Hz (no noise, 1% and 5%). Considering the number of monopoles, the phase configuration and type of sound, a total of 108 different configurations were made. As indicated in Section 1, the main objective of this research was to quantify the accuracy of the model as a function of the number of monopoles. From the perspective of the auralization of the sound in real time, it is important for the number of monopoles to be as small as possible without compromising the accuracy of the spectrum predicted in terms of sound quality. It was also of interest with respect to other studies [9] to study the precision of the model for different types of sound and with different phase configurations. The accuracy of the prediction in terms of the distance to the noise source was also evaluated for different receptor positions from different angles, see Figure 4.4, including two microphones in a binaural position. We can adduce that the angle with respect to the noise source was decisive in the precision of the model when the phase of the sound emitted by the loudspeakers was varied, and that, when the phase is the same for all the loudspeakers, configuration of the phase a), the precision of the model varies depending on the distance to the source.

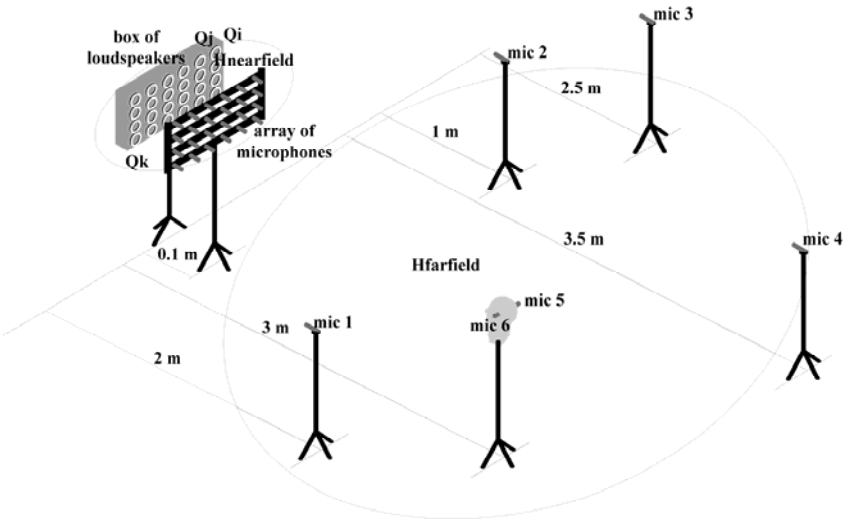

Figure 4.4. Configuration of the measurement set-up

4.1.1.5 Measurement set-up

The set-up used for this research consisted of a rectangular box with outer dimensions 902 mm x 602 mm x 190mm, with 24 loudspeakers separated from it at a distance of 100 mm. The nearest indicator microphones are positioned at a distance of 0.15 m from the loudspeaker cabinet, see Figure 4.5.

This loudspeakers array allows to simulate sources of increasing complexity, by means of the phase variation between the different loudspeakers in the array.

The set-up is placed inside a semi-anechoic room, where background levels remains below 35 dB(A). An LMS instrumentation series, consisting of a portable and multi-channel SCADAS meter, several Brüel and Kjaer (B&K) prepolarized free-field half-inch microphones model 4950 and prepolarized free-field quarter-inch microphone model 4954 were utilized as the measuring device. LMS Test.Lab was the measurement software package and all the microphones were calibrated with a B&K calibrator model 4231. Recorded measurements were sent to Matlab for post processing.

The measurements were taken with a sampling frequency of 20.480 kHz. The frequency resolution was 1.25 Hz and 50 spectral averages were implemented for analyses. Linear averaging was used to place equal emphasis on all spectra or time records. This type of averaging is helpful for the analysis of stationary signals.

Figure 4.5. Loudspeaker cabinet and microphone array

For the engine mock-up sound measurements, the height of the six free-field microphones above the ground was 1.2 m and the distance between the microphones and the loudspeakers is presented in Figure 4.4, following the ISO 365. All the microphones were pointed towards the source and situated parallel to the ground at different angles: microphones 1 and 2 at 45±10º, microphone 3 at 20±10º to the vertical plane, in line with the direction of the source, and microphones 5 and 6 were positioned in a binaural head, corresponding to human ears.

4.1.1.6 Evaluation of investigated models

Traditionally, acoustics engineers have employed measuring units such as dBA, which, in spite of showing a correlation with human perception, simply ponderates the effects of the different components in frequency of a complex sound. In this sense, it neglects an important mechanism within the ear transduction of pressure fluctuations into signals to the brain, namely frequency masking. By means of a study of the sound and psychoacoustic quality a more than mathematical interpretation is made of the pressure signals in order to correlate the acoustic stimulus with the hearing sensation [18].

To quantify the accuracy of the prediction, sound quality metrics were used. Among these metrics, the most important ones applied to the noise of a vehicle are: loudness, sharpness, roughness and fluctuation strength [19]. In this study, as the most significant ones, sharpness and Zwicker loudness were used to correlate, in this case, the noise of the engine. Therefore, these two metrics were fundamentally used throughout this study. Both metrics have been described in 2.1.3.5 of chapter 2.

4.1.2 Results and discussion

The study made involved a multitude of factors to be taken into account in the results, such as the number of monopoles, the phase configuration, the type of noise, the receptor position, regularization method, regularization parameter selection method, and all the parameters involved in this study, which made it difficult to evaluate all the possible combinations. Therefore, the study was initiated assessing the precision of the model in terms of relative error in loudness and sharpness for all the

phase configurations in a specific receptor position (microphone 4), without applying the regularization strategies and for all the types of noise studied. Next, the influence of the receptor position was studied without taking into account the regularization strategies for model 6M, which, according to the previous section, is the one presenting a smaller error. Finally, the influence of the regularization strategies were studied, contemplating the improvement in the regularization method proposed for different numbers of iterations with respect to traditional strategies.

4.1.2.1 Influence of the phase configuration

In Figure 4.3 the different phase configurations employed can be seen. For each of these, the relative error in sharpness and Zwicker loudness in the different models was studied fixing the receptor position (microphone 4), see Figures 4.6a and 4.6b blockwave noise and Figures 4.6c and 4.6d random noise. As can be deduced from these figures, the error in loudness was similar for the two types of sound studied; it was between 20-80% depending on the model, except for the models with 12M and 24M, which displayed a different behavior from the rest. For example, the model 24M succeeded in reaching an error 4 times greater in the random burst noise for the configuration of phase v3 than that of a blockwave noise.

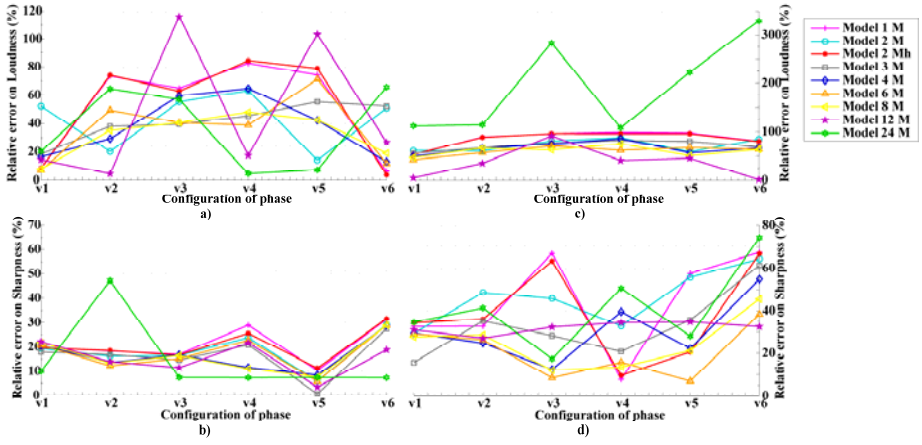

Figure 4.6. . a) and b) relative error loudness and sharpness blockwave noise; c) and d) relative error loudness and sharpness random noise

The error in sharpness varied between 8-72% for a random burst noise, whereas for a blockwave noise it was found in the interval 3-30%, except model 24M, which reached a value of over 45%. It shows that the accuracy achieved in terms of sharpness is better than loudness. On the other hand, also, it can be observed that when the number of monopoles is increased, the error both in total loudness and in sharpness decreases for the two types of noise. The model with 12 and 24 monopoles, as mentioned previously, presented a different behavior from the rest of the models and this was due to the problem of the conditioning of the matrix, as will be shown in Figure 4.8.

It was observed that the configuration of the model had a certain influence on the error since, considering the same number of monopoles, model 2hM presented a relative error in loudness of almost 20% greater than model 2M, with this greater difference becoming 45% in the configuration of phase v2. In this sense, it can also be noted that the models presenting similar configurations to those of phase**,** for example, model 4M and phase configuration v5, the error occurring is lesser both in Zwicker loudness and in sharpness in this phase configuration. Therefore, it can be concluded that the substitute source model requirements to include at least one substitute source on, or close to, each maxima in the radiation pattern of the original source.

4.1.2.2 Influence of the receptor position

As from Figure 4.7, it can be observed how, except for model 24M, all the rest, in general, have the same tendency to behave in terms of distance, both in total Loudness and in Sharpness for each one of the types of noises studied with the configuration of phase v1. The model with 24 monopoles presented a greater difference with respect to the value observed, and this could be explained, as in the previous case, by the conditioning problem presented by the model.

As from Figure 4.8, it may be inferred that the phase configuration influences on the accuracy of the model depending on the receptor position. It may be due to the fact that the microphone distribution is not in a line with the loudspeaker array which may be explained by Doppler effect, see Figure 5. For example, when all the loudspeakers have the same phase, case

v1, the distance at which the receptor is found is a factor to be taken into account. The error in total loudness reaches a value of over 100% in the prediction of the receptor position of microphone 4 when the phase configuration is the same for all the loudspeakers, see Tables 4.1 and 4.3 for error on total loudness and Tables 4.2 and 4.4 for error on sharpness.

Another consideration to be made is that the error committed in the microphones situated in a binaural position is different in spite of being at the same distance. This is due to the diffraction and reflection of the head and torso, which causes the sound field to be different, as was reported by Vorländer [2].

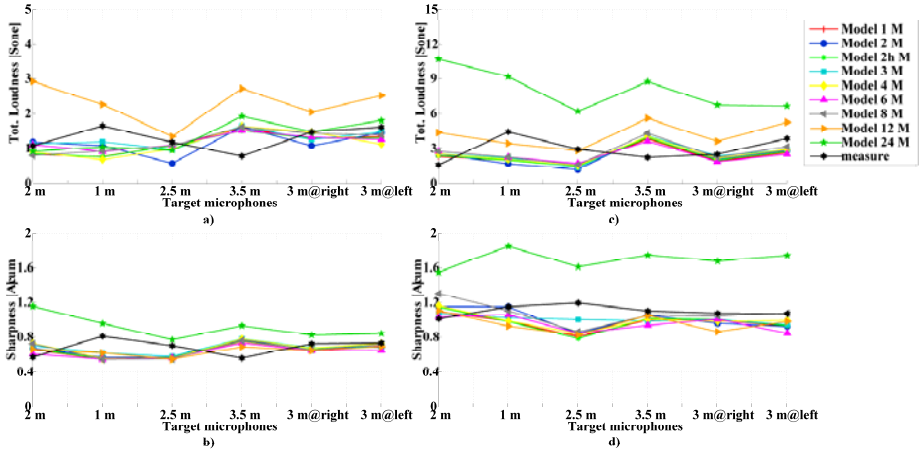

Figure 4.7. a) and b) error on total loudness and sharpness blockwave noise; c) and d) error on total loudness Sharpness for the different receptor positions

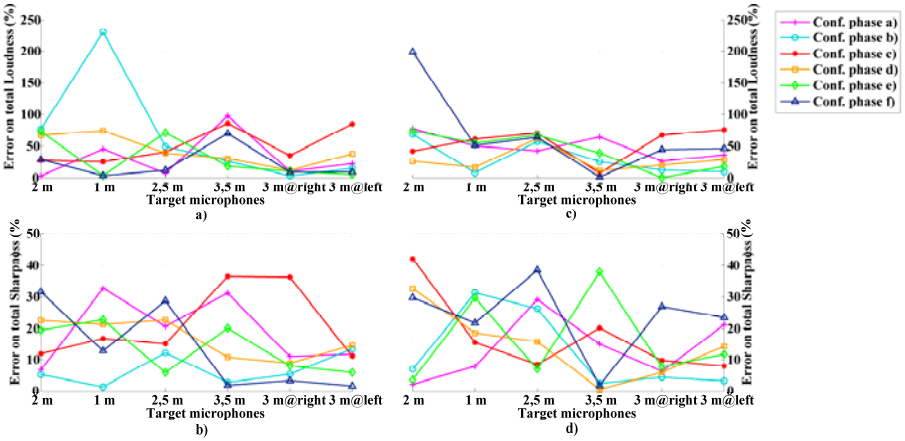

Figure 4.8. Error on total loudness and Sharpness of the phase configuration vs target microphones for model 6M, a) and b) for a blockwave noise; c) and d) for a random noise

Table 4.1. Error on total Loudness (%)as a function of the receiving distance for a Random burst noise

	Error on total Loudness (%)					
Mod.	**Mic 1**	**Mic 2**	**Mic 3**	**Mic 4**	**Mic 5**	**Mic 6**
1M	23.81	54.37	8.38	106.21	12.92	16.95
2M	10.60	34.84	52.32	110.88	27.20	10.11
2hM	21.76	54.97	8.55	96.89	12.45	19.23
3M	5.67	27.96	18.37	114.63	15.15	8.50
4M	17.11	59.49	16.59	112.43	0.40	30.51
6M	3.06	45.44	7.02	97.66	10.37	22.19
8M	26.32	44.54	7.95	110.75	3.09	13.99
12M	172	36.58	14.47	253.36	37.97	55.85
24M	15.25	37.25	20.32	148.83	0.20	11.22

Table 4.2. Error on Sharpness (%) as a function of the receiving distance for a Random burst noise

	Error on Sharpness(%)					
Mod.	**Mic 1**	**Mic 2**	**Mic 3**	**Mic 4**	**Mic 5**	**Mic 6**
1M	23.81	54.37	8.38	106.21	12.92	16.95
2M	10.60	34.84	52.32	110.88	27.20	10.11
2hM	21.76	54.97	8.55	96.89	12.45	19.23
3M	5.67	27.96	18.37	114.63	15.15	8.50
4M	17.11	59.49	16.59	112.43	0.40	30.51
6M	3.06	45.44	7.02	97.66	10.37	22.19
8M	26.32	44.54	7.95	110.75	3.09	13.99
12M	172	36.58	14.47	253.36	37.97	55.85
24M	15.25	37.25	20.32	148.83	0.20	11.22

Table 4.3. Error on total (%)in terms of the receptor distance for a Random burst noise with configuration of phase v1

	Error on total Loudness (%)					
Mod.	**Mic 1**	**Mic 2**	**Mic 3**	**Mic 4**	**Mic 5**	**Mic 6**
1M	46.69	56.05	52.93	73.75	24.20	32.23
2M	63.03	63.19	61.11	86.38	16.86	27.24
2hM	52.46	56.08	52.96	78.91	21.05	29.95
3M	63.94	51.72	55.42	85.56	6.25	25.63
4M	63.03	54.06	49.76	83.98	14.07	25.01
6M	77.82	50.17	42.46	64.34	26.05	36.18
8M	77.17	50.08	47.23	96.24	10.89	18.60
12M	185.21	22.84	4.80	153.75	46.22	36.26
24M	594.81	105.99	111.59	296.10	173.09	72.52

Table 4.4. Error on Sharpness in terms of the receptor distance for a Random burst noise with configuration of phase v1

	Error on Sharpness(%)					
Mod.	**Mic 1**	**Mic 2**	**Mic 3**	**Mic 4**	**Mic 5**	**Mic 6**
1M	8.26	14.43	32.61	9.47	6.97	13.34
2M	13.59	0.31	29.36	4.40	10.72	13.70
2hM	13.06	14.84	34.38	7.77	6.45	12.87
3M	5.53	10.85	15.67	10.54	6.73	11.71
4M	14.64	14.13	29.53	8.78	8.68	7.07
6M	2.12	7.82	29.18	15.09	6.18	21.30
8M	28.16	4.04	27.73	4.61	2.77	0.48
12M	9.21	19.43	31.05	4.63	19.93	8.32
24M	52.69	60.02	34.64	57.70	55.16	62.04

4.1.2.3 Regularization strategies

The inversion of the matrix *H* in this type of model presents the ill-conditioned problem. The quantification of the substitution sources depends on the conditioning of the problem and success is not guaranteed by only employing the simple least squares method [20]. Figure 4.9 represents the condition number as a function of the frequency for models 2-24. Some authors [9] indicates that a condition number is small when it reaches values of around 10^3. Observing Figure 4.9 we can affirm that only model 24M has a high condition number. In our case, the number of indicator microphones was the same for all the models, 24, which was higher than the number of monopoles in models 2-12M and the same as the number of monopoles in model 24M.

Note that the condition number increases at low frequencies. Starting from 1 kHz, the condition number becomes stable, around 2, which means that the smallest singular value is equal to 50 percent of the greatest one. For the source reconstruction this signifies a limitation in the resolution achieved. However, for the prediction of the resulting spectrum in the receptor position it is not a problem. Also, as established in [21], the conditioning improves when the geometry of the positions measured which are identical to the geometry of the source is selected, and when these measurements are made close to the source. In Figure 4.4 it can be seen how

these recommendations have been followed in carrying out the measurements in our research.

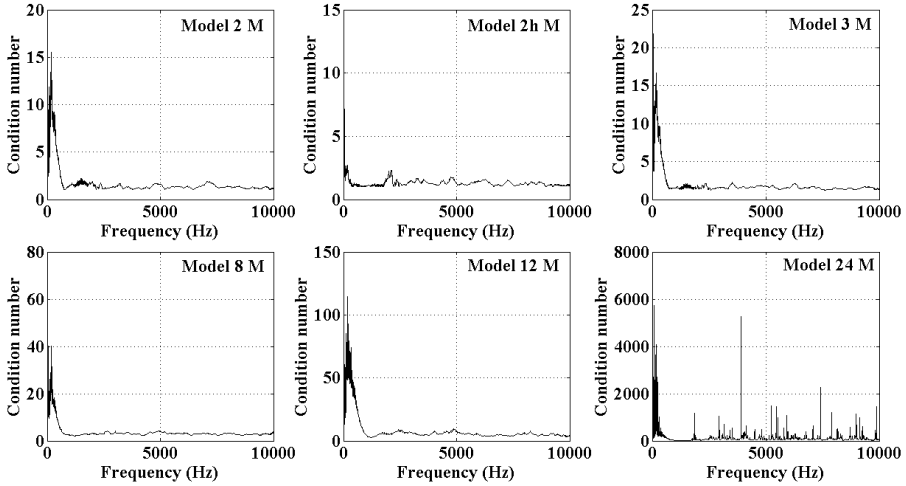

Figure 4.9. Condition number models 2-24M

Tables 4.5 and 4.6 show the relative errors on Zwicker Loudness (%) and Tables 4.7 and 4.8 show the relative errors on Sharpness (%) for the configuration of phase a) in the receptor position 4. The following abbreviations in these tables have been considered; Ti-L=Tikhonov L-curve; Ti-Gcv=Tikhonov-generalized cross validation; Ti-itxx=Tikhonov iterative with nºxx of iterations. Simulations of the iterative algorithm were made with a regularization parameter value: γ=1e-3.

By taking the values shown in the tables, it can be deduced that, as the number of monopoles increased the number of iterations necessary was lower in order to succeed in reducing the error. The superiority of the iterative algorithm developed compared to the traditional regularization strategies can be observed in most of the cases studied except for model 1 M. Kim and Nelson [21] report that the *L-curve* method is more effective than the *GCV* when the problem presents a well conditioned. In view of this, as the condition number varies with the frequency, some authors like Pézerat [15] propose a combination of both methods according to their

behavior as a function of the frequency.

Table 4.5. Relative error on loudness (%) for blockwave noise with γ=1e-3

Model	1M	2M	2hM	3M	4M	6M	8M	12M	24M
Ti-L	23.70	74.09	22.15	79.15	71.24	66.45	84.07	91.06	152.59
Ti-Gcv	23.70	74.09	22.15	63.47	71.11	61.27	75.13	82.77	63.47
No reg.	106.22	110.88	96.89	114.64	112.44	97.67	110.75	253.37	148.83
Ti-it5	100.00	100.00	100.00	100.00	100.00	100.00	100.00	100.00	100.00
Ti-it20	100.00	100.00	100.00	100.00	100.00	100.00	100.00	100.00	100.00
Ti-it50	100.00	100.00	100.00	100.00	100.00	99.35	97.80	94.17	84.84
Ti-it100	100.00	97.80	98.32	93.78	90.67	85.62	78.50	67.75	44.56
Ti-it200	90.54	78.11	80.44	67.23	57.12	48.19	31.35	**17.88**	**15.16**
Ti-it300	73.45	53.11	56.74	36.40	29.15	16.84	**4.66**	-	-
Ti-it400	56.74	30.57	35.75	**11.27**	**1.55**	**12.18**	-	-	-
Ti-it500	40.67	11.27	17.62	-	-	-	-	-	-
Ti-it600	25.26	**5.83**	**2.85**	-	-	-	-	-	-

Table 4.6. Relative error on loudness (%) for random burst noise with γ=1e-3

Model	1M	2M	2hM	3M	4M	6M	8M	12M	24M
Ti-L	3.85	36.65	19.14	37.15	43.03	36.33	62.53	81.22	153.57
Ti_Gcv	3.85	37.33	19.23	75.61	41.95	30.14	46.29	49.86	75.61
No reg.	73.76	86.38	78.91	85.57	83.98	64.34	96.24	153.76	296.11
Ti-it5	100.00	100.00	100.00	100.00	100.00	100.00	100.00	100.00	100.00
Ti-it20	100.00	100.00	100.00	100.00	100.00	100.00	100.00	100.00	99.68
Ti-it50	100.00	100.00	100.00	100.00	99.73	99.05	98.10	96.43	89.64
Ti-it100	99.77	98.19	98.19	96.70	94.98	91.40	87.29	81.00	56.88
Ti-it200	95.29	88.51	88.28	80.81	74.07	64.39	49.95	41.49	**3.30**
Ti-it300	86.33	71.54	70.81	58.96	48.91	37.19	16.11	**8.33**	-
Ti-it400	74.43	53.30	53.35	37.60	25.48	13.26	**8.73**	-	-
Ti-it500	60.77	35.93	36.52	17.69	**6.06**	**4.98**	-	-	-
Ti-it600	49.32	**19.77**	**20.00**	**1.76**	-	-	-	-	-

Table 4.7. Relative error on total sharpness (%) for blockwave noise with γ=1e-3

Model	1M	2M	2hM	3M	4M	6M	8M	12M	24M
Ti-L	23.48	16.61	23.79	21.11	22.05	17.40	22.23	29.11	52.74
Ti-Gcv	23.48	16.61	23.78	11.75	22.10	13.34	23.29	28.66	11.75
No reg.	34.71	37.60	35.42	40.42	39.75	31.24	36.72	23.23	68.00
Ti-it5	21.90	21.90	21.90	21.90	21.90	21.90	21.90	21.90	21.90
Ti-it20	21.90	21.90	21.90	21.90	21.90	21.90	21.90	21.90	21.90
Ti-it50	21.90	21.90	21.90	21.90	21.90	20.29	17.32	11.54	10.82
Ti-it100	21.90	17.25	18.20	11.71	11.76	11.19	8.23	6.96	**3.41**
Ti-it200	11.91	8.37	9.43	7.19	5.92	3.90	**0.97**	**1.15**	-
Ti-it300	8.17	5.33	5.59	**1.47**	**0.79**	**1.94**	-	-	-
Ti-it400	6.09	**1.23**	**1.35**	-	-	-	-	-	-
Ti-it500	2.41	-	-	-	-	-	-	-	-
Ti-it600	**0.37**	-	-	-	-	-	-	-	-

Table 4.8. Relative error on total sharpness (%) for random burst noise with γ=1e-3

Model	1M	2M	2hM	3M	4M	6M	8M	12M	24M
Ti-L	13.05	15.42	11.49	18.80	15.81	18.66	11.93	19.03	34.87
Ti-Gcv	13.05	16.63	11.38	18.07	19.53	27.08	18.06	19.76	34.07
No reg.	19.48	14.40	17.77	20.55	28.79	25.10	24.61	24.64	57.71
Ti-it5	67.33	67.33	67.33	67.33	67.33	67.33	67.33	67.33	67.33
Ti-it20	67.33	67.33	67.33	67.33	67.33	67.33	67.33	67.33	67.33
Ti-it50	67.33	67.33	67.33	68.49	67.60	65.57	63.51	63.52	45.19
Ti-it100	57.70	63.44	63.44	63.44	62.70	61.69	43.82	46.57	28.84
Ti-it200	43.00	53.68	51.57	46.37	40.84	40.56	27.44	30.76	18.33
Ti-it300	30.91	40.36	38.76	35.62	32.18	31.37	20.43	23.86	12.86
Ti-it400	20.89	33.72	33.11	28.66	26.48	25.55	16.97	18.91	10.37
Ti-it500	15.77	27.71	27.60	24.26	23.47	21.40	13.86	14.73	9.03
Ti-it600	**10.37**	**13.03**	**10.44**	**16.55**	**17.12**	**17.97**	**12.62**	**12.40**	**7.38**

Figure 4.10 shows the influence of the regularization for model 6M for the two types of noise studied. The effect of the regularization strategy is clear from the figure; the difference between the predicted and observed

values is lesser when the iterative algorithm developed is employed.

The spectrograms in Figure 4.11 show the error in 1/3rd octave band for the configuration of phase v1 in the target microphone 4 for a random burst noise. It can be observed graphically how the error diminishes when applying the regularization strategies. The superiority of the iteration algorithm with respect to traditional methods is also clear, with the result improving as from 200 iterations.

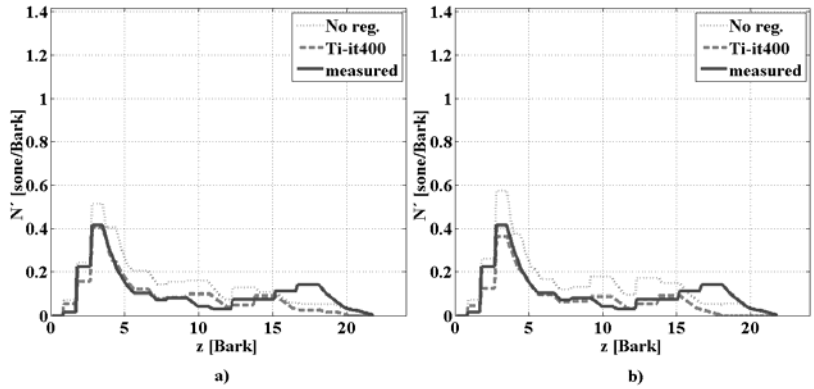

Figure 4.10. Influence of the regularization (Ti-iterative) on the Zwicker loudness predicted in model 6M for the configuration of phase a): a) blockwave noise. b) random burst noise

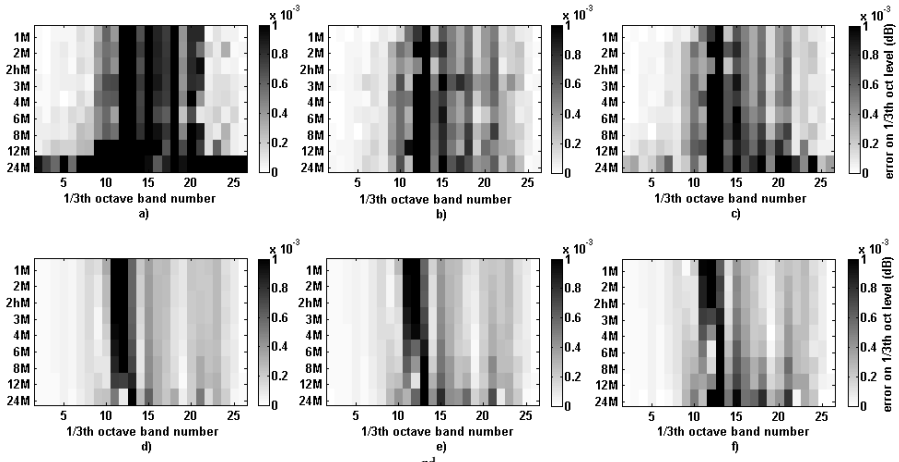

Figure 4.11. Error on 1/3rd octave band for random burst noise target microphone 4 configuration phase v1, a) without regularization, b) with GCV technique, c) L-curve technique, d) with Tikhonov iterative 200 it, e) with Tikhonov iterative 300 it and f) with Tikhonov iterative 400 it.

4.1.3 Conclusions

Using the monopole substitution technique, the noise of an engine has been experimentally characterized. Different models have been applied, varying the number of monopoles in order to quantify the number of descriptors necessary to obtain an acceptable precision. This precision was evaluated in terms of Zwicker loudness and Sharpness, with a higher level in the receiving spectrum predicted being obtained in the loudness than in the sharpness. That is to say, the loudness was much more influenced by the number of monopoles employed than the sharpness, which displayed a more homogeneous behavior. The relation between the number and position of the substitute sources on the hand, and the active radiation mode on the other hand, is the dominant effect that determines the best model performance. The substitute source model should have at least one substitute source on each maxima of the radiation pattern of the source.

The distance between the source and the target position regard to

the radiation mode is an important factor showing that the Doppler effect should be taken into account in the model.

The improvement in the regularization strategies was demonstrated even when the problem displayed a good conditioning. The results achieved with the Tikhonov iterative algorithm reveal their superiority compared to non iterative regularization techniques both in terms of Loudness and Sharpness. Moreover, it has been shown that the number of monopoles has influence on the number if iterations required. Future research could be aimed at studying other types of sources of vehicle sound and investigating more psychoacoustic parameters, which could be of interest for the characterization of the error committed in the model; as well as minimizing the number of iterations necessary in the regularization algorithm, fixing a criterion as a function of the error instead of establishing a number of fixed iterations.

4.2 Identification of sound source in vehicles using Evolutionary Product Unit Networks

4.2.1 Abstract

Auralization through binaural transfer path analysis and synthesis is a useful tool for analysis of how contributions from different sources affect the perception of sound. This paper presents a novel model based on auralization of sound sources by studying the behavior of the system with respect to the frequency. The proposed approach is a combined model using Airborne Source Quantification (ASQ) technique for low-mid frequencies (≤2.5 kHz) and an Evolutionary Product Unit Neural Networks (EPUNNs) for high frequencies (>2.5 kHz), what improves the overall accuracy. The accuracy of ASQ and novel combined models have been evaluated in terms of Mean Squared Error (MSE) and the Standard Error of Prediction (SEP), the combined model obtaining the smallest value for both measures. Moreover, the best prediction model was established based on sound quality metrics, the proposed method showing better accuracy than the ASQ technique at high frequencies in terms of loudness, sharpness and 1/3rd octave bands.

4.2.2 Introduction

Optimizing the acoustic package of a vehicle requires the identification of the sources radiating, and the analysis of the way they propagate. It is possible by means of the auralization, i.e. the process of rendering audible the sound field of a physical sound source in a space, in such a way as to simulate the listening experience at a given position in the modelled space [9, 22]. For auralization aims, sound synthesis models have been developed making possible to know both real listening experiences and the determination of sound quality with metrics. Generally, the first step assumed in these models involves the modelling of all contributing noise sources and the determination of all relevant transfer paths by a source-transmission path-receiver model. To determine the transfer paths, direct measurement techniques are in practice not applicable or very cumbersome, time consuming and expensive, and therefore, indirect techniques, such as sound intensity [11], nearfield acoustic holography (NAH) [15, 23-26] or airborne source quantification (ASQ) [9], are preferred. The main problem of indirect techniques is, generally, their limited resolution derivates from the ill-posed problem and the need of regularization strategies in the vast majority of cases.

In this sense, it should be possible to achieve more realistic and effective legislations by means of models based on auralization of sound such as the change in the ISO 362 procedure for vehicle Pass-by Noise testing. Therefore, achieving predictive models with acceptable accuracy based on the auralization of sound is very important, as well as using sound quality metrics for evaluating the error of the prediction.

Last years, Artificial Neural Networks (ANNs) have emerged as a powerful learning technique to perform complex tasks in highly nonlinear dynamic environments, one of the prime advantages being their ability to learn based on optimization of an approximation of nonlinear functions [27-30]. Different types of ANNs are being used for regression purposes [31], including, among others: MultiLayer Perceptron (MLP) neural networks, where the transfer functions are logistic or hyperbolic tangent functions, Radial Basis Functions (RBFs) [32], General Regression Neural Networks proposed by Specht [33], Product Unit Neural Networks (PUNNs) [34], etc. An additional problem related to the application of ANN models is the

selection of the most appropriate net architecture to be used. Classical neural network training algorithms assume a fixed architecture (number of layers, number of hidden layer nodes and number of connexions) but it is very difficult to establish beforehand the best structure of the network for a given problem. In the last few years, Evolutionary Algorithms (EAs) [35]have demonstrated their great accuracy in designing near optimal architectures, with different kinds of ANNs [36, 37].

In this work, a PUNN is trained to model and identify the transfer functions in the auralization of sound process. The main advantage of PUNNs is their capacity for reflecting the high order relationships between the inputs and the output. But PUNNs have a major drawback: their training is more difficult than the training of MLP or the RBFNN. In the standard sound synthesis model, the transfer functions between the sound source and the receptor are difficult to establish and the main drawback is their ill-conditioned problem what makes necessary apply regularization strategies involving a change of the accuracy depending on the regularization method used [7, 21, 38]. After studying the behaviour of the system with respect to the frequency, a novel strategy based on a combined model is proposed for the auralization of the sound source in sound synthesis. ASQ techniques for sound synthesis at low and mid frequencies ($f \leq 2.5$kHz) and a EPUNN model at high frequencies ($f > 2.5$kHz) were combined because the systems shows a bad conditioning at high frequencies as it will be proven. To evaluate the accuracy of the model proposed, different sound quality metrics were used assessing the real experience in a receptor position.

4.2.3 Modeling Techniques

In order to obtain the model of sound sources using reciprocal measurements source, monopole sound sources are required [5, 25, 38, 39]. This is due to the fact that there are very different space requirements of sound sources and sensors, the measurements of acoustic transfer functions being often much easier done by reciprocity, when source and sensor are interchanged. The quality of a monopole sound source is very important because it is the base of them in this kind of measurements [40]. If the source model performs the source from different manner than expected, the result of the complete procedure may become useless. As mentioned above, ($\lambda \gg L$), the simplest mathematical model of a sound source describing its

behaviour is a pulsating sphere with a radius a, being much smaller than the wavelength, expanding and contracting harmoniously with a perfect symmetry.

For the source models applied here, the substitute sources provide an appropriate description of generated sound field, without the need of describing all the physics involved. Once the model followed by the source is established, the next step in sound synthesis is fixing the type of descriptors and the quantification of them. A monopole sound source has a volume velocity output, in cubic meters per second, which is equal to the particle velocity, in meters per second, times the surface of the sound source. Therefore, the substitute sources are quantified by their volume velocity Q, which is a stable quantifier that suits the transfer path approach very well [5]. As mentioned before, several techniques for the quantification of noise sources, such as ASQ, are available. Although the measurement and post-process times can increase in some cases, an inverse ASQ method is well suited for the general sound synthesis approach [9]. The main problem associated with inverse ASQ method is that the transfer functions present an ill-conditioned problem, regularization strategies being needed. The conditioning is represented by the condition number, which is shown in Figure 4.12.Yoon and Nelson [21] established that the condition numbers can be said to be small when they are below 10^3. Therefore, it can be observe that for frequencies lower to 2.5 kHz the condition number remains low, indicating a good conditioned quantification problem. For high frequencies (f>2.5kHz), however, the condition number increases considerably and thus, regularization strategies will probably be useful to come up with a physically relevant solution.

This work considers two different models following the behavior of the system: Substitution Monopole model based on Airborne Source Quantification (ASQ) technique for all range of frequencies and a combined model using an ASQ technique for low and med frequencies and an EPUNNs model for high frequencies comparing the accuracy of the best model based on sound quality metrics.

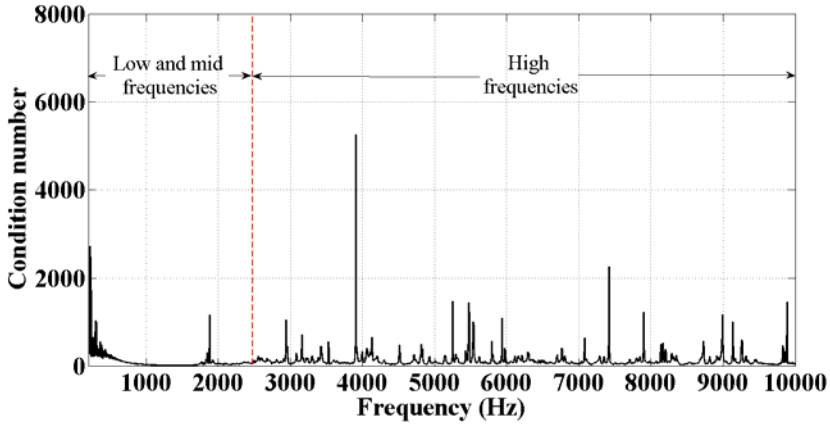

Figure 4.12. Condition number of the system

4.2.3.1 Substitution Monopole Model

As mentioned above, transfer Path Analysis (TPA) is defined as a procedure which allows the flow of vibro-acoustic energy to be traced from a source, through a set of known structures and air-borne pathways, to a given receiver position. When only airborne transfer paths are involved, TPA is referred to as ASQ [9]. In this technique, when the number of unknown source strengths Q_i is large in comparison to the number of indicator microphones, this inverse ASQ becomes badly conditioned. The number of indicators therefore always largely exceeds the number of sub-sources to be quantified. In our case, the number of indicators is the same of sub-sources, thus the ill-conditioned behavior of the inverse matrix H^{-1} complicates the definition of physically meaningful approximations of q. Observing the condition number of the transfer functions, shown in Figure 4.12, it can be concluded that, at high frequencies, the system presents peak values superior to $5 \cdot 10^3$. For the purpose of source reconstruction, this implies a restriction on achievable resolution [41]. However, this is not particularly problematic in our application, where a model of the noise source is required only to predict the resulting spectrum at a target position. The conditioning of the problem generally improves when the measurements are made at positions close to the acoustic sources and when the geometry of the measurement positions is chosen to match the geometry

of the source [41]. Despite taking into account these restrictions in our measurement set-up, the condition number rises considerably at high frequencies and thus, a novel method using ANNs has been proposed based on the behavior observed of the system with respect to the frequencies, in order to improve the accuracy of the prediction at these frequencies.

4.2.3.2 Combined ASQ-Evolutionary Product Unit Neural Networks Model

A combined linear ASQ and EPUNN model is proposed in this section, following the behavior of the system regarding the frequency:

$$f(\mathbf{x}, f, \boldsymbol{\theta}) = \begin{cases} ASQ \text{ model}, & \text{if } f \le 2.5kHz \\ f_{\text{PUNN}}(\mathbf{x}, \boldsymbol{\theta}), & \text{if } f > 2.5kHz \end{cases}., \qquad (4.13)$$

where f is the frequency, the ASQ model is presented in the section 4.2.3.1 and $f_{PUNN}(\mathbf{x}, \theta)$ is the EPUNN model which is developed in the section 4.2.3.3. For obtaining this model, only low-mid frequencies are used for fitting ASQ model and the high frequencies are used for adjusting $f_{\text{PUNN}}(\mathbf{x}, \theta)$ model where $\vec{\theta} = (\vec{w}, \vec{\beta})$ with $\vec{w} = (w_1, ..., w_m)$ and $\vec{\beta} = (\beta_0, \beta_1, ..., \beta_m)$ respectively.

4.2.3.3 Evolutionary Product Unit Neural Networks Model

PUNNs are an alternative to MLP or RBF neural networks, and are based on multiplicative nodes instead of additive ones.

As mentioned above, PUNNs have a major handicap: they have more local minima and a higher probability of becoming trapped in them [42].The main reason for this difficulty is that small changes in the exponents can cause large changes in the total error surface.

The structure of the PUNN considered is the following: an input layer with k nodes, a node for every input variable, a hidden layer with m nodes and an output layer with one node. There are no connections between the nodes of a layer and none between the input and output layers either. The activation function of the j-th node in the hidden layer is given by

$\Pi_j(\mathbf{x},\mathbf{w}_j)=\prod_{i=1}^{k} x_i^{w_{ji}}$, where w_{ji} is the weight of the connection between input node i and hidden node j and $\mathbf{w}_j=(w_{j1},...,w_{jk})$ the weight vector, k is the number of the inputs. The activation function of the output node is given in by $f_{\text{PUNN}}(\mathbf{x},\boldsymbol{\theta})=\beta_0+\sum_{j=1}^{m}\beta_j\Pi_j(\mathbf{x},\mathbf{w}_j)$, where β_j is the weight of the connection between the hidden node j and the output node. The transfer function of all hidden and output nodes is the identity function.

Evolutionary Algorithm. The Evolutionary Algorithm (EA) is developed in section 3.1.3.2 of chapter 3 and more details about the Evolutionary Programming (EP) operators can be found in Hervás-Martinez, *et al*. [43].

Hybrid Algorithms. In this work, different variants of hybrid EAs have been applied, all of them proposed by Martínez-Estudillo *et al*. [36]. The EP algorithm is the EA exposed in the previous section without either a local search or a clustering process. In the Hybrid EP (HEP), the EP is run without the local optimization algorithm and then it is applied to the best solution obtained by the EP in the final generation. This allows the precise local optimum around the final solution to be found. Another version of hybrid EA is the HEP with the Clustering algorithm (HEPC), which applies the clustering process over a large enough subset of the best individuals in the final population obtained by a 10-feed crossvalidations of the training set. The number of individuals in this subset and the number of clusters to be created are important parameters of the clustering process. Once clusters have been determined, the best individual in each cluster is selected and then optimized using the local search algorithm.

The clustering method selected is k-means clustering due to its simplicity and low cost computational, using a distance measure defined for the vectors of the different values obtained for each individual over the training dataset.

The local optimization procedure considered is the improved *Rprop* algorithm [44], which is based on *Rprop*. The *Rprop* algorithm is believed to be a fast and robust learning algorithm. It employs a sign-based scheme to update the weights in order to eliminate harmful influences of the

derivatives' magnitude on the weight updates, i.e., the magnitude of the update along each weight direction only depends on the sign of the corresponding derivative. The size of the update step along a weight direction is exclusively determined. The improved *Rprop* by a weight-specific "update-value" algorithm (denoted by *iRprop+*) applies a backtracking strategy. An adaptation of the *iRprop+* to the bass function and error was carried out.

The hybrid algorithms applied are summarized as follows:

Hybrid Evolutionary Programming (HEP)

1. Generate a random population of size $10N_p$ and select the best N_p individuals.
2. Repeat EP algorithm until the stopping criterion is fulfilled
3. Apply *iRprop+* algorithm to best solution obtained in the EP algorithm.
4. Return the optimized individual as the final solution.

Hybrid Evolutionary Programming with Clustering (HEPC)

1. Generate a random population of size $10N_p$ and select the best N_p individuals.
2. Repeat EP algorithm until the stopping criterion is fulfilled.
3. Apply *k*-means process to best N_C individuals of the population in the last generation and assign a cluster to each individual.
4. Apply *iRprop+* algorithm to best solution obtained in each cluster.
5. Select the best individual among optimized ones and return it as the final solution.

4.2.3.4 Description of the dataset and the experimental design

Instruments, apparatus, software used and experimental set up are depicted in depth in the section 4.1.3.5 of this chapter.

The engine mock-up is shows in Figure 4.4. From six target positions, the microphone 2 was randomly chosen. The height of the free-field microphone above the ground was 1.2 m and this was pointed towards

the source and situated parallel to the ground at 45±10º. The signal registered for this microphone was used for checking the accuracy of the model. The main drawback of the traditional methods is their low resolution at high frequencies and their quadratic performance at low-mid frequencies.

In addition, the phase of the loudspeakers in the set-up is modified individually and the signal transmitted via an amplifier to the loudspeakers varying the phase between 0º and 180º, and activing or not activing the loudspeakers. Figure 4.13 represents all the phase configurations studied v1, v2, v3, v4 and v5, respectively. For each case, there have been registered 8193 instances for the whole frequencies. In order to obtain the best model EPUNN, only 6143 instances have been used corresponding to high frequencies in the case v1. Once the best model EPUNN has been obtained, the other settings v2-v5 are used for generalizing the obtained ANN model training.

To start processing data in the EPUNN model, each of the input variables was scaled in the rank [1,2] by a simple linear rescaling, with x_i^* being the transformed variables.

The parameters used in the evolutionary algorithm for learning the EPUNN models are common to all methodologies: the $\mathbf{w}_j$ vector and the coefficients β_j are initialized in the [–5, 5] interval; the maximum number of hidden nodes is $m = 4$; the size of the population is $N_P = 1{,}000$. The number of nodes that can be added or removed in a structural mutation is within the [1, 3] interval, whereas the number of connections that can be added or removed in a structural mutation is within the [1, 7] interval. The *k-means* algorithm is applied to $N_C = 200$ best individuals in the population. The number of clusters is 6. For *iRprop+*, the adopted parameters are $\eta^- = 0.2$ (decreasing factor for stepsize), $\eta^+ = 1.2$ (increasing factor for stepsize), $\Delta_0 = 0.0125$ (the initial value of the step), $\Delta_{\min} = 0$ (minimum stepsize for the size for the weights), $\Delta_{\min} = 50$ (maximum stepsize for the weights), and $\text{epochs} = 500$ (number of epochs for the local optimization).

The performance of each model was evaluated using the MSE and the Standard Error of Prediction (SEP) an adimensional measurement in the

generalization set. SEP is defined as:

$$SEP = \frac{100}{|\bar{y}|} \times \sqrt{MSE} \quad . \tag{4.14}$$

The EP algorithm used for the EPUNN model is a stochastic method and, consequently, all methods are repeated 30 times and then the mean and the standard deviation of the error corresponding to the 30 models are recorded.

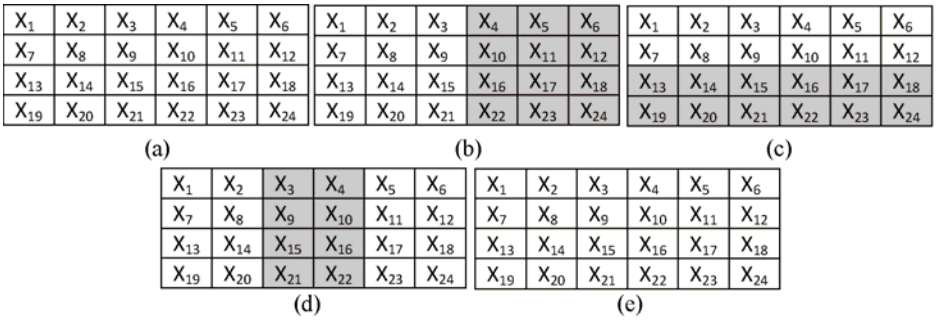

Figure 4.13. Overview of different studied models, where a) v1 is the model using for training set and b-e) v2-v5 are using for the generalization set. Light gray color: 0ºphase ,dark gray color: 180ºphase and white color: not active

Figure 4.14 shows the box plot obtained with the results of the different algorithms in MSE_G. Boxplots depict algorithm results according to the smallest observation, lower quartile, median, upper quartile and largest observation. As we can see in Figure 6, the HEPC method obtains the best result in term of MSE_G of all techniques compared. The differences in MSE_G are really important with respect to ASQ model for all cases in study. In general, these results show that the proposed approaches based on PUs are robust enough to identify the sound in vehicles in the interval of frequency 2.5-10 kHz since the system has linear or quadratic behavior at low or mid frequencies, obtaining better results than the ASQ approach.

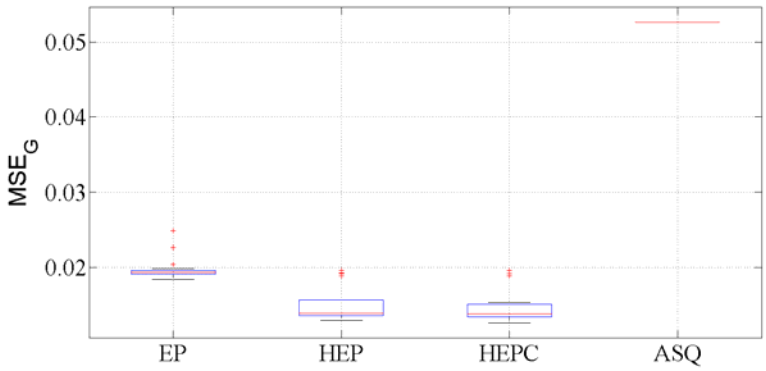

Figure 4.14. Box plot of the EP, HEP, HEPC and ASQ method

4.2.4 Results and discussion

Table 4.9 shows the results obtained with the different models. As explained above, the configuration data for v1 phase were used for training and other data corresponding to the phase configurations v2-v5 were used for generalization. The low and medium frequencies data are omitted in this set up design because of the error is similar for the two models studied in this work.

It is shows that MSE value is lower for all cases studied both in training and in generalization sets obtaining in this last case a MSE less than 10^{-8}, like case v5 where the lowest generalization error was found (35.02×10^{-9}). Since MSE values depends on the magnitude of the data, SEP values provided better comparisons between different models, observing a great difference between the two models in training 5013.61% for the ASQ model compared with 209.05% for combined ANN model. In generalization, the biggest difference is in the v2 case, obtaining a SEP value of 451.91% for ASQ model almost twice that of the ANN model (292.81%).

Table 4.9. Comparative performance of the ASQ and EPUNN models for high frequencies

Configuration of phase	Model Performance			
	ASQ		EPUNN	
	Mean MSE (dB)	SEP (%)	Mean MSE (dB)	SEP (%)
v1-Training	0.0302	5013.61	0.0136	209.06
v2-Generalization2	$14.93 \cdot 10^{-5}$	451.91	$16.55 \cdot 10^{-8}$	292.82
v3-Generalization3	$55.41 \cdot 10^{-6}$	228.81	$42.70 \cdot 10^{-8}$	220.06
v4-Generalization4	$34.46 \cdot 10^{-6}$	221.70	$28.72 \cdot 10^{-8}$	200.78
v5-Generalization5	$72.58 \cdot 10^{-7}$	236.00	$\mathbf{35.02 \cdot 10^{-9}}$	221.70

4.2.4.1 Sound Quality results

Predicting the overall sound levels is no longer sufficient, since human sound perception must be taken into account when aiming for a sound quality improvement. To quantify the accuracy of the prediction, sound quality metrics were used. There are various models and measurement techniques that are used to predict the human impression to the specific sound. Among these metrics, the most important ones applied to the noise of a vehicle are: loudness, sharpness, roughness and fluctuation strength. In this work, as the most significant one, Zwicker loudness was used to correlate the engine noise like in Berckmans, *et al*. [9]; Fouladi, *et al*. [45] and Nor, *et al*.[46], where the same sound quality metrics were evaluated. By means of Zwicker loudness, the subjective perception of loudness in the human ear is evaluated. Of the techniques currently available, only the method developed by Zwicker *et al*. [47] is valid for a broadband excitation, with or without tonal components in free and diffuse fields.

Figure 4.15 shows the comparison of observed and predicted signals for the ASQ method and EPUNN combined method based on Zwicker Loudness for all configurations studied in training set (v1) and in generalization set (v2-v5). It can be seen as at low-mid frequency range the signal is the same for the ASQ method and ANN combined method, but from the band 14, corresponding to 2.5 kHz, the signal predicted by ANN

combined method is better approximates to observed signal than the ASQ method. Therefore, using EPUNN model proposed the accuracy of the signal obtained has improved.

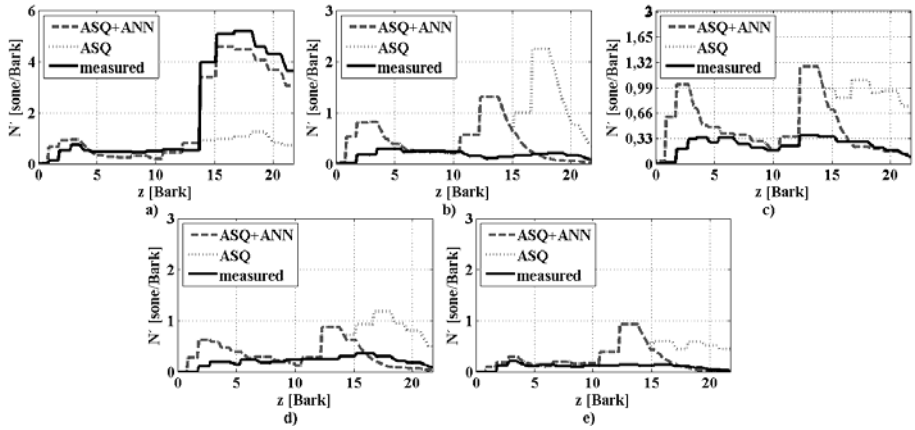

Figure 4.15. Comparison of the observed and predicted signal for ASQ method and ANN combined method by Zwicker Loudness, a) in training set v1, y b-e) in generalization set v2-v5

Observing the errors of both methods in terms of total loudness, defined as the sum of the partial specific loudness, see Figure 4.16, it can also be noted that the error for all cases in studies is less when using ANN, obtaining in generalization set an error less than twice achieved by the ASQ method.

Because most sounds are complex, fluctuating in amplitude and frequency content, the relationships between sound energy level and frequency are required for meaningful analysis. For most engineering applications, the greatest lies in the frequency range from 20 to 20 kHz. Although it is possible to analyze a source on a frequency by frequency basic, this is both impractical and time-consuming. For this reason, a scale of octave bands and one-third octave bands has been developed. Each band covers a specific range of frequencies and excludes all others. For this research, an one-third octave bands analyze has been choose.

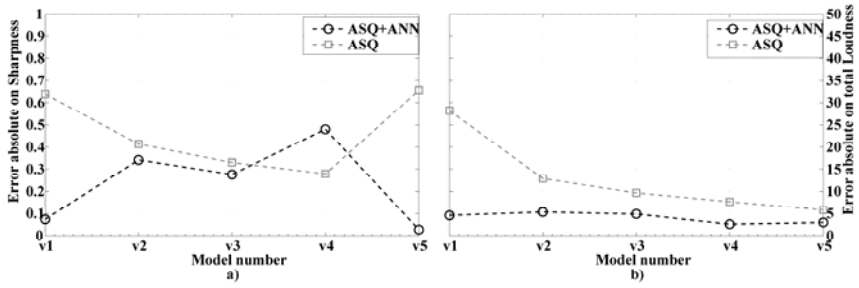

Figure 4.16. Error absolute on total loudness for ASQ method and combined ASQ and ANN method for all cases in study v1 (training) y v2-v5 (generalization)

Figure 4.17 shows a spectrogram of the error on one-third octave band for training set (v1) and generalization set (v2-v5) where the different colors perform the error level (dB) on the prediction obtained. From the band number 15 (2.5 kHz) can be seen as the method based on ANN the error is much smaller (below 0.2 dB) than when the ASQ method is used, while the error in this case is close to 1 -2dB (red color).

4.2.4.2 Comparison of the number of variables

Table 4.10 shows the variables for the EPUNN combined model. This model only need the signal of 20 sensors for identifying the sound sources, as can be seen, being necessary 24 signals for the ASQ method. This is a great advantage for high frequency signals based on more or less a non linear behavior, since the number of necessary microphones is less and therefore the cost of the set up of the experiment also.

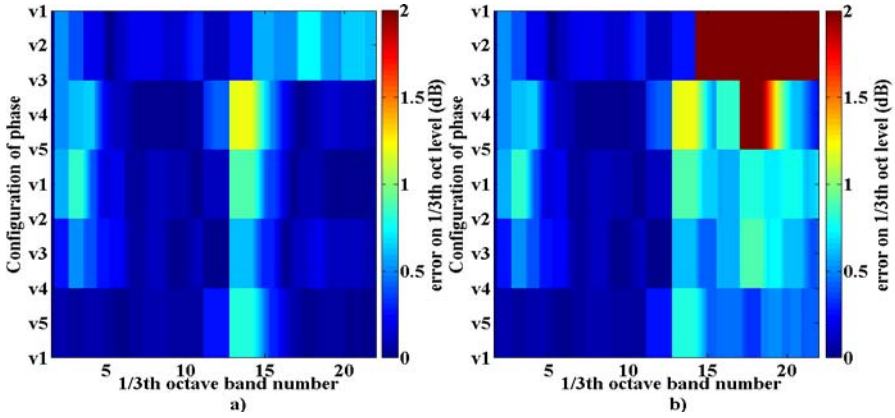

Figure 4.17. Error on 1/3 octave band for all configurations of phase v1 (training) and v2-5 (generalization) using: a) a combined model ASQ for low-medium frequencies and ANN for high frequencies; b) an ASQ model

x_1	x_2	x_3	x_4	x_5	x_6
x_7	x_8	x_9	x_{10}	x_{11}	x_{12}
x_{13}	x_{14}	x_{15}	x_{16}	x_{17}	x_{18}
x_{19}	x_{20}	x_{21}	x_{22}	x_{23}	x_{24}

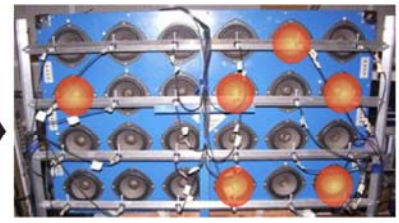

Figure 4.18. Critical variables for ANN model

Figure 4.18 shows most critical variables for each model. This study can determine the noise sources which are responsible for identifying engine noise in this model. These critical variables have been obtained by calculating the variation in the model output due to variations in the input variables. Finally, it was found by sensibility study that the critical variables for the ANN model at high frequencies in this model are $\{x_1, x_3, x_5, x_7, x_9, x_{10}, x_{11}, x_{12}, x_{15}, x_{19}, x_{20}, x_{21}, x_{22}, x_{24}\}$, see figure 4.18.

Table 4.10. Coefficients and variables of EPUNN model

Function	Coefficients
$f(x,\theta)=+0.14\left(x_3^{-0.15}x_5^{0.28}x_7^{0.20}x_9^{0.04}x_{12}^{0.73}x_{15}^{0.07}x_{19}^{-0.07}x_{20}^{0.01}x_{21}^{1.21}x_{22}^{-0.22}x_{24}^{0.16}\right)$ $+0.05\left(x_1^{0.007}x_3^{-1.10}x_9^{-0.96}x_{10}^{1.36}x_{11}^{-0.14}x_{20}^{-1.63}x_{22}^{2.05}\right)$ $+0.80$	

4.2.5 Conclusions

This study demonstrated the capability of EPUNN to identify noise in vehicles using a Pass-by Noise test at high frequencies. Adapting the solution of the problem through a combined method: ASQ method for low-mid frequencies and ANN method for high frequencies based on the behavior of the system studing the condition number of the problem. This regression problem is very complex due to the convoluted nature of the error function associated with the model. In this kind of problem, classical gradient-based algorithms tend to fall in local optima.

Therefore, the use of a stochastic global search procedure, an evolutionary algorithm, is justified to estimate the parameters of the models.

Through a statistical analysis based on the MSE and SEP have been shown that for high frequencies with the EPUNN model a better accuracy has been achieved in the generalization set. In addition, analyzing the perceived sound quality using the psychoacoustic parameters like a person could hear it, it has also been shown since the error obtained at high frequencies with ANN model is lower than ASQ model.

Finally, a study of the most important variables (sensors) was carried out. The conclusions arisen from this analysis help that the cost of futures noise studies can be reduced, because it is not necessary that all sensors are included in futures analysis.

4.3 Ensembles of evolutionary product unit or radial basis function neural networks for the identification of sound for pass by noise test in vehicles

4.3.1 Abstract

The successful development of new products relies on the capability of assessing the performance of conceptual design alternative in an early phase. In recent years, major progress was made hereto, based on the expensive use of prediction models, particularly in the automotive industry. Automotive manufactures invest a lot of effort and money to improve and enhance the vibro-acoustics performance of their products because they have to comply with the noise emission standards.

International standards, commonly known as pass-by and coast by noise test, define a procedure to measure the noise levels in vehicle at different receptor positions. The aim of this work is to develop a novel noise prediction model in vehicle using a pass-by-noise test based on ensembles of hybrid Evolutionary Product Unit or Radial Basic Function ERBFNN approaches have been used to develop different noise prediction models.

The results obtained using different ensembles of hybrid EPUNNs and ERBFNNs show that the functional model and the hybrid algorithms proposed provide very accurate prediction compared to other statistical methodologies used to solve this regression problem.

4.3.2 Introduction

Noise limits have become increasingly stringent over the years, but no corresponding reduction in noise levels has been observed in urban areas.

Reasons for this lack in traffic noise reduction are the trends towards the use of wider tires on cars, the non-representativeness of homologation tests and the increased traffic volume. In many communities, the problem of traffic noise has become an important political issue; simultaneously, along with this increase in exposure, people is more aware of noise due to media attention which make citizens criticize noise even in places where the levels measured were stable or in some cases even reduced.

For this reason, environmental noise is making European Union (EU) citizens more and more concerned and is now the focus of EU and national environmental legislation. The EU Directive (2002/49/EC) [48] related to the assessment and management of environmental noise was published in 2002 and it aims to create a quieter and more pleasant environment for European citizens within the framework of *'Sustainable Development and Growth in Europe'*. It deals mainly with the definition of universal noise indicators, strategic noise mapping, noise management action plans and methodologies for prediction. The European commission states that the harmful effects of noise exposure from all sources should be avoided and that quiet areas need to be preserved. Motivated by the appearance of new regularizations, automobile manufacturers are supervised to certify that their vehicles comply with noise emission standards by measuring noise levels according to procedures defined by international standards, commonly known as pass-by and coast-by noise tests. Furthermore, in order to establish the quality of their products, more and more companies try to achieve a high quality sound. In the automobile sector, exterior and interior sound quality in vehicles has become a

marketing feature to attract new consumers. This important change in viewpoint results in a need for new prediction models and noise abatement techniques. In this context, auralization techniques will play an important role. Auralization is the process of rendering audible the sound field of a physical sound source in a space, in such a way as to simulate the listening experience at a given position in the modelled space [9]. In auralizing spaces, one tries to simulate the effect of those rooms. The process of auralization is achieved by modelling the physical source in a sound synthesis model. Although there are some synthesis procedures that work purely in the time domain, there are numerous advantages in working partially in the frequency domain [49]. By means of the resulting real listening experience, a reliable method is established for the evaluation of the annoying sound quality. Modifications in, for example, an engine mount, tire tread pattern, the exhaust pipe, the acoustic transfer path, etc., can be evaluated thoroughly, quickly and economically. Sound synthesis models aim at auralizing the sound produced by a physical sound source at an arbitrary receiver location. These prediction methods are based on linear models [22]. The main advantage of these methods is their robustness, while the drawback is their resolution limitations at high frequencies since the system shows a nonlinear behavior.

On the other hand, various methods, such as Artificial Neural Networks (ANNs) and wavelet networks have been developed in recent years for analyzing and solving identification problems [50]. Depending on the basis function used in the hidden nodes the following ANNs [51], among others, can be distinguished: 1) ANNs based on projection basis functions, where the transfer functions are Sigmoidal Units (SUs) or the Product Units (PUs) [43], and 2) ANNs based on kernel basis functions, such as the Radial Basis Functions (RBFs) [32].

Kernel functions are functions of the local environment and have a greater ability to fit outliers. However, kernel function performance decreases drastically in global and high dimensionality environments. On the other hand, projection functions are functions of the global environment, and, due to their global nature, they present some difficulties for fitting outliers but do tend to perform better in high dimensionality problems. This paper focuses on two types of ANNs: Radial Basis Function Neural Networks (RBFNNs) and Product Unit Neural Networks (PUNN).

Although PUNNs and RBFNNs are very popular machine learning techniques, the search for the optimal ANN is still a challenging task: the ANN should learn input output mapping without overfitting the data, and training algorithms may get trapped in local minima. Evolutionary Algorithms (EAs) [34, 52] are good candidates for PUNN and RBFNN design, since they perform a global multi-point search, quickly locating areas of high quality, even when the search space is very complex. The combination of EAs and ANNs, called Evolutionary Neural Networks (ENNs), is a suitable candidate for topology design, due to the error surface features: 1) the number of nodes/connections is unbounded and 2) the mapping from the structure to its performance is indirect (similar topologies may present different performances, while distinct topologies may result in similar behavior). This paper analyses the good synergy between two types of ANNs (PUNNs and RBFNNs) and an EA: Evolutionary Product Unit and Radial Basis Function Neural Networks (EPUNNs and ERBFNNs).

Many researchers have shown that EAs perform well for global searching because they are capable of rapidly finding and exploring promising regions in the search space, although they take a relatively long time to converge to a local optimum [53]. Recently, new methods have been developed in order to improve the precision of EAs by adding local optimization algorithms. Within this context, the use of Lamarckian evolution [54] is a promising approach, where an EA is combined with a local search procedure (e.g. tabu-search or gradient based algorithm), improving the fitness of the individuals during their lifetime. Martínez-Estudillo *et al*.[34] proposed the hybrid combination of three methods for the design of Evolutionary PUNNs (EPUNNs) for regression: an EA, a clustering process and a local search procedure. Clustering methods create groups (clusters) of mutually close points that could correspond to relevant regions of attraction. Then, local search procedures can be started once in every such region. In this work, this methodology has been extended to kernel-type models: specifically it has been adapted to RBFNN models.

Two factors must be considered to make an ANN ensemble generalize adequately. One is diversity and the other one is the performance of the ANNs that comprise the ensemble. There is a trade-off as to what the optimal measures of diversity and performance should be [55]. Generally speaking, the approaches to design the ANN ensemble can be classified into

two groups. The first group of these approaches obtains diverse individuals by considering different architectures and settings of the parameters. The second one gets diverse individuals by training them on different training sets, such as bagging, boosting, cross validation [56-58]. Both of them directly generate a group of ANNs which are error uncorrelated. Partridge [59] experimentally compared the capabilities of the methods above and concluded that changing the ANN type and the training data are the two best ways to create ensembles of ANNs with the higher error diversity.

As we previously state, designing ANNs with EAs has emerged as a preferred alternative to the common practice of selecting the apparent best ANN [50]. Because EAs search from not only a single point but a large population of points, many researchers have actively exploited the combination of multiple ANNs from the last generation of the EA. However, these ANNs tend to be too similar between each other because the individual with the highest fitness frequently prevails after some generations. This phenomenon is known as premature convergence or genetic drift [60]. Trying to avoid this problem, in our proposal, the ensemble is composed of the best individuals from different generations of the EA. Since our EA designs the structure of the ANNs, the models obtained at different generations are suitable to be combined, each of them having distinct topological characteristics (diversity and performance). In summary, the main objective of this work is to assess the potential of ensembles of PUNNs and RBFNNs trained with different hybrid algorithms to reach the best approach in an industrial application, the identification of sound for the pass-by noise test for vehicles. The transfer functions between the source and receiver are established by means of these models, but using only the data corresponding to the frequency range 2.5-10 kHz, because the system has a predictable quadratic behavior at lower frequencies. Therefore, this novel strategy is proposed based on the auralization of sound to simulate the listening experience for high frequencies at a given position in the modelled space.

4.3.3 Description of the hybrid learning proposed

4.3.3.1 Product Unit Neural Networks (PUNNs) and Radial Basis Functions Neural Netwroks (RBFNNs)

Radial Basis Functions Neural Networks (RBFNNs) PUNNs are an alternative to MLPs, and are based on multiplicative neurons instead of additive ones. Product unit based neural networks have several advantages, including increased information capacity and the ability to express strong interactions between input variables. Despite these advantages, PUNNs have a major handicap: they have more local minima and more probability of finding themselves trapped in them [61]. The main reason for this difficulty is that small changes in the exponents can cause large changes in the total error surface.

On the other hand, RBFNNs can be considered a local approximation procedure, and the improvement in both its approximation ability as well as in the construction of its architecture has been note-worthy [32]. In RBFNNs, the main problem is how to determine the number of hidden centres and their locations. An interesting alternative is to evolve RBFNNs using EAs [29]. This study defines a common framework for both PUNNs and RBFNNs. The structure of the neural network considered has an input layer of k neurons, one neuron for each input variable, a hidden layer with m neurons and an output layer with one neuron. There is no connection between the neurons of a layer, and none between the input and output layers either. The activation function of the *j-th* neuron in the hidden layer is given by $B_j(x;w_j)$ and the activation function of the output neuron is given by:

$$f(x,\theta) = \beta_0 + \sum_{j=1}^{m} \beta_j B_j(x, w_j) \tag{4.15}$$

where β_j is the weight of the connection between the hidden neuron j and the output neuron and w_j is the weight vector of the connections of the hidden neuron j and the input layer. The transfer function of all hidden and output neurons is the identity function. The difference between PUNNs and RBFNNs is related to the activation function considered in the hidden layer.

Thus, Product Units (PUs) are considered for PUNNs:

$$B_j(x, w_j) = \prod_{i=1}^{k} x_i^{w_{ji}} \tag{4.16}$$

where w_{ji} is the weight of the connection between input neuron i and hidden neuron j and $w_j = (w_{j1}, ..., w_{jk})$ is the weight vector. On the other hand, Gaussian RBFs are considered for RBFNNs:

$$B_j(x, w_j) = exp\left(-\frac{\left\| x - c_j \right\|^2}{r_j^2} \right) \tag{4.17}$$

where $w_j = (c_j, r_j)$, $c_j = (c_{j1}; c_{j2}, ..., c_{jk})$ is the centre or average of the *j-th* Gaussian RBF transformation, r_j is the corresponding radius or standard deviation and $c_{ji}; r_j \in R$.

The error surface associated to the models is very convoluted. Thus, the parameters of the RBFNNs and PUNNs are estimated by means of Hybrid Evolutionary Algorithms (HEAs). The HEAs were developed to optimize the error function given by the Mean Squared Error (MSE) for N observations, which is defined for a model g of the population:

$$MSE(g) = \frac{1}{N} \sum_{i=1}^{N} \left(y_i - f\left(x_i, \theta\right) \right)^2 \tag{4.18}$$

where $f(x_i, \theta)$ are the values predicted by g and y_i are the real ones.

Evolutionary Programming Algorithm. In order to estimate the parameters and the structure of the PUNNs or RBFNNs that minimize the regression error function, an EA has been considered. The algorithm is similar to that proposed by [34]. This population-based evolutionary algorithm for architectural design and the estimation of real-coefficients has points in common with other evolutionary algorithms in the bibliography [52, 62]. The search begins with an initial population. This population is updated in each generation using a population-update algorithm, and it is subject to the evolutionary operations of replication and mutation. Crossover is not used

due to its potential disadvantages in evolving ANNs [52, 62]. For this reason, this EA belongs to the Evolutionary Programming (EP) paradigm. This algorithm is detailed in section 4.2.3.3 of this chapter.

The adjustment of both the weights and structure of the neural networks is performed by the complementary action of two mutation operators: parametric and structural mutation. Parametric mutation implies a modification in the coefficients (β and w_{ji}) of the model, using a self adaptive simulated annealing algorithm [63]. Structural mutation modifies the topology of the neural nets, helping the algorithm to avoid local minima and increasing the diversity of the trained individuals. Five structural mutations are applied sequentially to each network: neuron deletion, connection deletion, neuron addition, connection addition and neuron fusion. In order to define the topology of the neural networks generated in the evolutionary process, two parameters are considered: m and M_E. They correspond to the minimum and the maximum number of hidden neurons in the whole evolutionary process. More details about this EA can be found in [34]. For the experimental section, the RBFNNs obtained by the EP algorithm will be denoted as Evolutionary Radial Basis Functions (ERBF method) and the PUNNs obtained by this EP algorithm as Evolutionary Product Units (EPU method). More details about the HEAs can be found in section 4.2.3.3 of this chapter.

Ensembles approaches. All above-mentioned hybrid methodologies share the risk of overfitting training datasets. A local search procedure leads us to the closest local optimum for the current location in the training set, but sometimes the optimized model loses its generalization capability, especially in problems like the one addressed in this paper: on increasing the value of the signal, the dispersion with respect to the signal trend also increases (heteroscedasticity). Ensembles are presented here as a way to avoid this overfitting, by combining all the different PUNN or RBFNN models obtained through the evolution process. Recent studies in [37, 38] show that using different metamodels in the form of ensembles, generally leads to an improved generalization capacity and solution quality, representing some promising approaches for mitigating the effects of the *"curse of un- certainty"*. Thus, we consider the models obtained in three different generations of the evolutionary process, representing three stages of the evolution: the first one after a minimum number of generations (500

generations) (the procedure being more stationary and generally producing undertraining), the second one when the algorithm begins to become more elitist and has less diversity (1,000 generations) and the third one in the final generation (1,500th generation). In this way, a pool of individuals with different structures can be constructed and applied to the data as an ensemble. Models are extracted from the EP, HEP and HEPC algorithms at different moments in their evolution, so the set of individuals obtained will presumably gather neural nets with the most efficient and varied topologies to solve the identification of sound regression problems. To combine the outputs of all regression models in the ensemble, twelve different proposals are considered: mean EP, HEP and HEPC ensembles for the PUNN and RBFNN models (EPUMean, ERBFMean, HPUMean, HRBFMean, HCPUMean, and HCRBFMean) and median EP, HEP and HEPC ensembles for the PUNN and RBFNN models (EPUMedian, ERBFMedian, HPUMedian, HRBFMedian, HCPUMedian, and HCRBFMedian). Let $B = \{f_k, k = 1,...,s\}$, be the set of solutions obtained throughout the evolutionary process in a run of the EP, HEP, or HEPC algorithms. The output of the ensembles based on the mean $\left(\overline{f}\right)$ is calculated as the mean value of all the outputs of the elements of B, and the output of enssembles based on the median (f_M) is obtained as the median of the outputs of the elements in B:

$$\overline{f} = \frac{\sum_{1}^{8} f_k}{8}, F\left(f_M\right) = \frac{1}{2} \tag{4.19}$$

where F is the accumulative frequency function.

As shown in Figure 4.19, the evolutionary algorithm is stopped three times during the evolutionary process (every 500 generations, $s = 3$). When the algorithm stops at these generations, the solutions of the EP, HEP and HEPC algorithms are stored in a buffer. Once, the evolutionary process reaches the 1,500th generation, the ensembles associated with each methodology are composed of three models: the solutions of the EP, HEP and HEPC algorithms in the 500th, 1,000th and 1,500th generations.

The proposed methodologies are described in Figure 4.19 for PUs.

In the experimental Section, these methodologies are also applied using RBF instead of PU.

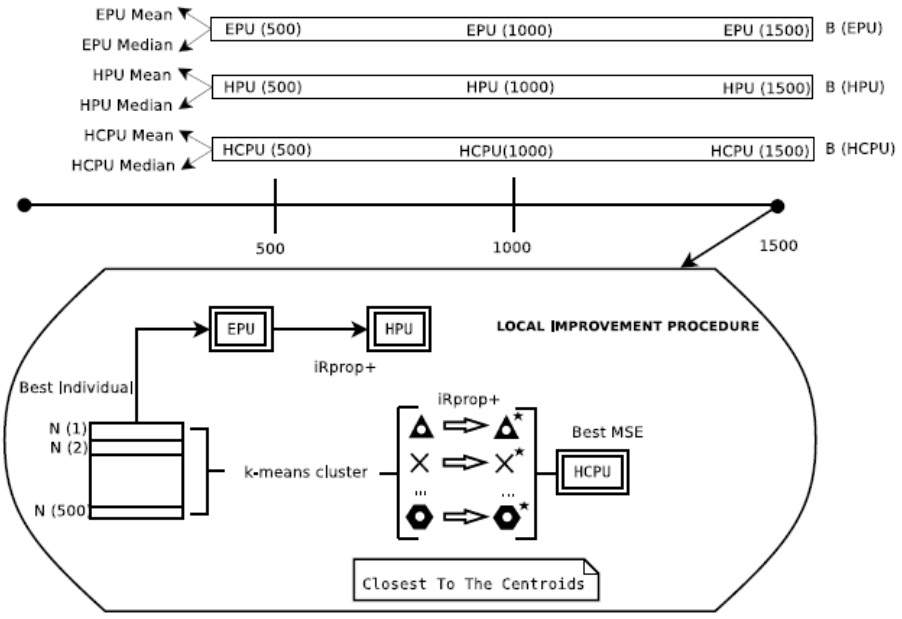

Figure 4.19. Proposed Methodologies for PUs

4.3.4 Experiments

4.3.4.1 Database Description

Instruments, apparatus, software used and experimental set up are depicted in depth in the section 4.1.3.5 of this chapter.

As mentioned above, the main drawback of the traditional methods is their low resolution at high frequencies (with a linear or quadratic behavior), only high frequencies have been used ($f > 2{,}5kHz$). Figure 4.12

shows the condition number at different frequency values ($f \leq 2{,}5kHz$ and $f > 2{,}5kHz$). Therefore, from 8,193 registered data, 6,000 data corresponding to high frequencies have served our propose. The experimental design was conducted using a holdout cross validation procedure with 4,000 instances for the training set and 2,000 instances for the generalization dataset.

4.3.4.2 Experimental Design

Different state-of-the-art statistical and artificial intelligence algorithms have been implemented for comparison purposes. Specifically, the results of the following algorithms have been compared to the hybrid techniques presented in this research:

A Gaussian Radial Basis Function Network (RBFN), deriving the centre and width of hidden units using *k-means*, and combining the outputs obtained from the hidden layer using linear regression. A Multilayer Perceptron (MLP) with sigmoid units as hidden nodes, obtained by means of the backpropagation algorithm. Ridged Linear Regression (RLR) where the Akaike Information Criterion (AIC) is used to select the variables to be included in the model. A Sequential Minimal Optimization (SMO) algorithm for training Support Vector Regression predictors. An Isotonic Regression (IR) model. This model picks the attribute that gives the lowest squared error. These algorithms have been selected for comparison since they are some of the best performing algorithms on regression problems in recent literature. Moreover, they are closely related to the proposals of this paper. The implementations of these algorithms are all available in the WEKA machine learning tool [64].

The parameter values used in the hybrid techniques proposed are the following: to start processing data, each of the input variables was scaled in the rank [1*;* 2] for PUNNs and [-2*;* 2] for RBFNNs. Weights are assigned using a uniform distribution defined throughout two intervals, [-2*;* 2] for connections of RBFNNs between the input layer and hidden layer, [-5*;* 5] for connections of PUNNs between the input layer and hidden layer, and, for all kinds of neurons, [-10*;* 10] for connections between the hidden layer and the output layer. The initial value of the radio r_j for RBFNNs is obtained as a random value in the interval [0*; dmax*], where *dmax* is the maximum distance between two training input examples. The minimum and

maximum number of hidden neurons for RBFNN models are $m = 8$ and $ME = 12$ respectively, and $m = 1$ and $ME = 4$ for PUNNs. The m and ME parameters have been determined by a 10-fold cross validation over the training set. The size of the population is $N_P = 500$. For structural mutations, the number of hidden neurons that can be added or removed in a structural mutation is within the [1*;* 2] interval. The stop criterion is reached when 1,500 generations are completed. The performance of each method was evaluated using the *MSE*.

4.3.5 Results

The experimental results presented in this paper are structured in two subsections. The first subsection studies which of the proposed hybrid techniques yields a better performance. The second subsection compares the best performing techniques to other statistical and artificial intelligence methods.

4.3.5.1 Comparison between the different hybrid techniques proposed

In this subsection, the different hybrid techniques presented in previous sections are compared to each other. In this way, the following methods are compared: Product Units methods: EPU, EPU_{Mean}, EPU_{Median}, HPU, HPU_{Mean}, HPU_{Median}, HCPU, $HCPU_{Mean}$ and $HCPU_{Median}$. Radial basis function methods: ERBF, $ERBF_{Mean}$, $ERBF_{Median}$, HRBF, $HRBF_{Mean}$, $HRBF_{Median}$, HCRBF, $HCRBF_{Mean}$ and $HCRBF_{Median}$.

The results obtained with all these methods are included in Table 4.11, where the *MSE* previously presented is obtained over the generalization set (MSE_G). The training results have not been considered, since it is well-known that the results in the training sample are upward-biased.

Table 4.11. Mean and standard deviation (SD) of the MSE_G results from 30 executions, using the different methods compared. Number of wins, draws and loses when comparing the different methods using the Mann-Whitney U rank sum test with $\alpha = 0:05$

	MSE_G	Mann-Whitney U test		
	Mean±SD	**Wins**	**Draws**	**Loses**
EPU	0.02248±0.00048	0	2	15
EPU Mean	0.02246±0.00045	0	2	15
EPU Median	0.02248±0.00048	0	2	15
HPU	0.01494±0.00195	12	5	0
HPU Mean	0.01472±0.00287	12	5	0
HPU Median	*0.01434±0.00105*	12	5	0
HCPU	0.01470±0.00134	12	5	0
HCPU Mean	0.01465±0.00322	12	5	0
HCPU Median	**0.01419±0.00091**	12	5	0
ERBF	0.02119±0.00059	3	6	8
ERBF Mean	0.02120±0.00057	3	6	8
ERBF Median	0.02123±0.00054	3	5	9
HRBF	0.02095±0.00054	3	8	6
HRBF Mean	0.02091±0.00053	6	5	6
HRBF Median	0.02096±0.00061	4	7	6
HCRBF	0.02096±0.00056	3	8	6
HCRBF Mean	0.02091±0.00053	6	5	6
HCRBF Median	0.02096±0.00062	3	**8**	6

The best result is in bold and the second best results in italic.

The mean and standard deviation values of these measures were calculated for the best models obtained in the 30 executions of the different algorithms and included in the table. From a quantitative point of view, the best mean results in MSE_G are obtained by $HCPU_{Median}$. Another aspect that is important to point out is that the $HCPU_{Median}$ method is far more robust than the rest of the PU methods, which can be observed on analyzing the values of standard deviation generated by the other PU methods.

Statistical tests have been applied in order to ascertain the statistical significance of the differences observed between the mean MSE_G of the best models obtained for each methodology. First of all, a non-parametric Kolmogorov-Smirnov test (KS-test) with a signification level $\alpha = 0{:}05$ was used to evaluate if the MSE_G values of all methods had a normal distribution. Normal distribution cannot be assumed because only 2 out of the 18 proposed methodologies obtained a *p*-value lower than the critical level. As a consequence, a non-parametric Kruskal-Wallis test was selected in order to check if the methodology applied significantly affects the results obtained. The test concludes that these differences are significant (with a *p*-value = 0.0001). So, we finish the statistical analysis applying the Mann-Whitney U rank sum test for all pairs of algorithms and the results are also included in Table 4.7. These results include, for each algorithm, the number of algorithms statistically outperformed (Wins), the number of draws (Draws) (non-significant differences) and the number of losses (Loses) (number of algorithms that outperform the method).

From the analysis of these results, hybrid methodologies based on PU have to be highlighted as the most competitive (with only five draws each one). Taking into account that the highest mean MSE_G is obtained by the $HCPU_{Median}$ method and that it also results in almost the lowest standard deviation (which means higher stability), the method selected to identify sound in vehicles is $HCPU_{Median}$. The performance of the ensembles is now compared to the performance of all the corresponding members, because this will highlight the necessity of forming a common response from the different members through the use of ensembles. Table 4.12 shows the results obtained by the ensemble and the average performance of individuals who comprise it. Ensembles-based methodologies are able to improve the results of the individuals who comprise the ensemble, for all cases when considering PUNNs. In the case of RBFNN, the results of the individuals of the last generation are usually equal to or better than the results of the ensemble. The reason for this is that the error function associated to PUNN models is by far more complex than the error function associated to RBFNNs models. The diversity of PUNN ensembles is greater given that it is easy to move from the current point of the search space by applying a very slight modification in the exponents of the PUs, which is more difficult for the case of RBFs.

Table 4.12. Analysis of the ANNs ensembles of different methodologies: Mean and standard deviation (SD) of the MSE_G results from 30 executions of the ensemble and the individuals who composed it (best individuals at 500th, 1,000th, and 1,500th generations)

	MSE_G	Models of the ensemble (MSE_G)		
	Mean±SD	**500th**	**1,000th**	**1,500th**
EPUMean	**0.02246** ± **0.00045**	0.02259 ± 0.00047	0.02253 ± 0.00049	0.02248 ± 0.00048
EPUMedian	**0.02248** ± **0.00048**	0.02259 ± 0.00047	0.02253 ± 0.00049	0.02248 ± 0.00048
HPUMean	**0.01472** ± **0.00287**	0.01730 ± 0.01589	0.01948 ± 0.02635	0.01494 ± 0.00195
HPUMedian	**0.01434** ± **0.00105**	0.01730 ± 0.01589	0.01948 ± 0.02635	0.01494 ± 0.00195
HCPUMean	**0.01465** ± **0.00322**	0.01951 ± 0.02863	0.01488 ± 0.00334	0.01470 ± 0.00134
HCPUMedian	**0.01419** ± **0.00091**	0.01951 ± 0.02863	0.01488 ± 0.00334	0.01470 ± 0.00134
ERBFMean	0.02120 ± 0.00057	0.02149 ± 0.00067	0.02130 ± 0.00053	**0.02119** ± **0.00059**
ERBFMedian	0.02123 ± 0.00054	0.02149 ± 0.00067	0.02130 ± 0.00053	**0.02119** ± **0.00059**
HRBFMean	**0.02091** ± **0.00053**	0.02110 ± 0.00059	0.02104 ± 0.00062	0.02095 ± 0.00054
HRBFMedian	0.02096 ± 0.00061	0.02110 ± 0.00059	0.02104 ± 0.00062	**0.02095** ± **0.00054**
HCRBFMean	**0.02091** ± **0.00053**	0.02109 ± 0.00055	0.02105 ± 0.00062	0.02096 ± 0.00056
HCRBFMedian	**0.02096** ± **0.00062**	0.02109 ± 0.00055	0.02105 ± 0.00062	**0.02096** ± **0.00056**

The best result is in bold face.

Following the above reasoning, it is easier to find diversity in PUNN ensembles because they are exponential models and their behavior

varies substantially by modifying the exponent values. This allows us to gather diverse PUNN models from different regions of the search space and they can cooperate to improve the results of the best individual who comprise the ensemble.

4.3.5.2 Comparison with other statistical and artificial in intelligence methods

This section focuses on the $HCPU_{Median}$ method, as it is the best in terms of MSE_G among the different hybrid approaches proposed in this paper. In order to complete the experimental section, this method has been compared to the well-known techniques for regression given in previous sections. Table 4.13 presents the results obtained with the different techniques, and the result obtained by the $HCPU_{Median}$ method. The results of the equivalent hybrid method for RBF ($HCRBF_{Median}$) are also shown for reference. Figure 4.20 shows the box plot obtained with the results of the different algorithms in MSE_G. Boxplots depict algorithm results according to the smallest observation, lower quartile, median, upper quartile and largest observation.

Table 4.13. Results of the MSE_G of the best hybrid method proposed compared to those obtained using different statistical and artificial intelligence methods

Method	**MSE_G**
	Mean±SD
RBFN	0.02312±0.00048
MLP	0.02415±0.00045
RLR	0.02210
SMO	0.02375
IR	*0.01544*
HCPU Median	**0.01419±0.00091**
HCRBF Median	0.02096±0.00062

The best result is in bold face and the second best result in italic.

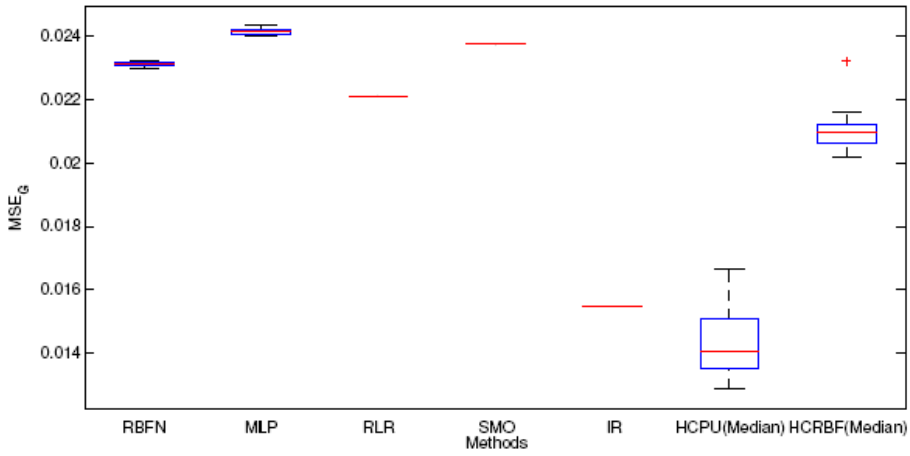

Figure 4.20. Box plots: Results of the RBFN, MLP, RLR, SMO, IR and hybrid methods proposed

As we can see in Table 4.13 and Figure 4.20, the $HCPU_{Median}$ method obtains the best result in terms of MSE_G from all the techniques compared. The differences in MSE_G are really important with respect to techniques such as RBFN, RLR, SMO or MLP. In general, these results show that the proposed approaches based on PUs are robust enough to identify the sound in vehicles in the interval of frequency 2.5-10 kHz (since the system has linear or quadratic behavior at a low or medium frequency), obtaining better results than the rest of the RBFs and state-of-the-art algorithms.

4.3.6 Discussion

The interpretation of the best model is based on the output of the $HCPU_{Median}$ ensemble, shown in Table 4.14. This is the model that shows the best performance in terms of MSE_G. Table 4.15 indicates which sensor corresponds to each input variable. As discussed above, the proposed model is an ensemble in which the model output is the median of the outputs of the three models obtained in the 500th, 1,000th and 1,500th generation. In an

ensemble-based model, it is extremely important that the set of models comprising the ensemble, presents the greatest possible diversity. In our proposal, this requirement should be fulfilled since the models were obtained from different stages of evolution. Intuitively, the greatest diversity should be found when comparing the first model to the next two models, because the EA is still quite stationary in the 500th generation and due to the genetic drift problem. The study of the influence of the input variables for each of the three models comprising the ensemble confirms this theory. Figure 4.27 shows most critical variables for each model, by calculating the variation in the model output due to variations in the input variables. This study can determine the noise sources which are responsible for identifying engine noise. Thus, we can state that the set of the most important variables in $f_1(\mathbf{x}; \theta)$ model is $\{x_6; x_8; x_{11}; x_{13}; x_{21}; x_{24}\}$, the set of the most important variables in $f_2(\mathbf{x}; \theta)$ model is $\{x_2; x_{12}; x_{16}; x_{18}\}$, and, finally, the set of the most important variables in $f_3(\mathbf{x}; \theta)$ model is $\{x_2; x_{12}; x_{16}; x_{18}; x_{21}; x_{22}\}$.

Figure 4.21 shows that the set of the most important variables of the $f_2(\mathbf{x}; \theta)$ model is very similar to the set of the most important variables of the $f_3(\mathbf{x}; \theta)$ model (since there is little difference between these two models). However, if we compare this set of variables with the set of critical variables of the $f_1(\mathbf{x}; \theta)$ model, considerable differences are found (since there is more diversity between the $f_1(\mathbf{x}; \theta)$ model with respect to $f_2(\mathbf{x}; \theta)$ and $f_3(\mathbf{x}; \theta)$ models).

In general, the number of variables selected is low, and some of them are the same for more than one member of the ensemble. For example, all the variables of the $f_2(\mathbf{x}; \theta)$ model are shared by the $f_2(\mathbf{x}; \theta)$ model. This is very important since more sensors imply a more expensive mock-up and by observing the distribution of the important variables, the microphones in the set up can be situated in different ways.

Table 4.14. Best ensemble model

Function	**Best HCPU$_{\text{Median}}$ model**
$f_1(x,\theta) =$	$+0.22(x_4^{0.093}x_7^{-0.058}x_8^{0.45}x_{12}^{0.27}x_{21}^{0.51}x_{22}^{0.58})$ $+1.12(x_1^{0.33}x_4^{0.61}x_6^{-2318.71}x_{10}^{0.95}x_{11}^{-0.92}x_{12}^{1.46}x_{13}^{0.27}x_{14}^{-0.034}x_{15}^{-571.58}x_{20}^{-4.97}x_{21}^{-3036.61})$ $+0.06(x_2^{0.24}x_5^{0.14}x_8^{-3.76}x_{11}^{1.69}x_{12}^{-1.92}x_{14}^{0.75})$ $+0.64(x_3^{-2074.40}x_5^{0.40}x_6^{-0.37}x_7^{-0.31}x_9^{-1.17}x_{10}^{0.13}x_{11}^{-1.47}x_{12}^{1.18}x_{13}^{-1254.30}x_{15}^{2.18}x_{16}^{-541.63}x_{19}^{-13.61}x_{20}^{-0.34}x_{22}^{-4.77}x_{24}^{0.49})$ $+0.72$
$f_2(x,\theta) =$	$+0.22(x_5^{0.25}x_7^{0.057}x_8^{0.14}x_9^{0.05}x_{12}^{0.48}x_{21}^{0.87}x_{22}^{-0.01})$ $+0.79(x_1^{-0.01}x_3^{-3.73}x_4^{1.30}x_5^{-0.52}x_6^{-946.13}x_{10}^{0.57}x_{13}^{0.18}x_{14}^{-0.21}x_{16}^{-1903.91}x_{19}^{-6.64}x_{20}^{-1.54}x_{21}^{-2056.49})$ $+1.86(x_2^{-5310.85}x_6^{-1.83}x_7^{-0.63}x_9^{-1.38}x_{10}^{0.16}x_{12}^{-4.63}x_{15}^{0.31}x_{18}^{-1863.00}x_{21}^{-1.17}x_{22}^{-0.59}x_{23}^{-0.50})$ $+0.70$
$f_3(x,\theta) =$	$+0.24(x_5^{0.26}x_7^{0.04}x_8^{0.16}x_9^{0.06}x_{12}^{0.38}x_{21}^{0.81}x_{22}^{0.04})$ $+0.78(x_1^{0.09}x_3^{-2.05}x_4^{1.22}x_5^{-0.64}x_6^{0.90}x_{10}^{0.33}x_{12}^{2.15}x_{13}^{0.59}x_{14}^{0.04}x_{16}^{-2455.43}x_{20}^{-2.44}x_{21}^{-3061.02})$ $+0.079(x_2^{-5370.46}x_6^{-3.60}x_7^{-0.76}x_9^{-1.35}x_{10}^{0.30}x_{12}^{-3.64}x_{15}^{-0.03}x_{18}^{-1761.91}x_{21}^{-1.34}x_{22}^{-0.45}x_{23}^{-0.38})$ $+0.68$
$f(x,\theta) =$	$F(f_M) = \frac{1}{2}$ where F is the cumulative frequency function.

Table 4.15. Position of each input variables in the array of microphones

x_1	x_2	x_3	x_4	x_5	x_6
x_7	x_8	x_9	x_{10}	x_{11}	x_{12}
x_{13}	x_{14}	x_{15}	x_{16}	x_{17}	x_{18}
x_{19}	x_{20}	x_{21}	x_{22}	x_{23}	x_{24}

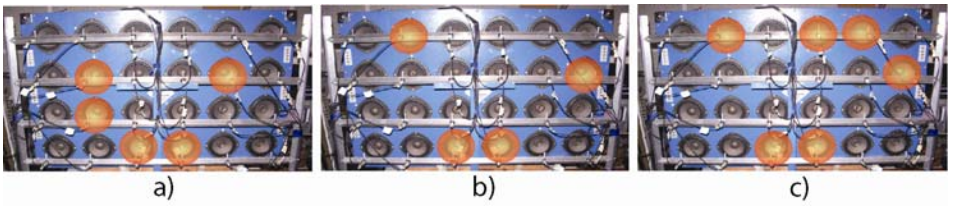

Figure 4.21. Critical variables for each model

4.3.7 Conclusions

This study evaluated the capability of EPUNNs and ERBFNNs to identify noise in vehicles using a pass-by noise test. This regression problem is very complex due to the convoluted nature of the error function associated to the model. In this kind of problem, classical gradient based algorithms tend to fall in local optima. Therefore, the use of a stochastic global search procedure, an evolutionary algorithm is totally justified to estimate the parameters of the models.

Three different EPUNN and ERBFNN algorithms (EP, HEP, and HEPC) were evaluated in training PUNNs and RBFNNs for the noise prediction problem. Additionally, ensemble-based approaches were considered to combine the outputs of the models from three different stages of the evolutionary process. EPUNN ensembles provided better accuracy than all the other proposals in the generalization set and they also outperformed alternative statistical approaches.

Finally, a study of the most important variables (sensors) was carried out. The conclusions arisen from this analysis help that the cost of futures noise studies can be reduced by discarding some of the microphones.

4.4 References

[1] M. Kloth, Vancluysen, K., Clement, F., Lars Ellebjerg, P., Silence project, in, European Comission, 2008.

[2] Y.H.Y. Haik, M.Y.E. Selim, T. Abdulrehman, Combustion of algae oil methyl ester in an indirect injection diesel engine, Energy, 36 (2011) 1827-1835.

[3] A. Albarbar, F. Gu, A.D. Ball, Diesel engine fuel injection monitoring using acoustic measurements and independent component analysis, Measurement, 43 (2010) 1376-1386.

[4] A. Albarbar, F. Gu, A.D. Ball, A. Starr, Acoustic monitoring of engine fuel injection based on adaptive filtering techniques, Applied Acoustics, 71 (2010) 1132-1141.

[5] J.W. Verheij, F.H. VanTol, L.J.M. Hopmans, Monopole airborne sound source with in situ measurement of its volume velocity, 1995.

[6] G. Leveque, E. Rosenkrantz, D. Laux, Correction of diffraction effects in sound velocity and absorption measurements, Measurement Science & Technology, 18 (2007) 3458-3462.

[7] D. Berckmans, B. Pluymers, P. Sas, W. Desmet, Numerical case-study on the development of acoustic equivalent source models for use in sound

synthesis methods, 2008.

[8] E. Mucchi, A. Vecchio, Acoustical signature analysis of a helicopter cabin in steady-state and run up operational conditions, Measurement, 43 (2010) 283-293.

[9] D. Berckmans, P. Kindt, P. Sas, W. Desmet, Evaluation of substitution monopole models for tire noise sound synthesis, Mechanical Systems and Signal Processing, 24 (2010) 240-255.

[10] P. Castellini, G.M. Revel, L. Scalise, Measurement of vibrational modal parameters using laser pulse excitation techniques, Measurement, 35 (2004) 163-179.

[11] M.G. Prasad, M.J. Crocker, Acoustical source characterization studies on a multi-cylinder engine exhaust system, Journal of Sound and Vibration, 90 (1983) 479-490.

[12] J.D. Maynard, E.G. Williams, Y. Lee, -Nearfield acoustic holography .1. Theory of generalized holography and the development of nah, Journal of the Acoustical Society of America, 78 (1985) 1395-1413.

[13] European Parliament, The Assessment and menagement of enviromental noise-Declaration by the Comission in the Conciliation Committee on the Directive relating to the assessment and management of environmental noise, Oficial Journal of the European Communities, 2002, pp. 14.

[14] A. Sarkissian, Near-field acoustic holography for an axisymmetrical geometry - a new formulation, Journal of the Acoustical Society of America, 88 (1990) 961-966.

[15] C. Pézerat, Q. Leclère, N. Totaro, M. Pachebat, Identification of vibration excitations from acoustic measurements using near field acoustic holography and the force analysis technique, Journal of Sound and Vibration, 326 (2009) 540-556.

[16] M. Hafner, M. Schuler, O. Nelles, R. Isermann, Fast neural networks for diesel engine control design, Control Engineering Practice, 8 (2000) 1211-1221.

[17] D. Berckmans, B. Pluymers, P. Sas, W. Desmet, Numerical Comparison of Different Equivalent Source Models and Source Quantification Techniques for Use in Sound Synthesis Systems Acta

Acustica united with Acustica, 97 (2011) 138-147.

[18] H. Fastl, The psychoacoustics of sound-quality evaluation, Acustica, 83 (1997) 754-764.

[19] M.R. Bai, Application of BEM (Boundary Element method)-based acoustic holography to radiation analysis of sound sources with arbitrarily shaped geometries, Journal of the Acoustical Society of America, 92 (1992) 533-549.

[20] S.H. Park, Y.H. Kim, Effects of the speed of moving noise sources on the sound visualization by means of moving frame acoustic holography, Journal of the Acoustical Society of America, 108 (2000) 2719-2728.

[21] Y. Kim, P.A. Nelson, Optimal regularisation for acoustic source reconstruction by inverse methods, Journal of Sound and Vibration, 275 (2004) 463-487.

[22] M.D. Redel-Macias, D. Berckmans, A.J. Cubero-Atienza, Model of Identification of Sound Source. Application to Noise Engine, Revista Iberoamericana De Automatica E Informatica Industrial, 7 (2010) 34-+.

[23] A.M. Pasqual, V. Martin, Optimal secondary source position in exterior spherical acoustical holophony, Journal of Sound and Vibration, 331 (2012) 785-797.

[24] V. Martin, T. Le Bourdon, A.M. Pasqual, Numerical simulation of acoustic holography with propagator adaptation: Application to a 3D disc, Journal of Sound and Vibration, 330 (2011) 4233-4249.

[25] Q. Leclere, B. Laulagnet, Nearfield acoustic holography using a laser vibrometer and a light membrane, Journal of the Acoustical Society of America, 126 (2009) 1245-1249.

[26] J.W. Maynard, E.; Lee, Y.,, Nearfield acoustic holography 1. Theory of generalized holography and the development of NAH, Journal of Acoustic Society of America, 78 (1985) 1395-1413.

[27] E. Ozkaya, M. Pakdemirli, Non-linear vibrations of a beam-mass system with both ends clamped, Journal of Sound and Vibration, 221 (1999) 491-503.

[28] J.S. Pei, A.W. Smyth, E.B. Kosmatopoulos, Analysis and modification of Volterra/Wiener neural networks for the adaptive identification of non-

linear hysteretic dynamic systems, Journal of Sound and Vibration, 275 (2004) 693-718.

[29] F. Tong, S.K. Tso, M.Y.Y. Hung, Impact-acoustics-based health monitoring of tile-wall bonding integrity using principal component analysis, Journal of Sound and Vibration, 294 (2006) 329-340.

[30] Y. Yu, YuDejie, J.S. Cheng, A roller bearing fault diagnosis method based on EMD energy entropy and ANN, Journal of Sound and Vibration, 294 (2006) 269-277.

[31] Haykin, Neural Networks and Learning Machines, 3st ed., Prentice HAll, 2009.

[32] M.C. Bishop, Pattern Recognition and Machine Learning, 1st ed., Hardcover, 2006.

[33] D.F. Specht, A general regression neural network, IEEE Transactions on Neural Networks, 2 (1991) 568-576.

[34] F.J. Martinez-Estudillo, C. Hervas-Martinez, P.A. Gutierrez, A.C. Martinez-Estudillo, Evolutionary product-unit neural networks classifiers, Neurocomputing, 72 (2008) 548-561.

[35] F.H.-M. Fernández-Navarro, C; Gutierrez, P. A.; Carbonero-Ruz, M., Evolutionary q-Gaussian radial basis functions neural networks for multi-classification, Neural Networks, 24 (2011).

[36] A.C. Martinez-Estudillo, C. Hervás-Martínez, F.J. Martinez-Estudillo, N. García-Pedrajas, Hybridization of evolutionary algorithms and local search by means of a clustering method, IEEE Transactions on Systems, Man, and Cybernetics, Part B: Cybernetics, 36 (2005) 534-545.

[37] X. Yao, Evolving artificial neural networks, Proceedings of the IEEE, 87 (1999) 1423-1447.

[38] Q. Leclere, Acoustic imaging using under-determined inverse approaches: Frequency limitations and optimal regularization, Journal of Sound and Vibration, 321 (2009) 605-619.

[39] F.J. Fahy, Some applications of the reciprocity principle in experimental vibroacoustics, Acoustical Physics, 48 (2003) 217-229.

[40] H.E. de Bree, Basten, T., Microflown based monopole sound sources for reciprocal measurements, SAE paper 2008-01-0503, (2008).

[41] Y. Kim, Nelson, P., Spatial resolution limits for there construction of acoustic source strength by inverse methods, Journal of Sound and Vibration, 265 (2003) 583-608.

[42] A. Ismail, A.P. Engelbrecht, I. Ieee, Pruning product unit neural networks, in: Proceeding of the 2002 International Joint Conference on Neural Networks, Vols 1-3, 2002, pp. 257-262.

[43] C. Hervas-Martinez, F.J. Martinez-Estudillo, M. Carbonero-Ruz, Multilogistic regression by means of evolutionary product-unit neural networks, Neural Networks, 21 (2008) 951-961.

[44] C. Igel, M. Husken, Empirical evaluation of the improved Rprop learning algorithms, Neurocomputing, 50 (2003) 105-123.

[45] M.H. Fouladi, M.J.M. Nor, A.K. Ariffin, Spectral analysis methods for vehicle interior vibro-acoustics identification, Mechanical Systems and Signal Processing, 23 (2009) 489-500.

[46] M.J.M. Nor, M.H. Fouladi, H. Nahvi, A.K. Ariffin, Index for vehicle acoustical comfort inside a passenger car, Applied Acoustics, 69 (2008) 343-353.

[47] E. Zwicker, H. Fastl, U. Widmann, K. Kurakata, S. Kuwano, S. Namba, Program for calculating loudness according to DIN 45631 (ISO 532B), Journal of Acoustic Society of Japan, 12 (1991) 3.

[48] D. 2009/28/EC, of the European Parliament and of the Council of 23 April 2009 on the promotion of the use of energy from renewable sources and amending and subsequently repealing Directives 2001/77/EC and 2003/30/EC, in, 2009.

[49] D. Vastfjall, M.A. Gulbol, M. Kleiner, T. Garling, Affective evaluations of and reactions to exterior and interior vehicle auditory quality, Journal of Sound and Vibration, 255 (2002) 501-518.

[50] S. Yao, C.J. Wei, Z.Y. He, Evolving wavelet neural networks for function approximation, Electronics Letters, 32 (1996) 360-361.

[51] I. Arasaratnam, S. Haykin, Nonlinear Bayesian Filters for Training Recurrent Neural Networks, in: A. Gelbukh, E.F. Morales (Eds.) Micai 2008: Advances in Artificial Intelligence, Proceedings, 2008, pp. 12-33.

[52] P.J. Angeline, G.M. Saunders, J.B. Pollack, An evolutionary algorithm

that constructs recurrent neural networks, IEEE Transactions on Neural Networks, 5 (1994) 54-65.

[53] Z. Michalewicz, Genetic algorithms+data structures=evolution programs, 2st ed., Springer-Verlag, Berlin and New York, 1994.

[54] P. Moscato, Cotta, C.,, A gentle introduction to memetic algorithms, in: Handbook of Metaheuristics, Springer New York, 2003.

[55] A. Chandra, Yao, X.,, Divace: Diverse and accurate ensemble learning algorithm, in: S. Berlin (Ed.) Proceeding of the Fifth International Conference on intelligent Data Engineering and Automated learning, Exeter, UK, 2005, pp. 619-625.

[56] D. Hernandez-Lobato, G. Martinez-Munoz, A. Suarez, Empirical analysis and evaluation of approximate techniques for pruning regression bagging ensembles, Neurocomputing, 74 (2011) 2250-2264.

[57] C.S. Zhang, Q.T. Cai, Y.Q. Song, Boosting with pairwise constraints, Neurocomputing, 73 (2010) 908-919.

[58] A.L.V. Coelho, D.S.C. Nascimento, On the evolutionary design of heterogeneous Bagging models, Neurocomputing, 73 (2010) 3319-3322.

[59] D. Partridge, Network generalization differences quantified, Neural Networks, 9 (1996) 263-271.

[60] A. Rogers, Pruegel-Bennett, A.,, Genetic drift in genetic algorithm selection schemes, IEEE Transactions on Evolutionary Computation, 4 (1999) 298.

[61] A. Ismail, Engelbrecht, P.,, Pruning product unit neural networks, in: International Joint Conference on Neural Networks, 2002, pp. 257-262.

[62] X. Yao, Liu, Y., A new evolutionary suystem for evolving artificial neural networks, IEEE Transactions on Neural Networks, 3 (1997) 694-713.

[63] S. Kirkpatrick, Gelatt, C.D., Vecchi, M.P., Optimization by simulated annealing Science, 4598 (1983) 671-680.

[64] H.I. Witten, Frank, E., Data Mining: Practical Machine Learning Tools and Techniques, Morgan Kaufmann (Elsevier), 2005.

Chapter 5

Sound quality in a tractor driver cabin based on biodiesel fatty acid composition

5.1 Evaluation of sound quality in a tractor driver cabin based on the effect of biodiesel fatty acid composition

5.1.1 Abstract

Nowadays, one of the main concerns for vehicle customers is comfort. This fact, together with the constraints imposed by legal regulations on noise emissions and human exposure to noise, have led to consider noise and vibration as important design criteria for agricultural machinery cabins. In this framework, experimental analysis procedures for rapid prototyping and prediction models for early design assessment are crucial.

This work presents a study of sound quality inside a tractor cabin mock up when the engine is fuelled with different biodiesel/diesel fuel blends. In this thesis, the influence of the chemical properties of biodiesel has been correlated to sound quality metrics, i.e. loudness and roughness, and thus, their influence on the comfort of the tractor driver cabin. It has been found that cetane number and unsaturation degree of biodiesel are strongly related to loudness, whereas viscosity and unsaturation degree are

strong indicators of roughness. Finally, to predict loudness and roughness based on biodiesel chemical properties, surface response models have been developed.

5.1.2 Introduction

Biodiesel has the opportunity to contribute to the gradual substitution of fossil fuels in order to achieve the 10% renewable energy target imposed by the EU [1]. Besides, an advantage of biodiesel is that it can be produced domestically, so farmers could manufacture their own biodiesel to run their agricultural machinery.

One problem associated to drivers of agricultural machinery is the high noise and vibration levels to which they are often exposed. Subsequently, drivers are suffering from fatigue, hearing damage and other health problems [2]. In this sense, the design of the tractor cabin, following noise and vibration comfort criteria, may be an important factor to take into account by manufacturers. For these reasons, to provide the optimal cabin design, the assessment of conceptual design alternatives in an early design phase is required. In fact, in recent years, this practice has become extensively used, particularly in the automotive industry [3].

Some authors have found meaningful differences from the noise radiated by an engine depending on the biodiesel used. It seems to be due to the combustion process, that it is strongly dependent on the biodiesel chemical properties, which affect the fuel-burning rate and injection timing advance, among others [4, 5]. When combustion take place, pressure and mechanical forces act over the engine block, producing the vibration of the block wall. In addition, the pressure gradients produced during combustion also cause the resonant oscillation of the gas in the combustion chamber. It depends mainly on the bowl geometry and the gas temperature, being the last one dependent on the chemical properties of biodiesel. The effect of engine vibration causes the cabin indoor noise by means of airborne excitation. Airborne excitation consists of sound that impinges on the exterior of the cabin and introduces cabin vibrations, which transmit sound to the interior. Therefore, it can be inferred that if the chemical properties of

biodiesel have influence on the noise radiated by the engine, thus they also may affect the noise perceived by the driver.

Although few decades ago research was focused on automotive noise reduction using active noise control techniques, nowadays efforts are mainly made to improve the sound quality inside the vehicle. Regarding this subject, research has been mainly concentrated on the study of the radiated engine noise [6-8]. Since auditory impressions are subjective, several investigations have been searching different metrics to describe them [9-11]. Although these procedures are frequently used to study sound quality in an engine when it is fuelled with diesel fuel, research concerning the influence of the chemical properties of biodiesel on sound quality in a tractor driver's cabin is insufficient, and due to the EU legislation related to the use of renewable energy, more research is needed.

For this reason, an experimental analysis for the evaluation of the airborne excitation in a tractor cabin model (based on sound quality metrics) for different biodiesel/diesel fuel blends at several engine operating condition has been developed. Moreover, the chemical properties of biodiesel blends have been correlated with the comfort inside the cabin using sound quality metrics. Finally, to find out the relationship between biodiesel chemical properties and the perception of noise in a driver's cabin based on sound quality parameters, several simple response surface models have been proposed.

5.1.3 Experimental layout

In a previous phase, the noise radiated by the engine fuelled with biodiesel blends and diesel fuel at several engine operating conditions was recorded. Next, recordings were used to both simulate the noise radiated by the engine and evaluate the effect of the use of biodiesel blends compared to diesel fuel on the perceived sound quality inside the tractor cabin. For this reason, a tractor cabin scaled model was built.

5.1.3.1 Description of the engine set up

A complete description of the experiment set up, equipments and procedures were described in detail in section 2.3.3.2, chapter 2.

5.1.3.2 Description of biodiesel optimization and properties

Methodology, apparatus and biodiesel properties have been explained in depth in section 2.3.3.1, chapter 2.

5.1.3.3 Tractor driver's cabin scaled model

The cabin scaled model consists of two components, the driver's cabin compartment (DC) and the engine compartment (EC), which are connected through a flexible firewall allowing noise generated in EC to be transmitted to DC. A sound source is placed in EC to simulate a primary excitation disturbance source. This source is connected to a computer where the measurement from the noise radiated by the engine is stored. DC comprises five flat rectangle shaped panels, glued together as shown in Figure 5.1. Panels have different thickness and are made of different types of plexiglass material (Table 5.1) to simulate the distinct structural parts of the cabin (roof, floor, doors, windscreen, etc.), each one having different dynamic characteristics. EC consists of four wood panels; dimensions and characteristics are also described in Table 5.1. The scaled cabin mock up is placed in small grooves located in a rubber mat, which is placed on the rigid floor of a semi-anechoic chamber.

One microphone was placed inside the cabin, approximately in the driver's place, at 130 cm height, 71 cm from the front part of the cabin and 61 cm from the left side (Figure 5.2). The characteristics of the microphone, calibrator and measuring equipment are detailed in section 2.1.

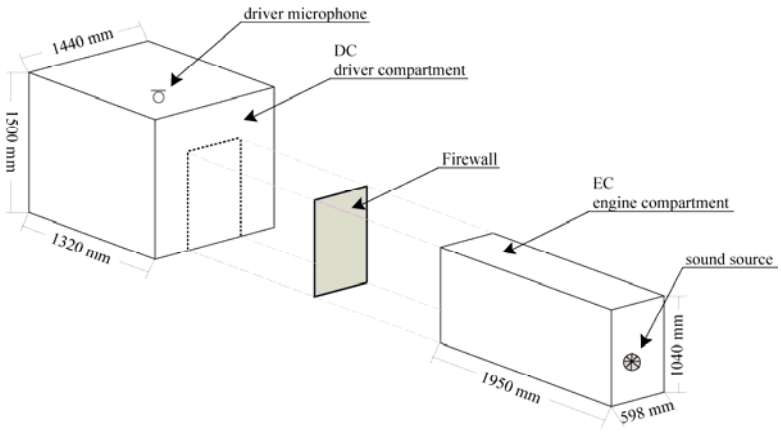

Figure 5.1. Description of the cabin mock up

Figure 5.2. Photo of the experimental setup: vibro-acoustic cabin mock-up inside the semi-anechoic chamber

Table 5.1. Materials characteristics

Tractor component	Dimensions (m^2)	Young's module, E (N/m^2)	Density, ρ (kg/m^3)	Thickness, e (m)
DC-windscreen	1.440x1.500	$2.3x10^9$	1138	$3.0x10^{-3}$
DC-backside	1.440x1500	$4.6x10^9$	1208	$2.3x10^{-3}$
DC-left/right side	1.320x1.500	$1.8x10^9$	1217	$6.0x10^{-3}$
DC-roof	1.320x1.440	$2.9x10^9$	1309	$2.3x10^{-3}$
firewall	0.598x1.040	$187.5x10^9$	8000	$15x10^{-3}$
EC-front/back side	0.598x1.040	$3.0x10^9$	755	$20x10^{-3}$
EC-left/right side	1.950x1.040	$3.0x10^9$	755	$20x10^{-3}$
EC-roof	0.598x1.950	$3.0x10^9$	755	$20x10^{-3}$

5.1.3.4 Noise characterization

Sound quality is related to the human appreciation of a determined auditive stimulus. Psychoacoustic involves more than the sole mathematical interpretation of pressure signals. In fact, it tries to go beyond, correlating acoustic stimuli with hearing sensation [12].

First, the most appropriate set of metrics for each application needs to be defined. According to the literature, loudness and roughness have been indicated as the most important metrics to describe engine noise [13, 14]. The subjective perception of loudness by the human ear is evaluated by means of both specific loudness and Zwicker loudness. From the available techniques, in the present research work, the procedure described in ISO 532B was followed [15]. According to this procedure, the specific loudness graph is presented in Sone/Bark units. The value for Zwicker loudness is defined as the integral of the specific loudness over Bark and is expressed in Sones. Roughness is related to high frequency modulation of the sound and its unit is the Asper. In this work, the model proposed by Aures for roughness calculation has been followed [16]. A more detailed description about both sound quality parameters can be found in section 2.1.3.5, chapter 2.

5.1.4 Results and discussion

Results on specific loudness are depicted in Figure 5.3 (a-d) for high engine power values and Figure 5.4 (e-h) for medium and low engine power values. In agreement with previous results, the most critical bands are situated below 5 Bark (below 570 Hz) for high power, extending to 7 Bark (840 Hz) for medium power [4, 5]. As a general trend, increasing the *CN*, an increment on specific loudness is observed at high engine power, while for medium power the opposite effect is achieved. This seems to be mainly due to the reduction of the maximum pressure, resulting from the improved *CN* and the reduced ignition delay period of the biodiesel/diesel fuel blends. However, there are some exceptions to this rule at specific engine operating conditions, i.e. mode # 6 from the 8-modes cycle, where biodiesel blends from olive pomace oil (OPME), coconut oil (CME) and palm oil (PME) show a higher increment of specific loudness. In this case, it may be attributed to their high oxygen content that provides a more complete combustion. This causes a higher in-cylinder pressure due to better fuel-air mixing, at medium engine power values. At low power, blends depict a similar behavior with regards to specific loudness. Similar results on noise radiation are in agreement with previous results [17, 18].

Figure 5.5 (a-c) illustrates the Zwicker loudness considering high, medium and low power values. In general terms, at high power, it can be seen that Zwicker loudness increases with the increase of *CN*, excepting for 50% linseed oil biodiesel/50% diesel fuel (LME50), which may be due to its high unsaturation degree. Moreover, the increase of Zwicker loudness may mean that the influence of higher *CN* of the blends on the advance of the fuel injection process increases the maximum pressure rise rate, which is expected to occur at high engine power. In general terms, at medium and low power, Zwicker loudness decreases with the increase of *CN*. In the same way as the increase of *CN* is responsible of the decreased ignition delay period and subsequently, of the maximum pressure rise rate, it is also responsible of an increase of Zwicker loudness. At medium power values, there are some exceptions corresponding to blends of coconut oil biodiesel (20% and 50%) with diesel fuel (CME20) and (CME50), which show the lowest unsaturation degree.

Figure 5.6 (a-c) shows the evolution of the roughness against μ. In this Figure, it can be observed that roughness increases slightly with μ at high and medium power. High viscosity leads to a poor atomization and mixing, burning slowly the fuel air mixture and releasing less heat [19]. The opposite tendency is noticed for lower power, where biodiesel blends with higher viscosity show the biggest decrease of roughness.

Additional results of specific roughness for the tested biodiesel blends sorted by their unsaturation degree at different engine operating conditions are presented in Figures 5.7 (a-d) and Figures 5.8 (e-h). At high engine power, the frequencies causing deterioration of the vehicle inner noise are in the range from 15 and 17 critical band rates (Bark) (2700-4000 Hz). In this case, it may be seen that higher unsaturation degree increases specific roughness. The higher the unsaturation degree of biodiesel the higher the ignition delay and the advance of the injection, consequently increasing specific roughness. At medium and low power, the most critical band rates (Bark) are the 5th and the 7th (510-700 Hz), showing the same trend as the unsaturation degree. It should be stressed that although roughness increase with the increase of the unsaturation degree, for some engine operating conditions the roughness value is very low (below 0.10 Asper). Therefore, the real sound quality equivalence should be verified with a jury test, which will be performed in future works.

5.1.4.1 Multiple regression models between fuel physical properties and sound quality metrics

To describe the relationship between the most significant fuel physical properties, Zwicker loudness and roughness measured inside the tractor cabin mock up, some multiple linear regression models have been developed. For each considered sound quality metric two models have been proposed; one based on *CN* and the other based on viscosity, as two main physical properties analyzed.

A holdout crossvalidation procedure was carried out in the experimental design using different functions from Matlab R2008a. The whole dataset *n* was divided into 3*n*/4 for training and *n*/4 for generalization proposes. Each model was performed using 88 points measured under the

engine 8-modes cycle for 10 biodiesel blends and diesel fuel. Moreover, 30 holdout processes with different random splits of the data (by means of iterative loop) achieving 30 models were performed. For each model, the mean square error (MSE) and the standard deviation (SD) were recorded. The best model was selected based on the value of these parameters in the generalization set (Table 5.2). Training results have not been considered since they are upward-biased.

Table 5.2. Comparative performance of the models based on medium standard error (MSE) for the generalization set

Method	**MSE_G(Mean±SD)**
Zwicker Loudness based on *CN*	2.591±0.0594
Zwicker Loudness based on μ	2.590±0.0618
Roughness based on *CN*	0.008±0.0002
Roughness based on μ	0.007±0.0001

[1]where G is the generalization set and SD is the standard deviation

Table 5.3 depicts the results of the best multiple response surface model applied to Zwicker loudness and roughness. The evaluation of these models was based on the MSE, coefficient of determination (R^2) and P-value in the generalization set. The P-value was lower than 0.0001 for all proposed models, meaning that there are statistically significant relationships between the variables with a confidence level above 99.9%. Results of the different models against MSE are plotted in Figures 5.9 and 5.10. Box plots depict algorithm results according to the smallest observation, lower quartile, median, upper quartile and largest observation.

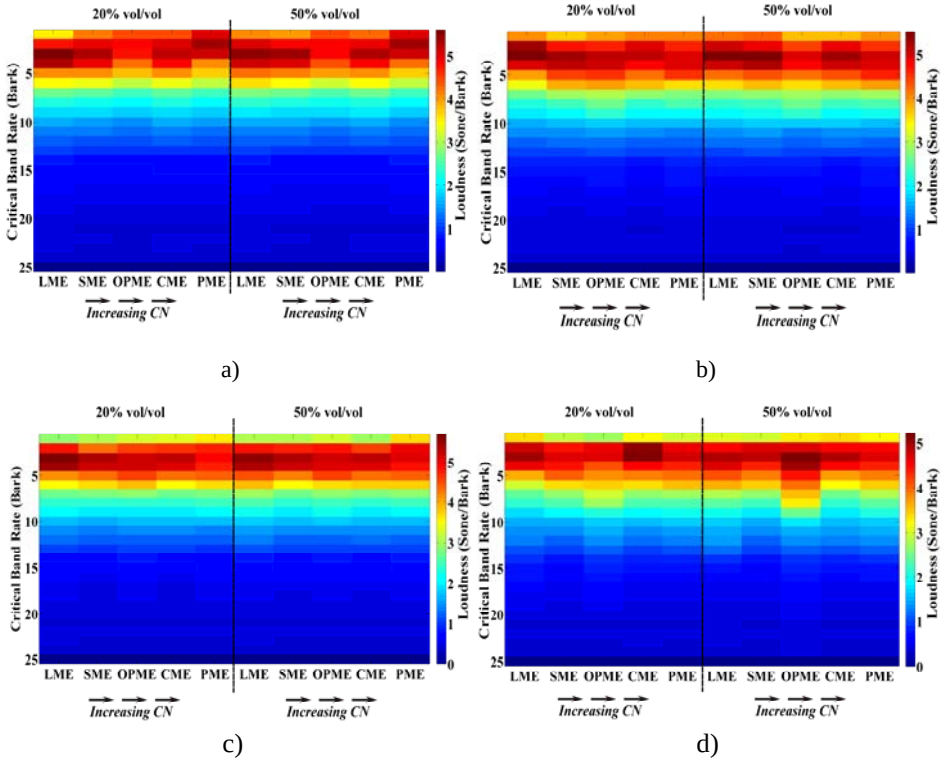

Figure 5.3. Spectrogram of specific loudness (Sone/Bark) for biodiesel blends at high power; modes 1-4 from the 8-mode cycle (a-d)

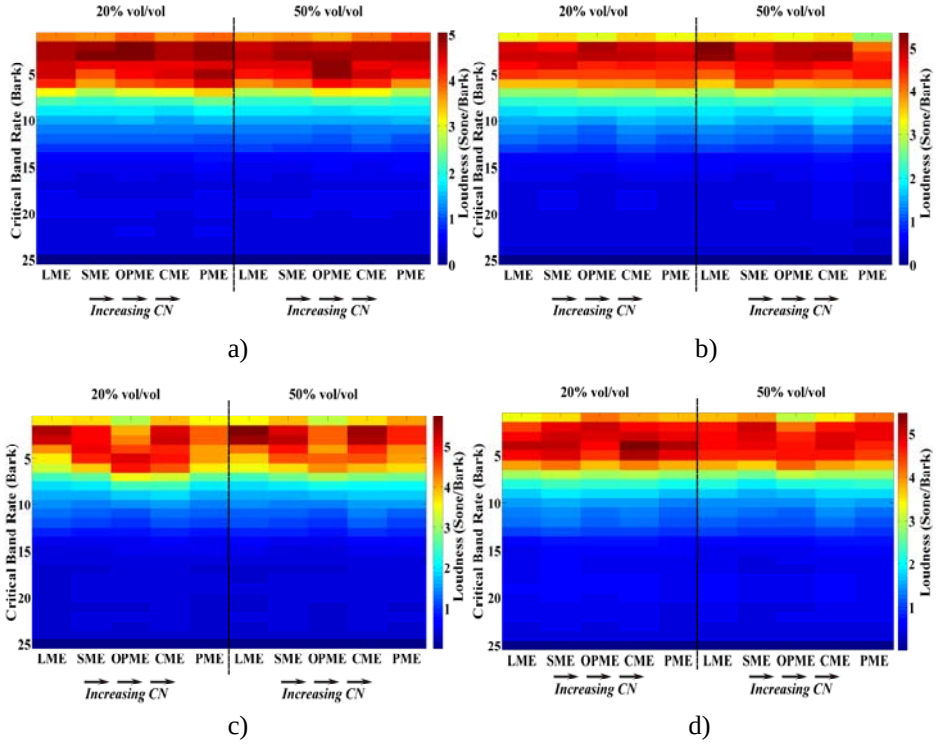

Figure 5.4. Spectrogram of specific loudness (Sone/Bark) for biodiesel blends at medium power (a-c) and low power d) considering the 8-mode cycle

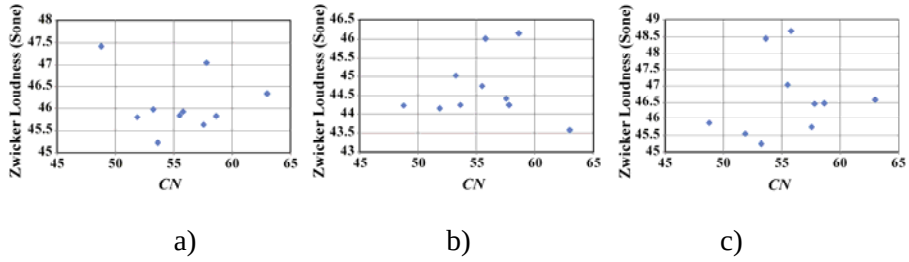

Figure 5.5. Zwicker loudness level (Sone) for different biodiesel blends

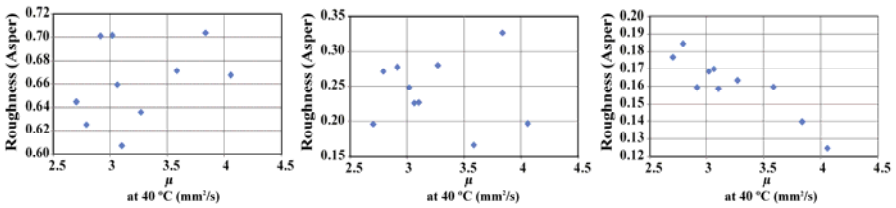

a) b) c)

Figure 5.6. Roughness level (Asper) for different biodiesel blends

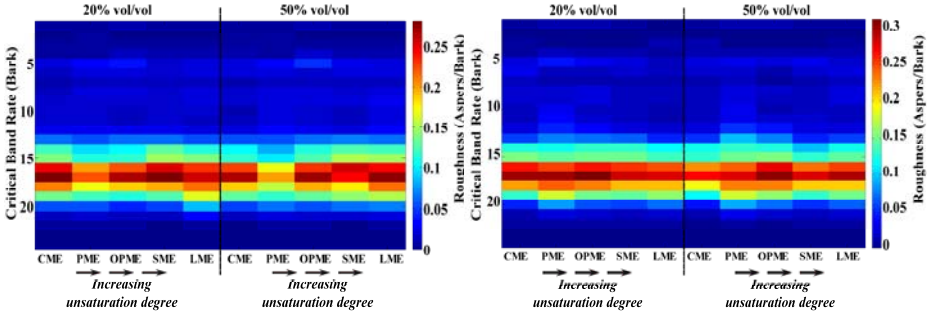

a) b)

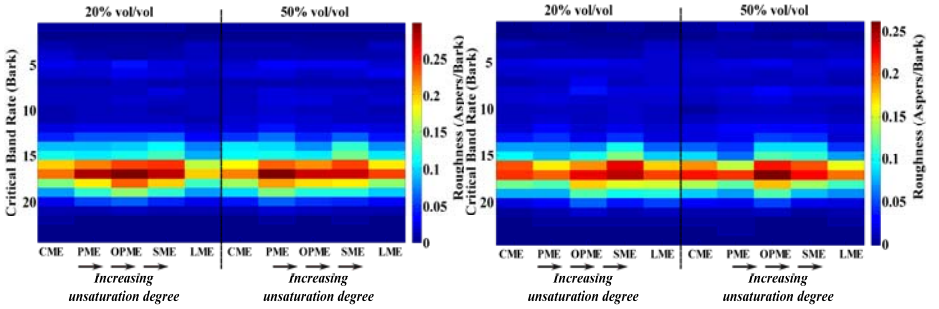

c) d)

Figure 5.7. Spectrogram of specific roughness level (Asper/Bark) for different biodiesel blends at high power; modes 1-4 from the 8-mode cycle (a-d)

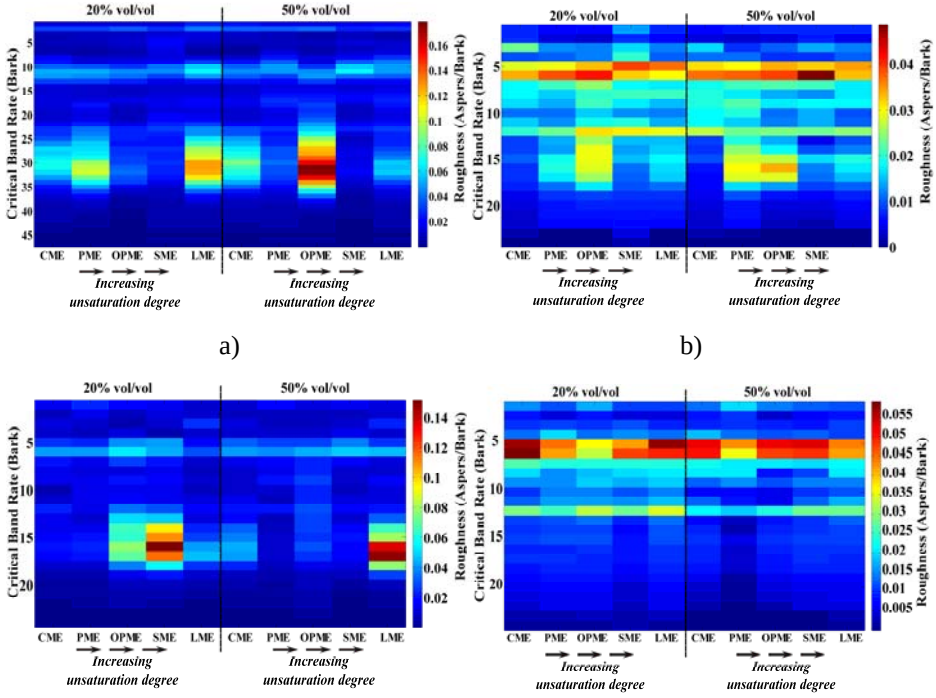

Figure 5.8. Spectrogram of specific roughness level (Asper/Bark) for different biodiesel blends at medium (a-c) and low power d) considering the 8-mode cycle

Table 5.3. Summary of the best models

MSE	R^2 (%)	models
2.44	99.26	$f_{loudness}(x)= 43.20861+0.02504\ x_{11} + 0.00108\ x_{12}– 0.03034\ x_{13}$
2.48	99.27	$f_{loudness}(x)= 43.95457 + 0.20398\ x_{21}+0.00108\ x_{22} – 0.03023\ x_{23}$
0.0076	91.02	$f_{roughness}(x)= -0.35086 – 0.00122\ x_{11}+ 0.00049\ x_{12}- 0.00187\ x_{13}$
0.0076	91.00	$f_{roughness}(x)= -0.43248 – 0.00508\ x_{21}+ 0.00049\ x_{22} - 0.00189\ x_{23}$

where: x_{11} is *CN*, x_{21} is μ, x_{12} and x_{22} are speed (rpm) and x_{13} and x_{23} are power (kW)

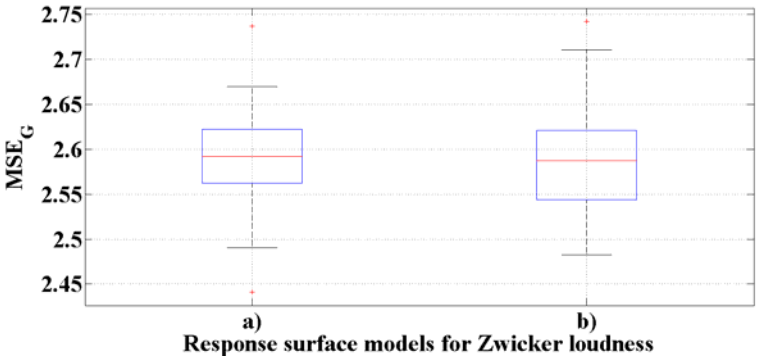

Figure 5.9. Box plot for Zwicker loudness models

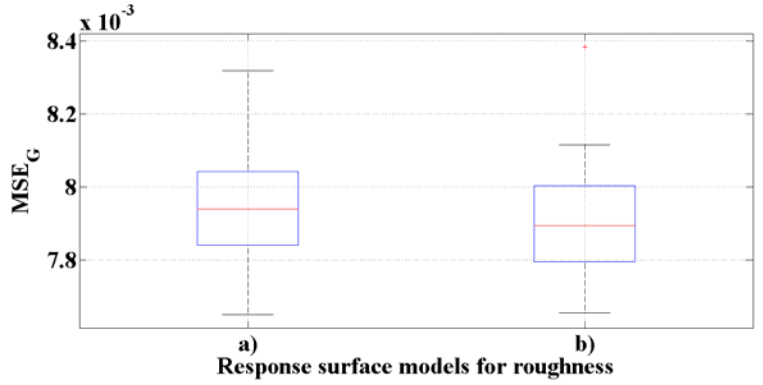

Figure 5.10. Box plot for roughness models

Prediction of Zwicker loudness. In order to predict Zwicker loudness, two important properties have been considered, namely *CN* and μ, besides engine power (*N*) and speed (*n*) due to their influence considering different engine operating conditions.

The two Zwicker loudness models show a good correlation, with a value of R^2 of 99.26% for *CN* and 99.27% for μ. The response surface models are as follows:

Zwicker loudness (Sone) = 43.20861+0.02504 CN + 0.00108 n (rpm) – 0.03034 N (kW)

Zwicker loudness (Sone) = 43.95457 + 0.20398 μ+0.00108 n (rpm) – 0.03023 N (kW)

As can be observed, both models are analogous and depict similar coefficients for speed and power. This indicates a clear effect of the speed and power on the Zwicker loudness; at high speed, the Zwicker loudness increases, while at high power it decreases proportionally to *CN* and μ. Although, the higher the *CN* the higher the Zwicker loudness value, the coefficient of μ shows that it is more significant with respect to *CN*. Similar results have been found in the literature [20, 21].

Prediction of roughness. Table 5.3 shows a value of R^2 of 91.02% and 91.00% for response surface models based on *CN* and μ, respectively. As found for the Zwicker loudness models, it can be seem that the speed and power present similar coefficient values in the models. However, the coefficients of *CN* and μ of the roughness models are lower than those of loudness models. This means that the effect of these properties is stronger for loudness.

The response surface models to predict roughness are given by the following expressions:

Roughness (Asper) = -0.35086 – 0.00122 CN + 0.00049 n (rpm) - 0.00187 N (kW)

Roughness (Asper) = -0.43248 – 0.00508 μ+ 0.00049 n (rpm) - 0.00189 N (kW)

The negative sign of *CN* and μ in the models means that roughness decreases as these properties increase. This statement is in agreement with the above explanation: *CN* is a relative measure of the delay between injection and auto-ignition of the fuel, while μ affects the atomization quality. High cetane number guarantees good start behavior and a smooth run of the engine. In contrast, fuels with low cetane number tend to increase the in-cylinder pressure because of incomplete combustion. On the other hand, fuel with high μ tend to form larger droplets on injection which can cause poor fuel atomization during the spray, increases the engine deposits, needs more energy to pump the fuel, and wears fuel pump elements and injectors and consequently leads to poor combustion [22, 23].

The main cause of roughness is due to the medium vibration originated from the dynamics of engine that move parts as crankshaft and camshaft, among others. This vibration is transmitted via the structure-borne to the tractor cabin and it penalizes the sound quality and comfort inside the driver's cabin. Therefore, it may be inferred that higher viscosity penalizes the comfort by means of roughness increase.

5.1.5 Conclusions

This work describes an experimental procedure, which can be used for the characterization of the sound quality in the driver's cabin of a tractor. In general terms, at high power, the higher the cetane number the higher the loudness. The opposite effect is found at medium and low power. For roughness, a strongly correlation with the unsaturation degree and viscosity has been found. In sum, the use of biodiesel blends is recommended to improve sound quality inside the tractor cabin, making the interior more comfortable for the driver.

5.2 References

[1] Directive 2009/28/EC of the European Parliament and of the Council of 23 April 2009 on the promotion of the use of energy from renewable sources and amending and subsequently repealing Directives 2001/77/EC and 2003/30/EC, in, 2009.

[2] W. Desmet, B. Pluymers, P. Sas, Vibro-acoustic analysis procedures for the evaluation of the sound insulation characteristics of agricultural machinery cabins, Journal of Sound and Vibration, 266 (2003) 407-441.

[3] L.P.R. de Oliveira, P.S. Varoto, P. Sas, W. Desmet, A state-space modeling approach for active structural acoustic control, Shock and Vibration, 16 (2009) 607-621.

[4] M.D. Redel-Macías, S. Pinzi, M.F. Ruz, A.J. Cubero-Atienza, M.P. Dorado, Biodiesel from saturated and monounsaturated fatty acid methyl esters and their influence over noise and air pollution, Fuel.

[5] M.D. Redel-Macías, S. Pinzi, D. Leiva, A.J. Cubero-Atienza, M.P. Dorado, Air and noise pollution of a diesel engine fueled with olive pomace oil methyl ester and petrodiesel blends, Fuel, 95 (2012) 615-621.

[6] N.W. Alt, J. Nehl, S. Heuer, M.W. Schlitzer, Prediction of combustion process induced vehicles interior noise, SAE paper 2003-01-1435, (2003).

[7] K. Genuit, The sound quality of vehicle interior noise: a challenge for the NVH-engineers, International Journal Vehicle Noise and Vibration, 1 (2004) 11.

[8] M.J.M. Nor, M.H. Fouladi, H. Nahvi, A.K. Ariffin, Index for vehicle acoustical comfort inside a passenger car, Applied Acoustics, 69 (2008) 343-353.

[9] T. Papenfus, K. Genuit, P. Blaschke, K.T. Kang, I. Jung, J. Jin, Method of NVH quality rating of diesel combustion noise using typical driving modes, SAE paper 2009-01-2078, (2009).

[10] F. Payri, A. Broatch, X. Margot, L. Monelletta, Sound quality assessment of Diesel combustion noise using in-cylinder pressure components, Measurement Science & Technology, 20 (2009).

[11] F. Payri, A.J. Torregrosa, A. Broatch, L. Monelletta, Assessment of diesel combustion noise overall level in transient operation, International Journal of Automotive Technology, 10 (2009) 761-769.

[12] L.P.R. de Oliveira, K. Janssens, P. Gajdatsy, H. Van der Auweraer, P.S. Varoto, P. Sas, W. Desmet, Active sound quality control of engine induced cavity noise, Mechanical Systems and Signal Processing, 23 (2009) 476-488.

[13] B. Brassow, M. Clapper, Powertrain sound quality development of the Ford GT, SAE paper 2005-01-2480, (2005).

[14] L.P.R. de Oliveira, M.M. da Silva, P. Sas, H. Van Brussel, W. Desmet, Concurrent mechatronic design approach for active control of cavity noise, Journal of Sound and Vibration, 314 (2008) 507-525.

[15] E. Zwicker, H. Fastl, U. Widmann, K. Kurakata, S. Kuwano, S. Namba, Program for calculating loudness according to DIN 45631 (ISO 532B), Journal of Acoustic Society of Japan, 12 (1991) 3.

[16] W. Aures, A procedure for calculating auditory roughness, Acustica, 58 (1985) 268-281.

[17] Y.H.Y. Haik, M.Y.E. Selim, T. Abdulrehman, Combustion of algae oil methyl ester in an indirect injection diesel engine, Energy, 36 (2011) 1827-1835.

[18] C.D. Rakopoulos, A.M. Dimaratos, E.G. Giakoumis, D.C. Rakopoulos,

Study of turbocharged diesel engine operation, pollutant emissions and combustion noise radiation during starting with bio-diesel or n-butanol diesel fuel blends, Applied Energy, 88 (2011) 3905-3916.

[19] D.B. Hulwan, S.V. Joshi, Performance, emission and combustion characteristic of a multicylinder DI diesel engine running on diesel-ethanol-biodiesel blends of high ethanol content, Applied Energy, 88 (2011) 5042-5055.

[20] M. Bunce, D. Snyder, G. Adi, C. Hall, J. Koehler, B. Davila, S. Kumar, P. Garimella, D. Stanton, G. Shaver, Stock and Optimized Performance and Emissions with 5 and 20% Soy Biodiesel Blends in a Modern Common Rail Turbo-Diesel Engine, Energy & Fuels, 24 (2010) 928-939.

[21] A.M. Peterson, P.I. Lee, M.C. Lai, M.C. Wu, C.L. DiMaggio, asme, Effects of b20 on combustion, emissions and performance of a light-duty diesel engine, 2009.

[22] L.F. Ramírez-Verduzco, B.E. García-Flores, J.E. Rodríguez-Rodríguez, A. Del Rayo Jaramillo-Jacob, Prediction of the density and viscosity in biodiesel blends at various temperatures, Fuel, 90 (2011) 1751-1761.

[23] L.F. Ramírez-Verduzco, J.E. Rodríguez-Rodríguez, A.D.R. Jaramillo-Jacob, Predicting cetane number, kinematic viscosity, density and higher heating value of biodiesel from its fatty acid methyl ester composition, Fuel, 91 (2012) 102-111.

Conclusions/Conclusiones

Conclusions

During this Phd thesis, the effect of biodiesel properties on exhaust and noise emissions has been studied and several noise prediction models have been developed. Moreover, the influence of biodiesel on sound quality has also been analyzed. The most important conclusions of this work are the following:

- Considering blends of biodiesel (covering a wide range of fatty acid composition) in diesel fuel, the higher the number of double bonds (higher unsaturation degree) the higher the emission of NO_x and the higher the reduction of CO and CO_2 emissions. In general terms, NO_x emissions increased when biodiesel was used to substitute diesel fuel, however a reduction of CO, CO_2 and noise emissions was achieved. In this sense, a linear correlation between kinematic viscosity (saturation level) and sound pressure level was found at high power values. In sum, the use of mono- and poly-unsaturated biodiesel as partial diesel fuel substitute is strongly recommended to improve CO and CO_2 emissions, besides engine sound quality, thus making the engine sound more pleasant.

- The capability of ANN to identify noise emitted by an engine fuelled with biodiesel from either olive pomace oil or palm oil at several

steady-state engine operating conditions has been demonstrated. MSE and SEP show that combined EPUNN and RBFNN model is the most appropriate. However, taking into account also the simplicity of the model, the best solution is provided by EPUNN model.

- To identify the sound source in a vehicle, different models have been applied. To quantify the number of descriptors necessary to achieve an acceptable precision, the number of monopoles have been changed. The precision was evaluated in terms of Zwicker loudness and sharpness, showing a higher level of prediction in the perceived spectrum when loudness was considered, instead of sharpness. Both, the relation between the number and position of the substitute sources and the active radiation mode are the dominant effects that determine the best model performance. It has been demonstrated that, even when the problem displays a good conditioning, the improvement of the regularization strategies is necessary. Results achieved with the Tikhonov iterative algorithm reveal their superiority compared to non-iterative regularization techniques, both in terms of loudness and sharpness. Moreover, it has been shown that the number of monopoles influence the required number of iterations.

- The potential of EPUNN to identify noise in vehicles using a Pass-by Noise test at high frequencies has been shown. A combined method (ASQ method for low-mid frequencies and ANN method for high frequencies) based on the behavior of the system studying the condition number of the problem has been used; the accuracy of the model has been improved. Statistical analysis based on MSE and SEP have shown that for high frequencies, the EPUNN model achieved the best accuracy in the generalization set. In addition, analyzing the perceived sound quality using the psychoacoustic parameters like a person could hear it, it has also been shown that the error obtained at high frequencies with the ANN model is lower than that of the ASQ model.

- The effect of the biodiesel blends in the tractor cabin comfort based on sound quality metrics has been studied. In general terms, the higher the cetane number the higher the loudness at high engine torque, while at medium and low torque the opposite effect was achieved. For

roughness, a strongly correlation with the unsaturation degree and hence with viscosity was found. In sum, the use of biodiesel blends is recommended to improve sound quality inside the tractor cabin, making the interior more comfortable for the driver.

Conclusiones

En esta tesis doctoral, se ha estudiado el efecto de las propiedades en las emisiones gaseosas y de ruido y se han desarrollado varios modelos de predicción de ruido. Además, se ha analizado la influencia del biodiésel en la calidad del sonido. Las conclusiones más importantes de este trabajo son las siguientes:

- Considerando las mezclas de biodiésel (a partir de aceites que cubran un amplio rango de composición de ácidos grasos) con gasóleo, se ha observado que las emisiones de NO_x se incrementan cuando se utiliza biodiésel como sustituto del gasóleo; sin embargo, se consigue una reducción de CO, CO_2 y de ruido emitido. Por otro lado, el aumento del número de dobles enlaces (aumento del grado de saturación), aumenta las emisiones de NO_x y reduce las de CO y CO_2. En este sentido, hay una correlación lineal entre la viscosidad cinemática (nivel de saturación) y la presión acústica a altos valores de par. En resumen, el uso de biodiésel mono y poli-insaturado como sustituto parcial del gasóleo mejora tanto las emisiones de CO como las de CO_2, así como la calidad del sonido del motor, de modo que éste sea mucho más placentero.

- Se ha demostrado la capacidad de las redes neuronales

artificiales (RNA) para identificar el sonido emitido por un motor cuando se emplea biodiésel de orujo de oliva bajo distintas condiciones de funcionamiento. Tanto el error medio cuadrático como la desviación estándar de la predicción han mostrado que el modelo combinado de redes basado en unidades producto y funciones de base es el más apropiado. Sin embargo, teniendo en cuenta la simplicidad de los modelos, la mejor solución la proporciona el modelo basado en redes unidades producto.

- Se han empleado diferentes modelos para identificar y cuantificar las fuentes de sonido en vehículos. La precisión de dichos modelos se ha evaluado en términos de *Zwicker loudness* y *sharpness*, mostrando mejor precisión cuando se emplea el primero. Además, se ha demostrado que tanto el número como la posición de los descriptores frente al modo de radiación son los factores determinantes en la precisión del modelo. Se ha demostrado que incluso aunque el problema muestre un buen condicionamiento, el uso de estrategias de regularización mejora la precisión del sistema. Los resultados logrados con el método iterativo Tikhonov mejoran notablemente los resultados obtenidos con los métodos no iterativos en términos de exactitud basados en *loudness* y *sharpness*. Además, el número de monopolos empleados es primordial en el número de iteraciones necesarias para lograr suficiente precisión.

- Se ha demostrado la potencialidad de las redes neuronales basadas en algoritmos evolutivos de unidades producto para identificar fuentes sonoras en vehículos a altas frecuencias. Se ha mejorado la precisión del modelo adaptando la solución del problema al comportamiento del sistema, basándose en el condicionamiento mostrado por el mismo, mediante un método combinado basado en la cuantificación de fuentes sonoras aéreas para bajas frecuencias y en redes neuronales artificiales para altas frecuencias. Este problema de regresión es un problema complejo debido a la naturaleza complicada de la función de error asociada al modelo. El análisis estadístico basado en el error medio cuadrático y en la desviación estándar en la predicción ha mostrado que para las altas frecuencias el modelo de redes neuronales basado en algoritmos evolutivos de unidades producto tienen mejor precisión en generalización. Además, el análisis psicoacústico del error

muestra que este modelo proporciona resultados más precisos que el de cuantificación de fuentes sonoras aéreas.

- El efecto de diversas mezclas de biodiésel sobre el confort en la cabina de un tractor ha sido estudiada considerando métricas de calidad del sonido. En términos generales, un aumento del número de cetano aumenta el parámetro *loudness* cuando el valor del par motor es alto, mientras que los valores medios y bajos de par proporcionan el efecto opuesto. Para el parámetro *roughness*, se ha encontrado una fuerte correlación con el grado de saturación y por tanto con la viscosidad. En resumen, se recomienda el uso de mezclas de biodiésel para mejorar la calidad del sonido en el interior de la cabina del tractor y, por tanto, el confort.

Future lines of research

Future lines of research

The research carried out in this Phd thesis shows a novel study, as there are no evidences about similar achievements in the literature. Once the conclusions have been presented, new lines of research may be proposed:

- To correlate the in-cylinder pressure with both the sound quality and the effect of the biodiesel chemical composition.

- To develop a Finite Element Model and Boundary Element Model of the tractor cabin to further simulate and validate the model with the tractor cabin mock up.

- To study the influence of the combustion oscillations due to the premixed flame on sound quality based on optical sensors placed in the combustion chamber.

- To study the influence on engine performance and air and noise emissions of higher percentages of biodiesel blended with diesel fuel, including straight biodiesel.

- To classify biodiesel sound quality by means of a jury test and then to check the correlation with sound quality metrics to provide an

ANN classification model.

- To test the sound quality inside a tractor cabin under several engine operating conditions and using different types of biodiesel, compared to straight diesel fuel.

References

References

(June 2002). "Official Journal of the European Communities, Directive 2002/49/EC of the European Parlianment and the Council ".

Agency, E. E. (2012). "http://www.eea.europa.eu/themes/noise."

GMBH, A. L. (2001). Community noise research strategy plan (CALM). Fifth Framework Programme G4RT-CT-2001-05043.

2009/28/EC, D. (2009). of the European Parliament and of the Council of 23 April 2009 on the promotion of the use of energy from renewable sources and amending and subsequently repealing Directives 2001/77/EC and 2003/30/EC.

European Parliament, C. (2002). The Assessment and menagement of enviromental noise-Declaration by the Comission in the Conciliation Committee on the Directive relating to the assessment and management of environmental noise, Oficial Journal of the European Communities. Directive 2002/49/EC: 14.

A

Abu-Jrai, A., J. A. Yamin, et al. (2011). "Combustion characteristics and engine emissions of a diesel engine fueled with diesel and treated waste cooking oil blends." Chemical Engineering Journal 172(1): 129-136.

Agarwal, A. K. and K. Rajamanoharan (2009). "Experimental investigations of performance and emissions of Karanja oil and its blends in a single cylinder agricultural diesel engine." Applied Energy 86(1): 106-112.

Agarwal, D., L. Kumar, et al. (2008). "Performance evaluation of a vegetable oil fuelled compression ignition engine." Renewable Energy 33(6): 1147-1156.

Albarbar, A., F. Gu, et al. (2010). "Diesel engine fuel injection monitoring using acoustic measurements and independent component analysis." Measurement 43(10): 1376-1386.

Albarbar, A., F. Gu, et al. (2010). "Acoustic monitoring of engine fuel injection based on adaptive filtering techniques." Applied Acoustics 71(12): 1132-1141.

Alt, N. W., Nehl, J., Heuer, S., Schlitzer, M. W., (2003). "Prediction of combustion process induced vehicles interior noise." SAE paper 2003-01-1435.

Anderton, D. (1979). "Relation between combustion system and noise." SAE paper 1979-790270.

Angeline, P. J. S., G. M.; Pollack, J, B. (1994). "An evolutionary algorithm that constructs recurrent neural networks." IEEE Transactions on Neural Networks 5(1): 54-65.

Arasaratnam, I. and S. Haykin (2008). Nonlinear Bayesian Filters for Training Recurrent Neural Networks. Micai 2008: Advances in Artificial Intelligence, Proceedings. A. Gelbukh and E. F. Morales. 5317: 12-33.

Arcaklioğlu, E. and I. Çelikten (2005). "A diesel engine's performance and exhaust emissions." Applied Energy 80(1): 11-22.

Aures, W. (1985). "A procedure for calculating auditory roughness." Acustica 58: 268-281.

Austen, A. E. W., Priede, T. (1959). "Origins of diesel engine noise." SAE paper 590127.

Azam, M., A. Waris, et al. (2005). "Prospects and potential of fatty acid methyl esters of some non-traditional seed oils for use as biodiesel in India." Biomass and Bioenergy 29(4): 293-302.

B

Ban-Weiss, G. A., J. Y. Chen, et al. (2007). "A numerical investigation into the anomalous slight NOx increase when burning biodiesel; A new (old) theory." Fuel Processing Technology 88(7): 659-667.

Bao, Y. D. and Y. He (2006). "Study on noise of rapeseed oil blends in a single-cylinder diesel engine." Renewable Energy 31(11): 1789-1798.

Basha, S. A., K. R. Gopal, et al. (2009). "A review on biodiesel production, combustion, emissions and performance." Renewable and Sustainable Energy Reviews 13(6-7): 1628-1634.

Bayhan, Y., E. Kilic, et al. (2010). "Effect of Pure Biodiesel on Fuel Injection Systems and Noise Level in Agricultural Diesel Engines." Ama-Agricultural Mechanization in Asia Africa and Latin America 41(4): 78-81.

Berckmans, D., B. Pluymers, et al. (2008). Numerical case-study on the development of acoustic equivalent source models for use in sound synthesis methods.

Berckmans, D., P. Kindt, et al. (2010). "Evaluation of substitution monopole models for tire noise sound synthesis." Mechanical Systems and Signal Processing 24(1): 240-255.

Bezaire, N., K. Wadumesthrige, et al. (2010). "Limitations of the use of cetane index for alternative compression ignition engine fuels." Fuel 89(12): 3807-3813.

Bishop, C. M. (2006). Pattern Recognition and Machine Learning, Hardcover.

Bishop, M. C. (1991). "Improving the generalization properties of radial basis function neural networks." Neural Computation 4(3): 579-581.

Bobrovnitskii, Y. I. and G. Pavic (2003). "Modelling and characterization of airborne noise sources." Journal of Sound and Vibration 261(3): 527-555.

Boehman, A. L., D. Morris, et al. (2004). "The Impact of the Bulk Modulus of Diesel Fuels on Fuel Injection Timing." Energy & Fuels 18(6): 1877-1882.

Bohn, C., A. Cortabarria, et al. (2004). "Active control of engine-induced vibrations in automotive vehicles using disturbance observer gain

scheduling." Control Engineering Practice 12(8): 1029-1039.
Boudy, F. and P. Seers (2009). "Impact of physical properties of biodiesel on the injection process in a common-rail direct injection system." Energy Conversion and Management 50(12): 2905-2912.
Brassow, B., Clapper, M., (2005). "Powertrain sound quality development of the Ford GT." SAE paper 2005-01-2480.
Bunce, M., D. Snyder, et al. (2010). "Stock and Optimized Performance and Emissions with 5 and 20% Soy Biodiesel Blends in a Modern Common Rail Turbo-Diesel Engine." Energy & Fuels 24: 928-939.
Bunce, M., D. Snyder, et al. (2011). "Optimization of soy-biodiesel combustion in a modern diesel engine." Fuel 90(8): 2560-2570.

C

Canakci, M., Sanli, H. (2008). "Biodiesel production from various feedstocks and their effects on the fuel properties." Journal of Industrial Microbiological and Biotechnology 35: 431-441.
Canakci, M., A. N. Ozsezen, et al. (2009). "Prediction of performance and exhaust emissions of a diesel engine fueled with biodiesel produced from waste frying palm oil." Expert Systems with Applications 36(5): 9268-9280.
Canakci, M., Sanli, H. (2008). "Biodiesel production from various feedstocks and their effects on the fuel properties." Journal of Industrial Microbiological and Biotechnology 35: 431-441.
Caresana, F. (2011). "Impact of biodiesel bulk modulus on injection pressure and injection timing. the effect of residual pressure." Fuel 90(2): 477-485.
Castellini, P., G. M. Revel, et al. (2004). "Measurement of vibrational modal parameters using laser pulse excitation techniques." Measurement 35(2): 163-179.
Chandra, A., Yao, X., (2005). Divace: Diverse and accurate ensemble learning algorithm. Proceeding of the Fifth International Conference on intelligent Data Engineering and Automated learning, Exeter, UK.
Chaparro, A., E. Landry, et al. (2006). "Transfer function characteristics of bluff-body stabilized, conical V-shaped premixed turbulent propane-air flames." Combustion and Flame 145(1-2): 290-299.

Chen, H., J. Wang, et al. (2008). "Study of oxygenated biomass fuel blends on a diesel engine." Fuel 87(15-16): 3462-3468.

Cho, Y. M. (1997). "Noise source and transmission path identification via state-space system identification." Control Engineering Practice 5(9): 1243-1251.

Choi, G. M., M. Tanahashi, et al. (2005). Control of oscillating combustion and noise based on local flame structure.

Coelho, A. L. V. and D. S. C. Nascimento (2010). "On the evolutionary design of heterogeneous Bagging models." Neurocomputing 73(16-18): 3319-3322.

Coen, T. J., N.; Van de Ponseele, P.; Goethals, I.; De Baerdemaeker, J.; De Moor, B. (2005). Engine sound comfortability: Relevant sound quality parameters and classification. Proceeding of IFAC 2005, Prague, Czech Republic.

Cremer, L. and M. Wang (1988). "Synthesis of Spherical Wave Fields to Generate the Sound Radiated from Bodies of Arbitrary Shape, its Realization by Calculation and Experiment." Die synthese eines von einem beliebigen koerper in luft erzeugten feldes aus kugelschallfeldern und deren realisierung in durchrechnung und experiment. 65(2): 53-74.

Cruz-Peragon, F. and F. J. Jimenez-Espadafor (2007). "Design and optimization of neural networks to estimate the chamber pressure in internal combustion engines by an indirect method." Energy & Fuels **21**(5): 2627-2636.

Cruz-Peragon, F. and F. J. Jimenez-Espadafor (2007). "A genetic algorithm for determining cylinder pressure in internal combustion engines." Energy & Fuels **21**(5): 2600-2607.

Cruz-Peragon, F., F. J. Jimenez-Espadafor, et al. (2009). "Influence of a Combustion Parametric Model on the Cyclic Angular Speed of Internal Combustion Engines. Part I: Setup for Sensitivity

D

de Bree, H. E., Basten, T. (2008). "Microflown based monopole sound sources for reciprocal measurements." SAE paper 2008-01-0503.

de Oliveira, L. P. R., K. Janssens, et al. (2009). "Active sound quality control of engine induced cavity noise." Mechanical Systems and

Signal Processing 23(2): 476-488.
de Oliveira, L. P. R., K. Janssens, et al. (2009). "Active sound quality control of engine induced cavity noise." Mechanical Systems and Signal Processing 23(2): 476-488.
de Oliveira, L. P. R., P. S. Varoto, et al. (2009). "A state-space modeling approach for active structural acoustic control." Shock and Vibration 16(6): 607-621.
Deh Kiani, M. K., B. Ghobadian, et al. (2009). "Application of artificial neural networks for the prediction of performance and exhaust emissions in SI engine using ethanol- gasoline blends." Energy 35(1): 65-69.
Demirbaş, A. (2000). "Direct route to the calculation of heating values of liquid fuels by using their density and viscosity measurements." Energy Conversion and Management 41(15): 1609-1614.
Desantes, J. M., J. Benajes, et al. (2004). "The modification of the fuel injection rate in heavy-duty diesel engines. Part 1: Effects on engine performance and emissions." Applied Thermal Engineering 24(17-18): 2701-2714.
Desantes, J. M., J. Benajes, et al. (2004). "The modification of the fuel injection rate in heavy-duty diesel engines: Part 2: Effects on combustion." Applied Thermal Engineering 24(17-18): 2715-2726.
Desmet, W., B. Pluymers, et al. (2003). "Vibro-acoustic analysis procedures for the evaluation of the sound insulation characteristics of agricultural machinery cabins." Journal of Sound and Vibration 266(3): 407-441.
Dorado, M. (2008). Raw materials to produce low cost biodiesel. Chapter 4. Biofuels refining and performance. A. Nag, McGraw Hill Professional: 107-148.
Dorado, M. P., E. Ballesteros, et al. (2003). "Testing waste olive oil methyl ester as a fuel in a diesel engine." Energy & Fuels 17(6): 1560-1565.
Dorado, M. P., E. Ballesteros, et al. (2003). "Exhaust emissions from a Diesel engine fueled with transesterified waste olive oil." Fuel 82(11): 1311-1315.
Dorado, M. P., F. Cruz, et al. (2006). "An approach to the economics of two vegetable oil-based biofuels in Spain." Renewable Energy 31(8): 1231-1237.
Dorado, M. P., S. Pinzi, et al. (2011). "Visible and NIR Spectroscopy to

assess biodiesel quality: Determination of alcohol and glycerol traces." Fuel 90(6): 2321-2325.

Dowling, A. P. and S. R. Stow (2003). "Acoustic Analysis of Gas Turbine Combustors." Journal of Propulsion and Power 19(5): 751-764.

Du, H., L. Zhang, et al. (2001). "Reconstructing cylinder pressure from vibration signals based on radial basis function networks." Proceedings of the Institution of Mechanical Engineers, Part D: Journal of Automobile Engineering 215(6): 761-767.

Duchaine, P., L. Zimmer, et al. (2009). Experimental investigation of mechanisms of sound production by partially premixed flames.

Ducruix, S., T. Schuller, et al. (2003). "Combustion Dynamics and Instabilities: Elementary Coupling and Driving Mechanisms." Journal of Propulsion and Power 19(5): 722-734.

F

Fahy, F. J. (2003). "Some applications of the reciprocity principle in experimental vibroacoustics." Acoustical Physics 48(2): 217-229.

Fastl, H. (1997). "The psychoacoustics of sound-quality evaluation." Acustica 83(5): 754-764.

Fastl, H. and E. Zwicker (2007). Psycho-Acoustics: Facts and Models. New York, Springer.

Fernández-Navarro, F. H.-M., C; Gutierrez, P. A.; Carbonero-Ruz, M. (2011). "Evolutionary q-Gaussian radial basis functions neural networks for multi-classification." Neural Networks 24(7).

Fogel, D. B. (1997). "Evolutionary Computation: A New Transactions." IEEE Transactions on Evolutionary Computation 1(1): 1-2.

Fouladi, M. H., M. J. M. Nor, et al. (2009). "Spectral analysis methods for vehicle interior vibro-acoustics identification." Mechanical Systems and Signal Processing 23(2): 489-500.

Freedman, B. and M. Bagby (1989). "Heats of combustion of fatty esters and triglycerides." Journal of the American Oil Chemists Society 66(11): 1601-1605.

G

Genuit, K. (2004). "The sound quality of vehicle interior noise: a challenge for the NVH-engineers." International Journal Vehicle Noise and Vibration 1: 11.

Godiganur, S., C. H. Suryanarayana Murthy, et al. (2009). "6BTA 5.9 G2-1 Cummins engine performance and emission tests using methyl ester mahua (Madhuca indica) oil/diesel blends." Renewable Energy 34(10): 2172-2177.

Goh, C. S. and K. T. Lee (2010). "Palm-based biofuel refinery (PBR) to substitute petroleum refinery: An energy and emergy assessment." Renewable & Sustainable Energy Reviews 14(9): 2986-2995.

Graboski, M. S. and R. L. McCormick (1998). "Combustion of fat and vegetable oil derived fuels in diesel engines." Progress in Energy and Combustion Science 24(2): 125-164.

Gutierrez, P. A., C. Hervas, et al. (2009). "Combined projection and kernel basis functions for classification in evolutionary neural networks." Neurocomputing 72(13-15): 2731-2742.

H

Haas, M. J., K. M. Scott, et al. (2001). "Engine performance of biodiesel fuel prepared from soybean soapstock: A high quality renewable fuel produced from a waste feedstock." Energy and Fuels 15(5): 1207-1212.

Hafner, M., M. Schuler, et al. (2000). "Fast neural networks for diesel engine control design." Control Engineering Practice 8(11): 1211-1221.

Haik, Y. H. Y., M. Y. E. Selim, et al. (2011). "Combustion of algae oil methyl ester in an indirect injection diesel engine." Energy 36(3): 1827-1835.

Haykin (2009). Neural Networks and Learning Machines, Prentice HAll.

Hampson, G. J., Patterson, M.A., Kong, S.C., Reitz, R.D. (1994). "Modeling the effects of fuel injection characteristics on diesel engine soot and NO_x emissions." SAE paper 940523 1994.

Hansen, K. F. and M. G. Jensen (1997). "Chemical and biological

characteristics of exhaust emissions from a diesel engine fuelled with rapeseed oil methyl ester (RME)." SAE paper 971689.

Harrington, K. J. (1986). "Chemical and physical properties of vegetable oil esters and their effect on diesel fuel performance." Biomass 9: 1-17.

Hashemi, N. and N. N. Clark (2007). "Artificial neural network as a predictive tool for emissions from heavy-duty diesel vehicles in Southern California." International Journal of Engine Research 8(4): 321-336.

Heckl, M. (1989). "Remarks on the calculation of sound radiation using the method of spherical wave synthesis." Bemerkung zur Berechnung der Schallabstrahlung nach der Methode der Kugelfeldsynthese 68(4): 251-257.

Hernandez-Lobato, D., G. Martinez-Munoz, et al. (2011). "Empirical analysis and evaluation of approximate techniques for pruning regression bagging ensembles." Neurocomputing 74(12-13): 2250-2264.

Herreros Arellano, J. M. (2010). Framework to optimise the use of alternative fuels. Case study: emission benefits in compression ignition engines. School of Apoplied Sciences, Cranfield University. MSc Motorsport Engineering and Management.

Hervas-Martinez, C., F. J. Martinez-Estudillo, et al. (2008). "Multilogistic regression by means of evolutionary product-unit neural networks." Neural Networks 21(7): 951-961.

Hickling, R., D. A. Feldmaier, et al. (1979). "Knock-induced cavity resonances in open chamber diesel engines." Journal of the Acoustical Society of America 65(6): 1474-1479.

Hulwan, D. B. and S. V. Joshi (2011). "Performance, emission and combustion characteristic of a multicylinder DI diesel engine running on diesel-ethanol-biodiesel blends of high ethanol content." Applied Energy 88(12): 5042-5055.

I

Igel, C. and M. Husken (2003). "Empirical evaluation of the improved Rprop learning algorithms." Neurocomputing 50: 105-123.

InSoo J., K. K. (2010). New experimental approach for developing combustion noise of diesel engines. Aachen Acoustic Colloquium,

Aachen.
Ismail, A., A. P. Engelbrecht, et al. (2002). Pruning product unit neural networks. Proceeding of the 2002 International Joint Conference on Neural Networks, Vols 1-3: 257-262.

J

Jayed, M. H., H. H. Masjuki, et al. (2011). "Prospects of dedicated biodiesel engine vehicles in Malaysia and Indonesia." Renewable & Sustainable Energy Reviews 15(1): 220-235.
Johnsson, R. (2006). "Cylinder pressure reconstruction based on complex radial basis function networks from vibration and speed signals." Mechanical Systems and Signal Processing 20(8): 1923-1940.

K

Kalam, M. A., H. H. Masjuki, et al. (2011). "Emission and performance characteristics of an indirect ignition diesel engine fuelled with waste cooking oil." Energy 36(1): 397-402.
Kara Togun, N. and S. Baysec (2010). "Prediction of torque and specific fuel consumption of a gasoline engine by using artificial neural networks." Applied Energy 87(1): 349-355.
Kim, G. T. and B. H. Lee (1990). "3-D Sound source reconstruction and field reprediction using the Helmholtz integral-equation." Journal of Sound and Vibration 136(2): 245-261.
Kim, Y. and P. A. Nelson (2004). "Optimal regularisation for acoustic source reconstruction by inverse methods." Journal of Sound and Vibration 275(3-5): 463-487.
Kim, Y., Nelson, P. (2003). "Spatial resolution limits for there construction of acoustic source strength by inverse methods." Journal of Sound and Vibration 265(3): 583-608.
Kloth, M., Vancluysen, K., Clement, F., Lars Ellebjerg, P. (2008). Silence project, European Comission.
Knothe, G. (2005). "Dependence of biodiesel fuel properties on the structure of fatty acid alkyl esters." Fuel Processing Technology 86(10): 1059-1070.

Knothe, G., C. A. Sharp, et al. (2006). "Exhaust emissions of biodiesel, petrodiesel, neat methyl esters, and alkanes in a new technology engine." Energy & Fuels 20(1): 403-408.

Knothe, G. (2008). ""Designer" Biodiesel: Optimizing Fatty Ester Composition to Improve Fuel Properties." Energy & Fuels 22: 1358-1364.

Koopmann, G. H., L. Song, et al. (1989). "A method for computing acoustic fields based on the principle of wave superposition." Journal of the Acoustical Society of America 86(6): 2433-2438.

Kotake, S. and K. Takamoto (1990). "Combustion noise: Effects of the velocity turbulence of unburned mixture." Journal of Sound and Vibration 139(1): 9-20.

L

Ladommatos, N., M. Parsi, et al. (1996). "The effect of fuel cetane improver on diesel pollutant emissions." Fuel 75(1): 8-14.

Lalor, N., Petit, M., (1975). "Modes of engine structure vibration as a source of noise." SAE paper 750833.

Lapuerta, M., O. Armas, et al. (2005). "Diesel emissions from biofuels derived from Spanish potential vegetable oils." Fuel 84(6): 773-780.

Lapuerta, M., O. Armas, et al. (2008). "Effect of biodiesel fuels on diesel engine emissions." Progress in Energy and Combustion Science 34: 198-223.

Lapuerta, M., J. M. Herreros, et al. (2008). "Effect of the alcohol type used in the production of waste cooking oil biodiesel on diesel performance and emissions." Fuel 87(15-16): 3161-3169.

Leclere, Q. (2009). "Acoustic imaging using under-determined inverse approaches: Frequency limitations and optimal regularization." Journal of Sound and Vibration 321(3-5): 605-619.

Leclere, Q. and B. Laulagnet (2009). "Nearfield acoustic holography using a laser vibrometer and a light membrane." Journal of the Acoustical Society of America 126(3): 1245-1249.

Leveque, G., E. Rosenkrantz, et al. (2007). "Correction of diffraction effects in sound velocity and absorption measurements." Measurement Science & Technology 18(11): 3458-3462.

Lin, L., Z. Cunshan, et al. (2011). "Opportunities and challenges for

biodiesel fuel." Applied Energy 88(4): 1020-1031.
Lin, S. L., W. J. Lee, et al. (2011). "Reduction in emissions of nitrogen oxides, particulate matter, and polycyclic aromatic hydrocarbon by adding water-containing butanol into a diesel-fueled engine generator." Fuel.
Luque R, P. S., Campelo JM, Ruiz JJ, Lopez I, Luna D, Marinas JM, Romero AA, Dorado MP (2010). Biofuels for Transport: Prospects and Challenges, in Emerging Enviromental Technologies, Springer:New York (USA).
Lu, X. C., J. G. Yang, et al. (2004). "Effect of cetane number improver on heat release rate and emissions of high speed diesel engine fueled with ethanol-diesel blend fuel." Fuel 83(14-15): 2013-2020.
Lü, X. C., J. G. Yang, et al. (2005). "Improving the combustion and emissions of direct injection compression ignition engines using oxygenated fuel additives combined with a cetane number improver." Energy and Fuels 19(5): 1879-1888.

M

Mallikappa, D. N., R. P. Reddy, et al. (2012). "Performance and emission characteristics of double cylinder CI engine operated with cardanol bio fuel blends." Renewable Energy 38(1): 150-154.
Martin, V., T. Le Bourdon, et al. (2011). "Numerical simulation of acoustic holography with propagator adaptation: Application to a 3D disc." Journal of Sound and Vibration 330(17): 4233-4249.
Martinez-Estudillo, A. C., C. Hervás-Martínez, et al. (2005). "Hybridization of evolutionary algorithms and local search by means of a clustering method." IEEE Transactions on Systems, Man, and Cybernetics, Part B: Cybernetics 36(3): 534-545.
Martinez-Estudillo, A. C., C. Hervás-Martínez, et al. (2005). "Hybridization of evolutionary algorithms and local search by means of a clustering method." IEEE Transactions on Systems, Man, and Cybernetics, Part B: Cybernetics 36(3): 534-545.
Martinez-Estudillo, F. J., C. Hervas-Martinez, et al. (2008). "Evolutionary product-unit neural networks classifiers." Neurocomputing 72(1-3): 548-561.
Mason, J. M. and F. J. Fahy (1990). "Development of a reciprocity

technique for the prediction of propeller noise transmission through aircraft fuselages." Noise Control Engineering Journal 34(2): 43-52.

Maynard, J. D., E. G. Williams, et al. (1985). "Nearfield acoustic holography .1. Theory of generalized holography and the development of nah." Journal of the Acoustical Society of America 78(4): 1395-1413.

Maynard, J. W., E.; Lee, Y., (1985). "Nearfield acoustic holography 1. Theory of generalized holography and the development of NAH." Journal of Acoustic Society of America 78: 1395-1413.

McCormick, R. L., M. S. Graboski, et al. (2001). "Impact of biodiesel source material and chemical structure on emissions of criteria pollutants from a heavy-duty engine." Environ. Sci. Technol 35: 1742–1747.

Meher, L. C., D. Vidya Sagar, et al. (2006). "Technical aspects of biodiesel production by transesterification--a review." Renewable and Sustainable Energy Reviews 10(3): 248-268.

Miskiewicz, A., Letowski, T. (1999). "Psychoacoustic in the automotive industry." Acustica 83: 5.

Michalewicz, Z. (1994). Genetic algorithms+data structures=evolution programs. Berlin and New York, Springer-Verlag.

Mittelbach, M. and C. Remschmidt (2004). Biodiesel: The Comprehensive Handbook. Graz, Austria, Martin Mittelbach.

Monarca, D., M. Cecchini, et al. (2009). Safety and health of workers: Exposure to dust, noise and vibrations. 845: 437-442.

Moscato, P., Cotta, C., (2003). A gentle introduction to memetic algorithms, in: Handbook of Metaheuristics, Springer New York.

Mucchi, E. and A. Vecchio (2010). "Acoustical signature analysis of a helicopter cabin in steady-state and run up operational conditions." Measurement 43(2): 283-293.

N

Nivesrangsan, P., J. A. Steel, et al. (2005). "AE mapping of engines for spatially located time series." Mechanical Systems and Signal Processing 19(5): 1034-1054.

Nor, M. J. M., M. H. Fouladi, et al. (2008). "Index for vehicle acoustical comfort inside a passenger car." Applied Acoustics 69(4): 343-353.

O

Ochmann, M. (1995). "Source simulation technique for acoustic radiation problems." Acustica 81(6): 512-527.

Oh, Y.-K., H.-J. Kim, et al. (2008). "Metabolic-flux analysis of hydrogen production pathway in Citrobacter amalonaticus Y19." International Journal of Hydrogen Energy 33(5): 1471-1482.

Oğuz, H., I. Saritas, et al. (2010). "Prediction of diesel engine performance using biofuels with artificial neural network." Expert Systems with Applications 37(9): 6579-6586.

Ozkaya, E. and M. Pakdemirli (1999). "Non-linear vibrations of a beam-mass system with both ends clamped." Journal of Sound and Vibration 221(3): 491-503.

P

Papenfus, T., Genuit, K., Blaschke, P., Kang, K. T., Jung, I., Jin, J., (2009). "Method of NVH quality rating of diesel combustion noise using typical driving modes." SAE paper 2009-01-2078.

Park, S. G., H. J. Sim, et al. (2009). "Analysis of the HVAC system's sound quality using the design of experiments." Journal of Mechanical Science and Technology 23(10): 2801-2806.

Partridge, D. (1996). "Network generalization differences quantified." Neural Networks 9(2): 263-271.

Pasqual, A. M. and V. Martin (2012). "Optimal secondary source position in exterior spherical acoustical holophony." Journal of Sound and Vibration 331(4): 785-797.

Payri, F., A. Broatch, et al. (2005). "New methodology for in-cylinder pressure analysis in direct injection diesel engines - application to combustion noise." Measurement Science & Technology 16(2): 540-547.

Payri, F., A. J. Torregrosa, et al. (2009). "Assessment of diesel combustion noise overall level in transient operation." International Journal of Automotive Technology 10(6): 761-769.

Payri, F., A. Broatch, et al. (2009). "Sound quality assessment of Diesel combustion noise using in-cylinder pressure components."

Measurement Science & Technology 20(1).

Payri, R., F. J. Salvador, et al. (2011). "The effect of temperature and pressure on thermodynamic properties of diesel and biodiesel fuels." Fuel 90(3): 1172-1180.

Pei, J. S., A. W. Smyth, et al. (2004). "Analysis and modification of Volterra/Wiener neural networks for the adaptive identification of non-linear hysteretic dynamic systems." Journal of Sound and Vibration 275(3-5): 693-718.

Pessina, D. and M. Guerretti (2000). "Effectiveness of hearing protection devices in the hazard reduction of noise from used tractors." Journal of Agricultural Engineering Research 75(1): 73-80.

Peterson, A. M., P. I. Lee, et al. (2009). Effects of b20 on combustion, emissions and performance of a light-duty diesel engine.

Pézerat, C., Q. Leclère, et al. (2009). "Identification of vibration excitations from acoustic measurements using near field acoustic holography and the force analysis technique." Journal of Sound and Vibration 326(3-5): 540-556.

Pinzi, S., I. L. Garcia, et al. (2009). "The ideal vegetable oil-based biodiesel composition: a review of social, economical and technical implications." Energy & Fuels 23: 2325–2341.

Pinzi, S., F. P. Capote, et al. (2009). "Flow injection analysis-based methodology for automatic on-line monitoring and quality control for biodiesel production." Bioresource Technology 100(1): 421-427.

Pinzi, S., F. J. Lopez-Gimenez, et al. (2010). "Response surface modeling to predict biodiesel yield in a multi-feedstock biodiesel production plant." Bioresource Technology 101(24): 9587-9593.

Pinzi, S., D. Leiva, et al. (2011). "Multiple response optimization of vegetable oils fatty acid composition to improve biodiesel physical properties." Bioresource Technology 102(15): 7280-7288.

Pinzi, S., J. M. Mata-Granados, et al. (2011). "Influence of vegetable oils fatty-acid composition on biodiesel optimization." Bioresource Technology 102(2): 1059-1065.

Pinzi, S., P. Rounce, et al. (In press). "The effect of biodiesel fatty acid composition on combustion behavior and diesel engine exhaust emissions." Fuel.

Prasad, M. G. and M. J. Crocker (1983). "Acoustical source characterization studies on a multi-cylinder engine exhaust system." Journal of Sound and Vibration 90(4): 479-490.

Pruvost, L., Q. Leclere, et al. (2009). "Diesel engine combustion and mechanical noise separation using an improved spectrofilter." Mechanical Systems and Signal Processing 23(7): 2072-2087.

R

Rakopoulos, D. C., C. D. Rakopoulos, et al. (2010). "Effects of butanol-diesel fuel blends on the performance and emissions of a high-speed DI diesel engine." Energy Conversion and Management 51(10): 1989-1997.

Rakopoulos, C. D., A. M. Dimaratos, et al. (2011). "Study of turbocharged diesel engine operation, pollutant emissions and combustion noise radiation during starting with bio-diesel or n-butanol diesel fuel blends." Applied Energy 88(11): 3905-3916.

Ramírez-Verduzco, L. F., B. E. García-Flores, et al. (2011). "Prediction of the density and viscosity in biodiesel blends at various temperatures." Fuel 90(5): 1751-1761.

Ramírez-Verduzco, L. F., J. E. Rodríguez-Rodríguez, et al. (2012). "Predicting cetane number, kinematic viscosity, density and higher heating value of biodiesel from its fatty acid methyl ester composition." Fuel 91(1): 102-111.

Ramos, M. J., C. M. Fernandez, et al. (2009). "Influence of fatty acid composition of raw materials on biodiesel properties." Bioresource Technology 100(1): 261-268.

Redel-Macias, M. D., D. Berckmans, et al. (2010). "Model of Identification of Sound Source. Application to Noise Engine." Revista Iberoamericana De Automatica E Informatica Industrial 7(3): 34-+.

Redel-Macías, M. D., S. Pinzi, et al. (2012). "Air and noise pollution of a diesel engine fueled with olive pomace oil methyl ester and petrodiesel blends." Fuel 95: 615-621.

Ren, Y., Z. Huang, et al. (2008). "Combustion and emissions of a DI diesel engine fuelled with diesel-oxygenate blends." Fuel 87(12): 2691-2697.

Riazi, R., M. Farshchi, et al. (2010). "An Experimental Study on Combustion Dynamics and NOx Emission of a Swirl Stabilized Combustor with Secondary Fuel Injection." Journal of Thermal Science and Technology 5(2): 266-281.

Rogers, A., Pruegel-Bennett, A., (1999). "Genetic drift in genetic algorithm selection schemes." IEEE Transactions on Evolutionary Computation 4(3): 298.

Rounce, P., A. Tsolakis, et al. (2010). "A comparison of diesel and biodiesel emissions using dimethyl carbonate as an oxygenated additive." Energy and Fuels 24(9): 4812-4819.

Rounce, P., A. Tsolakis, et al. (2009). "Diesel Engine Performance and Emissions when First Generation Meets Next Generation Biodiesel." SAE paper 2009-01-1935

Russell, M. F. (1982). "Diesel Engine Noise: Control at source." SAE paper 820238.

Russell, M. F. and R. Haworth (1985). "Combustion noise from high speed direct injection Diesel engines." SAE paper 850973.

S

Sarkissian, A. (1990). "Near-field acoustic holography for an axisymmetrical geometry - a new formulation." Journal of the Acoustical Society of America 88(2): 961-966.

Sayin, C., H. M. Ertunc, et al. (2007). "Performance and exhaust emissions of a gasoline engine using artificial neural network." Applied Thermal Engineering 27(1): 46-54.

Schmidt, K. and J. Van Gerpen (1996). "The Effect of Biodiesel Fuel Composition on Diesel Combustion and Emissions." SAE paper 961086.

Schober, S., I. Seidl, et al. (2006). "Ester content evaluation in biodiesel from animal fats and lauric oils." European Journal of Lipid Science and Technology 108(4): 309-314.

Schönborn, A., N. Ladommatos, et al. (2009). "The influence of molecular structure of fatty acid monoalkyl esters on diesel combustion." Combustion and Flame 156(7): 1396-1412.

Selim, M. Y. E. (2009). "Reducing the viscosity of Jojoba Methyl Ester diesel fuel and effects on diesel engine performance and roughness." Energy Conversion and Management 50(7): 1781-1788.

Senatore, A., Cardone. M., Rocco, V., Prati, MV. (2000). "A comparative analysis of combustion process in DI diesel engine fueled with

biodiesel and diesel fuel." SAE paper 2000-01-0691.
Sharp, C. A., Howell, S., Jobe, J. (2000). "The efect of biodiesel fuels on transient emissions from modern diesel engines-part I:regulated emissions and performance." SAE paper 2000-01-1967.
Singh, K. K., S. H. Frankel, et al. (2004). "Study of spectral noise emissions from standard turbulent nonpremixed flames." Aiaa Journal 42(5): 931-936.
Solecki, L. (2000). "Duration of exposure to noise among farmers as an important factor of occupational risk." Annals of Agricultural and Environmental Medicine 7(2): 89-93.
Specht, D. F. (1991). "A general regression neural network." IEEE Transactions on Neural Networks 2(6): 568-576.
Stanković, L. and J. F. Böhme (1999). "Time-frequency analysis of multiple resonances in combustion engine signals." Signal Processing 79(1): 15-28.
Szybist, J. P., J. H. Song, et al. (2007). "Biodiesel combustion, emissions and emission control." Fuel Processing Technology 88(7): 679-691.

T

Tat, M. E., J. H. Van Gerpen, et al. (2000). "Speed of sound and isentropic bulk modulus of biodiesel at 21 °C from atmospheric pressure to 35 MPa." JAOCS, Journal of the American Oil Chemists' Society 77(3): 285-289.
Tokhi, M. O. and R. Wood (1997). "Active noise control using radial basis function networks." Control Engineering Practice 5(9): 1311-1322.
Tong, F., S. K. Tso, et al. (2006). "Impact-acoustics-based health monitoring of tile-wall bonding integrity using principal component analysis." Journal of Sound and Vibration 294(1-2): 329-340.
Torregrosa, A. J., A. Broatch, et al. (2007). "Combustion noise level assessment in direct injection Diesel engines by means of in-cylinder pressure components." Measurement Science & Technology 18(7): 2131-2142.
Torregrosa, A. J., A. Broatch, et al. (2011). "Suitability analysis of advanced diesel combustion concepts for emissions and noise control." Energy 36(2): 825-838.
Torres-Jimenez, E., M. P. Dorado, et al. (2011). "Experimental investigation

on injection characteristics of bioethanol-diesel fuel and bioethanol-biodiesel blends." Fuel 90(5): 1968-1979.

Tsolakis, A., A. Megaritis, et al. (2008). "Application of exhaust gas fuel reforming in diesel and homogeneous charge compression ignition (HCCI) engines fuelled with biofuels." Energy 33(3): 462-470.

Tousignant, T., Wellmann, T., Govindswamy, K., (2009). "Application of combustion sound level (CSL) analysis for powertrain NVH development and benchmarking." SAE paper 2009-01-2168.

Tsolakis, A., A. Megaritis, et al. (2007). "Engine performance and emissions of a diesel engine operating on diesel-RME (rapeseed methyl ester) blends with EGR (exhaust gas recirculation)." Energy 32(11): 2072-2080.

V

Vastfjall, D., M. A. Gulbol, et al. (2002). "Affective evaluations of and reactions to exterior and interior vehicle auditory quality." Journal of Sound and Vibration 255(3): 501-518.

Verheij, J. W., F. H. VanTol, et al. (1995). Monopole airborne sound source with in situ measurement of its volume velocity.

W

Wang, X., C. S. Cheung, et al. "Diesel engine gaseous and particle emissions fueled with diesel-oxygenate blends." Fuel.

Witten, H. I., Frank, E. (2005). Data Mining: Practical Machine Learning Tools and Techniques, Morgan Kaufmann (Elsevier).

Y

Yao, S., C. J. Wei, et al. (1996). "Evolving wavelet neural networks for function approximation." Electronics Letters 32(4): 360-361.

Yao, X. (1999). "Evolving artificial neural networks." Proceedings of the IEEE 87(9): 1423-1447.

Yao, X., Liu, Y. (1997). "A new evolutionary suystem for evolving artificial

neural networks." IEEE Transactions on Neural Networks 3(8): 694-713.

Yap, W. K. and V. Karri (2011). "ANN virtual sensors for emissions prediction and control." Applied Energy 88(12): 4505-4516.

Yoshizaki, T., Nishida, K., Hiroyasu, H., (1993). "Approach to low NO_x and smoke emission engines by using phenomenological simulation." SAE paper 930612 1993.

You, Y., Jeon, Y. (2007). Just noticeable differences of sound quality metrics of refrigerators noise. Proceedings of 19th ICA. Madrid.

Yu, Y., YuDejie, et al. (2006). "A roller bearing fault diagnosis method based on EMD energy entropy and ANN." Journal of Sound and Vibration 294(1-2): 269-277.

Yuan, Z. C., H. Fang, et al. (2011). The Experiment Research on Related Factors of Influencing Combustion Noise of Diesel Engine. Advances in Mechanical Design, Pts 1 and 2. J. M. Zeng, Z. Y. Jiang, T. Li, D. G. Yang and Y. H. Kim. 199-200: 1005-1009.

Yücesu, H. S., A. Sozen, et al. (2007). "Comparative study of mathematical and experimental analysis of spark ignition engine performance used ethanol-gasoline blend fuel." Applied Thermal Engineering 27(2-3): 358-368.

Yusaf, T. F., D. R. Buttsworth, et al. (2010). "CNG-diesel engine performance and exhaust emission analysis with the aid of artificial neural network." Applied Energy 87(5): 1661-1669.

Yuste, A. J. and M. P. Dorado (2006). "A neural network approach to simulate biodiesel production from waste olive oil." Energy & Fuels 20(1): 399-402.

Z

Zhang, C. S., Q. T. Cai, et al. (2010). "Boosting with pairwise constraints." Neurocomputing 73(4-6): 908-919.

Zimont, V. L. (1979). "Theornumbersy of turbulent combustion of a homogeneous fuel mixture at high Reynolds " Combustion, Explosion, and Shock Waves 15: 305-311.

Zwicker, E., Fastl, H., (1999). Psychoacoustic: Facts and Models. Heidelberg.

Zwicker, E., Fastl, H., Dalmayr, C. (1984). "BASIC-program for calculating

the loudness of sounds from their 1/3-oct band spectra according to ISO 532B." Acustica 55: 4.

Zwicker, E., Fastl, H., Widmann, U., Kurakata, K., Kuwano, S., Namba, S. (1991). "Program for calculating loudness according to DIN 45631 (ISO 532B)." Journal of Acoustic Society of Japan 12(1): 3.

Appendix

Appendix. List of Publications

Journal articles

[1] M.D. Redel-Macías, S. Pinzi, D. Leiva, A.J. Cubero-Atienza, M.P. Dorado, Air and noise pollution of a diesel engine fueled with olive pomace oil methyl ester and petrodiesel blends, Fuel, 95 (2012) 615-621.

[2] M.D. Redel-Macías, S. Pinzi, M.F. Ruz, A.J. Cubero-Atienza, M.P. Dorado, Biodiesel from saturated and monounsaturated fatty acid methyl esters and their influence over noise and air pollution, Fuel.D.O.I.: 10.1016/j.fuel.2012.01.070.

[3] M.D. Redel-Macías, C. Hervás-Martínez, S. Pinzi, P.A. Gutiérrez, A.J. Cubero-Atienza, M.P. Dorado, Noise prediction of a diesel engine fueled with olive pomace oil methyl ester blended with diesel fuel, Fuel. *Accepted for their publication.*

[4] M.D. Redel-Macías, F. Fernández-Navarro, P.A. Gutiérrez, A.J. Cubero-Atienza, C. Hervás-Martínez, Ensembles of evolutionary product unit or RBF neural networks for the identification of sound for pass-by noise test in vehicles. Neurocomputing. *Accepted for their publication.*

[5] M.D. Redel-Macías, D. Berckmans, A.J. Cubero-Atienza, Model of Identification of Sound Source. Application to Noise Engine, Revista Iberoamericana De Automatica E Informatica Industrial, 7 (2010) 34-+.

Chapter of books

[1] M.D. Redel-Macias, F. Fernandez-Navarro, A.J. Cubero-Atienza, C. Hervas-Martinez, Identification of Sound for Pass-by Noise Test in Vehicles Using Generalized Gaussian Radial Basis Function Neural Networks, in: A. GasparCunha, R. Takahashi, G. Schaefer, L. Costa (Eds.) Soft Computing in Industrial Applications, 2011, pp. 327-336.

[2] M.D. Redel-Macias, P.A. Gutierrez, A.J. Cubero-Atienza, C. Hervas-Martinez, Sound Source Identification in Vehicles Using a Combined Linear-Evolutionary Product Unit Neural Network Model, in: E. Corchado, V. Snasel, J. Sedano, A.E. Hassanien, J.L. Calvo, D. Slezak (Eds.) Soft Computing Models in Industrial and Environmental Applications, 2011, pp. 379-386.

[3] M.D. Redel-Macias, A.J. Cubero-Atienza, P. Sas, L. Salas-Morera, Algorithms for Active Noise Control, Omatu, J.M. Corchado (Eds.) Distributed Computing, Artificial Intelligence, Bioinformatics, Soft Computing, and Ambient Assisted Living, 2009, pp. 1240-1247.

International peer reviewed conferences

[1] M.D. Redel-Macías, A.J. Cubero-Atienza, D. Berckmans, Design and experimental validation of a sound source model for engine of vehicles, in ACS/IEEE International Conference on computer systems and applications, AICCSA, 2010.

[2] M.D.Redel-Macías, D. Santamaría-García, A.J. Cubero-Atienza. A novel design strategy for iterative learning control based on approximate fuzzy data model (AFDM) for active noise control: Theoretical background. International Conference on noise and vibration engineering-ISMA2010.

[3] M.D. Redel-Macías, AJ Cubero-Atienza, L Salas-Morera, A Arauzo-Azofra, L García-Hernández. Review of Algorithms for Active noise control. AEIPRO. International Conference on Project Engineering. Badajoz, España Julio (2009).

[4] MD Redel-Macías, D Berckmans, AJ Cubero-Atienza. Modelo de Identificación de fuentes de ruido. AEIPRO. International Conference on Project Engineering. Badajoz, España Julio (2009).